

RESONANCE: THE SCIENCE BEHIND THE ART OF SONIC DRILLING

by

Peter Andrew Lucon

A dissertation submitted in partial fulfillment
of the requirements for the degree

of

Doctor of Philosophy

in

Engineering

MONTANA STATE UNIVERSITY
Bozeman, Montana

April 2013

©COPYRIGHT

by

Peter Andrew Lucon

2013

All Rights Reserved

APPROVAL

of a dissertation submitted by

Peter Andrew Lucon

This dissertation has been read by each member of the dissertation committee and has been found to be satisfactory regarding content, English usage, format, citation, bibliographic style, and consistency and is ready for submission to The Graduate School.

Dr. David Miller (Co-Chair)
Dr. Douglas Cairns (Co-Chair)

Approved for the Department of Mechanical and Industrial Engineering

Dr. Christopher H.M. Jenkins

Approved for The Graduate School

Dr. Ronald W. Larsen

STATEMENT OF PERMISSION TO USE

In presenting this dissertation in partial fulfillment of the requirements for a doctoral degree at Montana State University, I agree that the Library shall make it available to borrowers under rules of the Library. I further agree that copying of this dissertation is allowable only for scholarly purposes, consistent with “fair use” as prescribed in the U.S. Copyright Law. Requests for extensive copying or reproduction of this dissertation should be referred to ProQuest Information and Learning, 300 North Zeeb Road, Ann Arbor, Michigan 48106, to whom I have granted “the right to reproduce and distribute my dissertation in and from microform along with the non-exclusive right to reproduce and distribute my abstract in any format in whole or in part.”

Peter Andrew Lucon

April 2013

ACKNOWLEDGEMENTS

I would like to thank some of the many people who from the beginning of this work have been instrumental in its final success. Without the support, encouragement, and training from Lawrence C. Farrar and the staff at Resodyn Corporation this work would never have come to fruition.

Without the financial support of Resodyn Corporation, it would not have been possible to start the journey nor finish strong. Funding from the Department of Energy SBIR Phase I Program made it possible to perform tests and collect test data while operating a sonic drill. Special thanks also goes out to Dr. Jeffery Barrow for allowing us the use of his sonic drill as well as the multitude of facts and stories about sonic drilling. I would also like to thank Rob Dobush of Blue Star Enterprises Northwest for assembling and operating the sonic drill for our tests and Brian Seaholm for writing the data acquisition program, recording the test data and traveling with me to take the sonic drill data.

Without the support of my family this work would not have been completed. Janice, especially, was and currently is a constant source of encouragement, who through all the other distractions, including the birth of our first born, Helen, kept me on task so I could focus on this endeavor and finish.

Finally, I would like to dedicate this body of work to my parents Francis and Mary Lucon, for providing continual support and encouragement throughout to my life.

TABLE OF CONTENTS

1. INTRODUCTION	1
Sonic Drilling Background	1
How Sonic Drilling Works	6
The Sonic Drill Head	6
The Resonator	7
Drilling with Sonics	9
Sonic Drilling Modeling	12
Motivation for Continued Research in Sonic Drilling	22
Background of Microhole Drilling	23
Anticipated Public Benefits	24
Carbon-Sequestration	26
Coalbed Methane Basins (CBM)	26
Market Potential	27
Research Direction	28
2. SONIC DRILL VARIABLES OF INFLUENCE	29
Introduction	29
Penetration Rate	35
Weight on Bit	35
Input Force Frequency	36
Input Force	36
Speed of Rotation	37
Flush Fluid Flow	40
Mass of Sonic Head	40
Mass of Drill Bit	42
Air Spring Rate at Sonic Head	43
Damping along the Length of the Drill String	43
Damping at the Drill Bit	45
Sonic Driver Damping	46
Stored Energy along the Length	46
Drill Bit Coupling	47
3. MODELING	48
Introduction	48
Single Degree of Freedom System	49
Sonic Drill System	56
Mathematical Model	56
Boundary Condition Solution Method	62
Sonic Drill Parameters	65

TABLE OF CONTENTS – CONTINUED

Finite Element Method Model.....	80
Control Derivations	84
Resonant Condition	84
Power Delivery and Measurement.	89
Real-time Monitoring of Drilling Condition	93
Choosing an Operational Resonant Mode	95
4. MATHEMATICAL MODELS	97
Introduction	97
Closed Form Boundary Solution	97
Finite Element Method	101
5. MODEL RESULTS.....	104
Introduction	104
Boundary Condition Solution.....	104
Conditions except Damping	106
Variable Effects of the Strata Being Drilled.....	115
Variable Effects of the Strata Damping.....	120
Finite Element Solution	125
Resonant Modes	127
Constant Damping and Restoring.....	134
FEM with Equivalent Damping and Restoring	137
Boundary Condition Results Summary	140
Finite Element Results Summary	145
6. EXPERIMENTAL VERIFICATION	147
Introduction	147
Test and Measurement Setup.....	147
Data Analysis.....	150
Test Data and Data Construction.....	150
Phase Angle and Resonance	151
Push or Pull Force and Resonance	153
Power	155
Experimental Results.....	166
Experimental Conclusions.....	171
7. SYSTEM CONTROL VARIABLES	173
Introduction	173
Measurements above Ground	175
Sonic Drill Head Response.....	175

TABLE OF CONTENTS – CONTINUED

Phase Relation and Input Power	176
Rate of Penetration	177
Mathematically	178
Empirically	182
Other Measurement Control Conditions	184
8. CONTROL APPLICATIONS	187
Introduction	187
Sonic Drilling	188
Non-resonant Systems	201
9. CONCLUSIONS	202
10. FUTURE WORK	208
REFERENCES CITED	210
APPENDICES	
APPENDIX A: MATLAB [®] Code	216
APPENDIX B: Supplemental Data and Graphs	224

LIST OF TABLES

Table	Page
1.1. Relation of the electrical analog variables with the corresponding mechanical variables.	12
1.2. Summary of results from CO ₂ /EOR analysis.....	27
3.1. RSD 750 rig specifications	66
3.2. Mechanical properties of various soil types and other well known materials.....	71
3.3. Soil properties survey for sands and clays.....	72
3.4. Physical parameters of rocks for simulation. (31)	75
3.5. Modeling variables.....	76
3.6. Soil damping and spring constants for various strata.	78
3.7. Soil elasticity and damping constants for various strata.....	79
3.8. Relations between the undamped natural frequency and the maximum amplitude frequencies.	87
4.1. Summary of Assumptions for the Different Models.....	98
5.1. Design of Experiments Used for the Boundary Conditions Solutions	105
5.2. DOE results for factors of influence of the resonant frequency.	108
5.3. DOE results for factors of influence of the drill bit amplitude.	109
5.4. DOE results for factors of influence of the ratio of the sonic drill head to the drill bit amplitude.....	111
5.5. DOE results for factors of influence of the resonant frequency.	116

LIST OF TABLES - CONTINUED

Table	Page
5.6. DOE results for factors of influence of the drill bit amplitude.	117
5.7. DOE results for factors of influence of the ratio of the sonic drill head to the drill bit amplitude.	119
5.8. DOE results for factors of influence of the resonant frequency.	121
5.9. DOE results for factors of influence of the drill bit amplitude.	122
5.10. DOE results for factors of influence of the ratio of the sonic drill head to the drill bit amplitude.	124
5.11. Finite Element Sonic Drill Variables.	127
5.12. FEA design of experiments listed variables to determine the significance of the damping and elastic coupling along the drill string length.	135
5.13. Variable Damping and Restoring Along the Drill String Length.	138
5.14. Boundary Condition Variables of Influence.	141
5.15. Boundary Condition Variables of Influence, sorted by Measured Variable.	141
6.1. Difference in power for the displacement, velocity, and acceleration maximum amplitude natural frequencies.	163
6.2. Calculated undamped natural frequency and damping ratio.	165
7.1. Sonic Drill Variables used for Example.	178
7.2. Equivalent damping and spring constants along the length of the drill string without RMS correction.	181
7.3. Equivalent damping and spring constants along the length of the drill string with RMS correction.	182

LIST OF TABLES - CONTINUED

Table	Page
10.1. DOE results for factors of influence of the resonant frequency.	225
10.2. DOE results for factors of influence of the drill bit amplitude.	226
10.3. DOE results for factors of influence of the ratio of sonic drill head amplitude to the drill bit amplitude.....	227
10.4. DOE results for factors of influence of the resonant frequency.	228
10.5. DOE results for factors of influence of the drill bit amplitude.	229
10.6. DOE results for factors of influence of the ratio of sonic drill head amplitude to the drill bit amplitude.....	230
10.7. DOE results for factors of influence of the resonant frequency.	231
10.8. DOE results for factors of influence of the drill bit amplitude.	232
10.9. DOE results for factors of influence of the ratio of sonic drill head amplitude to the drill bit amplitude.....	233
10.10. Axial Mode Frequencies for Various Drill Pipe Lengths.	234
10.11. Torsional Mode Frequencies for Various Drill Pipe Lengths.....	235
10.12. First 50 Bending Modes for Various Drill Pipe Lengths.....	236
10.13. Bending Modes 51 – 100 for Various Drill Pipe Lengths.	237
10.14. Bending Modes 101 – 147 for Various Drill Pipe Lengths.	238

LIST OF FIGURES

Figure	Page
1.1. Sonic drill head. Picture provided courtesy of Resodyn Corporation.	4
1.2. Resonant sonic drill diagram. Picture provided courtesy of Resodyn Corporation.	4
1.3. Resonant peak for drill steel.	5
1.4. Drill bits with buttons.	11
1.5. Sonic drilled four inch hole through a granite bolder.	11
1.6. Dynamic representation of the pile and driver pile to soil system.....	16
1.7. Power and tip amplitude versus frequency, computer curves -example.....	18
1.8. Well construction for geophone deployment.	25
2.1. Resonance condition	30
2.2. Potential and kinetic energy plotted over two oscillation cycles for a system on mechanical resonance (a) and one that is operating at a frequency lower than that of mechanical resonance (b).....	31
2.3. High-level schematic of the sonic drill.	32
2.4. Sonic drill control center.....	34
2.5. Button location and rotation to impact virgin material.	38
2.6. Rotational angle for a 0.25" button to impact virgin material at various button radii.	38
2.7. Minimum rotational speed for 0.25" buttons to impact virgin material at various button mounted radiuses and sonic drill operational frequencies of 60 hz, 120 hz, 150 hz, and 200 hz.....	39

LIST OF FIGURES - CONTINUED

Figure	Page
2.8. Coefficient of internal friction vs. acceleration	44
3.1. Single degree of freedom system.....	51
3.2. Free body diagram of the single degree of freedom system.	51
3.3. Rotating eccentric mass.	54
3.4. Dual eccentric force vectors.....	55
3.5. Sonic drill model.....	58
3.6. Sonic drill boundary conditions.....	63
3.7. RSD 750 drill rig.....	67
3.8. 9 inch outer diameter sonic drill pipe.	71
3.9. Damping and coupling types.	81
3.10. Normalized mode shape.....	83
3.11. The max displacement ' ω_M ', max velocity ' ω_v ', and max acceleration ' ω_A ' angular frequencies are located at different frequencies, because velocity and acceleration are related to the displacement by the operating frequency and operating frequency squared; respectively. The max velocity angular frequency ' ω_v ' is the most important because the power is maximized at this location.	85
3.12. The change in frequency for the maximum amplitude cases for the constant force and eccentric driven systems, with varying damping.....	88
3.13. The phase change of the maximum displacement, velocity, and accelerating points are for both constant and eccentric driven force systems with varying damping.	89

LIST OF FIGURES - CONTINUED

Figure	Page
3.14. A typical system with a power factor of 1 should have the following measurement signal from the input force, velocity response, power and average power.	90
3.15. A typical system that has a lagging power factor of 0.174. this takes power away from the system to do actual work. The average power thus used by the system to do work has now dropped to 6.6 hp as opposed to a power factor 1 with 37.9 hp.	91
3.16. Force and velocity with a lagging power factor of 0. A typical system with a lagging power factor of 0. The system is storing power from the source and then rejecting it back to the source thus doing no actual work, results in to zero average power.	92
3.17. The relation between the real power 'P', reactive power 'R', and apparent power 'S' is shown above. As the angle ' Φ_v ' increases, more of the total power from the source (diesel engine) is rejected back to the source, which causes the available power 'P' to do real work to decrease, thus performing less work onto the system.	93
3.18. Hypothetical human machine interface drilled strata profile available to the sonic drill operator if the system response variables are used to model the strata.	94
3.19. High and low frequency resonant mode shapes with corresponding damping along the length.	96
5.1. Example of an Axial Resonant Mode Shape of 6.	107
5.2. Half - Normal Plot of the DOE results for the significant factors that effect the sonic drill axial resonant frequency.	108
5.3. Half - Normal Plot of the DOE results for the significant factors that effect the sonic drill bit amplitude.	110
5.4. Half - Normal Plot of the DOE results for the significant factors that effect the ratio of the sonic drill head amplitude to the sonic drill bit amplitude.	111

LIST OF FIGURES - CONTINUED

Figure	Page
5.5. (a) Sonic drill head to drill bit amplitude ratio vs. drill bit spring rate with different curves with various drill bit masses, 500 kg sonic drill head mass, and 1,751,268 N/m sonic drill head spring rate. (b) Sonic drill head to drill bit amplitude ratio vs. drill bit spring rate with different curves with various drill bit masses, 2000 kg sonic drill head mass, and 12,258,879 N/m sonic drill head spring rate.....	112
5.6. (a) Sonic drill head to drill bit amplitude ratio vs. drill head spring rate with different curves with drill bit mass of 0.1 kg, various sonic drill head masses, and the extreme sonic drill head spring rates. (b) Sonic drill head to drill bit amplitude ratio vs. drill head spring rate with different curves with drill bit mass of 113 kg, various sonic drill head masses, and the extreme sonic drill head spring rates.....	113
5.7. Sonic drill head to drill bit amplitude ratio vs. sonic drill head mass with different curves for varying drill bit masses.	114
5.8. Half - Normal Plot of the DOE results for the significant factors that effect the sonic drill axial resonant frequency.	117
5.9. Half - Normal Plot of the DOE results for the significant factors that effect the sonic drill bit amplitude.	118
5.10. Half - Normal Plot of the DOE results for the significant factors that effect the ratio of the sonic drill head amplitude to the sonic drill bit amplitude.....	119
5.11. Half - Normal Plot of the DOE results for the significant factors that effect the sonic drill axial resonant frequency.	121
5.12. Half - Normal Plot of the DOE results for the significant factors that effect the sonic drill bit amplitude.	123
5.13. Half - Normal Plot of the DOE results for the significant factors that effect the ratio of the sonic drill head amplitude to the sonic drill bit amplitude.....	124
5.14. Example of an axial resonant mode resultant mode shape.	126

LIST OF FIGURES - CONTINUED

Figure	Page
5.15. Example of a bending resonant mode resultant mode shape.	126
5.16. Example of a torsional resonant mode resultant mode shape.	127
5.17. ANSYS® Model Boundary Conditions.	128
5.18. Axial resonant modes for different drill string lengths.	131
5.19. Bending resonant modes for different drill string lengths.	131
5.20. Lateral coupling with the primary axial resonant mode. (a) is the 6th resonant mode for a 750 ft. long drill string and (b) is the 4th resonant mode for a 500 ft. long drill string. The lateral mode is 0.2 Hz away from the axial for the 750 ft. long drill string mode, and 1.1 Hz away for the 500 ft. long drill string.	132
5.21. Torsional resonant modes for different drill string lengths.	133
5.22. FEA test condition 3 results. (a) Amplitude response of the sonic head and drill bit. (b) Phase response for the sonic head and the drill bit.	136
5.23. FEA test condition 3, 4, and 5 results. (a) Amplitude response of the sonic head and drill bit. (b) Phase response for the sonic head and the drill bit.	137
5.24. Damping Values and the normalized mode shape at 66 Hz.	139
5.25. FEA linear and step condition results. (a) Amplitude response of the sonic head and drill bit. (b) Phase response for the sonic head and the drill bit.	139
5.26. FEA impulse node and anti-node condition results. (a) Amplitude response of the sonic head and drill bit. (b) Phase response for the sonic head and the drill bit.	140
5.27. Bit Amplitude Normalized Factors of Influence. 1 being most influential.	142

LIST OF FIGURES - CONTINUED

Figure	Page
5.28. Ratio of Head to Bit Normalized Factors of Influence. 1 being most influential.	142
5.29. Resonant Frequency Normalized Factors of Influence. 1 being most influential.	143
6.1. Water development technologies sonic drill system.....	149
6.2. Accelerometer and eddy current sensor.....	150
6.3. Accelerometer and eddy current sensors.	150
6.4. Measured signals and reconstructed eccentric motion.....	152
6.5. While drilling at a depth of 80 feet of drill string, the displacement vs. input force phase angle ' Φ_d ' is shown to peak over -70 degrees, which allows the drill string to pass through -90 degrees while moving into resonance.	153
6.6. While drilling with 120 feet of drill string, the system becomes heavily damped because the operator incorrectly applied too high of a down force (9000 lbf).	156
6.7. While drilling with 80 feet of drill string the operator increases the down force from 9,000 lbf to 13,800 lbf in an attempt to increase the penetration rate, but in doing so it decreases the amount of input power delivered to the drill string that could be utilized for drilling.....	156
6.8. While drilling with 70 feet of drill string, the power input to the drill tip for drilling reached a maximum value of 300 hp. The large amount of power transfer was possible by an appropriately matched downward force for the length of drill string.....	157
6.9. The same down force of 9,000 lbf upon the drill string results in a power to drop from 300 hp to 175 hp by adding 10 feet of drill string to the system – Extension from 70 to 80 feet in length.	158

LIST OF FIGURES - CONTINUED

Figure	Page
6.10. While drilling with 120 feet of drill string, high down force causes heavy damping of the system which leads to the separation of total input power (kilo VA) and the actual useful power (kW).	160
6.11. While Drilling with 120 Feet of drill string the system became so heavily damped that the resonant peak was not discernible, making it very unlikely that the operator could find resonance. The actual useful power is also below 100 hp where at 9,000 lbf of load the useful power can be as high as 225 hp.....	161
6.12. While drilling with 120 feet of string, the high down force of 9,000 lbf caused a heavily damped system, increasing the difficulty for a human operator.	161
6.13. The maximum displacement ' ω_M ', max velocity ' ω_v ', and max acceleration ' ω_A ' angular frequencies.....	162
6.14. The phase between the force input and the corresponding velocity changes between the maximum displacement, velocity, and acceleration amplitude frequencies.....	164
6.15. The drill string mass is aiding in the push down force for penetration. Based on the tests the Equivalent pull down force for a heavy damped system was calculated and found to be very close to the drill string's own weight at about 400 feet. This is the onset of where the drill string will behave more like a pile driver than a sonic drill. The drill will still penetrate, but at a reduced rate to the maximum depths between the 500 and 700 foot ranges.	166
6.16. Sonic drilling performance data.....	168
6.17. Sonic drilling efficiency.....	170
7.1. Sonic drill mode shapes for a 76.2 m (250 ft) long drill string. (a) 2 nd mode shape and (b) 3 rd mode shape.	179

LIST OF FIGURES - CONTINUED

Figure	Page
7.2. Normalized mode shape for a 76.2 m (250 ft) long drill string.	179
7.3. Three different damping conditions along the length of the drill string.	180
7.4. Three different spring rate conditions along the length of the drill string.	181
7.5. Half-power bandwidth method to determine the damping ratio. (40)	183
7.6. Sonic drill operating conditions for drilling through rock and a void.	185
8.1. RST™ instrumentation and control system schematic. (Courtesy of Resodyn Corporation.).....	189
8.2. Eccentric speed and push-pull control loops. (Courtesy of Resodyn Corporation.).....	192
8.3. High level RST™ flowchart. (Courtesy of Resodyn Corporation.).....	192
8.4. Sonic drill starting control algorithms.	194
8.5. Sonic drill control algorithms.	195
8.6. Block diagram of the supervisory safe conditions control system.	196
8.7. RST HMI control center replacement.	199
8.8. Manual control screen.	200

NOMENCLATURE

a.....	Pile shaft elasticity constant.....	(s^{-2})
A.....	Cross sectional area of the drill pipe	(m^2, in^2)
A.....	Area of the pile	(m^2, in^2)
a'.....	Spring constant	($N \cdot m^{-4}, lbf \cdot in^{-4}$)
a(x,t).....	Acceleration relative to time and distance along the length of the drill string	($m \cdot s^{-2}, in \cdot s^{-2}$)
A _{ds}	Cross sectional area of the drill string.....	(m^2, in^2)
a _{eq}	Equivalent spring constant for the restoring forces along the length of the drill string.....	($N \cdot m^{-1}, lbf \cdot in^{-1}$)
A _n	Inward acceleration.....	($m \cdot s^{-2}, in \cdot s^{-2}$)
A _o	Sonic drill response amplitude coefficient.....	(m, in)
A _r	Radial acceleration	($m \cdot s^{-2}, in \cdot s^{-2}$)
b.....	Pile shaft damping constant	(s^{-1})
b'.....	Damping constant	($N \cdot s \cdot m^4, lbf \cdot s \cdot in^4$)
b _{eq}	Equivalent damping constant for the damping along the length of the drill string	($N \cdot s \cdot m^{-1}, lbf \cdot s \cdot in^{-1}$)
B _o	Sonic drill response amplitude coefficient.....	(m, in)
c.....	Speed of Sound in drill pipe.....	($m \cdot s^{-1}, ft \cdot s^{-1}$)
c.....	Damping constant	($N \cdot s \cdot m^{-1}, lbf \cdot s \cdot in^{-1}$)
c _{SDB}	Damping rate at the sonic drill bit.....	($N \cdot s \cdot m^{-1}, lbf \cdot s \cdot in^{-1}$)
c _{SDP}	Damping rate along the sonic drill pipe.....	($N \cdot s \cdot m^{-1}, lbf \cdot s \cdot in^{-1}$)
c _{SDH}	Damping rate at the sonic drill head	($N \cdot s \cdot m^{-1}, lbf \cdot s \cdot in^{-1}$)
c _{bit}	Damping rate at the sonic drill bit.....	($N \cdot s \cdot m^{-1}, lbf \cdot s \cdot in^{-1}$)
c _{cr}	Critical damping constant	($N \cdot s \cdot m^{-1}, lbf \cdot s \cdot in^{-1}$)
C _e	Electrical capacitance.....	(Farads)
C _m	Mechanical compliance	($N \cdot s \cdot m^{-1}, lbf \cdot s \cdot in^{-1}$)
C _o	Sonic drill response amplitude coefficient.....	(m, in)
c _{sh}	Damping rate at the sonic drill head	($N \cdot s \cdot m^{-1}, lbf \cdot s \cdot in^{-1}$)
d ² x(t)/dt ²	Acceleration relative to time	($m \cdot s^{-2}, in \cdot s^{-2}$)
D _o	Sonic drill response amplitude coefficient.....	(m, in)
du.....	Deflection along the length of the drill string	(m, in)

xx
NOMENCLATURE – CONTINUED

dv.....	Velocity along the length of the drill string ...	(m·s ⁻¹ , in·s ⁻¹)
dx(t)/dt.....	Velocity relative to time.....	(m·s ⁻¹ , in·s ⁻¹)
E.....	Drill pipe elastic constant.....	(Pa, psi)
e(N)	Correction factor	(kg·m ⁻³ ·s ² , slug·in ⁻³ ·s ²)
E _{ds}	Young's moduls of the drill string.....	(Pa, psi)
F	Oscillator force 'Fo*sin(ωt)'	(N, lbf)
F	Mechanical Force.....	(N, lbf)
F _{ecc}	Eccentric Force	(N, lbf)
f _n	Natural Frequency.....	(Hz)
F _o	Mechanical Force.....	(N, lbf)
F _o (t)	Input Force	(N, lbf)
G _s	Soil shear modulus	(Pa, psi)
i	Electrical current.....	(Amps)
j	Imaginary Unit	√(-1)
k.....	Spring constant	(N·m ⁻¹ , lbf·in ⁻¹)
k'.....	Soil spring constant per unit area.....	(N·m ⁻³ , lbf·in ⁻³)
k _{bit}	Spring rate at the sonic drill bit.....	(N·m ⁻¹ , lbf·in ⁻¹)
k _{SDB}	Spring rate at the sonic drill bit.....	(N·m ⁻¹ , lbf·in ⁻¹)
k _{SDP}	Spring rate along the length of the sonic drill pipe	(N·m ⁻¹ , lbf·in ⁻¹)
k _{SDH}	Spring rate of the air spring at the sonic drill head	(N·m ⁻¹ , lbf·in ⁻¹)
k _j	Spring constant of spring between the jth and (j+1)th elements	(N·m ⁻¹ , lbf·in ⁻¹)
k _{sh}	Spring rate of the air spring at the sonic drill head	(N·m ⁻¹ , lbf·in ⁻¹)
k _{sj}	Elastic soil spring constant imposed on jth element	(kg·m ⁻¹ , slug·in ⁻¹)
k _t	Spring rate of soil at the drill bit	(N·m ⁻³ , lbf·in ⁻³)
L	Electrical inductance	(Henry)
L _{ds}	Length of the drill string	(m, in)

xxi
NOMENCLATURE – CONTINUED

L_p	Length of the pile	(m, in)
l_{pipe}	Length of drill string	(m, in)
M	Mechanical mass	(kg, lbm)
m	Mass	(kg, lbm)
m_{bit}	Mass of the drill bit	(kg, lbm)
m_e	Mass of eccentric	(kg, lbm)
m_j	Mass of jth element	(kg, lbm)
m_{sh}	Mass of the sonic drill head	(kg, lbm)
m_{SDH}	Mass of the sonic drill head	(kg, lbm)
N	Total number of elements	
NMS	Normalized mode shape along the drill string length	
p	Pile perimeter	(m, in)
P	Mechanical power	(W, hp)
Q	Ratio of ωM to R	
q	Body force	($N \cdot m^{-3}$, $lbf \cdot in^{-3}$)
R	Distance to center of mass of eccentric from the rotation axis	(m, in)
R	Reactive power	V_{ars} V_{ars}
r_b	Radius of the drill bit button	(m, in)
r_g	Area of the pile divided by the pile perimeter squared	($m^2 \cdot m^{-2}$, $in^2 \cdot in^{-2}$)
R_m	Mechanical resistance 'friction'	($N \cdot s \cdot m^{-1}$, $lbf \cdot s \cdot in^{-1}$)
R_m	Electrical resistance	(Ohms)
r_t	Radius of the drill bit	(m, in)
s	Laplace domain complex number	
S	Apparent power	(Volt-Amp or VA))
t	Time	(s)
T	Kinetic energy	(J, BTU)
$u(x,t)$	Deflection along the length of the drill string relative to time	(m, in)
V	Electrical voltage	(Volts)

xxii
NOMENCLATURE – CONTINUED

v	Vibration velocity amplitude	$(m \cdot s^{-1}, in \cdot s^{-1})$
v	Lateral deflection in the y direction along the length of the drill string relative to time	(m, in)
ν	Poisson's ratio for the soil	
V	Mechanical velocity	$(m \cdot s^{-1}, in \cdot s^{-1})$
$v(x,t)$	Velocity relative to time and distance along the length of the drill string	$(m \cdot s^{-1}, in \cdot s^{-1})$
W	External work energy	(J, BTU)
W	Mechanical work.....	$(Watts, hp)$
w	Lateral deflection in the z direction along the length of the drill string relative to time	(m, in)
w_p	Piles weight per unit length	$(N \cdot m^{-1}, lbf \cdot in^{-1})$
X	Displacement amplitude	(m, in)
x	Distance along the drill string	(m, in)
$x(t)$	Displacement relative to time	(m, in)
x_N	Oscillation displacement amplitude at N node	(m, in)
x_{N_ddot}	Oscillation acceleration amplitude at N node	$(m \cdot s^{-2}, in \cdot s^{-2})$
x_{N_dot}	Oscillation velocity amplitude at N node	$(m \cdot s^{-1}, in \cdot s^{-1})$
Z_e	Electrical impedance.....	(Ω)
Z_m	Mechanical impedance.....	$(N \cdot s \cdot m^{-1}, lbf \cdot s \cdot in^{-1})$
γ	Damping ratio	
γ_p	Drill pipe specific weight.....	$(N \cdot m^{-3}, lbf \cdot in^{-3})$
δ	Change in displacement	(m, in)
Δt	Time between the peak force and the peak displacement	(s)
ϵ_{xx}	Strain along the x axis.....	$(m \cdot m^{-1}, in \cdot in^{-1})$
ϵ_{xy}	Shear Strain in the xy plane	$(radian)$
ϵ_{yy}	Strain along the y axis.....	$(m \cdot m^{-1}, in \cdot in^{-1})$
ϵ_{yz}	Shear Strain in the yz plane	$(radian)$
ϵ_{zx}	Shear Strain in the zx plane	$(radian)$

xxiii
NOMENCLATURE – CONTINUED

ϵ_{zz}	Strain along the z axis	$(m \cdot m^{-1}, in \cdot in^{-1})$
ζ	Damping ratio	
θ	Fourier domain variable (radial frequency) ...	$(radian \cdot s^{-1})$
θ_f	Radial oscillation frequency along the drill string length	$(radian \cdot m^{-1})$
μ	Shaft soild damping coefficient per unit area	$(N \cdot s \cdot m^{-3}, lbf \cdot s \cdot in^{-3})$
μ_t	Damping at the drill bit per unit of area.....	$(N \cdot s \cdot m^{-3}, lbf \cdot s \cdot in^{-3})$
ξ_j	Viscous soil damping coefficient on the jth element	$(kg \cdot s^{-1}, slug \cdot s^{-1})$
π	Strain energy	(J, BTU)
ρ_{ds}	Density of drill string material	$(kg \cdot m^{-3}, lbm \cdot in^{-3})$
ρ_{pipe}	Density of drill string material	$(kg \cdot m^{-3}, lbm \cdot in^{-3})$
ρ_{soil}	Density of the soil	$(kg \cdot m^{-3}, lbm \cdot in^{-3})$
σ_{xx}	Stress along the x axis	(Pa, psi)
σ_{xy}	Stress strain in the xy plane	(Pa, psi)
σ_{yy}	Stress along the y axis	(Pa, psi)
σ_{yz}	Stress Strain in the yz plane	(Pa, psi)
σ_{zx}	Stress Strain in the zx plane	(Pa, psi)
σ_{zz}	Stress along the z axis	(Pa, psi)
Φ_a	Phase angle offset between the input forcing sinusoidal function and the acceleration of the sonic drill head	$(radian)$
Φ_d	Phase angle offset between the input forcing sinusoidal function and the displacement of the sonic drill head	$(radian)$
Φ_v	Phase angle offset between the input forcing sinusoidal function and the velocity of the sonic drill head	$(radian)$
ω	Angular frequency	$(radian \cdot s^{-1})$
ω_A	Maximum acceleration angular frequency	$(radian \cdot s^{-1})$
ω_d	Damped angular natural frequency	$(radian \cdot s^{-1})$
ω_f	Input forcing angular frequency	$(radian \cdot s^{-1})$
ω_L	Undamped angular resonant frequency	$(radian \cdot s^{-1})$
ω_M	Maximum displacement angular frequency ..	$(radian \cdot s^{-1})$

xxiv
NOMENCLATURE – CONTINUED

ω_nUndamped angular resonant frequency(radian·s⁻¹)
 ω_vMaximum velocity angular frequency(radian·s⁻¹)

ABSTRACT

The research presented in this dissertation quantifies the system dynamics and the influence of control variables of a sonic drill system. The investigation began with an initial body of work funded by the Department of Energy under a Small Business Innovative Research Phase I Grant, grant number: DE-FG02-06ER84618, to investigate the feasibility of using sonic drills to drill micro well holes to depths of 1500 feet. The Department of Energy funding enabled feasibility testing using a 750 hp sonic drill owned by Jeffery Barrow, owner of Water Development Co. During the initial feasibility testing, data was measured and recorded at the sonic drill head while the sonic drill penetrated to a depth of 120 feet. To demonstrate feasibility, the system had to be well understood to show that testing of a larger sonic drill could simulate the results of drilling a micro well hole of 2.5 inch diameter. A first-order model of the system was developed that produced counter-intuitive findings that enabled the feasibility of using this method to drill deeper and produce micro-well holes to 1500 feet using sonic drills.

Although funding was not continued, the project work continued. This continued work expanded on the sonic drill models by understanding the governing differential equation and solving the boundary value problem, finite difference methods, and finite element methods to determine the significance of the control variables that can affect the sonic drill. Using a design of experiment approach and commercially available software, the significance of the variables to the effectiveness of the drill system were determined. From the significant variables, as well as the real world testing, a control system schematic for a sonic drill was derived and is patent pending. The control system includes sensors, actuators, personal logic controllers, as well as a human machine interface.

It was determined that the control system should control the resonant mode and the weight on the bit as the primary two control variables. The sonic drill can also be controlled using feedback from sensors mounted on the sonic drill head, which is the driver for the sonic drill located above ground

CHAPTER 1

INTRODUCTION

Sonic Drilling Background

Using vibrations to penetrate the earth is not a new idea; driving piles to support structures has dated as far back as the Roman Empire. Penetration is accomplished through brute force; huge, heavy machines create cyclic, vertical vibrations at low frequency to overcome the earth's elastic resistance. Several companies have tried to create higher-frequency, higher horsepower vibration machines, only to have these forces destroy the machines.

The determination of Albert G. Bodine, Jr. led him to discover a method to not only generate high frequency vibrations with very high force output, but also have this machine resist destruction while passing the vibrations on to the object being resonated. In the thirty years since Bodine's original work, various companies and individuals have made incremental refinements of the technology, but the fundamental methodology remains a mystery to most and has received limited exposure in both literature and use in the field. At the time of Bodine's untimely death in 1990, he had received over 300 U.S. patents for his inventions and was world renowned for his pioneering work in "orboresonance." This work and body of knowledge has been acquired by Resodyn Corporation through an asset purchase. Resodyn Corporation holds the rights to all of the active Bodine patents in this area, as well as prototype equipment, development records and test results.

Today, there are only 3 major sonic drill companies worldwide. The major companies are Sonic Drill group, Boart Longyear, and SonicSampDrill (SSD). Sonic Drill group is based in British Columbia and was started by Ray Roussy. (1; 2; 3; 4) Ray Roussy worked under Hawker Siddeley, who Bodine was developing Sonic Drills for. When Hawker Siddeley decided to abandon their sonic drill technology Ray Roussy left and took his ideas about sonic drilling and started to make his own sonic drilling rigs. Boart Longyear has been developing sonic drills for over 15 years and has over 120 sonic rigs (5). Boart Longyear has traditionally kept their sonic drilling equipment in-house, but has recently begun to sell drill rigs and other equipment to third parties (5). Since 2006, Fons Eijkelkamp established a European manufacturing company for sonic drilling equipment, SSD.

Sonic drills are being utilized more in the mining industry, but are typically limited use in the creation of shallow wells, frequently for water, or to take very efficient samples of the underground strata. The sampling recovery rates by this method are commonly approaching 100% (5). In recent years, the technology has also proved well-suited for sampling of the following soil types: 1) heap-leach formations, 2) bauxite, 3) mineralized sands, 4) manganese, 5) uranium, 6) nickel laterites, 7) tailings, 8) coal spoils, and 9) disseminated gold (5). Because sonically drilled shallow holes are typically drilled much more rapidly than conventional drilling, it is becoming the method of choice for quick, shallow jobs. However, sonic drilling is often more expensive than traditional drilling per hour of operation because of the requirement for highly trained operators as well as the greater consequences of drilling with low experience operators.

These consequences typically come from the operator controlling the resonant system beyond its allowable stresses. In order for operators to attempt to control the resonance system within safe operating conditions, they have gained knowledge from experience and through the standard knowledge of sonic drilling portrayed in the following paragraphs.

The sonic drill is an advanced, hydraulically-driven system. Through the use of a sonic drill head, shown in Figure 1.1, a series of high-frequency, sinusoidal wave vibrations are imparted to a steel drill pipe to create a cutting action at the bit face. In its resonant condition, each energy pulse imparted to the drill pipe is exactly superimposed on each reflected energy pulse wave, Figure 1.2. In this condition, the direction and magnitude of movement of each molecule in relation to another stays the same, and creates a situation where the energy stored in the pipe can greatly exceed the energy being dissipated in the form of “work” on the medium being drilled.

In a non-resonating state (as occurs with traditional vibratory equipment), the energy waves are not superimposed in a reinforcing pattern and tend to cancel each other out as they move up and down the pipe. Consequently, the pipe is unable to utilize higher horsepower inputs from the drill head and the drilling rate is greatly reduced.

Presently, sonic drill rigs are operated primarily by “feel” and by “ear”. Although provided with numerous gages, successful sonic drilling is accomplished through the expertise of the operator; less practiced drillers do not perform well on sonic rigs. Drilling with resonance is unlike any other drilling method.

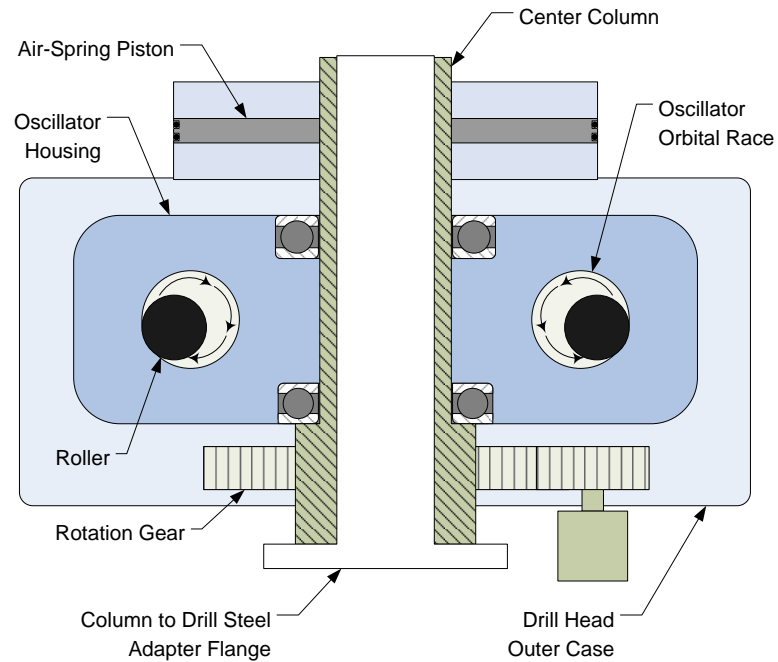


Figure 1.1. Sonic drill head. Picture provided courtesy of Resodyn Corporation.

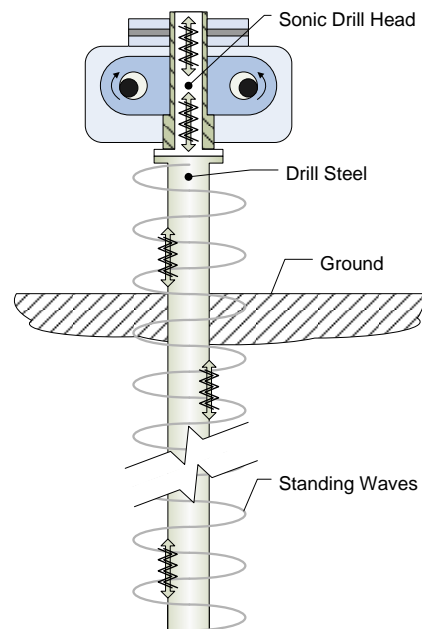


Figure 1.2. Resonant sonic drill diagram. Picture provided courtesy of Resodyn Corporation.

There are a number of factors working against the operator in maintaining resonance. A few of the factors commonly known by industry are given:

- As the length of the drill string increases, the friction on the pipe increases the damping of the system and decreases the energy delivered to the bit face. As shown in Figure 1.3, the resonant peak becomes less pronounced and more difficult to discern with increased damping.

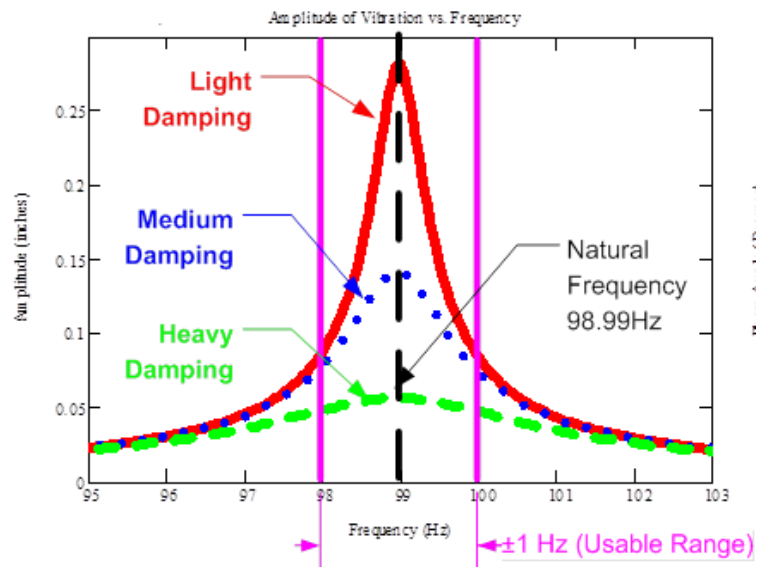


Figure 1.3. Resonant peak for drill steel.

- As the depth of the drill pipe increases, the number of different formations the pipe is exposed to increases. Each formation will act upon the drill pipe differently, thus creating a very complex and dynamic system. Under these circumstances, manually tuning the system frequency to yield maximum power efficiency becomes nearly impossible.
- At any moment in time, the formation surrounding the resonating drill pipe may dramatically change the system impedance due to underground formation

collapse, sloughing shale, or heaving sands. Over a longer period, swelling clay may act on the drill pipe to damp resonance.

- The manually-operated hydraulic systems currently in use in industry do not have the sensitivity necessary to accurately maintain resonance within 1 Hz. As shown in Figure 1.3, the resonant peak of the system is very steep; if the operator is just 1% off peak (1 Hz), the power delivered to the bit face drops by more than 60%. Typically, the sonic drill system tends to pass through resonance without the drilling knowing it.

Because the sonic drill is such a complex system, it is imperative to understand the function of each of the major system components prior to evaluating the complete system.

How Sonic Drilling Works

The sonic drilling system is comprised of three primary components: the sonic drill head, the resonator (in this case the steel drill pipe or drill rod), and the formation being drilled. All three interdependent components must work in harmony to allow the method to work effectively.

The Sonic Drill Head The sonic drill head, Figure 1.1, utilizes hydraulic power to create linear forces. By developing vertically oriented, mechanically-induced pressure waves, the sonic head can deliver forces ranging from 50,000 pounds to 280,000 pounds at frequencies approaching 150 Hz. The key to effectiveness of the sonic drilling method is efficient transfer of massive vibrational wave energy put into the top of the steel drill

pipe to the bottom bit, with very little power loss in the process. The linear forces are commonly generated by counter rotating rollers or eccentrics. The bottom bit does not cut, but pulverizes or bludgeons the rock into dust or moves dirt or clay to the side. Little optimization can be done with the bit other than using harder and more durable materials with tungsten carbide or other more durable materials. Ultimately, the rate of penetration is not how good the drill bit is, but how well the energy is transferred from the top of the drill string to the bit to perform drilling.

The Resonator The purpose of the sonic drill head is to impart as much force as needed to the top of the drill pipe and to have as much of that energy as possible transfer to the bottom of the drill pipe where it can do the most useful work in penetrating the formation. In the standing wave condition there are points of maximum movement and corresponding velocity called antinodes and points of minimum movement and corresponding velocity called nodes. The location of the nodes and antinodes are related to the length of the drill pipe, material properties of the pipe, and the frequency of the vibrational energy. The fundamental axial (movement in the length direction) resonance frequency of any length of drill pipe is determined by the following formula, Equation 1.1.

$$f_n = \frac{c}{2 \cdot l_{pipe}} \quad (1.1)$$

Where f_n is the natural frequency, in hertz (Hz), at which resonance occurs, c is the speed of sound for the media in feet per second, and l_{pipe} is the length of the pipe in feet. This formula defines the one-half wavelength resonance condition and is strictly

true only when the pipe is free at the top and bottom. Since the speed of sound through steel is approximately 16,500 feet per second, for a 100 foot length of any size or weight of drill steel, the natural frequency becomes 82.5 Hz as shown in Equation 1.2.

$$\frac{16,500 \text{ ft} \cdot \text{sec}^{-1}}{2 \cdot (100 \text{ ft})} = 82.5 \frac{\text{cycles}}{\text{sec}} \quad (1.2)$$

Assuming no other intervening variables, a 100 foot length of steel drill pipe will resonant when cyclic forces are imparted at a rate of 82.5 cycles per second. This fundamental one-half wavelength resonance condition creates a situation where a single node is located at the middle of the pipe length along with two antinodes, one at the top and one at the bottom. As drilling progresses and more sections of pipe are added, the frequency of energy input must change according to the formula in order to maintain the one-half wavelength condition.

As the steel drill pipe gets longer, a lower frequency of input energy is required to bring the drill string into resonance. The force generated by the sonic head is directly proportional to the square of the angular frequency ‘ ω ’. Hence as the length of pipe increases, the force exerted on the pipe is reduced dramatically. To address this problem, multiples of the natural frequency, called “overtones” may be utilized. Therefore, if a 100 foot length of steel pipe has a fundamental frequency of 82.5 cycles per second, doubling this frequency to 165 cycles per second produces the first overtone, or full wavelength resonant frequency. As the length of the drill pipe increases, adding multiples of the fundamental frequency yields the desired condition of resonance, keeping the antinodes near the top and bottom of the length of drill pipe. More importantly, however, is the fact that as drilling gets deeper, operating the sonic head at

higher frequencies produces the required increase in force output allowing continued penetration at greater depths.

Drilling with Sonics

The focus to this point has been on the sonic drill head and the effects that occur in the steel drill pipe as a result of coupling the two elements together. When the sonic drill head and the drill steel pipe are brought into a condition of resonance, the resonating drill steel literally “fluidizes” the surrounding soil within a quarter of an inch of the drill pipe wall, thus reducing the frictional forces that serve to constrain the pipe. (6) Because of aforementioned fluidization action, the industry preference is to use non-upset pipe (such as core rod) to keep loose material from sloughing onto the pipe. The loose material results in higher damping and restoring coupling effects along the length.

In loose sand and gravel formations, the drilling action of the resonating steel pipe is one of displacement wherein the elastic bonds of the particles are easily separated by the drill bit and the sand grains become re-arranged and move to the outside of the bit face. The more porous and saturated the formation, the more easily it accepts soil particles displaced from the bit.

Clay type soils present a larger challenge to sonic drilling. Due to their cohesive nature, clays do not displace as easily as sands and gravels. Consequently, a shearing type drilling action must occur at the bit face to effectively separate the elastic bonds of most clay formations. Clay is actually fluidized in a small circumferential area around the bit face and along the side wall providing the necessary liquefaction to inhibit the clay from aggressively bonding to the steel wall of the resonating drill. When the squeezing

actions of more cohesive clays against the drill pipe become severe, it becomes more difficult for the sonic energy to flow efficiently from the drill head to the bit face. As a result, when drilling in this type of lithology (7), the depth of the well is limited and earlier restriction to further penetration can be encountered.

The penetration of rock or consolidated formations with the sonic drill is accomplished by a fracturing action. Special bit designs containing tungsten carbide inserts to provide a durable surface for sonically fracturing rock formations. When drilling consolidated formations, however, a flushing medium, typically air or water, is often necessary to sweep away cut material and to maintain exposure of the bit to virgin material. It is also important to note, that rotation of the drill string is required so that the tungsten carbide inserts, also referred to as buttons, constantly impact virgin material. An example of drill bits with buttons is shown in Figure 1.4. If the drill pipe is not rotated, the inserts, which intensify the impact energy onto the rock, would hit the same spot fractured in the previous cycle, decreasing drilling efficiency. When drilling alluvial fans, it is not uncommon to encounter large boulders within sands, clays, and smaller gravels. If the boulder is small enough, the resonating drill bit will quite literally move the boulder aside as long as the formation is loose enough to accept it. However, if the boulder is of sufficient size or the surrounding formation is sufficiently dense, the bit must drill through the boulder. As shown in Figure 1.5, with the right bit the sonic drilling system can penetrate large boulders.

Because of complex resonance conditions and ever changing drilling material properties it is necessary to have a model of how the drill is going to respond at given

situations. Once a model has been developed and verified, it can then be used as the foundation of control algorithms that will be implemented into an automated control system.

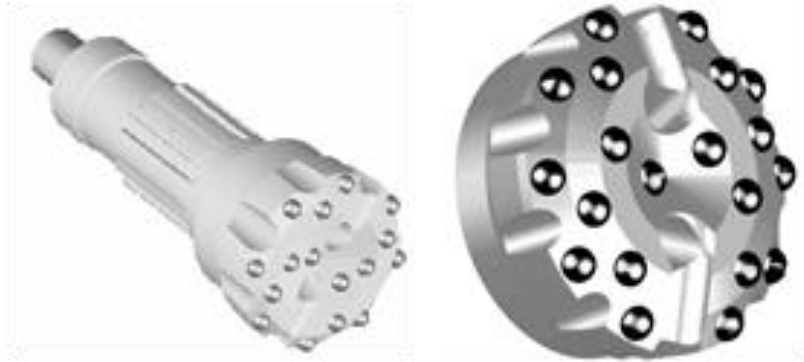


Figure 1.4. Drill bits with buttons. (8)

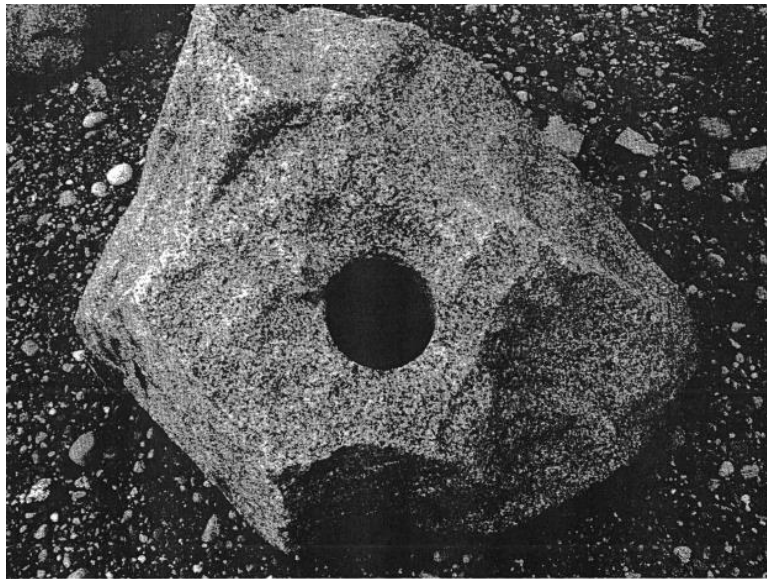


Figure 1.5. Sonic drilled four inch hole through a granite bolder.

Sonic Drilling Modeling

Modeling was first performed by Mr. Albert Bodine Jr. and his models are well documented in numerous patents and a select few are referenced here (9; 10; 11; 12; 13; 14; 15; 16; 17). Albert Bodine derived his models from the textbook titled “Sonics”, by Hueter and Bolt (18). Using the methods outlined in the second chapter of the book “Sonics”, the mechanical system is modeled using an electrical analog. The electrical analog relates the acoustically vibrating circuit to an equivalent oscillating electrical circuit. When using this type of analog, the mechanical system variables must have an equivalent circuit representation. The mechanical to electrical variables are outlined in Table 1.1.

Table 1.1. Relation of the electrical analog variables with the corresponding mechanical variables.

Mechanical Variable	Mechanical Variable Symbol	Electrical Variable	Electrical Variable Symbol
Force	F	Voltage	V
Velocity	v	Current	i
Mechanical Compliance	C_m	Capacitance	C_e
Mass	M	Inductance	L
Resistance ‘Friction’	R_m	Resistance	R
Impedance	Z_m	Impedance	Z_e

The model is based off of the assumption that a member is elastically vibrated along the length of the drill pipe by means of an acoustical sinusoidal forcing function. The model he developed neglected all the other resonant modes such as flexure, torsion, and breathing as well as the boundary conditions of the sonic drill. The damping and restoring forces along the length of the drill string were incorporated in the ‘ R_m ’ and ‘ C_m ’ terms in Equation 1.3. As is presented later in this body of work, these neglected salient features of the system should not have been omitted in Bodine’s model. No mention in the Bodine’s patents why the longitudinal direction of the sonic drill was considered, while the other sonic drill degrees of freedom where ignored. Bodine stated that the model relation was the equation shown in Equation 1.3.

$$Z_m = R_m + j(\omega M - 1/\omega C_m) = F_o \sin(\omega t / tv) \quad (1.3)$$

When the system is on mechanical resonance, the term ‘ $\omega \cdot M$ ’ is equal to ‘ $1/\omega \cdot C_m$.’ This shows that the forces from the masses are directly offset by the forces of the compliance (spring forces). When a resonant state occurs, the kinetic energy of the mass is directly transferred into potential energy in the compliance member and vice versa, which allows any further input energy to go directly to damping of the system and not to drive the mechanical system. Therefore, the mechanical impedance ‘ Z_m ’ is equal to the mechanical resistance ‘ R_m ’. Under this condition, the vibration velocity amplitude ‘ v ’ is maximized, the power factor is one, and the energy is more efficiently delivered to a load to which the resonant system may be coupled (drilling).

The sonic drill is described to have a “lock-in” attribute that allows the system to essentially lock in to the resonant frequency. The “lock-in” phenomenon will be explained further in the modeling section, below.

Bodine claimed that the sonic resonant system needed to have a high acoustic “Q” to increase the efficiency of the vibration which would lead to the maximum amount of power. The “Q” as was defined by Bodine as “the sharpness of resonance thereof and is indicative of the ratio of the energy stored in each vibration cycle to the energy used in each such cycle” (9). The “Q” is also mathematically equal to the ratio of ωM to R . He also noted that the total effective resistance, mass, and compliance in the acoustically vibrating system are represented in Equation 1.3 and that these parameters are typically distributed throughout the system rather than being lumped at a single location. By using this type of model, an overall representation is given, but it doesn’t provide the operator any indication if the drill is behaving differently at the drill head than anticipated.

In an attempt to give the operator a little more feel and understanding of what may be happening to the drill while drilling, a different modeling approach was applied by discretizing the drill and string, as opposed to the lumped parameter approach. The new models were developed by SoniCo, Incorporated, which was a subsidiary of the Shell Oil Company. The research was published by W. C. Rockefeller in The American Society of Mechanical Engineers (ASME) publication (19). Rockefeller continued to build on Bodine’s models of impedance and the ‘Q’ of the system. The ‘Q’ is defined as a dimensionless ratio of the energy stored by the resonant system to the energy dissipated over one cycle. Rockefeller showed that the mass in a vibratory system with a high “Q”

The pipe spring constants 'k_j' were derived to give the correct mode shapes for the analysis. The spring constant 'k_j' is derived from Equation 1.5.

$$k_j = \frac{E w_p}{\gamma_p L_p} (N - 1) e(N) \quad (1.5)$$

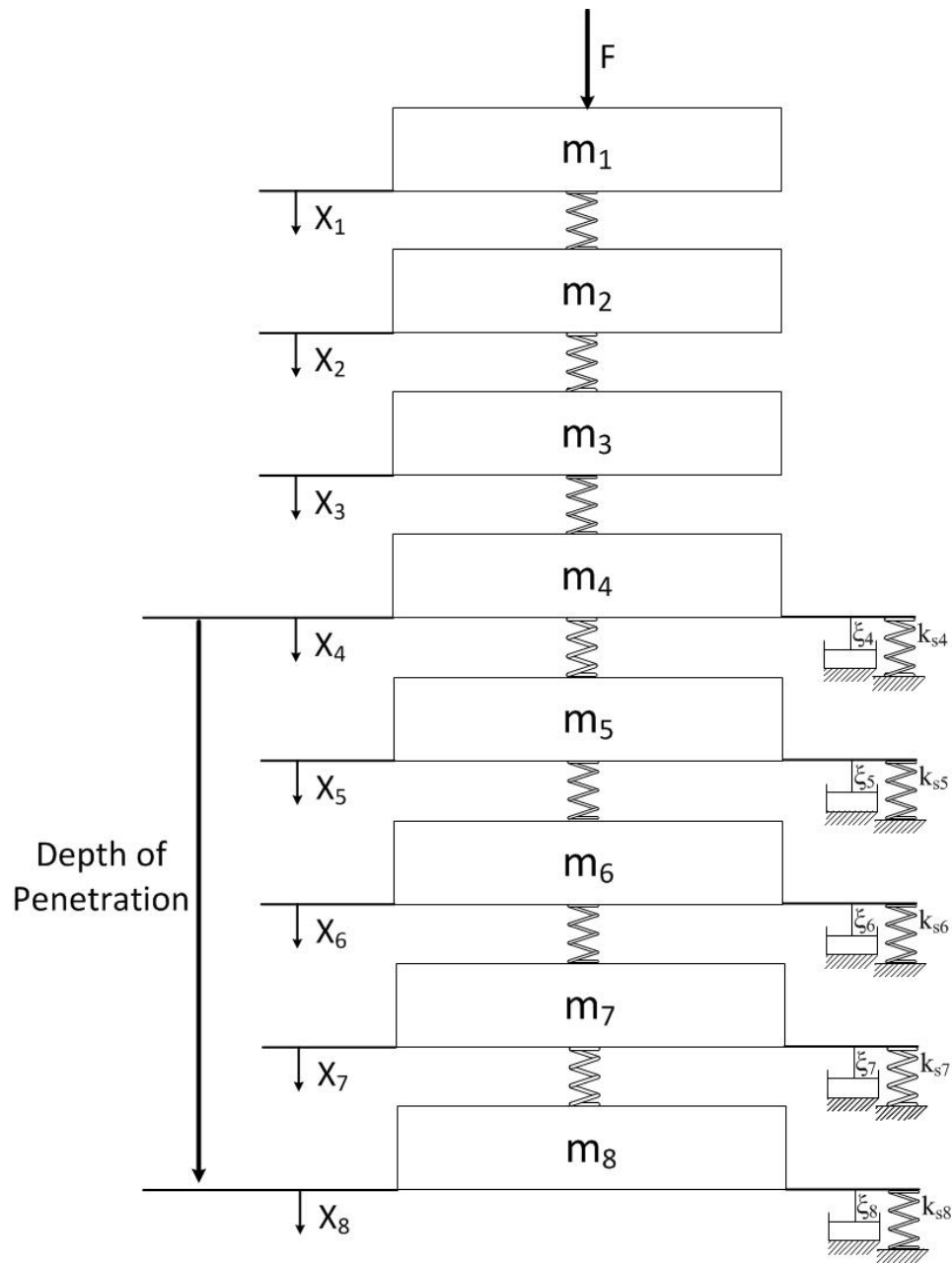


Figure 1.6. Dynamic representation of the pile and driver pile to soil system.

Where 'E' is the pipe elastic constant, ' γ_p ' is the pipe specific weight, ' w_p ' is the piles weight per unit length, ' L_p ' is the length of the pile, and $e(N)$ is a correction factor given by equation 1.6.

$$e(N) = \frac{\pi^2}{N(N-1)} \frac{\gamma_p}{\omega^2} \quad (1.6)$$

The damping and spring values for the soil were bounded to $10^3 \leq \xi_j \leq 10^6$ slugs/sec and $0 \leq k_{sj} \leq k_j$ lb/ft. The model was run with realistic loads and input force functions of the tested sonic drill. The model predictions are plotted with two data point in Figure 1.7 in the paper published in 1967 (19) which were recorded at a drill depth of 5 ft, labeled points 'A' and 'B'.

Point 'A' is when the drill was penetrating, 310 hp, and point 'B', 540 hp, is when the drill was taking a great deal of energy but exhibited no penetration. The model had good correlation with point 'A', but under no conditions would the model correlate with point 'B'. Mr. Rockefeller stated, "Obviously, increased damping values should be tried to gain better agreement". Systems with higher 'Q' have more energy than is able to be input and transferred in the system, therefore, his system must have had a higher 'Q' when it exhibited no penetration. In order to achieve a higher 'Q', the end bit would have to have become coupled to the bottom, to create a fixed joint that will act as a reflection of all the acoustic energy. But with the method of breaking the system into discrete masses, if the bottom mass suddenly became fused, the model would predict the correct resonant condition with the end as a node. When a fused condition occurs, the drill bit amplitude approaches zero, but the small motion still generated heat due to friction. The reduced displacement causes the bit to heat up because less of the heat can be dissipated

through the strata or by the flushing fluid moving the dislodged strata away from the bit. However, Rockefeller was assuming he was just far away from a primary mode while still having the same mode shape. Therefore, Rockefeller did not predict that the reflected end condition would result in a separate resonant mode with his model, which would not occur unless the reflected wave force was sufficient to displace or fracture the rock in pure compression.

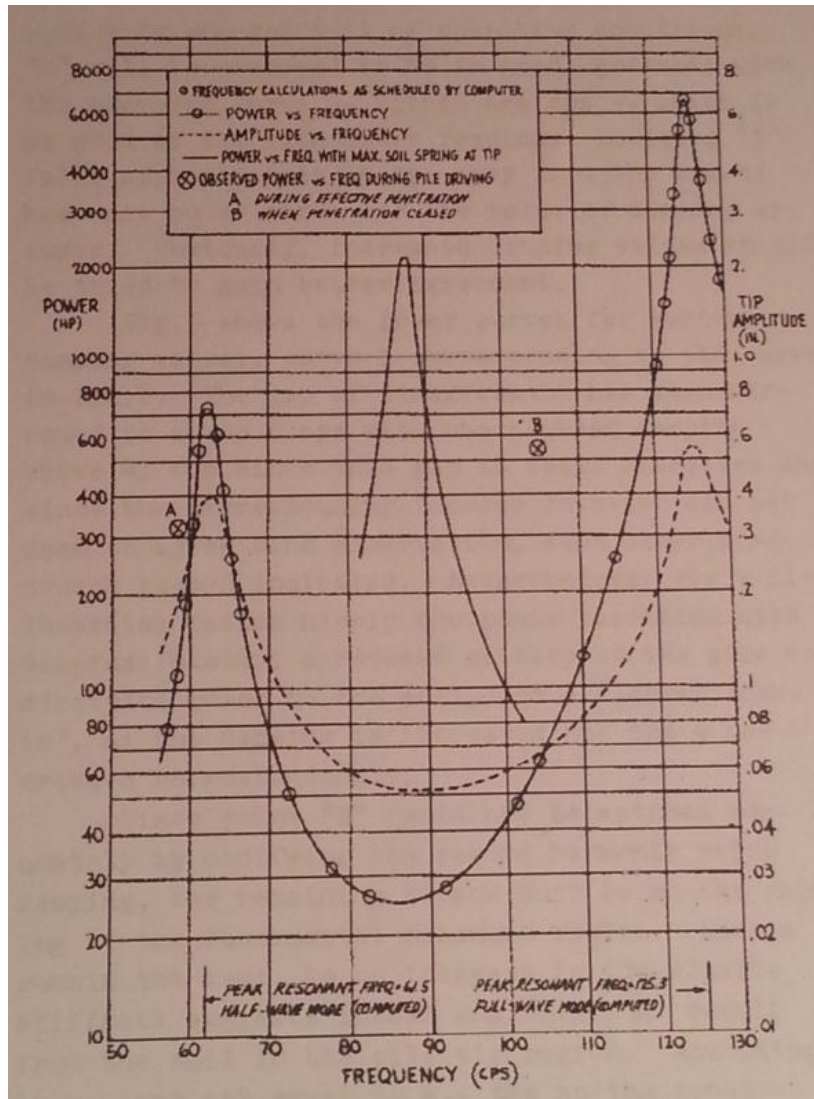


Figure 1.7. Power and tip amplitude versus frequency, computer curves -example. (19)

Rockefeller accounted the lack of drilling to high soil elastic “clamping”. Rockefeller’s team applied more lift on to the cable holding the sonic drill up and the driving point “A” was again achieved. They didn’t know how to account for this, but by applying boundary conditions to their model, this condition can be well defined and represented. However, by modeling the continuous system in all direction, taking into account the boundary conditions, and by including his drill operating parameters in the model, he would have been able to more accurately model the sonic drill system and explain his empirical results. Using Rockefeller’s own model, his value that was claimed to have good correlation indicates that it was off of resonance, but with further investigation and use of a more accurate model it was in fact on resonance, however the end conditions changed the mode shape and frequency of the resonant condition. Rockefeller did notice that down force did change the condition between penetration and not penetrating, but through more accurate models this is verified and quantified.

More accurate models may have been developed, but they have been developed by industry under private funding and have not been published since the work by Rockefeller. However, some modeling was performed under a Cooperative Research and Development Agreement (CRADA) between Water Development Hanford Corporation, and the U.S. Department of Energy. The scope of the work was to use a commercial finite-element structural code called ANSYS[®] to perform the dynamic analysis of Water Development’s ResonantSonic[®] Drill and evaluate instrumentation options for the drilling system. Some earlier work was described in a preliminary report (20) that described that a drill rig was instrumented to aid the operators and provide data to refine a

drilling simulator developed by the Colorado School of Mines. However, the instrumented rig was Water Development Hanford's rig #114 (150/300 series ResonantSonic[®] drill), which was used for routine use at Hanford. The test data included data from an instrumentation system that contained commercial transducers and signal conditions of reasonable quality. The collected data was reduced and curves were plotted, but the significance of the data was not apparent or reported.

Testing under the CRADA between Water Development Hanford and the DOE continued with the modeling effort lead by the Engineering Mechanics Group of the Department of Energy's Pacific Northwest National Laboratory (PNNL). Variables that were measured during tests were: 1) Drill String load, 2) Oscillator Head Acceleration, 3) Oscillator Head Displacement, 4) Oscillatory Head Velocity, 5) Differential Hydraulic Pressure Across the Oscillator drive motor, 6) Oscillatory Head Frequency, and 7) Acoustic Sensor response (Microphone). Through testing, it was discovered that the accelerometer and the load cell were the only transducers that produced any significant information. This is surprising, because the sonic drill operators rely on feel and sound feedback from the sonic drill, so it was expected that the sound would have some relevance.

Modeling effort using ANSYS[®] was also performed by PNNL, but unfortunately the data is not available in the report. However, through phone conversations and personal meetings (21) with Water Development President, Jeffrey Barrow, that "no definitive data" to base a control system on or accurate mathematical modeling came out of this project. It was concluded, however, that the load cell data could be used to

determine operation regimes that would be damaging to the drill string or other equipment, if it was coupled to an accurate computer model.

However, renewed research is being performed by Farid Arvani at Memorial University of Newfoundland in St. John's, Canada. He is the project manager for the Advanced Exploration Drilling Technology group at Memorial University. Through a phone interview with Farid; he and his group are performing research on sonic drills, but have yet to publish any of their research (22).

Similar models for sonic drilling have been developed for low frequency sonic (typically <30Hz), for exciting and retrieving stuck liners, tubing, casing, and drill pipe. Dr. Gonzalez published the modeling of the use of a sonic drill head to free stuck liners, tubing, casing, and drill pipe down holes (23). By 1980, low frequency sonic drill heads freed 50 of 81 stuck liners, 3 of 16 stuck tubing, and *one of four* drill pipes. From 1983-1987, there were 73 successes out of 125 attempts from as little as 67 feet to over 8500 feet stuck lengths. In the work by Dr. Gonzalez, he specifies that acoustic measurements have been measured at a depth of 11,000 feet, and the deepest stuck pipe retrieved was up to 9,000 feet. These impedance models were derivatives of the equations outlined by Rockefeller (19), and he went further to show what a model would look like for a stuck drill pipe with casing. The following research builds on Dr. Gonzalez's mechanical impedance models as well as outlines the shortcomings of the low frequency oscillations. Some of the short comings are the lack of power using low frequencies and the time to build the resonant oscillations. In order to address these shortcomings, higher frequency

vibrations are utilized to build the resonant condition more quickly and harness more available power using the same input force amplitude.

Motivation for Continued Research in Sonic Drilling

The Department of Energy first sent out a call from proposals under a small business innovative research solicitation fall of 2005. Under the solicitation, it called for a method for exploration and development of new energy resources in remote and environmentally sensitive areas. The Department of Energy particularly expressed a need for a way to reduce the size of the associated equipment and operations currently used in remote and environmentally sensitive areas. Microhole technology can significantly reduce the drilling operation size and cost of well construction; however microhole technology that could meet this call, at the time, were all very large and not very mobile. The ultimate goal of the Department of Energy small business innovative research (SBIR) project is to provide reliable, small footprint instrumentation deployment systems that can operate at lower cost and in environmentally sensitive areas not accessible to conventional drilling systems. Thus, sonic drilling was chosen for investigation to determine if it could meet the above requirements.

The sonic drilling method has the potential to be a highly effective method for placing microhole wells in environmentally sensitive areas. In most unconsolidated formations it operates without mud, air, or other circulating medium, and produces no excess cuttings. In consolidated formations, a significantly reduced amount of drilling fluid is required to remove cuttings from the bit face. The method has achieved high

rates of penetration and can easily drill at any angle through formations of rock, clay, sand, boulders, permafrost, or glacial till.

Although sonic drilling has advantages over conventional drilling in many applications, its primary use has been limited to the environmental drilling industry. In addition to being a comparatively new drilling method, the inability of sonic drilling to penetrate depths greater than 500 - 1000 feet has been a substantial barrier to broader industry acceptance. The principal reason for its restricted depth is that it is difficult for the operator to manually keep the drill string in resonance as it penetrates through various formations. Thus, another primary goal of Department of Energy SBIR research was to prove that with automated control to keep the drill string on resonance, the sonic drill would be able to infiltrate the earth with a microhole sized string to depths of 1500 feet.

Background of Microhole Drilling

Microhole technology refers to the size of the bore hole involved, typically 2-3/8 inches in diameter and smaller (the surface casing is only 4-1/2 inches). Within the drilling industry, the term microhole drilling is often synonymous with coiled-tubing drilling. This was an unfortunate result of the Department of Energy Microhole Program being de-funded by DOE/NETL when only part way through. The actual focus of the program was "Systems Approach" for encouraging the use of purpose build rigs. Tom Gipson's CT rig commercialized 1 trillion cubic feet of Niobrara shallow tight gas. However, industry had been drilling through this area for decades because drilling cost prevented it from being commercialized. Sonic drilling was the perfect "system" for drilling seismic holes because it represented an even greater step reduction in drilling cost

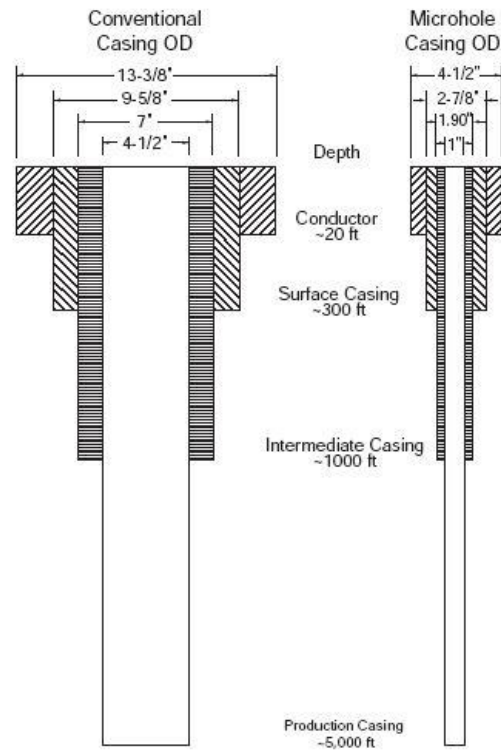
and system complexity. However, coiled-tubing rigs have traditionally been used primarily in well intervention activities including cleaning up or initiating flow in existing well bores, and within the last two decades their use in drilling all sizes of boreholes has dramatically increased in the lower 48 United States as their cost effectiveness has been demonstrated enough to offset the false economics previously associated with their higher day-rate. This is primarily due to the advent of stronger tubing, better bottom-hole assemblies (BHA), and other advancements in the technology (24).

Irrespective of the equipment used to drill the microholes, a significant advantage to microhole drilling development and increased use is in the reduced size and cost of the casing, as shown in Figure 1.8. The smaller size of the casing and associated drill strings further justifies sonic drilling for placement of microholes. In many instances, the depth of the sonic-drilled bore was limited solely by the lift capacity of the drill head if the sonic drill maximum depth was not impeded by the operator's inability to keep the drill on resonance. The smaller-sized pipe allows the use of current sonic heads to drive longer lengths of pipe to greater depths.

Anticipated Public Benefits

Geophysicists are continually exploring a means to reduce costs associated with the deployment of seismic instrumentation. Seismic instrumentation in the subsurface yields many benefits including reduced noise, reduced travel paths, and greatly improved signal-to-noise ratios. The use of conventional well construction is too expensive for monitoring alone, and production wells are generally too noisy for gathering quality data.

The development of an environmentally-friendly microhole drilling system capable of being deployed to remote locations will be of a great benefit to geophysical exploration. The use of microholes in exploration efforts can improve conventional reflection surveying, locating sources of natural seismicity, vertical seismic profiling (VSP), and cross-well imaging capabilities.



Conventional			Microhole		
OD (in.)	Cost (\$)	Casing Weight (lbs)	OD (in.)	Cost (\$)	Casing Weight (lbs)
13-3/8	763	1,090	4-1/2	147	210
9-5/8	6,783	9,690	2-7/8	1,754	2,505
7	16,100	23,000	1.90	2,030	2,900
4-1/2	36,750	52,500	1	4,750	4,250
Total	60,396	86,280	Total	8,681	9,865

Figure 1.8. Well construction for geophone deployment. (25)

Carbon-Sequestration

Another likely application for inexpensive microhole well monitoring is in the implementation and management of carbon-sequestration. Microhole wells could be used for monitoring the carbon injection and long-term storage of CO₂ in depleted reservoirs. In the short term, this will support efforts for enhanced oil recovery (EOR) and eventually sequestration as a possible national policy solution in response to global warming. In a recent economic analysis performed for the National Energy Technology Laboratory, two cases for carbon sequestration combined with oil recovery were considered (24). As shown in Table 1.2, the results suggest that if CO₂ sequestration is pursued by the U.S., nearly 12,700 million tons of CO₂ would be sequestered, 26,000 million barrels of incremental oil reserves would be recovered, and thousands of monitoring wells would be required.

The cost of the monitoring wells may be one of the greater barriers to a more widespread use of VSP for implementation of CO₂ in increased oil recovery (IOR). To properly monitor the movement of the CO₂ and oil bank within a reservoir, between three and five surveys are required, each costing \$400,000 (24). Reducing the construction cost of the monitoring well will make VSP more affordable for IOR projects and help it become the monitoring tool of choice for sequestration.

Coalbed Methane Basins (CBM)

At least 25 native Alaskan communities have been identified as potential sites for coalbed methane production as an alternative to paying for diesel-generated, state-subsidized electricity at rates that are three to ten times greater than the national average

(26). According to economic studies (27), the current high costs associated with site preparation, transportation of equipment, rig mobilization, and operating costs only present a marginal economic case for developing CBM at remote Alaskan locations. It is estimated that nearly 250,000 lbs of drilling, well-completion, and logging equipment is required for exploration at any given Alaskan site (28). Developing a less costly and environmentally benign drilling system will enable greater exploration, characterization, and development of these natural resources for economic benefits.

Table 1.2. Summary of results from CO₂/EOR analysis.

	Case 1	Case 2
Total # of Fields	290	780
Estimated # Monitoring Wells	7,250	19,500
CO ₂ Sequestered, Million Tons	4,686	12,658
Total Oil Recovered, Million bbls	9,763	26,370

Market Potential

The market for sonic drilling equipment has grown ten-fold over the past decade. Further growth in the broader drilling industry is plausible if an automated control system is developed that works. In addition, new technologies such as carbon fiber drill pipe with “purpose designed” Young’s Moduli could potentially allow more effective deep drilling systems using more “sonically efficient” combination drill strings. This represents the newest frontier for complex sonic drill modeling such as developed in this body of work.

Research Direction

The first chapter outlined the available information about sonic drilling in peer reviewed literature as well as marketing information from various private companies. Chapter 2 provides definitions of the sonic drill variables, by providing a review and summary of current knowledge with rules of thumb. The modeling, Chapter 3, included background of how a sonic drill system is similar to a single degree of freedom spring-mass-damper system. The same tools used to analyze a single degree of freedom model were also used to analyze the sonic drill system. Governing differential equations of motion for the sonic drill were derived from both force balance and energy balance. Closed form boundary condition solutions and numerical solutions using finite element models were used to solve for the system dynamics. The assumptions for each model were provided. Chapter 4 describes the design of experiments that was used to determine the sensitivity of the sonic drill variables which include: 1) sonic drill head mass, 2) sonic drill head spring rate, 3) sonic drill bit spring rate, 4) sonic drill bit mass, 5) resonant mode, 6) strata types, 7) sonic drill bit damping, and 8) sonic drill length.

The results for the design of experiments are described in Chapter 5. Chapter 6 describes the sonic drill experimentation and testing. The variables that are used for the control system are described in Chapter 7. The control system, which is patent pending, primarily for Resonant Sonic Drilling and other applications that utilize the control methodologies were described in Chapter 8. Chapter 9 summarizes the conclusions for the body of work, while Chapter 10 outlines the future work.

CHAPTER 2

SONIC DRILL VARIABLES OF INFLUENCE

Introduction

Sonic drills are a resonant system, and are one of the few mechanical systems designed to operate on mechanical resonance. Engineers are typically taught that mechanical resonance is a phenomenon to avoid. However, resonant systems offers two unique advantages. The first advantage is the ability of transferring energy without expending much energy in the mechanical system itself and the second advantage is the ability to store great amounts of energy in the mechanical system, which allows for higher amplitudes. Because of these unique attributes, the sonic drill is able to transfer mechanical energy generated and input at the top of the drill string by an oscillator called a sonic drill head, which is located above the surface of the earth, and then transmit the mechanical energy efficiently to the drill bit to perform drilling. A resonant system is said to be on resonance when the input power is being directly transferred to the damping of the system, while expending little to no energy within the mechanical system itself. This phenomenon occurs at particular frequencies where the ability of the system to store kinetic energy is directly matched with its ability to store potential energy. As the system oscillates, the potential and kinetic energies are transferred back and forth between the two energy types. An example of the resonant condition is displayed in Figure 2.1, where in the resonant frequency is located where the velocity amplitude is maximized and the input power is minimized.

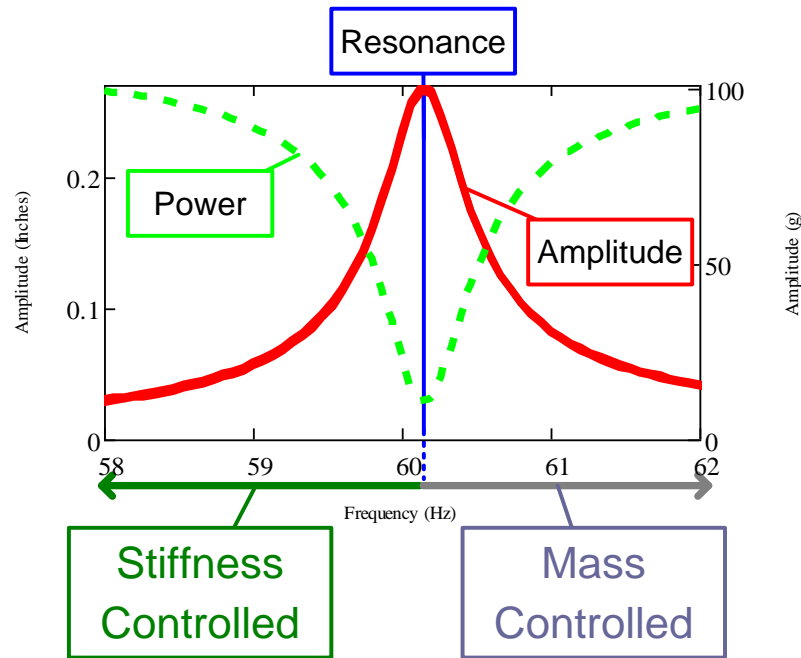


Figure 2.1. Resonance condition

The resonant condition allows for the additional energy to flow through the system without being absorbed as either potential or kinetic energy during the mechanical oscillations of the system. As the system grows in amplitude on mechanical resonance the total energy stored in the system as potential or kinetic energy increases. In fact, on mechanical resonance, the total energy stored as either potential or kinetic energy in the system is constant, Figure 2.2a. If the system is being operated below mechanical resonance additional power must to be added to the system to continually charge the potential energy, because the system can store more potential energy than kinetic energy for a given oscillation amplitude, Figure 2.2b. In other words: the oscillator has to add additional energy to drive the system which is used to continually charge the potential energy of the system, because the system cannot store enough of the potential energy in the form of kinetic energy, which would then be transferred back to potential energy later

on in the oscillation cycle. When the potential and kinetic energies are not matched, the oscillator must continually put additional energy in to the system to sustain the desired oscillatory amplitude, Figure 2.2b.

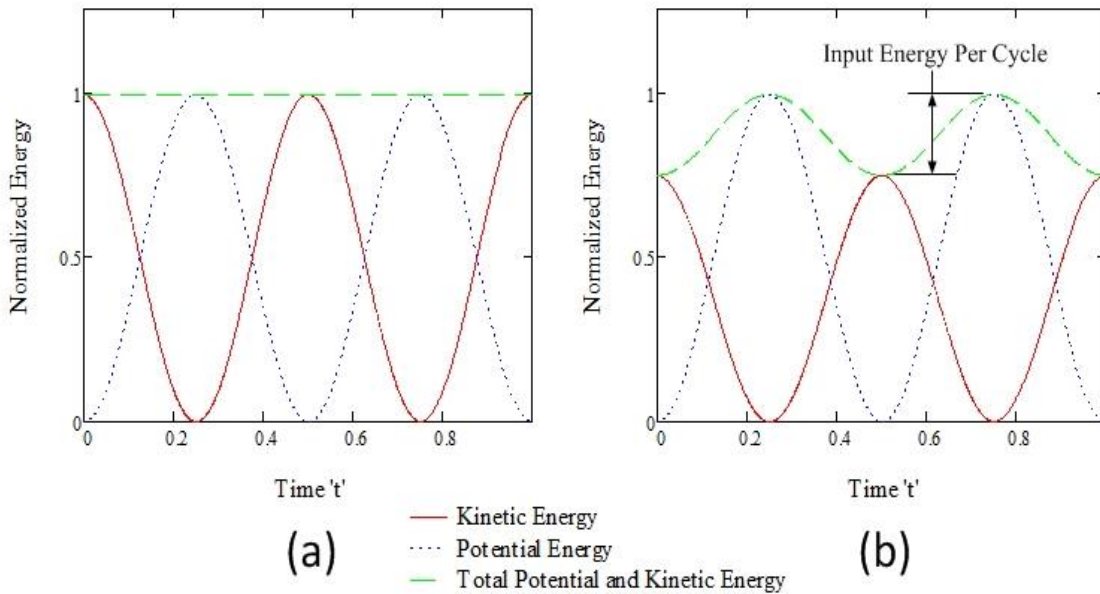


Figure 2.2. Potential and kinetic energy plotted over two oscillation cycles for a system on mechanical resonance (a) and one that is operating at a frequency lower than that of mechanical resonance (b).

Similarly, at frequencies above mechanical resonance more energy must be input into the system because not enough potential energy can be stored to recharge the kinetic energy that is required to oscillate the system. When on mechanical resonance, the system will charge up to a maximum energy stored as potential or kinetic energy so that the energy flowing into the system is passed through and absorbed by the damper. When the system is charging, it is referred to as when the input energy is being stored as kinetic or potential energy as the system is growing in oscillatory amplitude. A high-level

schematic of the sonic drill system displaying the driver, potential and kinetic energy storage reservoir, and the load/damper is displayed in Figure 2.3.

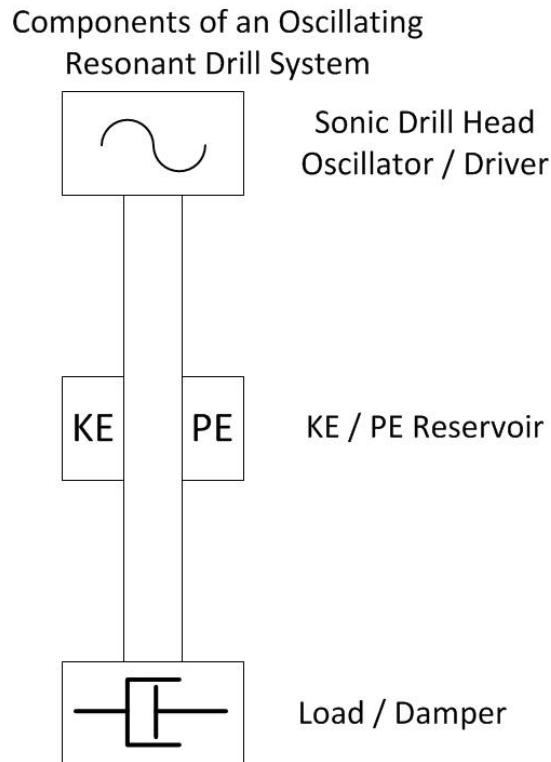


Figure 2.3. High-level schematic of the sonic drill.

If the damper cannot absorb all the energy going into the system, then the system oscillation amplitude will continue to grow until the system fails. Failures in the sonic drilling system have been as common as overstressing the joints that tie the drill pipe together as well as over stressing the sonic drill driver by applying excessive acceleration at the drill head. However, the resonant condition can also help the operator, usually, by what is called ‘lock-in’ frequency. Operators typically operate the sonic drill by increasing the driving frequency until the system starts increasing frequency by itself, due to the lower power required to operate on mechanical resonance. Once the resonant

frequency is reached, much more power is required to drive it to even higher frequencies and move through the resonant condition, so the system will automatically “lock-in”, and operate on mechanical resonance. However, later in this work, it describes how the “lock-in” does not work to ensure the system is operating on mechanical resonance with efficient energy transfer to the drill bit to perform drilling.

To prevent the system from failing, an understanding of the mechanical resonant system is needed. The system can be broken down into 13 major components, which are: 1) Penetration Rate, 2) Weight on Bit, 3) Input Force Frequency, 4) Input Force, 5) Speed of Rotation, 6) Flush Fluid Flow, 7) Mass of Sonic Head, 8) Mass of Drill Bit, 9) Air Spring Rate at Sonic Head, 10) Damping along the Length of String, 11) Damping at the Drill Bit, 12) Sonic Driver Damping, and 13) Stored Energy along the Length of the Drill String. Sonic drills are currently operated by operator feel and experience. A picture showing the typical control panel for a sonic drill rig is displayed in Figure 2.4.

The research presented here could serve as rules of thumb for sonic drill operators, but in many cases a drilling operator cannot react as fast as required necessitating an automated control system. A disconnect exists between the current control variables and the system variables that affect drilling. The above sections listed the system variables and the control variables, the definitions of each and the reasons why they are important will now be discussed.



Figure 2.4. Sonic drill control center.

Penetration Rate

The penetration rate is defined as the net distance of drill bit travel into the earth per unit time. In drilling, the penetration rate is a critical performance indicator that determines how long the drill rig and team will be engaged in a particular job. With increased duration of the drilling operation more money is being spent on the project, eroding profit. One of the goals of this research is to identify the importance of the other variables listed and determine methods to adjust these independent variables to maximize the dependent variable 'Penetration Rate', while still operating the sonic drill in safe conditions. Needless to say, the penetration rate is the most important variable, as it is the variable the drilling industry wants to maximize without added costs.

Weight on Bit

Weight on bit is defined as the static force that is applied onto the drill string at the drill rig. Some companies actually define this value as force of the drill rig and the weight of the drill string and bit. The weight on the bit is very important for rotary drilling, because weight has to be applied to ensure the drill bit is engaged and is able to shear and break the rock formations. However, in sonic drilling if too much force is applied, the drill bit can become essentially fused to the bottom of the hole and the resonant condition will change from free – free to fixed – free. If this occurs, the sonic drill resonant frequency will change due to the lack of relative motion of the drill bit. When a lack of relative motion occurs to the drill bit, essentially turns into a 'node', the bit will have reduced penetration of the earth even when the drill system is operated on

mechanical resonance. In this condition, little to no damping is occurring at the drill bit, and the probability of mechanical breakage increases significantly.

Input Force Frequency

The input force frequency is a key operating parameter and primary point of tuning for a mechanical resonant system. As discussed earlier, in order to transfer energy efficiently the frequency must be such that the kinetic and potential energies in the system have equal magnitudes and are allowed to transfer energy freely between each other. In many sonic drills the input force frequency is generated by the speed of the rotating eccentric masses. Sonic drills typically operate in the frequency range of 60 Hz to 200 Hz. This is because at low frequencies, the eccentric masses generate little force, as the force is directly related to the square of the angular frequency. In addition, the frequency range of the drill should be such that the next higher axial resonant frequency of the sonic drill is reachable while the current mode is still within the operational range on the low end of the frequency spectrum.

Input Force

The input force is typically fixed, as it is dependent on the size of the eccentrics and on the square of the angular frequency. As more force is generated at higher oscillation speeds it is typically better to operate at the highest axial resonance mode available for drilling. Depending on the down-hole conditions, sometimes it may be beneficial to operate at a lower mode, thus sacrificing some input force and ultimately power to gain efficiency of the energy going to the drill bit. Examples of these

conditions are swelling clays or high damping regions at anti-node locations of the higher frequency: when the lower frequency mode is excited, the anti-node location shifts and the damping at that particular location is absorbing less energy and allowing more energy to be transferred to the drill bit.

Speed of Rotation

The speed of rotation helps in two respects: the first is the radial orientation of the impact of the drill bit changes over time, but it also allows for movement along the drill string that lowers the axial friction, damping, along its length.

The speed of rotation is important on hard rock and strata that isn't easily displaced into itself. Ideally, the speed of rotation would be high enough to rotate the bit buttons to impact virgin material each oscillation. The button location and rotation needed to impact virgin material is displayed in Figure 2.5, wherein the bottom of a drill bit with a single button is displayed.

Based on the size of the drill diameter, button placement, and the oscillation frequency (nominally between 60 Hz and 200 Hz) the optimum rate of rotation may be hard to achieve. A typical size for drilling buttons is 0.25". The angle of rotation for various buttons at different radii on a drill bit can be calculated with Equation 2.1, where d_{but} is the diameter of the button and r_b bit button location radius. The angle of rotation for a 0.25" diameter button to impact virgin material is plotted in Figure 2.6.

$$Rotation\ angle = \frac{d_{but}}{2\pi r_b} 360\ degrees \quad (2.1)$$

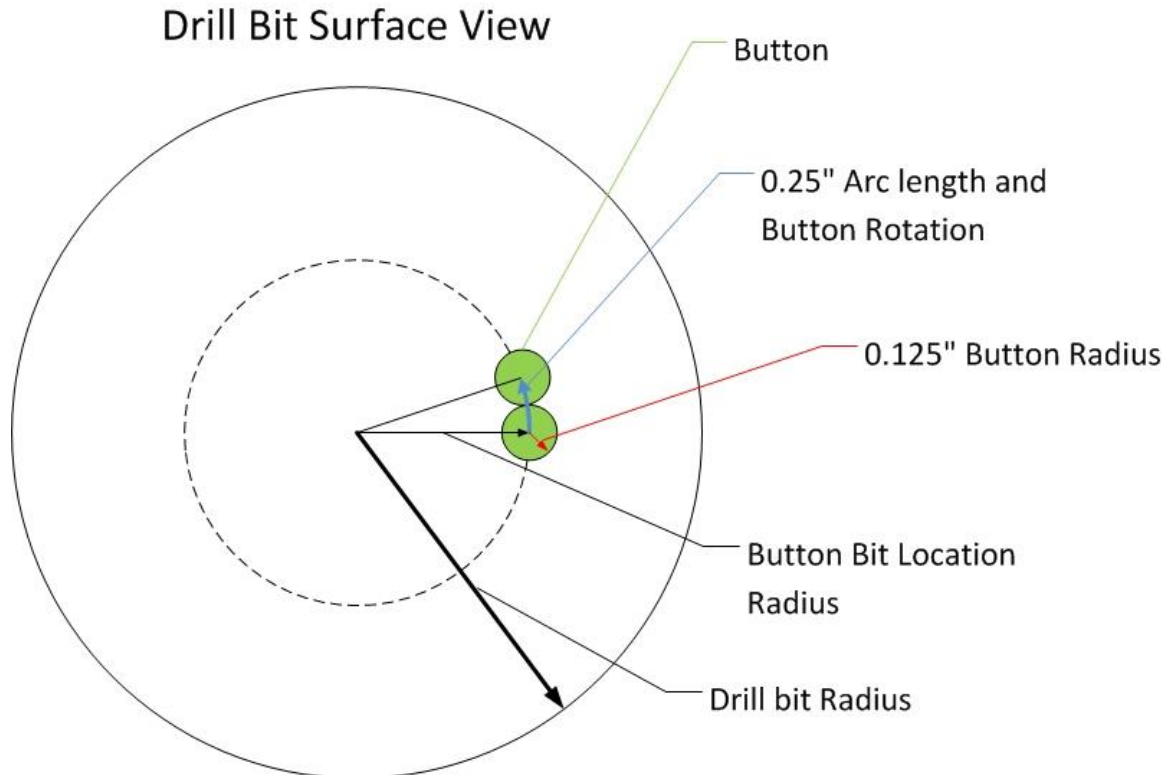


Figure 2.5. Button location and rotation to impact virgin material.

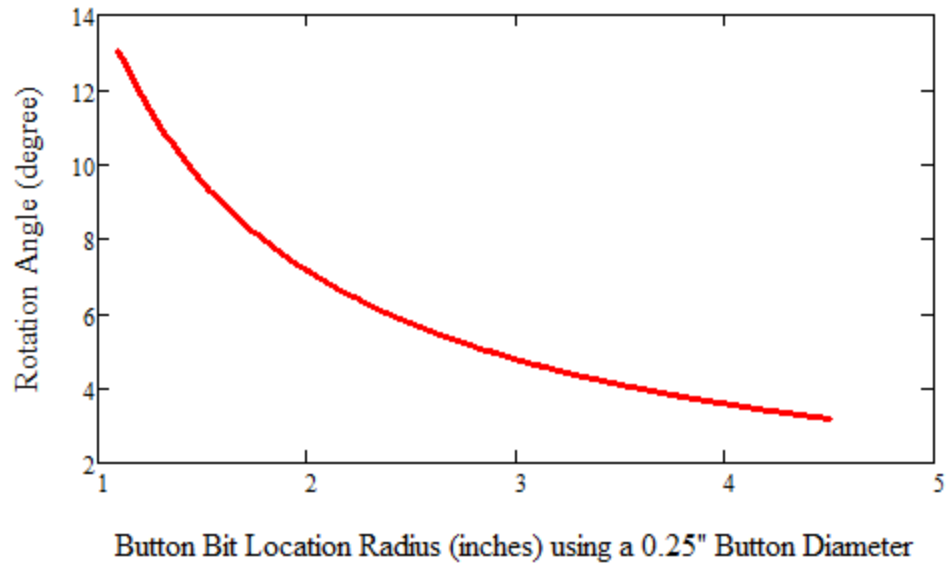


Figure 2.6. Rotational angle for a 0.25" button to impact virgin material at various button radii.

The minimum rotational frequency for buttons to impact virgin material at various sonic drilling speed of rotation are shown in Figure 2.7. The four operational frequencies given in Figure 2.7 where chosen because 120 Hz, 150 Hz, and 200 Hz are typical maximum frequencies for the different types of sonic drills in industry. Also, the 60 Hz value is a typical low end operational frequency. The equation for the minimum rotational frequency in revolutions per minute (rpm) is Equation 2.2, where ‘SDSR’ is the sonic drill speed of rotation (Hz).

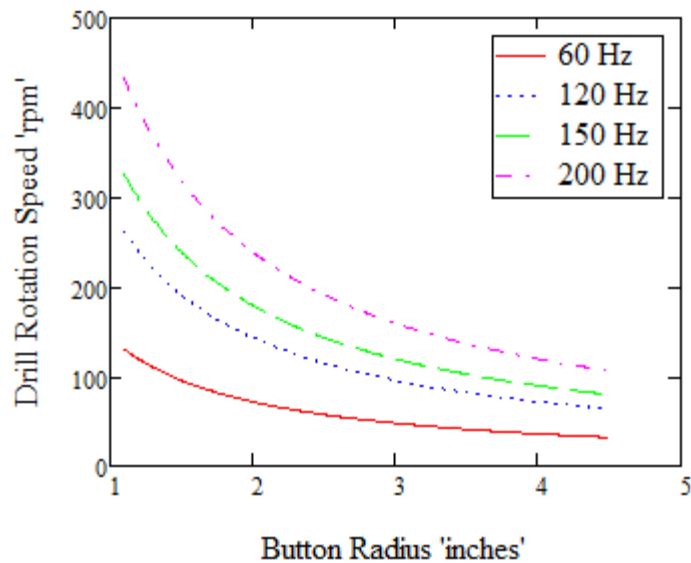


Figure 2.7. Minimum rotational speed for 0.25" buttons to impact virgin material at various button mounted radiuses and sonic drill operational frequencies of 60 hz, 120 hz, 150 hz, and 200 hz.

$$Drill\ Rotation\ Speed\ (rpm) = \frac{Rotation\ angle}{360\ degree} * SDSR\ (Hz) * 60$$

(2.2)

While drilling using an 9” outer diameter drill pipe with 0.25” diameter buttons on the outside diameter, it would require at a minimum of 32 rpm with a sonic drill

operating at 60 Hz compared to 106 rpm for a sonic drill operating at 200 Hz for the drill button to impact virgin material. It may be advantageous to have the rotational speed slightly off by a multiple of the minimal rotational speed to ensure that the bits will not impact the same location after a complete revolution.

Flush Fluid Flow

In many sonic drilling conditions flushing fluid is not required. In rotary drilling, fluid is required to move the drilled material out of the way of the bit, so it can drill virgin material. Flushing media for sonic drilling can be as simple as air and water, as complicated as the fluids required for rotary drilling. A sonic drill bit oscillates vertically thus creating turbulent flow at the drilling interface which naturally lifts loose drilled material out of the way. When flushing media is required, the actual amount required is small compared to rotary drilling. This is another benefit that promotes, sonic drilling as the drill rig of choice for areas where there is concern of environmental impact or instances of drilling in contaminated areas, such as nuclear test sites or storage areas and extraterrestrial drilling. (20) (7) (29)

Mass of Sonic Head

The sonic driver mass is defined as the mass of the sonic driver between the drill string and the compliant (sonic driver spring) member to the frame. The sonic drill mass is a boundary condition of the governing differential equation model of motion of the system. To solve the governing differential equation, the mass of the sonic head has significance to the resultant sonic drill dynamics. The primary impact to the system

dynamics is that as the mass of the sonic head increases, the sonic drill head moves less relative to the pipe below the surface. Because the sonic drill head is located where the input force is applied, the decreased amplitude greatly affects the amount of energy going into the system. If the sonic drill head boundary condition were to move more, by using a smaller mass, more energy would be delivered because work is defined by force applied over a distance. If the mass is infinitely large, it would act as a fixed boundary condition and little to no energy will excite the sonic drill system, even though it has the same input force and the rest of the system may be identical. The sonic drill head mass is one of the major constituents in the boundary condition of the sonic drill model and design.

On the other hand, the system can almost control itself if the sonic drill mass is lighter. This perceived notion is because the drill string has more impedance relative to the sonic driver and the machine operator observes system responses that are more representative of what happens below ground. This condition is commonly referred to as the sonic drill's ability to 'lock-in' to the resonant mode. As the mass of the sonic drill head is reduced the sonic drill head oscillation amplitude increases and is able to provide more power into the system given the same amount of input force. Ultimately, by minimizing the drill head mass, the sonic drill can provide more power given the same size of eccentric masses and frequency. In this configuration the resonant system requires less power to achieve higher amplitudes on mechanical resonance, allowing the eccentrics to rapidly drive the system into resonance. Once it reaches resonance more power will be required to push through resonance to a higher frequency, and thus the system will naturally seek resonance ('lock-in'). However, there is some minimum mass

that must be used to ensure the acceleration stresses on the sonic drill driver do not fatigue and ultimately fail the driver. The system power also reaches a minimum at resonance if operated correctly, thus the hydraulic motors will automatically drive to the optimum condition. However, lock-in is only as good as the controller and if the system's input force is not well matched to the size of drill pipe, the system can become unstable and kick the mechanical system out of mechanical resonance or frequency will oscillate back and forth through resonance, not fully utilizing the advantage of the resonant condition. The push and pull force and other variables affect the system parameters; the system doesn't self-regulate and can actually drive away from the optimal operation conditions.

In summary, it has been common practice to design the sonic drill head as light as possible, so that more energy can be implemented with a smaller input force. However, if design constraints allow for less sonic drill amplitude, then a larger driver mass may be used to reduce the amount of drill stresses, but larger eccentrics to increase the input force must be used to make up for the reduced driver amplitude.

Mass of Drill Bit

The drill bit mass is defined as the lumped mass at the end of the drill pipe, which comes into contact with the earth. The mass of the drill bit also acts as a means to limit the sonic drill bit oscillation amplitude. Additional bit mass reduces the oscillation amplitude relative to the rest of the sonic drill string. The mass at the end also gives an added advantage while drilling: as the mass is increased it will add inertia, while drilling in an oscillatory impact manner. In this case the drill bit absorbs more energy and more

of the impact load, as opposed to being sent up the drill string causing damage due to large compressive strain rates. Thus, an optimization of drill bit mass to drilling penetration rate would be ideal, but is beyond the scope of this work.

Air Spring Rate at Sonic Head

The sonic driver spring is typically an air spring that is used to mechanically decouple the sonic forces from the drill rig frame. The air spring is designed for a drill string size and the depth requirement of the drilling rig. The drill string can be lifted by forces through the air spring when it is being pulled up out of the drilled hole. The air spring also applies the static load on the bit. The air spring at the sonic head acts as part of the boundary condition of the sonic drill. Because the sonic forces are high frequency, typical vibration isolation equations apply and the air spring is designed with the lowest amount of spring rate that still yields a stable system. When the spring rate is low, it has very little effect the sonic drill system.

Damping along the Length of the Drill String

The damping along the length of the drill string accounts for the drilled sections of earth contacting the side of the drill pipe along its length. Various damping conditions can occur along the length of the drill string. These damping conditions are due to sand, clay, rock, liquid, bubbly liquid, paste, etc. The amount of damping is greatly affected by the frequency and amplitude of the oscillation at the local area. In particular, strata types that are located at anti-node locations will have a much greater affect onto the drill system than materials located at node locations. Research in this field indicates that little

acceleration- typically a few 'g' can greatly reduce the friction coefficient between the drill pipe and the surrounding sand, Figure 2.8 (6; 30; 31; 32). As the sonic drill has higher localized accelerations due to higher displacements and higher frequencies, the friction onto the pipe from the surrounding media is greatly reduced. Acceleration rates will be calculated in the modeling section, and most of the drill string (unless at an anti-node) is typically greater than 8 g of acceleration during operation. (6)

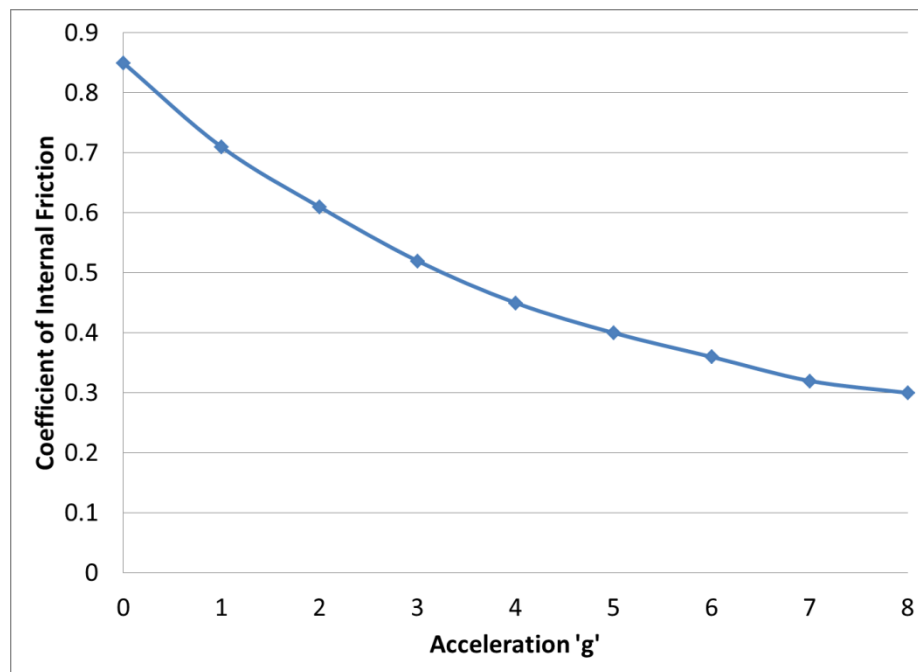


Figure 2.8. Coefficient of internal friction vs. acceleration (30)

The impact of material along the sides of the drill string are typically considered small relative to the damping on the drill tip because the primary mode of vibration is in a shear plane that facilitates damping and restoring effects of the side material. The drill string however does expand and contract due to Poisson's effect; however this is a much smaller factor than the main axial mode. Because the drill bit is in the direction of the

primary mode, it presents the majority of the system damping. Also, most soil bonds fail at frequencies below 30 Hz (33). Thus, at driving frequencies above 30 Hz, the sonic drill is decoupled from the surrounding soil as most sonic drill systems operate between 60 and 200 Hz. Because of the mismatch of frequencies, the ground doesn't transmit the sonic energy because it fails to couple with the sonic drill string along its length. Due to the decoupled nature, many sonic drill advertisements include a still glass of water next to the sonic drill in operation even though it is right next to the drill while it is drilling. Because damping along the length is very low, the sonic drill operator has to be very careful not to overstress the drill string at resonance when the bottom drill tip is not engaged in drilling.

In addition to the strata damping along the length, there can be internal damping of the drill string material. Typically, steel is the material of choice because of its high strength and good fatigue properties when operated under the “knee” in a stress versus number of cycles (S-N) fatigue curve. The material loss factor and damping factor for steel are $1 \cdot 10^{-4} - 1 \cdot 10^{-2}$ and $5 \cdot 10^{-5} - 5 \cdot 10^{-3}$, respectively. (34) Because the material damping is so low, the intrinsic losses of the drill pipe are ignored.

Damping at the Drill Bit

Damping at the drill bit is defined as the amount of energy consumed by drilling or displacing the strata into itself. The damping at the drill bit is the most important variable of the drilling system, as it defines the drilling work that is taking place.

Damping at the drill bit can be used to correlate to the strata type being drilled through at the time. Common knowledge from sonic drilling experts would say that hard rock has the highest amount of damping. Hard rock, in theory, should become broken and then become fluidized in a similar fashion to a fluidized sand. Thus, hard rock should have a higher damping constant than sand because the drill bit first has to fracture the rock and then fluidize the fractured rock. Clays should have the highest damping constant because they have absorbing properties due to their viscoelastic nature. Not only does the drill have to displace the clay, but it also has to break the shear forces holding the clay together. Therefore, damping at the drill bit has yet to be defined and quantified for all different types of strata, but the above rules of thumb were intuitively derived. However, some types of clays, such as marl, tend to stick to the drill string. Dr. George Cooper, U.C. Berkeley, has demonstrated that it is possible to eliminate/minimize this effect by imposing a small DC charge on the drill string.

Sonic Driver Damping

The sonic driver damping occurs at the drill head and consists of air friction losses, losses of pumping the air spring, and viscoelastic losses in the air spring material. These losses are negligible as they typically account for less than 1% of the losses of the system.

Stored Energy along the Length

The stored energy along the drill length is defined as the strata's ability to couple potential energy to the drill string along its length. The stored energy along the length of

the drill string is negligible for fluidized media. During normal operation this stored energy is minimized. However, if the media has collapsed, swelled, or pinched, there is a potential for the media to store energy. The media can store energy in two directions: The first being the axial or primary direction of motion of the drill string, and the second is the lateral or breathing direction. The breathing stored forces can be much greater, as there is a higher coupling in this direction due to the pinch, swelling, or collapse forces. In the primary axial direction the friction forces are less than the primary holding forces of the pinch, swelling, or collapse forces, thus this mode is more easily decoupled. A decoupled state is when the surrounding strata has minimum to no influence onto the drill string.

Drill Bit Coupling

The drill bit coupling is defined as the amount of restoring forces being imparted by the strata onto the drill bit. As the drill bit coupling increases to the actual strata mechanical stiffness, the boundary condition approaches a fixed state from the normally assumed free condition. The drill bit coupling is also known as drill bit spring rate in this body of work.

CHAPTER 3

MODELING

Introduction

The modeling section is the backbone of the work presented in this dissertation. The modeling provides a base understanding of what the system dynamics of the sonic drill are and will ultimately be the cornerstone for a sonic drill control system. First, a system with a simple single degree of freedom is analyzed to determine the salient features of a resonant condition. A sonic drill's governing differential equation of motion can be derived through either force balance or energy balance. Only the derivation of the longitudinal vibration governing differential equations are presented in this body of work. The governing differential equation can then be manipulated similarly to the single degree of freedom system which will give a simplistic understanding of the system. The simplistic approach works well for a free – free system where the end conditions do not contribute much to the system. However, once the end conditions are no longer negligible then other, more advanced modeling techniques are required, such as a closed form solution and finite element analysis. The closed form solution chosen only solves the boundary condition problem with no damping or spring forces along the length of the drill pipe. A new solution would need to be found for each changing boundary condition and length of drill pipe, which would limit the utility of this method for industry. A full closed-form solution with damping and spring forces along the length would require a great deal amount of mathematical solutions for each set of boundary conditions and

conditions along the length, these permuted configurations are beyond the scope of this work. However, to account for the damping and spring affects along the drill pipe, a finite element model was developed. The finite element model uses equivalent damping and soil coupling along the length of the drill string. These equivalent damping and spring constants are derived in the finite element section.

Chapter 3 lays the foundation of the boundary condition model for the longitudinal vibration of the drill string, relations of real world soil characteristics at the drill bit and along the length of the drill string, and the foundation for the finite element model of the sonic drill that models the longitudinal, torsion, flexure, and breathing vibrations of the sonic drill system. The assumptions for each modeling system are outlined for each. The boundary condition model was developed to investigate the significance of the sonic drilling variables have on drilling and ultimately the penetration rate. The sonic drilling variables included the mechanical sonic drilling parameters and also the soil characteristics. The soil characteristics (coupling and damping) provided cover the range of strata types that could be encountered while sonic drilling that include voids, sands, clays and rock. These strata characteristics are tabulated later in the chapter, which are also the values used for the design of experiments to determine the significance of all the sonic drilling parameters.

Single Degree of Freedom System

A resonant system is on resonance when the input power is being directly transferred to the damping of the system, expending little to no energy within the mechanical system itself. This phenomenon occurs at particular frequencies where the

kinetic energy (stored in the masses) and the potential energy (stored in the springs) are matched so that energy used to move the system is conserved once charged. The resonant condition is best illustrated by a single degree of freedom system, also known as a simple lumped parameter system. The single degree of freedom system (displayed in Figure 3.1) has a single mass connected to the ground through means of a spring and a damper. The spring has a spring constant, 'k', that defines the spring's resultant force when compressed or elongated a specific distance. The damper has a damping constant, 'c', associated with it that defines the resultant force when the damper is being compressed or elongated at some velocity.

Please note that damper is not to be confused with the term 'dampening', which means to wet or moisten. In recent years, the term dampen and dampening have been used incorrectly, that the dictionaries have been adding them to also mean the same as damp. Thus, in this document, only terms such as damp, damped, or damping are used. Terms such as dampen, dampened, and dampening are not standard practice in vibrations or sound literature.

By analyzing the diagram displayed in Figure 3.1 and drawing the corresponding free body diagram (displayed in Figure 3.2) the governing differential equation (GDE) of motion (depicted in Equation 3.1) can be derived from Newton's second law of motion or force balance as shown by Equation 3.2. Newton's second law states that the force resultant acting on an object is equal to the product of its mass and the resultant acceleration. The governing differential equation relates all the known system constants to the input force through means of the resultant motion of the system 'x(t)'.

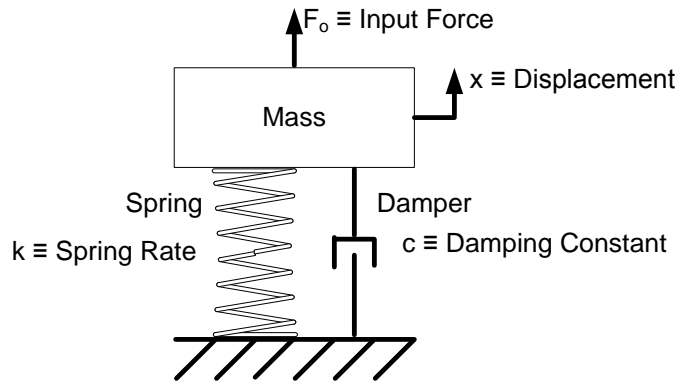


Figure 3.1. Single degree of freedom system.

The input force is sinusoidal, so the resultant motion solution $x(t)$ is assumed to also be sinusoidal (displayed in Equation 3.3) where ‘X’ is the displacement amplitude, ‘ ω_f ’ is the input forcing angular frequency, ‘t’ is time, and ‘ Φ_d ’ is the phase angle offset between the input forcing sinusoidal function and the displacement. The assumed solution (Equation 3.3) is then placed into the governing differential equation (GDE) (Equation 3.1) and the resulting equation is shown in Equation 3.4.

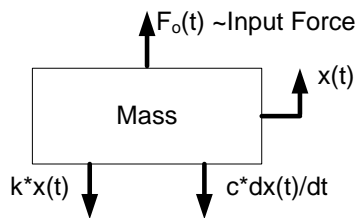


Figure 3.2. Free body diagram of the single degree of freedom system.

$$\underbrace{m \cdot \frac{d^2}{dt^2} x(t)}_{\text{Inertia Forces}} + \underbrace{c \cdot \frac{d}{dt} x(t)}_{\text{Damping Forces}} + \underbrace{k \cdot x(t)}_{\text{Stored Forces}} = \underbrace{F_o \cdot \sin(\omega_f t)}_{\text{Input Forces}} \tag{3.1}$$

$$\sum \mathbf{F} = \mathbf{m} \cdot \mathbf{a} \quad (3.2)$$

By examining Equation 3.4 it can be observed that there will be a specific frequency at which the inertia forces, a function of the mass, will directly offset the stored force, established by the spring. This frequency is defined as the undamped natural frequency 'ω_n' of the system and can be found to have the relation: the square root of the spring rate divided by the mass (as shown in Equation 3.5). At the system's undamped natural frequency, 'ω_n', the phase angle between the input force and the spring force is always -90 degrees. This condition makes the damping forces in phase with the input forces.

$$x(t) = X \cdot \sin(\omega_F t + \phi_d) \quad (3.3)$$

$$-m \cdot X \cdot \omega_F^2 \cdot \sin(\omega_F t + \phi_d) + c \cdot \omega_F X \cdot \cos(\omega_F t + \phi_d) + k \cdot X \cdot \sin(\omega_F t + \phi_d) = F_0 \cdot \sin(\omega_F t)$$

Inertia Forces
Damping Forces
Stored Forces
Input Forces

$$(3.4)$$

$$\omega_n = \sqrt{\frac{k}{m}} \quad (3.5)$$

In order to examine the resonant system, the GDE must be solved and the solution must be analyzed. By applying trigonometric relations to the manipulated GDE, Equation 3.6, the displacement amplitude 'X', and phase angle 'Φ_d' are found (displayed in Equation 3.6 and Equation 3.7, respectively).

From these two relations, if the damping constant is very large then it will override the inertia and spring effects and not allow the oscillating system to utilize the

input force to perform work using the damping of the system. In other words, as the damping constant 'c' gets larger, the displacement amplitude 'X' gets smaller.

$$X = \frac{F_0}{\left[\left(k - m \cdot \omega_f^2 \right)^2 + c^2 \cdot \omega_f^2 \right]^{0.5}} \quad (3.6)$$

$$\phi_d = \tan^{-1} \left(\frac{c \cdot \omega_f}{k - m \cdot \omega_f^2} \right) \quad (3.7)$$

This allows less energy to be utilized by the system damper. An analogy to this is the larger the resistors placed into an alternating current (AC) circuit (at constant voltage amplitude) the less flow of electrons the circuit will allow, and less power is consumed through the resistor. In order to more easily quantify when the damping will take control of a system the damping ratio ' ζ ' (displayed in Equation 3.8) will be defined as the ratio of the damping constant 'c' to the critical damping value ' c_{cr} '. The critical damping value ' c_{cr} ' is defined as the value of damping that will not allow the system to oscillate during a transient situation. The transient vibration frequency ' ω_d ' or damped natural frequency is found by the relation displayed in Equation 3.9.

$$\zeta = \frac{c}{c_{cr}} = \frac{c}{2 \cdot m \cdot \omega_n} \quad (3.8)$$

$$\omega_d = \omega_n \cdot \sqrt{1 - \zeta^2} \quad (3.9)$$

As the damping ratio approaches one, ω_d approaches zero. However, this is not the frequency where the max displacement occurs for a forced system. By taking the derivative of the displacement amplitude (Equation 3.6) and solving for the frequency at which the derivative of the displacement amplitude is zero, the max displacement

frequency ' ω_M ' (displayed in Equation 3.10) may be derived. ω_M is real only when ζ is greater than one half of the square root of two. If ζ is large enough so that ω_M is zero or imaginary, then X is maximized only at zero input frequency.

$$\omega_M = \omega_n \cdot \sqrt{1 - 2 \cdot \zeta^2} \quad (3.10)$$

Sonic drills are typically powered by eccentric driven oscillators. The eccentric creates the input force in the direction outward from the axis of rotation through the eccentric mass as shown in Figure 3.3.

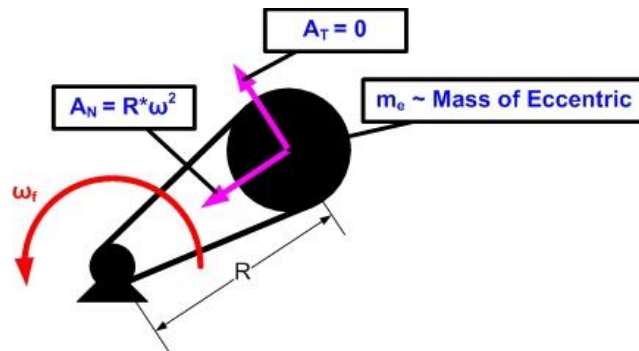


Figure 3.3. Rotating eccentric mass.

The force that is generated onto the supporting structure is equivalent to the inward acceleration ' A_N ' multiplied by the eccentric mass ' m_e ', shown in Equation 3.11.

$$F_{ecc} = m_e \cdot R \cdot \omega_f^2 \quad (3.11)$$

In a single-mass system the force vector is circumferentially-oriented about the axis of rotation. In order to only have the force vector in a single-axis-parallel to the drill string a second eccentric that is counter rotating, must be included in the same supporting structure to cancel out all unwanted lateral forces and reinforce the desirable axial forces.

The two eccentric force vectors are displayed in Figure 3.4 and show how the axial forces in the X direction are reinforced, but the lateral forces in the Y direction are cancelled.

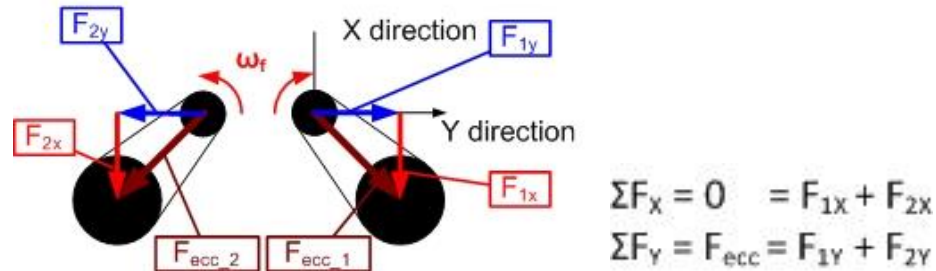


Figure 3.4. Dual eccentric force vectors.

Because sonic drills are driven by eccentrics, the GDE changes to include the input force (Equation 3.12) as the force amplitude.

$$\underbrace{m \cdot \frac{d^2}{dt^2} x(t)}_{\text{Inertia Forces}} + \underbrace{c \cdot \frac{d}{dt} x(t)}_{\text{Damping Forces}} + \underbrace{k \cdot x(t)}_{\text{Stored Forces}} = \underbrace{m_e \cdot R \cdot \omega_f^2 \cdot \sin(\omega_f t)}_{\text{Input Forces}} \quad (3.12)$$

By analyzing the same single degree of freedom system displayed above in Figure 3.1, with a similar forcing function, the sonic drill system model will give an accurate representation of the sonic drill system performance. The new GDE with the eccentric input forcing function is displayed in Equation 3.13.

$$\frac{d^2}{dt^2} x(t) + 2 \cdot \zeta \cdot \omega_n \cdot \frac{d}{dt} x(t) + \omega_n^2 \cdot x(t) = m_e \cdot R \cdot \omega_f^2 \cdot \sin(\omega_f t) \quad (3.13)$$

With an eccentric driven system, the undamped natural frequency ' ω_n ', damped natural frequency ' ω_d ', phase angle ' Φ_d ', and damping ratio ' ζ ' are still found the same way as described previously and have the same values. The maximum displacement

amplitude frequency ‘ ω_M ’, displayed in Equation 3.14, is also found the same way, but is now higher than the undamped natural frequency. As the damping ratio increases up to one divided by the root of two, the maximum amplitude natural frequency ‘ ω_M ’ converges to infinity.

$$\omega_M = \frac{\omega_n}{\sqrt{1 - 2\zeta^2}} \quad (3.14)$$

The GDE is written in terms of the damping ratio ‘ ζ ’ and undamped natural frequency ‘ ω_n ’. The above section was included to help make the transition from the single degree of freedom system to the sonic drill system.

Sonic Drill System

Mathematical Model

Sonic drills are essentially long thick walled steel tubes. The modeling effort is broken into 4 models, which are longitudinal vibration in tubes, torsional vibration in tubes, transverse vibration in beams, and breathing vibration in tubes. Because the sonic drill rod is a tube, the breathing modes can be present, but for solid shafts this mode is usually much stiffer and is frequently neglected in vibrational models.

For initial examination, only a single axis model of the longitudinal vibration for the sonic drill is investigated. However, this same methodology can be applied to the torsional vibration and transverse vibration in the sonic drill. For further reference in these particular degrees of freedom please refer to the text, *Vibration of Continuous System* by Singiresu S. Rao (35). To analyze the system, the free body diagram displayed in Figure 3.5 must first be drawn. Then, by applying Newton’s second law of

motion to the free body diagram the governing differential equation can be derived, shown in Equation 3.15. The damping forces are from the earthen materials along the length of the drill string. The stored forces are from the internal stiffness (or springiness) of the drill string and the coupling between the ground material and the drill string along the length of the drill string. The input forces are defined as any body forces that are applied along the drill string and, for the sonic drill, there are none. Damping and soil restoring forces along the length are modeled separately from body forces. Inertial forces are caused by the mass of the drill string and local accelerations of the drill string. The solution to this system is the deflection along the length of the drill string relative to time, $u(x,t)$. The damping constant 'b' and the spring constant 'a' are derived and explained further in the work by Don C. Warrington (36) and in the finite element section below. The soil conditions while drilling can range from void, sand, clay, and rock. Later in this chapter, these soil constants for various damping and coupling conditions are tabulated, which will be used in a design of experiments approach to determine the significance of the drilling parameters with respect to the drill penetration rate.

The governing differential equation for sonic drills can also be derived using energy methods. Sonic drills can also be thought of as continuous pipe.

Models for pipes vary from simple axial models assuming that the deformation of the cross section in the y and z directions (v and w bar displacements) are assumed to be negligible. The displacements are then given in equation 3.16, the strains in equation 3.17, and the stresses in equation 3.18.

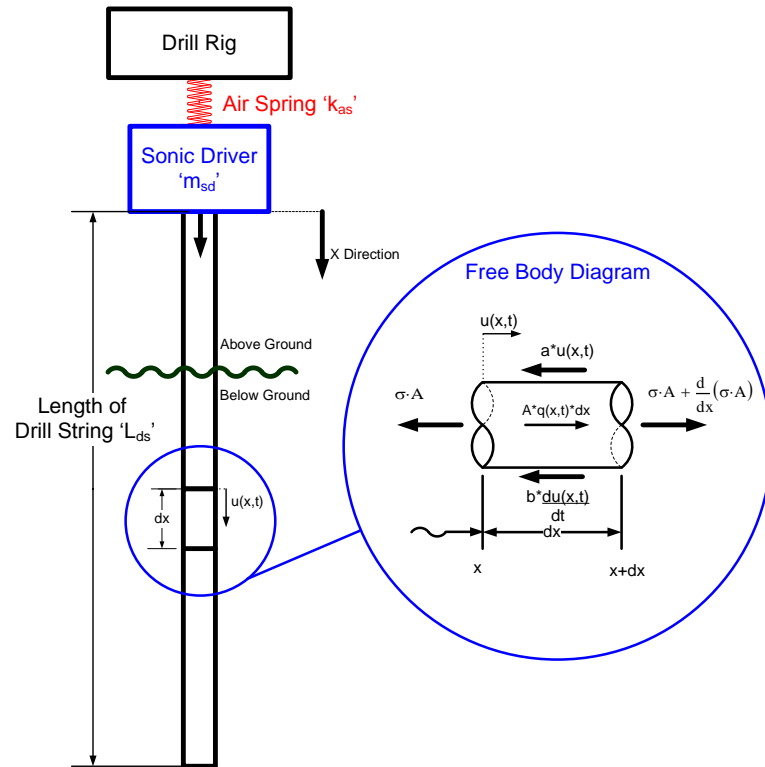


Figure 3.5. Sonic drill model.

$$\underbrace{\rho * A * dx * \frac{\partial^2 u(x,t)}{\partial t^2}}_{\text{Inertia Forces}} + \underbrace{2 * b * A * dx * \frac{\partial u(x,t)}{\partial t}}_{\text{Damping Forces}} + \underbrace{\left(a * A * dx * u(x,t) - E * A * dx * \frac{\partial^2 u(x,t)}{\partial x^2} \right)}_{\text{Stored Forces}} = \underbrace{q(x,t) * A * dx}_{\text{Input Forces}}$$

(3.15)

$$u = u(x, t), v = 0, w = 0 \quad (3.16)$$

$$\varepsilon_{xx} = \frac{\partial u}{\partial x}, \quad \varepsilon_{yy} = \varepsilon_{zz} = 0, \quad \varepsilon_{xy} = \varepsilon_{yz} = \varepsilon_{zx} = 0 \quad (3.17)$$

$$\sigma_{xx} = E \frac{\partial u}{\partial x}, \quad \sigma_{yy} = \sigma_{zz} = 0, \quad \sigma_{xy} = \sigma_{yz} = \sigma_{zx} = 0 \quad (3.18)$$

The governing differential equation of motion for the axial direction (along the length of the drill string) can be determined either by force balance or energy balance. If energy balance is used, then the strain (π), kinetic (T), and external work (W) energies of

the pipe are found, equations 3.19, 3.20, and 3.21, where ‘A’ is the cross sectional area of the pipe and ‘ρ’ is the density of the drill pipe.

$$\pi = \frac{1}{2} \int_0^l \sigma_{xx} \varepsilon_{xx} A dx = \frac{1}{2} \int_0^l EA \left(\frac{\partial u}{\partial x} \right)^2 dx \quad (3.19)$$

$$T = \frac{1}{2} \int_0^l \rho A \left(\frac{\partial u}{\partial t} \right)^2 dx \quad (3.20)$$

$$W = \int_0^l f(x, t) u dx \quad (3.21)$$

The generalized Hamilton’s principle is used to derive the governing differential equation from the energy components of the system. Simply stated, the Hamilton’s principle employs that of all possible time histories of displacement conditions, which comply with the compatibility equations and the kinematic boundary conditions and that also satisfy the conditions at initial and final times t_1 and t_2 , the history corresponding to the actual solution makes the Lagrangian function a minimum. Therefore the generalized Hamilton’s principle is expressed in equation 3.22.

$$\delta \int_{t_1}^{t_2} L dt = 0 \quad (3.22)$$

And for this system the Hamilton’s principle equation is displayed in equation 3.23.

$$\delta \int_{t_1}^{t_2} (T - \pi + W) dt = 0 \quad (3.23)$$

Once equations 3.19, 3.20, and 3.21 are incorporated into equation 3.23, the governing differential equation and the boundary condition are determined, equation 3.24.

$$\frac{\partial}{\partial x} \left(EA \frac{\partial u}{\partial x} \right) + f = \rho A \frac{\partial^2 u}{\partial t^2}$$

$$EA \frac{\partial u}{\partial x} \delta u \Big|_0^l = 0 \quad (3.24)$$

Note: Equation 3.24 is for the conservative system (non-damping).

However, by manipulating and transforming the force balance derived GDE (Equation 3.15) for the sonic drill from the time domain into the Fourier and then the Laplace domains results in Equation 3.25.

$$s^2 + 2 \cdot b \cdot s + c^2 \cdot \theta^2 + a = F_0 \quad (3.25)$$

Then by applying the same tools to define the damping ratio ‘ ζ ’ for the single degree of freedom, the damping ratio ‘ γ ’ can be defined for the sonic drill system, as shown in Equation 3.26.

$$\gamma = \frac{b}{\sqrt{c^2 \cdot \theta^2 + a}} \quad (3.26)$$

The GDE for the sonic drill can then be rewritten with the damping ratio ‘ γ ’ (displayed in Equation 3.27).

$$s^2 + 2 \cdot \gamma \cdot \omega_L \cdot s + \omega_L^2 = F_0 \quad (3.27)$$

This equation is of the same form as the single degree of freedom system expressed in Equation 3.13, previously. Because the sonic drill GDE shares the same form as the single degree of freedom system, the same measurement techniques and control system can also be used for the sonic drill system. This concept is critical, because the sonic drill system is very complex and would normally need a very complex control algorithm and an assortment of measurement equipment to fully characterize and control the system. But because the GDE has been manipulated into a useful equation

that allows the use of measurable quantities, such as the phase angle ' Φ_d ', the entire system can be characterized and monitored during the drilling process. This eliminates the need for other sensors below the ground. This simplification results because the string is a continuous system, which will relate the below ground information to the sensors above ground. The relationship between the single degree of freedom system and the sonic drill allows for the control system to be able to monitor the ground conditions and adjust the sonic drill to its optimum operating conditions.

The assumed solution of the governing differential equation of the sonic drill, displayed in Equation 3.28, is a function of both the length along the drill string ' x ' and time ' t ', while also being in the same form as the sinusoidal input force, shown in Equation 3.29.

$$u(x,t) = (A_o \cdot \sin(\theta_f x) + B_o \cdot \cos(\theta_f x)) \cdot (C_o \cdot \sin(\omega_f t) + D_o \cdot \cos(\omega_f t)) \quad (3.28)$$

$$F(t) = F_{ecc} \cdot \sin(\omega_f t) \quad (3.29)$$

The ' x ' radial frequency ' θ_f ' with respect to the length along the drill string ' x ' is related to the forcing angular frequency ' ω_f ' by the relation depicted by Equation 3.30, that shows that the square of the ratio between ' ω_f ' and ' θ_f ' is equal to the Young's Modulus ' E_{ds} ' of the drill string divided by the drill string density ' ρ_{ds} '.

$$\frac{\omega_f^2}{\theta_f^2} = c^2 = \frac{E_{ds}}{\rho_{ds}} \quad (3.30)$$

In order to solve this problem and find the unknown coefficients ' A_o , B_o , C_o , and D_o ' for the assumed solution for the model dynamics of the sonic drill system, the

boundary conditions for the sonic drill system must be defined, as displayed in Figure 3.6.

Boundary Condition Solution Method

The sonic driver mass, the input force from the sonic driver, and the air spring all reside, where 'x' is equal to zero. The sonic driver mass and the air spring are always boundary conditions, however the input force can either be a boundary condition, or an input into the sonic GDE as $q(0,t)$.

At the drill tip of the string, where 'x' is equal to length of the drill string ' L_{ds} ', a boundary condition caused by coupling of the sonic drill tip to the material being drilled through exists. All boundary conditions are located on the ends of the drill string and because of this, all the conditions have to equal the apparent forces at the end conditions. The forces for the ends are found by taking the drill string's elastic constant ' E_{ds} ' multiplied by the cross sectional area of the drill string ' A_{ds} ' and also multiplied by the partial derivative of the local deflection 'u' with respect to the location in space 'x' and setting this equal to the boundary condition, displayed in Equation 3.31.

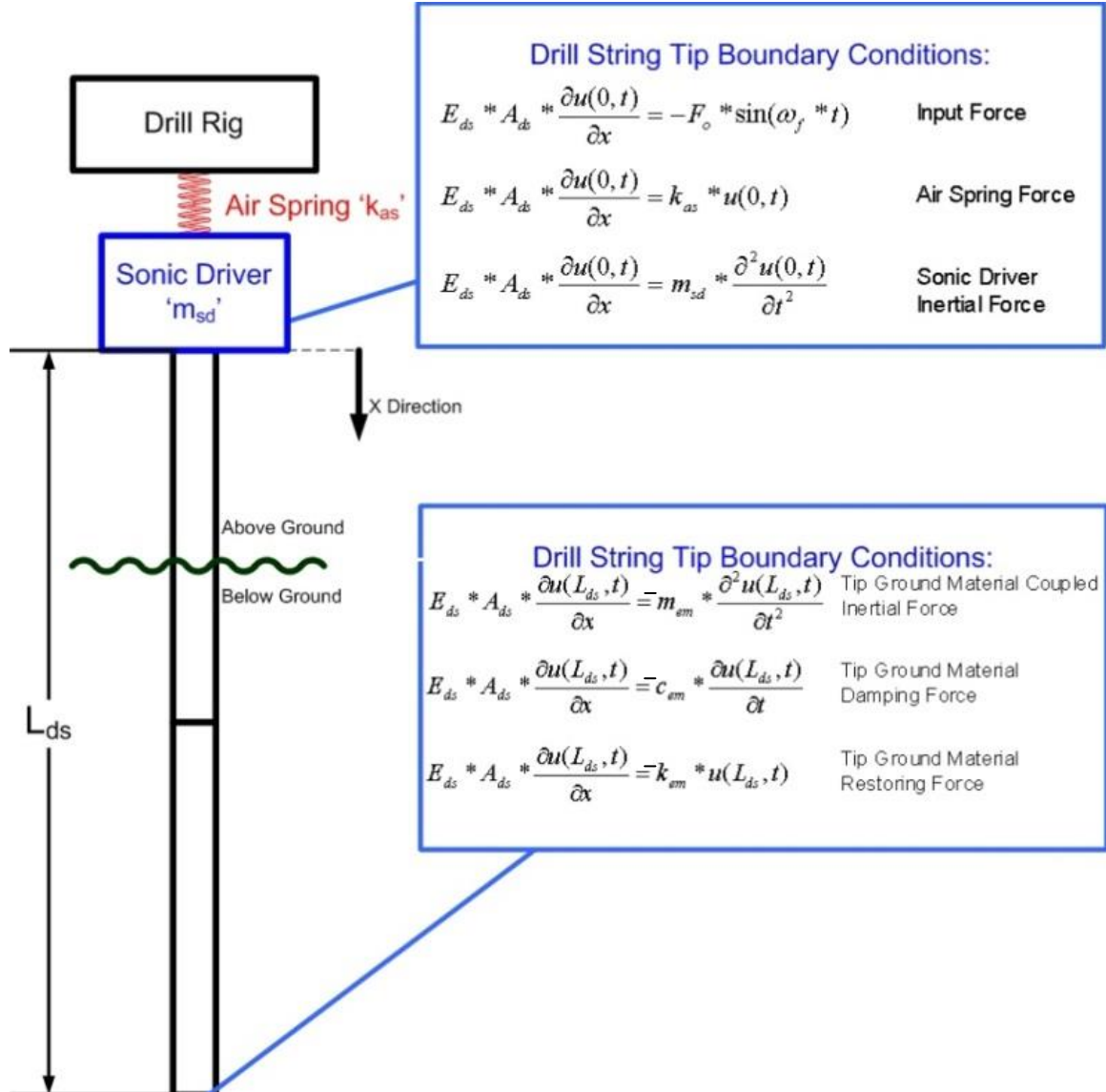


Figure 3.6. Sonic drill boundary conditions.

$$E_{ds} * A_{ds} * \frac{\partial u(x,t)}{\partial x} = \text{Boundary_Condition} \quad (3.31)$$

If the drill string tip was held in place on the ends, then the end condition would be fixed, making the local displacement always equal to zero, displayed in Equation 3.32.

$$u(L_{ds}, t) = 0 \quad (3.32)$$

For example, if the drill string is being pushed onto a rock formation before it is allowed to resonate, the end will act as if it were fused to the rock formation (fixed end). The other extreme is if the drill string is lifted off the bottom of the drilled hole so that the tip does not come into contact with any material, this will be called a free end. However, the drill system will be drilling into the material and thus interacting with it. The material could be very sandy and thus have little effective mass because it will be fluidized at the drill tip. This sandy media will damp the string, but provide no effective spring rate because of the soil fluidization. While drilling through rock formations, the effective mass, effective spring rate, and damping will be insignificant. This is due to impacts and brittle fracture of rock causing very little energy absorption, but the drill string will be excited with all the higher frequency vibrations because of these impacts.

Clays are the hardest and most complex materials to analyze because they have an “effective mass,” and also have very high damping, as well as a spring rate. The drilled material spring rate is negligible compared to the rest of the system; however, the damping is not. The possible boundary conditions are displayed in Equations 3.33 and 3.34.

$$E_{ds}A_{ds} \frac{\partial u(0, t)}{\partial x} = m_{em} \frac{\partial^2 u(0, t)}{\partial t^2} - F_o \sin(\omega_f t) + k_{em} u(0, t) \quad \text{Top Boundary Condition} \quad (3.34)$$

$$E_{ds}A_{ds} \frac{\partial u(L_{ds}, t)}{\partial x} = -m_{em} \frac{\partial^2 u(L_{ds}, t)}{\partial t^2} - c_{em} \frac{\partial u(L_{ds}, t)}{\partial t} - k_{em} u(L_{ds}, t) \quad \text{Tip Boundary Condition} \quad (3.33)$$

The boundary conditions for both the driver (top) and bit (tip) ends of the drill string form two separate independent equations, displayed in Equations 3.33 and 3.34. The modeling

values for these constants are explained and tabulated in the following section “Sonic Drill Parameters”. These values include real world coupling and damping along the drill string for soil types (void, sand, clay and rock) as well as estimated values for the strata coupling and damping at the drill bit. By placing the assumed solution to the governing differential equation, displayed in Equation 3.28, into these two independent boundary condition equations, the unknown solution coefficients, ‘ A_o , B_o , C_o , and D_o ’, can then be solved. These coefficients can be solved by the two independent equations because each equation can also split into two more independent equations, where one includes the sine terms and the other the cosine terms, creating four independent equations for the four unknown coefficients. Now that model has been developed, the perturbation parameters used to determine the significant factors of the sonic drill system are defined.

Sonic Drill Parameters

The variables used for this study have come from various sources and methods. The most prominent source of the variables listed are from the sonic drill (RSD750) which was used to drive a 9” OD drill pipe 120 ft into the ground. Other sources include the work by Memorial University (37), various reports written by Jeffrey Barrow (29), (7), (20), an ASME publication by W. C. Rockefeller (19), and the work by Henry Bernat, Founder of Vibration Technology, L.L.C. (6). The sonic drill modeled is the RSD 750, which was developed by Bodine, but refined by Water Development Corporation under the direction of Jeffrey Barrow. The sonic drill machine specifications for the RSD 750 drilling rig are given in Table 3.1, and are described in the following paragraphs. A picture of the system is also displayed in Figure 3.7.

Table 3.1. RSD 750 rig specifications

Item	Description
Rig Structure	
Length	43.4 ft.
Width	8.5 ft.
Weight	74320 lbs.
Fuel Tank Size	224 gallons
Head Travel	24.5 ft.
Head Drive	4" Cylinder at 3500 psi
Hoist Pull	65,000 lbs.
Hoist Push	21,000 lbs.
Casing Adapters	Up to 36" diameter casing can be driven
Drill Angle	Up to 45° Angle off of vertical
Sonic Driver	RSD*1000
Breakout wrench System	
Movement or mounting of Barber rotary table	12 foot stroke 2.5" hydraulic cylinders
Leveling Jacks	Three 48" stroke cylinders with built-in holding valves
Engines	
Oscillator and Lubrication Oil Pump	725 hp Detroit Diesel
Other rig functions	325 hp Detroit Diesel
Hydraulic system	
RSD*1000 Drive	240 gpm at 5000 psi
Cooling	266 gallon hydraulic oil reservoir
Rotation of Drill	60 gpm at 3500 psi
Hoist Cylinder	60 gpm at 5000 psi
Leveling jacks, breakout system, etc.	Three stack fixed displacement hydraulic pump
Cable Hoisting Systems	
Mainline System	
Rated Pull	17,500 lbf at 260 fpm
Maximum Line Speed	520 fpm at 8,750 lbf.
Cable	700 ft. of 5/8" diameter cable.
Brake	Multiple disc, spring engaged hydraulic release arrangement.
Sand reel System	
Line Pull	5,500 lbf.
Line Speed	400 - 800 fpm
Cable	2500 ft. of 3/8" diameter cable.
Jib Line System	4000 lbf single line pull
Breakout wrench System	
Pipe Sizes	4" to 16"
Torque	37,350 ft-lbf
Clamp Force	74,660 lbf.
Water Injection System	
Injection Pump	CAT 2520 hydraulically powered water injection pump
Reservoir	291 gallon water tank



Figure 3.7. RSD 750 drill rig.

The sonic drill carrier is a 4 Axle Crane Carrier, with Hendrickson Suspension, Allison Automatic Transmission, 10.00 – 20 Load Range F tires on rear axles and 16.5 – 22.5 16 Ply Load Range H tires on the front axles. The carrier is Serial No. AL745 and License No. 3AYC104. The height of the rig is 14 feet 2 inches and the width is 8 feet 6 inches. The vehicle length is 35 feet 8 inches and the overall length including the mast is 43 feet 6 inches. The weight of the rig without the drill head is 74,320 pounds with 28,540 pounds on the front axles and 45,780 pounds on the rear axles. The rig height, weight, and length are legal for travel in all contiguous states. The rig has a 224 gallon diesel fuel tank that feeds both engines.

The rig structure is described as a base rig built by Pacific Welding & Fabrication in Bakersfield, CA who also built Hopper and IDECO Oilfield Workover Drilling Rigs.

All engineering calculations and dimensions performed by Derrick Dance, formerly chief engineer of Hawker Siddeley for their Bodine Soundrive programs. Rig design is based on the Foremost Barber dual rotary 12/26 configuration. The hoist feed is by hydraulic cylinder; no cables, sheaves, chains, or sprockets are used. Heavy duty box and tubular steel is used in the design. The length of the head travel is 24 feet 6 inches, powered by a 5 inch diameter cylinder with 4 inch rod pressured to 3500 psi. The system has both fast feed, rapid retract, and slow feed for drilling applications. The hoisting system has 65,000 pounds of hoisting capacity and 21,000 pounds of pull down force. The breakout wrench system is attached to two 12 foot stroke 2 1/2" hydraulic cylinders for vertical movement or mounting of Barber rotary table. Three 48" stroke cylinders with built-in holding valves are used for leveling jacks. Up to 36" diameter casing can be driven with the rig with the breakout cylinders removed. The mast is configured to slide such that work can be performed at up to a 45 degree angle off vertical.

The rig is driven by two engines: The **Resonant Sonic Drill (RSD)*1000** oscillator driver is a 16V71 turbo charged Detroit diesel rated at 725 horsepower at 2100 rpm with N80 injectors. This engine functions to run the oscillator only and the 20 gpm lubrication oil pump for the Sonic Head lubricating system. All other rig functions are driven by an 8V71T Detroit diesel engine generating 325 horsepower at 2100 RPM. It transmits power through an Allison automatic transmission which uses a Chelsea 5P223 and is **power take off (PTO)** enabled to deliver power to drive-train axles or to operate hydraulic pumps for drill rig operations.

The RSD*1000 oscillator system is powered by four Sundstrand model 23 variable flow piston pumps connected to a Marco DP41 hydraulic pump drive transfer case with a 1.15 to 1.00 reduction. Each pump delivers 60 gpm at 5000 psi for a total flow to the two Sundstrand model 26 motors of the RSD*1000 oscillator of 240 GPM. The oil is cooled by a Young hydraulic oil cooler attached to the 16V71T engine radiator and circulates to a 266 gallon hydraulic oil reservoir for suction and discharge.

The rotation system of the RSD*1000 is driven by a separate Sundstrand model 23 variable flow piston pump producing 60 gpm at 3500 psi delivered to the two Charlynn series 6000 motors. A Dennison A7V variable displacement hydraulic piston pump is also powered by the 8V71 engine through a two-pad KF1-04 Terrell Double Pump Drive case yielding 60 gpm at 5000 psi capability. This pump feeds the hoist cylinder for slow and rapid feed as well as the mainline and sand line winches. A commercial three-stack fixed displacement hydraulic pump feeds the A-20 commercial valves for all other functions on the rig including leveling jacks, breakout system, water injection, tilt cylinders, and mast cylinders. A separate 157 gallon hydraulic oil reservoir tank and hydraulic oil coolers are used for these systems. Drill head holdback features are designed into the hydraulic system.

The cable hoist system includes a mainline system, sand reel system, and jib line system. The mainline system included a variable speed, hydraulic Drawworks winch manufactured by Dresser Industries. Maximum bare drum single line pull of 17,500 lbf. at 260 fpm. Maximum line speed of 520 fpm at 8,750 lbf. single line pull. Grooved cable drum for 5/8" diameter cable. Drum diameter is 20.5" and length is 21". Spooling

capacity is 700 feet. The break is a multiple disc, spring-engaged hydraulic release arrangement.

The sand reel system includes a hydraulic drive sand reel winch with 10.75" diameter drum holding 2500' of 3/8" cable. Bare drum line pull of 5,500 lbf. with a bare drum line speed of 400 fpm and full drum line speed of 800 fpm.

The jib line system was a Braden manufacturing winch with 4000 lbf. Single line pull.

The sonic drill also contained a water injection system that included a 2520 CAT hydraulically powered water injection pump with a 291 gallon water tank for supply. Water injection was not used in this project.

The drill string used was a 9" OD drill pipe in 10 foot long sections. A picture of the sections are shown in Figure 3.8. The drill bit of the 9" OD pile was a 1" thick steel plate welded to bottom of the first drill string. The mass of the flat plate was 18 lbs. The media being drilled through was primarily unconsolidated sands. Before the boundary conditions at the drill bit can be defined, first the different types of soil and how they will react to the sonic drill must be understood. Typical earthen types include sands, clays and hard rock. The mechanical properties of these types of materials as well as other well-known materials are displayed in Table 3.2 (38) (39) (40).

From the soil properties displayed in Table 3.2, the boundary condition properties for sands, clays, and hard rock can be determined through the use of the stiffness and damping terms developed by Don Warrington. The soil values used by Don Warrington are listed in Table 3.3 (36) (41). These values are very similar except that the clay soil in

Table 3.2 has the clay soil elastic modulus as high as 29 ksi, where the soil properties in Warrington had a maximum of 3.5 ksi.



Figure 3.8. 9 inch outer diameter sonic drill pipe.

Table 3.2. Mechanical properties of various soil types and other well known materials.

Material	Density (ρ)	Young's Modulus (E)	Poisson's ratio (ν)	Shear Modulus (G)
Sandy Soil	0.065 lb./in ³	1 - 7 ksi	0.25-0.4	0.4 - 3 ksi
Gravel Soil	0.072 lb./in ³	10 - 25 ksi	0.15-0.35	4 - 11 ksi
Silty Soil	0.076 lb./in ³	ksi		ksi
Clay Soil	0.069-0.076 lb./in ³	1 - 29 ksi	0.3-0.5	0.4 - 11 ksi
Mafic igneous rocks	0.108 lb./in ³	ksi		ksi
Felsic igneous rocks	0.098 lb./in ³	ksi		ksi
Metamorphic rocks	0.098 lb./in ³	ksi		ksi
Sedimentary rocks	0.094 lb./in ³	ksi		ksi
Granite	0.098 lb./in ³	1450 - 10153 ksi	0.1-0.3	580 - 4641 ksi
Shale	0.090 lb./in ³	145 - 10153 ksi	0.2-0.4	44 - 4206 ksi
Limestone	0.098 lb./in ³	2176 - 7977 ksi	0.18-0.33	1015 - 3336 ksi
Chalk	0.076 lb./in ³	ksi	0.35	ksi
Sandstone	0.072 lb./in ³	145 - 2901 ksi		ksi
Steel	0.289 lb./in ³	29008 ksi	0.3	11168 ksi
Concrete	0.060-0.110 lb./in ³	ksi		ksi
Water	0.036 lb./in ³	ksi		ksi

Table 3.3. Soil properties survey for sands and clays.

Soil Type	Young's Modulus (E)				Poisson's ratio (v)			Density (ρ)	
	min	-	max	Unit	min	-	max	Average	Unit
Loose Sand	1.5	-	3.5	ksi	0.2	-	0.4	0.054	lb./in ³
Medium Dense Sand	2.5	-	4.0	ksi	0.25	-	0.4	0.058	lb./in ³
Dense Sand	5.0	-	8.0	ksi	0.3	-	0.45	0.058	lb./in ³
Silty Sand	1.5	-	2.5	ksi	0.2	-	0.4	0.058	lb./in ³
Sand and Gravel	10.0	-	25.0	ksi	0.15	-	0.35	0.072	lb./in ³
Soft Clay	0.3	-	0.8	ksi		-		0.061	lb./in ³
Medium clay	0.8	-	1.5	ksi	0.2	-	0.5	0.061	lb./in ³
Stiff Clay	1.5	-	3.5	ksi		-		0.061	lb./in ³

The 'a' and 'b' values derived by Don Warrington, work well for the closed form simple wave equation, but to relate the equations to an equivalent damping and spring constant of the soil, it is proposed to use 'a'' and 'b'', which are related to 'a' and 'b' by pipe density 'ρ' in the following relations, equations 3.35 and 3.36, where ρ_{pipe} is the density of the drill pipe.

$$a' = a * \rho_{pipe} \quad (3.35)$$

$$b' = b * \rho_{pipe} \quad (3.36)$$

The new constants are then defined as outlined in equations 3.37 and 3.38.

$$a' = \frac{k'}{\sqrt{A * r_g}} \quad (3.37)$$

$$b' = \frac{\mu}{2\sqrt{A * r_g}} \quad (3.38)$$

Where:

$$k' = \pi * G_s * \sqrt{\frac{r_g}{A}} \quad (3.39)$$

$$r_g = \frac{A}{p^2} \quad (3.40)$$

$$\mu = \sqrt{G_s * \rho_{soil}} \quad (3.41)$$

‘k’ is the soil spring constant per unit area (lbf/in³) (Equation 3.39), G_s is the soil shear modulus, r_g is the area of the pile ‘A’ divided by the pile perimeter ‘p’ squared (Equation 3.40), ρ_{soil} is the density of the soil. The previous equations are used to find the damping and spring constants along the length of the pile. However, the spring and damping at the end of the drill bit are assumed using Equations 3.42 and 3.43 which were outlined by Warrington (36), but were cited from works of Lysmer, 1965 (42), and Holeyman, 1988 (43).

$$k_t = \frac{4 * G_s * r_t}{(1 - \nu) * A_t} \quad (3.42)$$

Where ‘ k_t ’ is the spring rate of soil at the drill bit (lbf/in³), r_t is the radius of the drill bit, ‘A’ is the drill bit cross sectional area, and ‘ ν ’ is Poisson’s ratio for the soil.

$$\mu_t = \frac{3.4 * r_t^2 * \sqrt{G_s * \rho_{soil}}}{(1 - \nu) * A_t} \quad (3.43)$$

Where ‘ μ_t ’ is the soil damping at the drill bit per unit of area (lbf*s/in³).

Because the sand becomes decoupled easily, the spring rate at the end of the drill bit was estimated from 0 – 80,000 lbf/in (assuming a 9” OD drill bit), which was calculated from a bulk density of sandy soil of 0.065 lb/in³ (39) and shear modulus as high as 8 ksi. The spring rate is calculated by multiplying ‘ k_t ’ (found in equation 3.42) by the frontal area of the drill bit. The damping of consolidating and displacing the sand

into itself was estimated from 0 – 67,000 lbf*s/in. The damping was found by dividing ‘ μ_t ’ (in equation 3.43) it by the drill bit frontal area and the bit perimeter. The damping and spring rate of clays were derived from the shear modulus and density of Winnipeg clay as outlined in an article by J. Graham in 1983 and various other sources (39; 36; 44).

Some spring and damping values for solid rock were generated from stiffness and damping values measured by Farid Arvani’s team at Memorial University (37). The damping and stiffness constants were measured on a small 2.5” OD drill string with a 44 lb. drill bit. To relate these values to the larger sonic drill, the relations must first be normalized to soil characteristics. The relations and assumptions used to derive the damping and stiffness constants to soil characteristics are those derived by Don C. Warrington (36), equations 3.35 – 3.41.

The values used to find the equivalent spring rate and damping are displayed in Table 3.4. The shear modulus of the Hackensack Siltstone was found to be 9.32×10^6 lbf/in² and 2.11×10^8 lbf/in² using k and b given in Table 3.4, respectively. The density used for Hackensack Siltstone was 0.094 lb/in³ (2,590 kg/m³) (45). Showing that the shear modulus is within reason by using the damping and spring rate relations, checks both the validity of the relations outlined by Warrington, as well as the measured parameters given in Table 3.4. However, by relating the shear modulus to Young’s modulus and Poisson’s ratio that are also given as 4,350ksi (30 GPa) and 0.09, respectively in the book Petroleum Related Rock Mechanics (45), shows the shear modulus should be 2×10^6 lbf/in², which is roughly 20% of the calculated values published by Memorial University.

Table 3.4. Physical parameters of rocks for simulation. (37)

Rock Type	D, kip	k, lbf/in	b, lbf*s/in
Hackensack Siltstone	85.4	1.27×10^7	1.3×10^3
Berea Sandstone	46.3	6.6×10^6	8.56×10^2
Pierre Shale I	7.6	3.95×10^5	2.22×10^2
Drill Bit Mass	44 lb.		
Effective bit Radius (r)	1.24 inches		

The sonic drill head had a mass close to 2200 lb (1000 kg) and the air spring had an adjustable spring rate, but was held close to 35,000 lbf/in for all testing. The air spring damping at the drill string top was assumed negligible.

The sensitivity of the sonic drilling to the following boundary variables for the 9” OD drill pipe and RSD 750, given in Table 3.5, will be investigated. These values were derived from the above information given in Table 3.2 and Table 3.4 as well as by using equations 3.35 – 3.43.

These boundary conditions provide an indication of how the sonic drill behaves under drilling conditions when the damping and restoring forces along the length of the drill string are neglected. When the drilling system is first starting to drill (less than a couple hundred feet of the surface) or when drilling through sands and hard rock, the damping along the length can be neglected.

Because the input force is acting on the drill string at the boundary, the system of equations can be simplified to the boundary conditions and subsequently solved by using only the boundary conditions. However, if the damping and restoring forces along the length of the drill pipe are not neglected, the boundary value solution method cannot be used and other means must be employed to solve the governing differential equation.

Table 3.5. Modeling variables.

Variable	Nomenclature	Value	Value
Sonic Drill Head Mass	m_{SDH}		
Low		1,100 lb	500 kg
Medium		2,200 lb	1000 kg
High		4,400 lb	2000 kg
Sonic Drill Head Spring	k_{SDH}		
		10,000 lbf/in	1,751,268 N/m
		35,000 lbf/in	6,129,439 N/m
		70,000 lbf/in	12,258,879 N/m
Sonic Drill Head Damping	c_{SDH}	0 lbf*s/in	0 N*s/m
Sonic Drill Bit Mass	m_{SDB}		
No end Bit		0 lb	0 kg
Trap Door for Sampling		10 lb	5 kg
1" Flat Plate		18 lb	8 kg
Intermediate Mass		100 lb	45 kg
Rock Hog Drill Bit		250 lb	113 kg
Sonic Drill Bit Spring	k_{SDB}		
No Spring Rate		0 lbf/in	0 N/m
Sand Loose		16,160 lbf/in	2,830,050 N/m
Sand Dense		79,180 lbf/in	13,866,543 N/m
Medium Clay		11,160 lbf/in	1,954,416 N/m
Extreme Clay		297,400 lbf/in	52,082,722 N/m
Rock (Granite)		1.00E+08 lbf/in	17,582,734,736 N/m
Sonic Drill Spring Rate Along the Length	k_{SDP}		
No Spring Rate		0 lbf/in	0 N/m
Sand Loose		3,808 lbf/in	666,883 N/m
Sand Dense		21,770 lbf/in	3,812,511 N/m
Medium Clay		2,848 lbf/in	498,761 N/m
Extreme Clay		75,920 lbf/in	13,295,630 N/m
Rock (Granite)		2.76E+07 lbf/in	4,833,500,784 N/m
Sonic Drill Bit Damping	c_{SDB}		
No Damping Rate		0 lbf*s/in	0 N*s/m
Sand Loose		31.554 lbf*s/in	5,526 N*s/m
Sand Dense		66.783 lbf*s/in	11,695 N*s/m
Medium Clay		26.815 lbf*s/in	4,696 N*s/m
Extreme Clay		138 lbf*s/in	24,195 N*s/m
Rock (Granite)		3097 lbf*s/in	542,368 N*s/m
Sonic Damping Along the Length	c_{SDP}		
No Damping Rate		0 lbf*s/in	0 N*s/m
Sand Loose		17.493 lbf*s/in	3,063 N*s/m
Sand Dense		43.195 lbf*s/in	7,565 N*s/m
Medium Clay		16.105 lbf*s/in	2,820 N*s/m
Extreme Clay		83 lbf*s/in	14,563 N*s/m
Rock (Granite)		2003 lbf*s/in	350,779 N*s/m
Operating Frequency	f_{Hz}	60-115 Hz	60-115 Hz
Mass of Eccentric and Eccentric Eccentricity	$m_{ecc} * r_{ecc}$	148 lb*in	1.7 kg*m

Other methods including the use of mathematical relations and techniques to solve the governing differential equation directly to obtain a closed form solution exist, but are very time consuming and only can be used for a single, steady-state configuration. This method is very time consuming, and only valid for specific damping and restoring forces along the length of the pile. Because of the large amount of time required, this method would not be practical to use in industry. Discretizing the sonic drill into finite difference nodes that follow the governing differential equation at the nodal scale was investigated, as the changing damping and restoring forces can be applied at each node and easily updated to obtain a solution. However, this method was computationally intensive and each iteration for a single frequency required of many hours to converge to a solution. The finite difference method was found to not be able to achieve results in a reasonable amount of time. A finite element method was used, because it was found to have computational advantages. The finite element method was able to solve the conditions to determine the sensitivity of the remaining variables.

In order to use the variables derived in the governing differential equation and ultimately input into the finite element analysis, the following variables listed in Table 3.6 and Table 3.7 were converted from Table 3.5 by using Equation 3.35 through Equation 3.43.

Table 3.6. Soil damping and spring constants for various strata.

Variable	Nomenclature	Value	Value
Sonic Drill Bit Spring			
No Spring Rate	k_t	0.00E+00 lbf/in ³	0.00E+00 N/m ³
Sand Loose		2.54E+02 lbf/in ³	6.89E+07 N/m ³
Sand Dense		1.25E+03 lbf/in ³	3.38E+08 N/m ³
Medium Clay		1.75E+02 lbf/in ³	4.76E+07 N/m ³
Extreme Clay		4.68E+03 lbf/in ³	1.27E+09 N/m ³
Rock (Granite)		1.58E+06 lbf/in ³	4.28E+11 N/m ³
Sonic Drill Spring Rate Along the Length			
No Spring Rate	k'	0.00E+00 lbf/in ³	0.00E+00 N/m ³
Sand Loose		5.99E+01 lbf/in ³	1.62E+07 N/m ³
Sand Dense		3.42E+02 lbf/in ³	9.29E+07 N/m ³
Medium Clay		4.48E+01 lbf/in ³	1.22E+07 N/m ³
Extreme Clay		1.19E+03 lbf/in ³	3.24E+08 N/m ³
Rock (Granite)		4.34E+05 lbf/in ³	1.18E+11 N/m ³
Sonic Drill Bit Damping			
No Damping Rate	μ	0.00E+00 lbf/in ³	0.00E+00 N*s/m ³
Sand Loose		4.96E-01 lbf/in ³	1.35E+05 N*s/m ³
Sand Dense		1.05E+00 lbf/in ³	2.85E+05 N*s/m ³
Medium Clay		4.22E-01 lbf/in ³	1.15E+05 N*s/m ³
Extreme Clay		2.17E+00 lbf/in ³	5.89E+05 N*s/m ³
Rock (Granite)		4.87E+01 lbf/in ³	1.32E+07 N*s/m ³
Sonic Damping Along the Length			
No Damping Rate	μ_t	0.00E+00 lbf/in ³	0.00E+00 N*s/m ³
Sand Loose		2.75E-01 lbf/in ³	7.46E+04 N*s/m ³
Sand Dense		6.79E-01 lbf/in ³	1.84E+05 N*s/m ³
Medium Clay		2.53E-01 lbf/in ³	6.87E+04 N*s/m ³
Extreme Clay		1.31E+00 lbf/in ³	3.54E+05 N*s/m ³
Rock (Granite)		3.15E+01 lbf/in ³	8.55E+06 N*s/m ³

Table 3.7. Soil elasticity and damping constants for various strata.

Variable		Nomenclature	Value
Sonic Drill Bit Spring			
No Spring Rate			0.00E+00 1/s ²
Sand Loose		a _t	4.45E+05 1/s ²
Sand Dense			2.18E+06 1/s ²
Medium Clay			3.07E+05 1/s ²
Extreme Clay			8.19E+06 1/s ²
Rock (Granite)			2.76E+09 1/s ²
Sonic Drill Spring Rate Along the Length			
No Spring Rate			0.00E+00 1/s ²
Sand Loose		a	1.05E+05 1/s ²
Sand Dense			5.99E+05 1/s ²
Medium Clay			7.84E+04 1/s ²
Extreme Clay			2.09E+06 1/s ²
Rock (Granite)			7.60E+08 1/s ²
Sonic Drill Bit Damping			
No Damping Rate			0.00E+00 1/s
Sand Loose		b _t	4.34E+02 1/s
Sand Dense			9.19E+02 1/s
Medium Clay			3.69E+02 1/s
Extreme Clay			1.90E+03 1/s
Rock (Granite)			4.26E+04 1/s
Sonic Damping Along the Length			
No Damping Rate			0.00E+00 1/s
Sand Loose		b	2.41E+02 1/s
Sand Dense			5.94E+02 1/s
Medium Clay			2.22E+02 1/s
Extreme Clay			1.14E+03 1/s
Rock (Granite)			2.76E+04 1/s

Finite Element Method Model

The finite element approach will be analyzed with ANSYS[®]. The models will be used to compare three types of strata damping and coupling. The three types are: 1) constant; 2) linear; and 3) step function, as shown in Figure 3.9. The three types are chosen because:

- 1) Constant values will be used to verify that the numeric model is correct with respect to the previously developed closed form models;
- 2) The linear increase condition describes the linear increase of the hydrostatic pressure of the strata as the drill pipe penetrates deeper into the ground; and
- 3) A step function can model the drilling condition where a new layer of strata is encountered causing the amount of damping and coupling onto the drill bit to change instantaneously.

A fourth condition will also be explored, which is impulse damping. This will model the condition where a part of the hole is unstable and pinches the drill pipe at a specific location while not impacting much of the length. It is assumed that particular resonant frequencies with nodes at the pinch site will not be affected by pinch damping, but to free the bar, a resonant frequency with an anti-node at the pinch location must be used.

The models analyzed in ANSYS[®] were created in SolidWorks[®] as a three-dimensional model. This three-dimensional model was imported into ANSYS[®], meshed, the system was configured, and the full model was then be solved. The three dimensional model was used to examine the interaction between the axial and the other primary vibration modes. Because a drill string is a continuous system, the modes are coupled by

weak springs, which excite the other modes, even though the primary forcing function is in the axial direction.

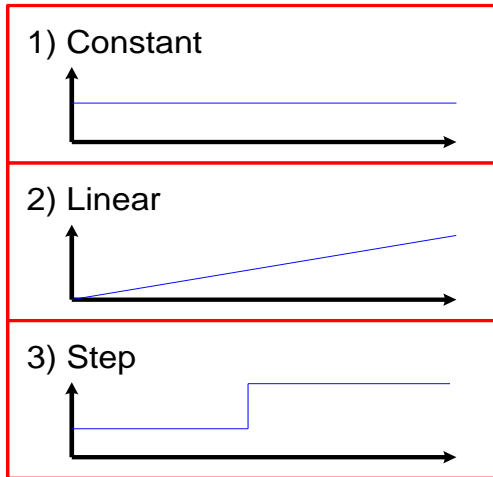


Figure 3.9. Damping and coupling types.

The ANSYS[®] finite element model is more computational efficient when a damping ratio is used. To use ANSYS[®] a method to determine the equivalent damping ratio must be identified, which is derived below.

The damping ratio was derived above in equation 3.26, but is rewritten in the variables used equation 4.44. The damping ratio is again defined as ‘ γ ’.

$$\gamma = \frac{b_{eq}}{\sqrt{c^2 \theta_L^2 + a_{eq}^2}} \quad (3.44)$$

The GDE for the sonic drill can then be rewritten with the damping ratio ‘ γ ’, displayed in Equation 3.27, but for clarity is included in the governing differential equation here (3.45).

$$s^2 + 2\gamma \cdot \omega_L \cdot s + \omega_L^2 = F_o \quad (3.45)$$

The radial frequency ‘ θ ’ was defined in equation 3.30. However, the coefficients ‘ b_{eq} ’ and ‘ a_{eq} ’ are not as straightforward as simply using the values derived above as b' and a' in equations 3.35 – 3.38. The coefficients ‘ b_{eq} ’ and ‘ a_{eq} ’ are equivalent damping constants along the entire length of drill pipe. Thus to get equivalent damping and restoring forces along the drill pipe, the resonant mode shapes must be used along with the damping profile along the drill string length. Damping along the length is given as the local damping constant changes along the length, defined as $b'(x)$: a function of the distance along the length of the drill string ‘ x ’. The mode shape is found and normalized to 1. A sample mode shape and how it is normalized to ‘1’ is displayed in Figure 3.10. The length of the drill string is along the x-axis and the u-axis is the relative displacement along the x-axis in the x-direction. Local damping along the drill string is defined as the local damping at each location along the length. Sample plots of the damping and spring rate along the length are displayed in Figure 3.9.

To find equivalent damping along the length, the normalized mode shape must be incrementally multiplied by the damping value at the x location of the damping. The values of these products are then summed and divided by the length of the drill string, as in equation 3.46 – 3.47. The equivalent damping could also be computed by integrating over the drill string length and applying the product of the damping and normalized mode shape (equations 3.48 – 3.49).

$$b_{eq} = \sqrt{2} * \sqrt{\frac{\sum_{n=1}^{L_n} (b_n ' * NMS_n)^2}{L_n}} \quad (3.46)$$

$$a_{eq} = \sqrt{2} * \sqrt{\frac{\sum_{n=1}^{L_n} (a_n' * NMS_n)^2}{L_n}} \quad (3.47)$$

$$b_{eq} = \frac{\int_0^L (b'(x) * NMS(x))^2 dx}{L} * \sqrt{2} \quad (3.48)$$

$$a_{eq} = \frac{\int_0^L (a'(x) * NMS(x))^2 dx}{L} * \sqrt{2} \quad (3.49)$$

Where the normalized mode shape 'NMS' is the mode shape normalized to '1' and 'L' is the length of the drill string.

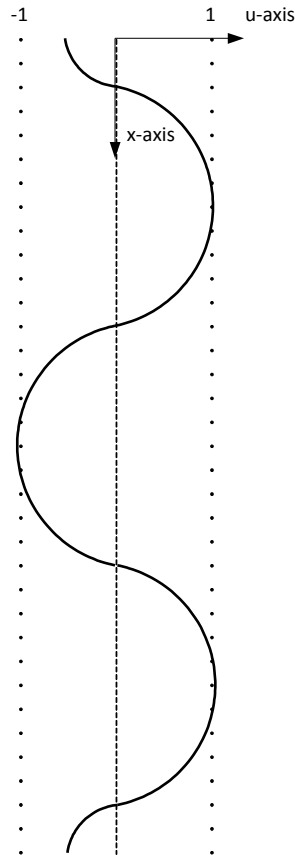


Figure 3.10. Normalized mode shape.

Now that the equivalent damping and spring rate have been found, they can be used to determine the significance of each variable. These equations effectively take the root mean square of the damping and the normalized mode shape and converting it back to a peak value. There will be error with lower mode shapes, but the error decreases with higher order mode shapes. However, these equations can be used as a tool to determine the optimum mode to operate regardless, because it will give accurate relative values for comparison.

Control Derivations

Resonant Condition

In order to take advantage of resonance for the sonic drilling process it is necessary to not only understand the salient factors developed above, but the process must be instrumented so that it can be tracked through active feedback during the drilling process. The parameters which affect the drilling system power requirements and complex interactive effects of mechanical forces on the drill string, are presented below.

The resonance tracking scheme measures the phase angle between the input force and the displacement ' Φ_d ', velocity ' Φ_v ', and acceleration ' Φ_a ' of the sonic head. The system is designed to be an eccentric-driven continuous resonant system. The system has three distinct frequencies that correspond to: the maximum displacement ' ω_M ' (displayed in Equation 3.14) max velocity ' ω_v ', and max acceleration ' ω_A ', respectively. The velocity and acceleration amplitude peaks are always located at higher frequencies than the displacement peak. ' ω_A ' and ' ω_v ' are located at higher frequencies than ' ω_M ' because the acceleration ' $a(x,t)$ ' is related to the displacement ' $u(x,t)$ ' by the negative square of

the forcing frequency ' ω_f ', shown in Equation 3.50, and the velocity ' $v(x,t)$ ' is related to the displacement by the forcing frequency ' ω_f ', presented in Equation 3.51.

$$a(x,t) = -\omega_f^2 \cdot u(x,t) \quad (3.50)$$

$$v(x,t) = \omega_f u(x,t) \quad (3.51)$$

In Figure 3.11, the difference in frequencies between the max displacement, velocity, and acceleration amplitudes are shown.

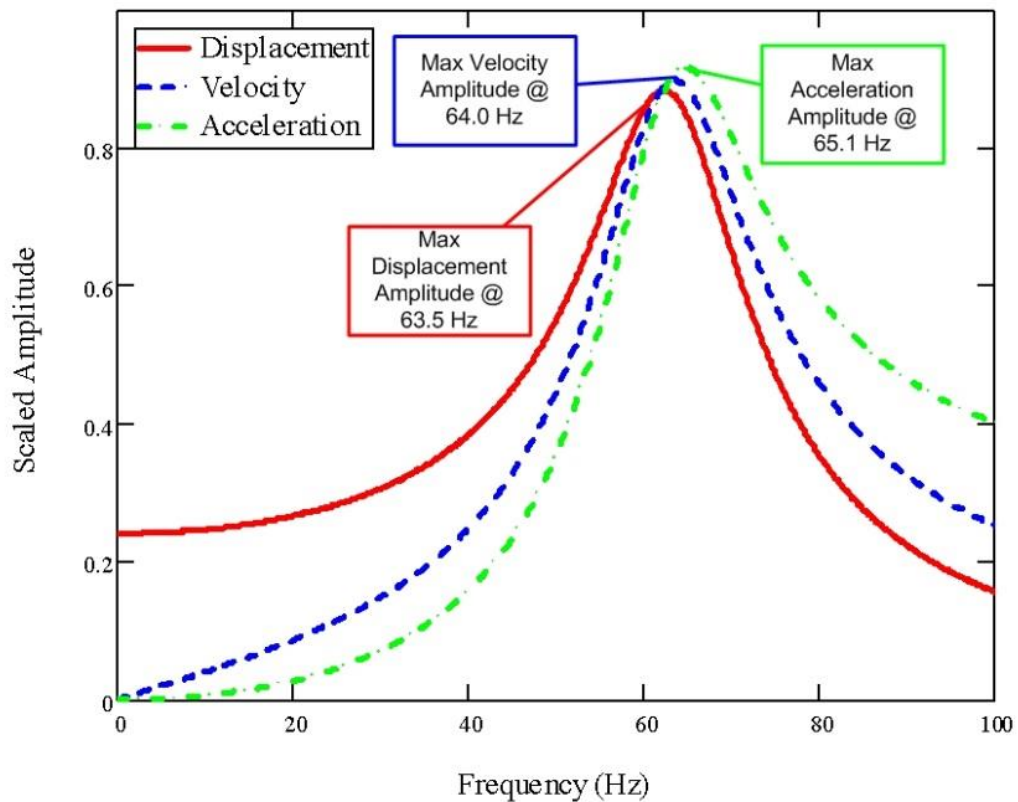


Figure 3.11. The max displacement ' ω_M ', max velocity ' ω_v ', and max acceleration ' ω_A ' angular frequencies are located at different frequencies, because velocity and acceleration are related to the displacement by the operating frequency and operating frequency squared; respectively. The max velocity angular frequency ' ω_v ' is the most important because the power is maximized at this location.

For sonic drill systems, the most important resonant frequency is that of ' ω_v '. ' ω_v ' is the frequency where maximum power is transferred to the drill string. The maximum power is located at ' ω_v ', because work ' W ' is defined by the integral of the force ' F ' multiplied by deflection ' du ', Equation 3.52.

$$W = \int F du \quad (3.52)$$

However, power ' P ', displayed in Equation 3.53, is defined by the integral of the force multiplied by the velocity ' dv '.

$$P = \int F dv \quad (3.513)$$

The max work is located at ' ω_M ' while the max power values are located at ' ω_v '. The resonant tracking scheme will use these phase angles to track the frequency at which the maximum velocity amplitude ' ω_v ' is found by taking the derivative of Equation 3.51. Finding ' ω_v ' for the sonic drill string is very advantageous because this is the point at which the most energy will be transmitted to the bit for drilling.

The maximum amplitude frequencies are useful for a control system, because it provides a means to control to a defined variable. However, this defined variable constantly changes with the impedance of the drill string and changing boundary conditions. Relationships of the maximum amplitude frequencies to the undamped natural frequency are displayed in Table 3.8. There are separate relationships for those with a constant force system, defined as a system where the force does not vary with frequency, and the eccentric forced system, where the input force amplitude changes with frequency.

Table 3.8. Relations between the undamped natural frequency and the maximum amplitude frequencies.

Forcing System	Condition	Relation
Constant Force System	Maximum Displacement Amplitude	$\omega = \omega_n \cdot \sqrt{1 - 2 \cdot \zeta^2}$
	Maximum Velocity Amplitude	$\omega = \omega_n$
	Maximum Acceleration Amplitude	$\omega = \frac{\omega_n}{\sqrt{1 - 2 \cdot \zeta^2}}$
	Maximum Efficiency	$\omega = \omega_n$
Eccentric Forced System	Maximum Displacement Amplitude	$\omega = \frac{\omega_n}{\sqrt{1 - 2 \cdot \zeta^2}}$
	Maximum Velocity Amplitude	$\omega = \omega_n \cdot \sqrt{2.0 - 1.0 \cdot \sqrt{16.0 \cdot \zeta^4 - 16.0 \cdot \zeta^2 + 1.0 - 4.0 \cdot \zeta^2}}$
	Maximum Acceleration Amplitude	$\omega = \omega_n \cdot \sqrt{1.5 - 0.5 \cdot \sqrt{36.0 \cdot \zeta^4 - 36.0 \cdot \zeta^2 + 1.0 - 3.0 \cdot \zeta^2}}$
	Maximum Efficiency	$\omega = \omega_n$

These relations are displayed pictorially in Figure 3.12, where the natural frequency is found to be at 60 Hz. As the damping ratio increases, max amplitude

frequencies will further deviate from the undamped natural frequency, except for the maximum velocity amplitude in the constant force system will be constant at the undamped natural frequency. Also note that the undamped natural frequency is always the frequency at which maximum efficiency occurs for both constant and eccentric-forced systems. The relationship of phase angles between the input force and the displacement amplitude is shown in Figure 3.13

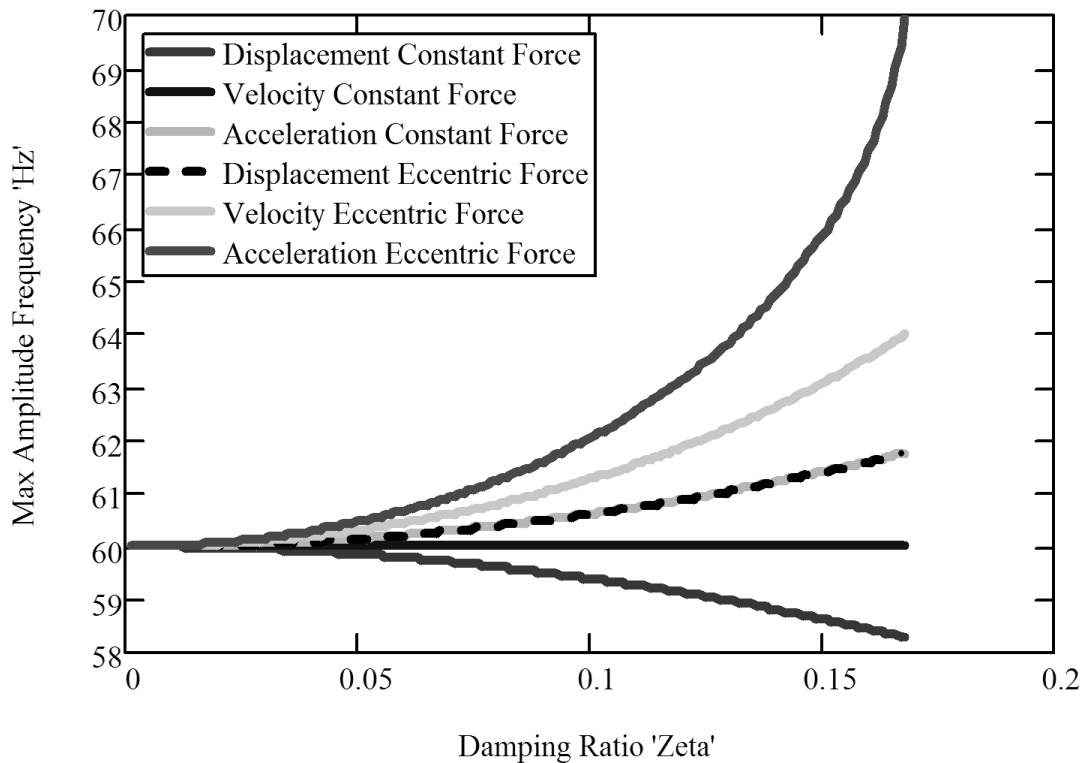


Figure 3.12. The change in frequency for the maximum amplitude cases for the constant force and eccentric driven systems, with varying damping.

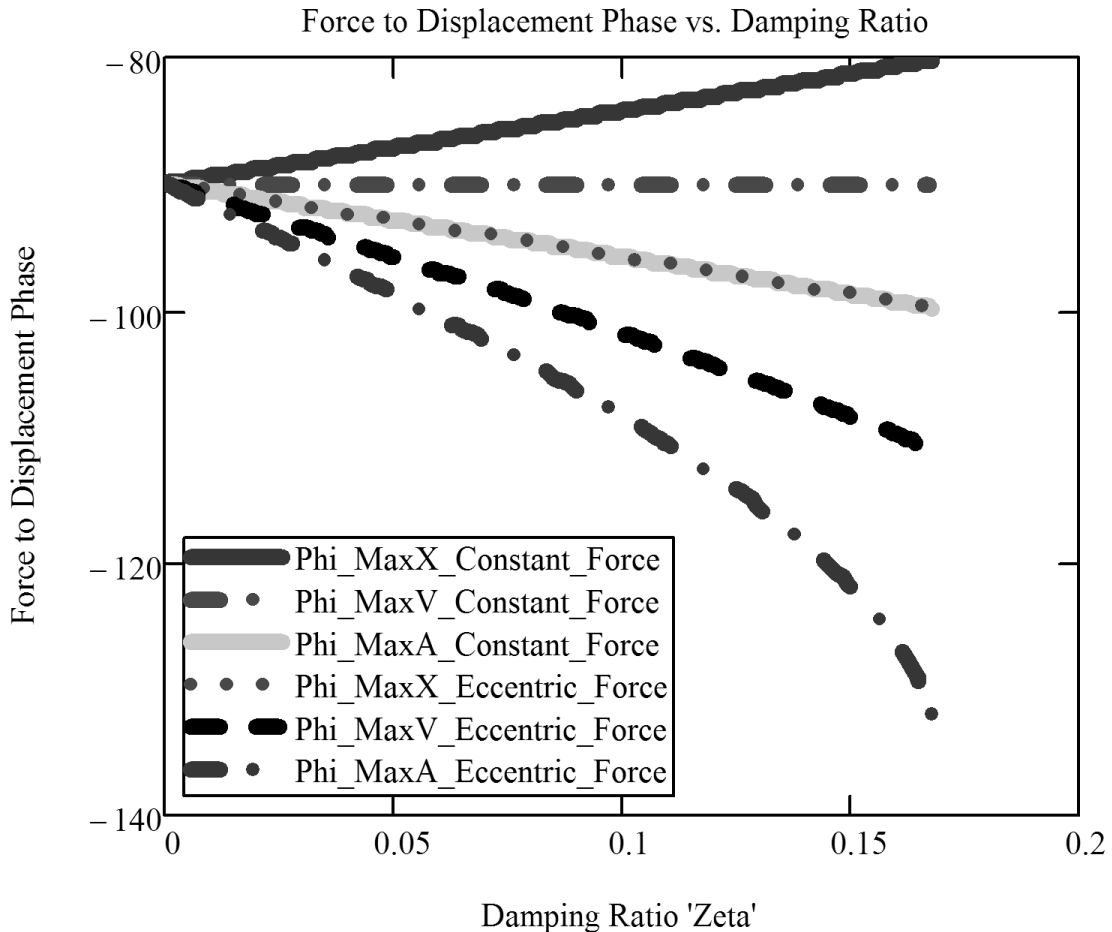


Figure 3.13. The phase change of the maximum displacement, velocity, and accelerating points are for both constant and eccentric driven force systems with varying damping.

Power Delivery and Measurement. The power used to drive the sonic drill is typically supplied by a diesel motor. The motor is delivering the power through a hydraulic system to the eccentric of the sonic drill. The sonic drill takes the energy input from the eccentric and turns this into useful work. The power exerted onto the system from the eccentrics is the actual physical power (in watts). However, this power is not always the power required to operate the system. The system can also store energy and reflect that energy back into the hydraulics, where pressures in the hydraulic lines may be higher than necessary for the actual work being done on the sonic drill. This condition

can be described by use of a power factor. The power factor is the relationship between the actual power 'P' (useful power utilized by the drill string) divided by the apparent power 'S' (generated power from the diesel engine), described in Figure 3.14.

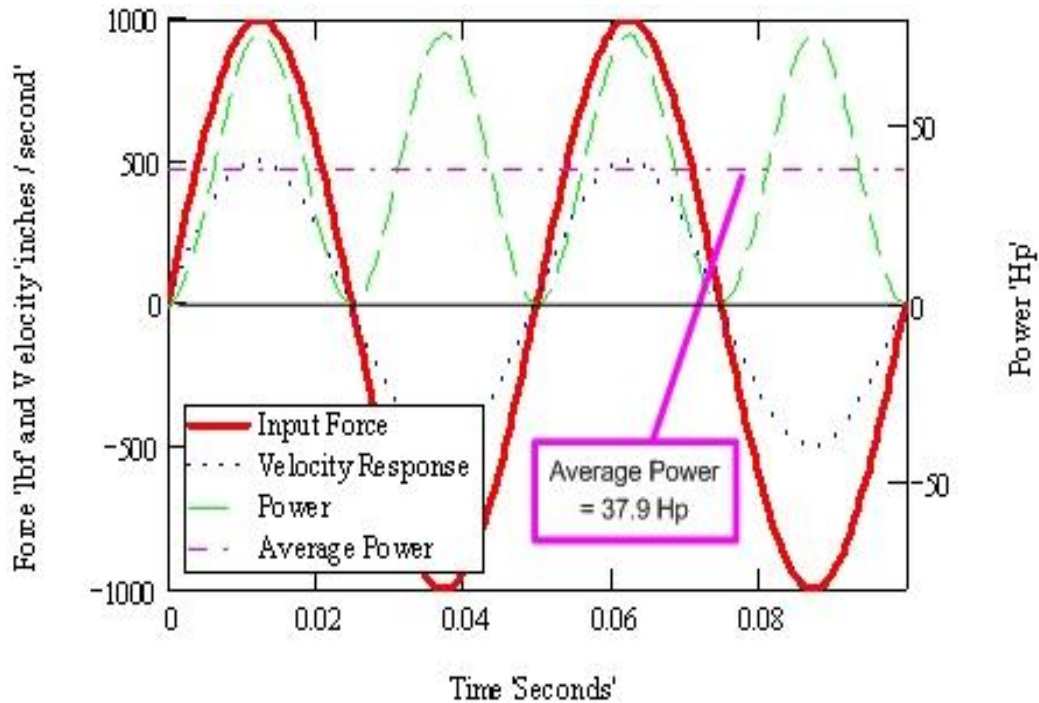


Figure 3.14. A typical system with a power factor of 1 should have the following measurement signal from the input force, velocity response, power and average power.

A system is said to have a power factor of 1 when the input force is in phase with the system's velocity, as shown in Figure 3.15, above. The typical system presented in Figure 3.14, uses an input force amplitude of 1,000 lbf to excite the system to exhibit a velocity amplitude of 500 inches/second. During this operating condition the actual power, shown in green, is always above zero (positive) and thus, always doing real work. The average power going into the system is a measure of the power that is doing physical work. However, when the system has a velocity phase lag or lead ' Φ_v ' respect to the

force, like that demonstrated in Figure 3.16, the actual average physical power becomes very low even though the diesel engine is still supplying the same amount of apparent power.

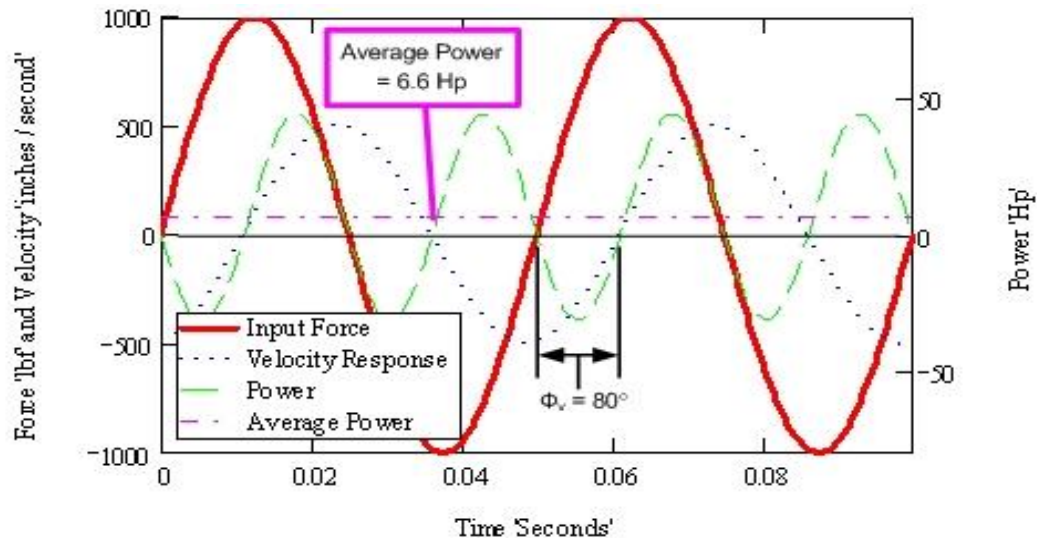


Figure 3.15. A typical system that has a lagging power factor of 0.174. this takes power away from the system to do actual work. The average power thus used by the system to do work has now dropped to 6.6 hp as opposed to a power factor 1 with 37.9 hp.

When the power factor approaches zero, the physical average power approaches zero, thus zero net physical work is done. At this point the system is merely storing and rejecting the energy back to the diesel engine and thus fighting the input power from the diesel engine and in turn performing no physical work. This particular concept becomes of great importance to the sonic drill industry because conventional knowledge states that the maximum power input to the sonic drill is a direct 1 to 1 correlation with the maximum power generated from the diesel engine. When the power factor goes to 0, displayed in Figure 3.16, the average power also heads to zero. At this operating point

the power from the source (diesel engine) is stored by the system and is thus rejected or released back to the source (diesel engine).

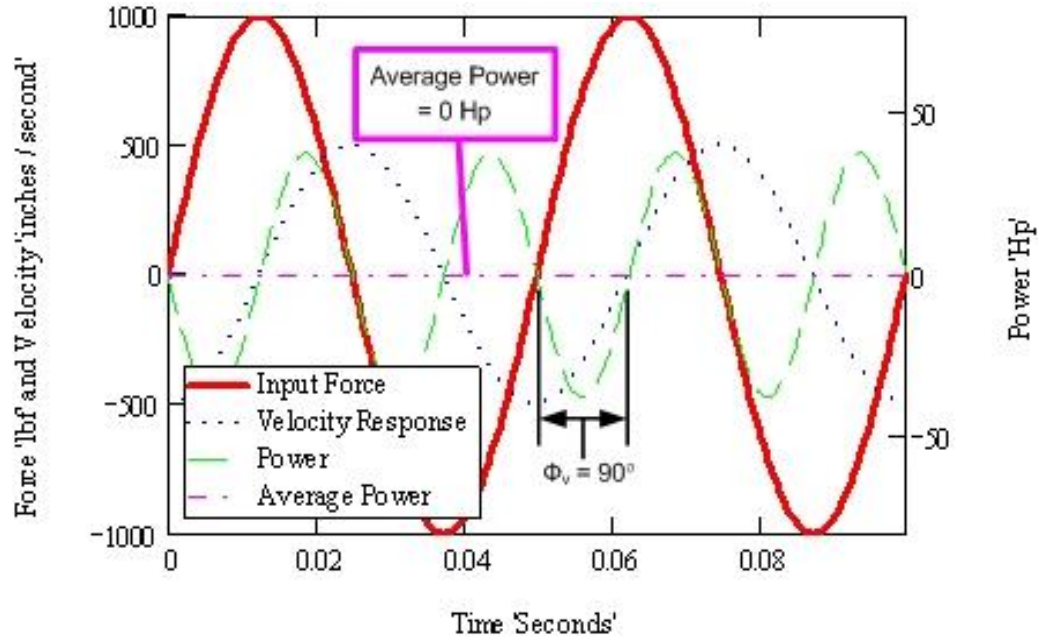


Figure 3.16. Force and velocity with a lagging power factor of 0. A typical system with a lagging power factor of 0. The system is storing power from the source and then rejecting it back to the source thus doing no actual work, results in to zero average power.

Power factor can also be defined as the relationship between the real ‘P’, reactive ‘R’, and apparent ‘S’ power, given in Equation 3.52 and has units of ‘Volt-Amps’ and also visualized in Figure 3.17. They are related to each other through the phase angle ‘ ϕ_v ’. The reactive power ‘R’, units of ‘Vars’, is the measure of the power that is stored and rejected back to the source (diesel engine) without being able to do physical work to the system.

$$S = P \cdot \cos(\phi_v) + R \cdot \sin(\phi_v) \cdot i \quad (3.52)$$

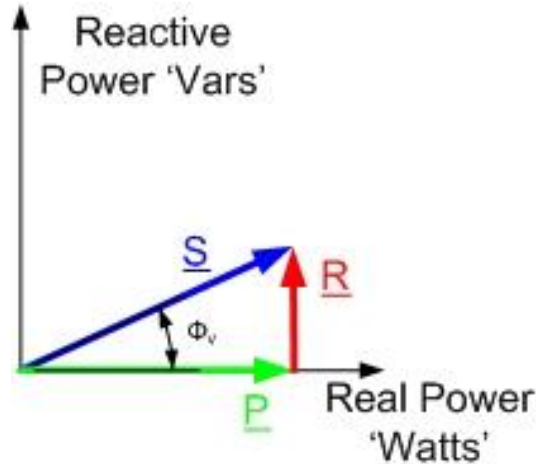


Figure 3.17. The relation between the real power 'P', reactive power 'R', and apparent power 'S' is shown above. As the angle ' Φ_v ' increases, more of the total power from the source (diesel engine) is rejected back to the source, which causes the available power 'P' to do real work to decrease, thus performing less work onto the system.

The phase angle ' Φ_d ' found earlier, the phase difference between the input force and the displacement, is related to ' Φ_v ' by a difference of 90 degrees. When ' Φ_d ' is -90 degrees ' Φ_v ' is zero degrees. While the system is operating in this condition, it is swapping energy back and forth between inertial and stored energy elements and cannot store energy thus rejecting energy back to the source. This condition is then the location of *the* maximum efficiency of the drill string with respect to energy generated by the diesel engine delivered to the drill string tip. The frequency at which this occurs is ' ω_n '. However, this frequency is not where the max power will be delivered to the drill string, which instead is ' ω_v '.

Real-time Monitoring of Drilling Condition

When drilling with a sonic drill, the operator has no indication of the type of media they are drilling because there is an incomplete understanding of how drilling media and operating controls affect the effectiveness of the sonic drill system and

ultimately the rate of penetration. However, by utilizing the models developed above as well as measurement variables above ground such as the: 1) sonic drill driver acceleration (or velocity), 2) sonic drill driver phase relative to the driver force, 3) sonic drill push or pull force, 4) length of drill pipe, 5) rate of rotation, as well as the 6) input force frequency and 7) amplitude of the sonic driver, the strata type being drilled can be predicted.

An artistic rendition of what a human machine interface would display as the final drilled strata to the operator while drilling is displayed in Figure 3.18.

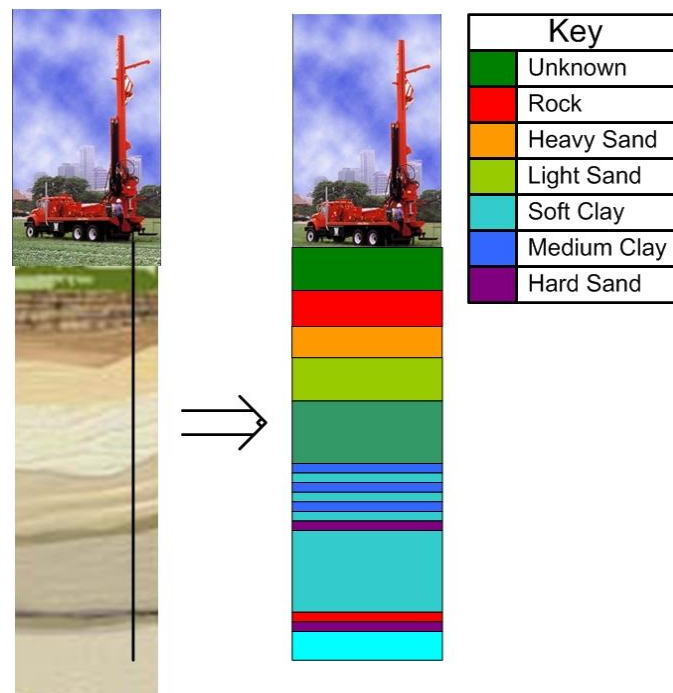


Figure 3.18. Hypothetical human machine interface drilled strata profile available to the sonic drill operator if the system response variables are used to model the strata.

The above variables are measured and used to determine the drilled strata. While drilling through different strata, the sonic drill will be affected by different damping and

spring rates at the drill bit due to the changing strata types. These changing damping and spring rates can be determined in real time from the above measured variables and the amount of energy that is being absorbed while drilling. The drill bit should be first taken off the bottom of the hole to obtain a baseline reading of the amount of damping along the length of the drill string. Additional damping due to drilling when not engaged and during drilling can be used to determine the strata being drilled through. Also, previously drilled strata can also be used to verify the damping along the length of the drill string, using equations 3.46 and 3.47. The strata equations will have to be verified with real world conditions, but such verification is beyond the scope of this research effort.

Choosing an Operational Resonant Mode

Because the sonic drill is a continuous system, operating at a variable frequency from ~ 60 Hz to 115 Hz, and typically has a changing input force relative to the frequency due to the eccentric drives, multiple axial resonant modes may be available for the operator to choose. A sonic drill operator knows that a higher force is generated at higher frequencies, and therefore more power can be used for drilling if a higher frequency mode is utilized. Using the developments discussed here damping along the length of the drill string may be located at higher frequency anti-nodes. At the lower frequency modes, it may be located at nodes, which could lead to additional energy delivered to the drill bit using a lower frequency mode. For example, in Figure 3.19, the high damping region is at the midpoint of the drill string. The low frequency mode shape has a node located at the midpoint of the drill string, while the higher frequency mode shape has an anti-node located at the mid-point of the drill string. Using equation 3.48,

damping is greater in the higher frequency mode than the low frequency mode. Thus, for an operational standpoint, more energy could be transmitted to the drill bit using a lower frequency mode than a higher frequency resonant mode.

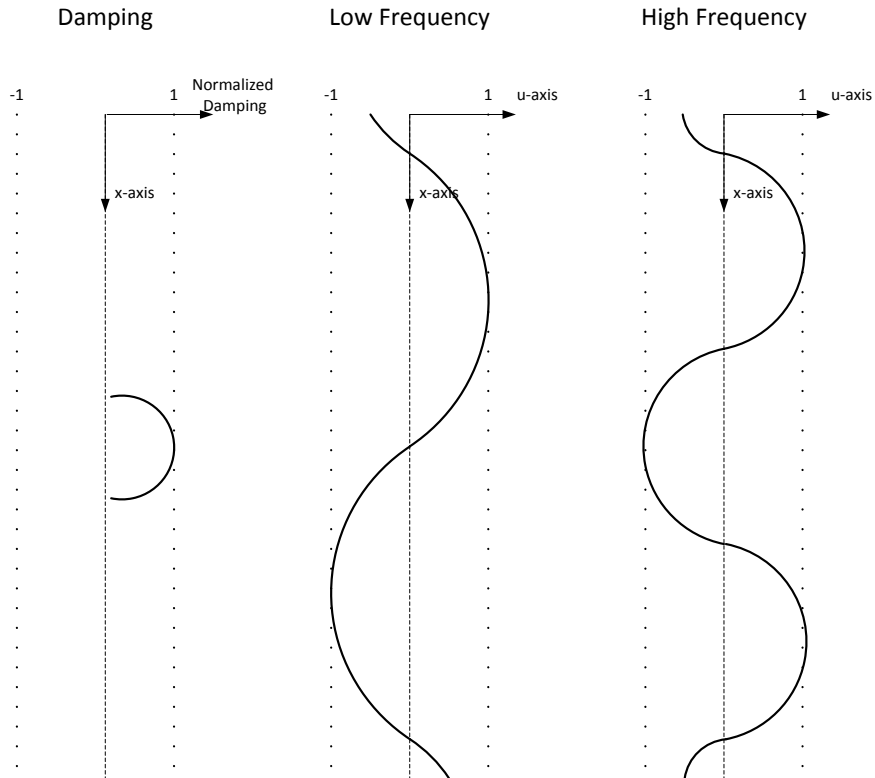


Figure 3.19. High and low frequency resonant mode shapes with corresponding damping along the length.

In choosing a resonant mode, the strain rate of the drilling action may affect performance at the drill bit. The drilling performance could ultimately be linked to equivalent damping and spring constants at the drill bit, but this modeling and verification is beyond the scope of this body of work.

CHAPTER 4

MATHEMATICAL MODELS

Introduction

This chapter outlines the mathematical model and variables that were used. The variables were outlined in Chapter 3, but this chapter goes through the design of experiments on selection of the variables and models used with defined variables to be investigated. Two types of models are used: 1) Closed form boundary solution and 2) Finite Element. Each modeling system has its advantages and disadvantages. The models used can generate data more rapidly and are therefore more useful to industry are chosen. For example the closed form boundary model is very efficient to solve the system response for all boundary conditions as well as changing lengths of the pipe, but cannot be easily adapted to solving with damping or restoring forces along the length of the drill string. A summary table, Table 4.1, of the assumptions of the various models presented in this body of work. These models included the closed form boundary system, finite element model, Bodine model, and the Rockefeller model. This table can be used as a reference for comparison between the different models.

Closed Form Boundary Solution

The closed form boundary model is to be used for the following real world situations. The two closed form models represent the following conditions:

- 1) Little to no damping (Represents the sonic drill when it is pulled off the bottom of the hole and the drill bit is not engaged with the strata);
- 2) Spring coupling at the drill bit with drill bit damping held constant (neglecting interactions of strata along the length of the drill string);
- 3) Damping due to the drill bit (represents the sonic drill while drilling assuming damping and coupling spring from the strata along the length of the drill string are negligible);

Table 4.1. Summary of Assumptions for the Different Models.

Assumptions	Models						
	Bodine's Model Equation 1.3	W.C. Rockefeller's Model	Closed form Boundary Condition			Finite Element Model	
			DOE 1	DOE 2	DOE 3	Resonant Modes	Damping and Coupling Along the Length
Plane Surfaces Remain Plane	<input checked="" type="checkbox"/>						<input checked="" type="checkbox"/>
Motion takes place in a single Plane	<input checked="" type="checkbox"/>						
Motion takes place in Multiple Planes						<input checked="" type="checkbox"/>	<input checked="" type="checkbox"/>
Forces act parallel to the direction along which the point of application moves	<input checked="" type="checkbox"/>						
Boundary Conditions are Ignored	<input checked="" type="checkbox"/>	<input checked="" type="checkbox"/>					
Damping and Restoring Forces along the length of the drill string are ignored			<input checked="" type="checkbox"/>	<input checked="" type="checkbox"/>	<input checked="" type="checkbox"/>		

The model will also be used to vary the boundary conditions such as masses of the sonic drill head and the drill bit as well as the sonic drill air spring rate. The drill string will be modeled at five different drill string lengths, which are 80 ft, 120 ft, 500 ft, 1000 ft, and 1500 ft. The two lower lengths are chosen because test data exists for these particular lengths of drill pipe. The two longer lengths are chosen because they are

typical lengths of drill pipe for sonic drills, but 1500 ft is currently the upper limits of a sonic drilling rig's depth capability. The sonic drill head mass, drill head spring rate, bit mass, bit spring rate, and bit damping are all listed in Table 3.5.

A full design of experiments will be performed over the listed variables. The total number of variable combinations are 8,100 from 5 pipe lengths, 3 sonic drill head masses, 3 sonic drill head springs, 5 sonic drill bit masses, 6 sonic drill bit spring rates, and 6 sonic drill bit damping constants. However, sonic drill bit spring rates and damping constants do not vary relative to one another, thus reducing the total solutions to 1350 combinations. To decouple the sonic drill bit spring rate and the drill bit damping, the first DOE holds the damping at the drill bit constant at 0.1 N*s/m .

To determine how drill bit damping affects the sonic drill system, a smaller DOE with fixed drill bit spring rate while varying the drill bit damping was performed. This drill bit damping DOE was performed with a 500 ft. sonic drill string length.

Another critical item is that the damping at the drill bit must be less than the critical damping to enable the oscillation of the bit. If the damping is greater than the critical damping, then the drill bit essentially becomes fused with the strata and the boundary conditions change. Critical damping for a single degree of freedom system was determined as shown in Equation 3.8, above. Similar methods were applied to determine critical damping at the drill bit; however boundary equations are used to determine the critical damping at the drill bit. The equations originally shown as Equation 3.33 are displayed again and referenced as equation 4.1.

$$\begin{aligned}
E_{ds}A_{ds} \frac{\partial u(0, t)}{\partial x} &= m_{sh} \frac{\partial^2 u(0, t)}{\partial t^2} - F_o \sin(\omega_f t) \\
&+ c_{sh} \frac{\partial u(L_{ds}, t)}{\partial t} + k_{sh} u(0, t) && \text{Top Boundary Condition} \\
-E_{ds}A_{ds} \frac{\partial u(L_{ds}, t)}{\partial x} &= -m_{bit} \frac{\partial^2 u(L_{ds}, t)}{\partial t^2} - c_{bit} \frac{\partial u(L_{ds}, t)}{\partial t} - k_{bit} u(L_{ds}, t) && \text{Tip Boundary Condition}
\end{aligned}
\tag{4.1}$$

Using the equations specified in equation 4.1 and setting them equal to zero while looking at the homogenous case ($F_o=0$) The critical damping constant can be found by solving the equations for the damping constant with an assumed solution for the governing differential equation of motion given in equation 4.2.

$$u(x, t) = Ae^{st} B e^{\frac{s}{c}x} \tag{4.2}$$

The critical damping constants for the sonic drill head and drill bit are given in equation 4.3 and 4.4, respectively.

$$c_{cr} = 2m_{sh} \sqrt{\frac{k_{sh}}{m_{sh}}} + \frac{E_{ds}A_{ds}}{c} \tag{4.3}$$

$$c_{cr} = 2m_{bit} \sqrt{\frac{k_{bit}}{m_{bit}}} + \frac{E_{ds}A_{ds}}{c} \tag{4.4}$$

All the damping values found were under the critical damping values of the system boundary conditions. The generated data will be used to give indications of the sensitivity of the system to each variable with respect to the resonant frequency, drill bit amplitude, and the ratio of amplitude of the sonic drill head with the drill bit. The drill bit displacement amplitude and the ratio of amplitude of the sonic drill head with the drill bit are assumed to be the most important parameters with respect to the rate of penetration. When the sonic drill bit displacement amplitude is less relative to the sonic

drill head greater amounts of energy can be delivered and stored in the drill bit to perform drilling. The variables examined will include the sonic drill head vibration velocity (at the head) as well as the input force and phase of the drill string. Other variables examined include the relative displacement at the top of the drill string (drill head) and at the drill bit.

The model was solved using code written in MATLAB[®] and a copy of the code is documented in Appendix A. The code iterates and solves the boundary system problem for the resonant frequencies and calculates the four unknowns, 'A_o', 'B_o', 'C_o', and 'D_o' as described in equation 3.28, above. The solutions found for all the sonic drill lengths and modes were then exported to an Excel file.

Commercially available design of experiments software (Design – Expert 8.0.7.1) was used to perform the design of experiments. Some of the relationships were plotted in Excel for a graphic representation and to further verify the DOE solutions found by the Design – Expert software.

Finite Element Method

The finite element model (FEM) characterizes the differences of various drilling strata along the length of the drill pipe. The FEM will be used to show the effect of varying relative effects of restoring forces onto the drill pipe along its length from the strata. The changing strata conditions are outlined in Figure 3.9, which includes evaluation of both spring rate and damping.

All conditions are important to model to quantify all operational modes of the sonic drill system, but the finite element model is more efficient and more easily implemented than the finite difference method. During this analysis the strata variables along the length as well as the drill bit interaction will be investigated within reason with respect to the drill chosen for this experiment. The phase angle between the input force and the velocity of the sonic drill head will be used as a metric to monitor these properties at above ground measurement points: one of the major breakthroughs of this research. The drill bit velocity amplitude will also be recorded and used for comparison.

As previously mentioned, the finite element method is a well-known technique to achieve approximate results of an actual system. These approximate results greatly depend on the assumptions chosen and how well the modeling system represents the actual system. The finite element method was used instead of a finite difference method, because it required less computational power. A modal analysis using ANSYS® will be used as the commercially off the shelf (COTS) finite element method.

ANSYS® will also be used to determine the resonant effects of lateral motion of the sonic drill system. By performing a modal analysis using a three dimensional model the relative influence of the lateral to the axial modes can be determined. If there is interaction between the lateral and axial resonant modes, it will be apparent in the modal analysis.

The models performed using a Finite Element Analyses are as follows:

- 1) Modal analysis including all resonant modes (axial, lateral, torsion, and breathing) from 60 – 120 Hz using drill lengths from 60 – 1000 ft. The drill rig and string conditions are the same as outlined in Table 3.1;
- 2) A comparison of lateral modes to axial modes will be demonstrated using a modal analysis to show that unless a lateral mode is excited on resonance, little excitation deflection is generated, even with large loads.
- 3) No damping or spring coupling along the length, but with boundary conditions to verify the model from the boundary value solutions with a drill string length of 250 ft;
- 4) Uniform spring coupling along the length of the drill string;
- 5) Varying damping along the length of the drill string as outlined in Figure 3.9;
- 6) Uniform damping and spring coupling along the length of the drill string; and
- 7) Varying damping along the length of the drill string as outlined in Figure 3.9.

CHAPTER 5

MODEL RESULTS

Introduction

This chapter describes the mathematical model results and conditions that were used to generate the results. Two types of models are used: 1) Closed form boundary condition solution and 2) Finite Element. The closed form boundary condition solution results are first described and the significant variables are determined out of the eight independent variables included in the design of experiments. The resonant modes were listed for drill string lengths from 50 ft to 1000 ft. The finite element model results are then listed for constant, linear, step, and impulse damping and restoring loads along the length. The level of significance is listed for each variable examined.

Boundary Condition Solution

The boundary condition solutions mapped the sensitivities of the parameters specified in Table 5.1, with respect to: 1) Ratio of sonic drill head to drill bit amplitude, 2) resonant frequency, and 3) drill bit amplitude.

Three different design of experiments were chosen to determine the different variable sensitivities with respect to the above 3 criteria. The boundary condition solution results include solutions from variable relationship curves using Excel as well as significance values for the design variables as calculated from a design of experiments software. By using the boundary condition equations, relations for all non-damping

conditions were generated over 5 different sonic drill lengths. The boundary condition equations were then used to determine the combined significance of the drill bit damping and spring rate using data generated for a drill string length of 1500 ft. Lastly, the boundary condition model was used to determine the relative significance of drill bit damping.

Table 5.1. Design of Experiments Used for the Boundary Conditions Solutions

Variable	Variable Designation	Design of Experiment		
		1	2	3
Sonic Drill Head Mass	A	X	X	X
Sonic Drill Head Spring Rate	B	X	X	X
Sonic Drill Bit Mass	C	X	X	X
Sonic Drill Bit Spring Rate	D	X		
Sonic Drill Bit Damping	E			X
Strata Types (Combination Bit Rate and Damping)	F		X	
Resonant Mode	G	X*	X	X
Sonic Drill Length	H	X		
* Overlap in data and not used. Cannot generate curves over multiple drill lengths.				

The first DOE was to generate data and determine the variable sensitivities using a constant drill bit damping value, while iterating over all the other available variables listed in Table 5.1. A second DOE was to generate data and determine the sensitivities for as many variables while including damping coupled with the particular spring rates associated with different strata types. A third DOE was also used to generate data and determine the sensitivities for as many variables while including the drill bit damping and holding the drill bit spring rate constant. Through the combination of all three DOEs the

variables can be compared with respect to each other and the highest-impact variables will be determined.

Conditions except Damping

First a Design of Experiments (DOE) was performed over the following system design variables: 1) sonic drill head mass, 2) sonic drill head spring rate, 3) sonic drill bit spring rate, 4) sonic drill bit mass, and 5) resonant mode. The design variables are outlined in Table 3.5 and these variables tested by the model at sonic drill lengths of 80 ft, 120 ft, 500 ft, 1000 ft, and 1500 ft. Under this DOE, the drill bit damping was held constant at 0.1 N*s/m. Solutions were found at frequencies 1 Hz below the resonant frequency, because the damping was very low. Generation of all results at 1 Hz below the resonant frequency gave realistic relationships of the relative amplitude of the sonic drill head and the drill bit amplitude. It also provided a constant offset to show the difference of the changing amplitude between the drill bit and the sonic drill head. The three variables that were assumed to be influenced by the boundary condition variables were: 1) Ratio of the sonic drill head to drill bit amplitude, 2) Resonant Frequency, and Drill bit amplitude. In addition the mode shape results were found for each drill string length for frequencies between 60 and 120 Hz. The mode shapes are described by the number of anti-nodes present in the axial mode shape. An example of a resonant mode of 6 is displayed in Figure 5.1, below.

The first variable measured was the resonant frequency including the above variables which were analyzed by the DOE software. A full factorial DOE was performed and all factors and combinations of factors were investigated. The most

significant variables were found to be, in the order of most important to least important:

- 1) Combination of the sonic drill head mass and the sonic drill length,
- 2) Sonic drill length,
- 3) Sonic drill length and the sonic drill bit spring rate,
- 4) Sonic drill head mass,
- and 5) Combination of the sonic drill head mass and the sonic drill bit spring rate.

The results of the DOE are listed in Table 10.1 and a summary of the most influential variables are displayed in Table 5.2. The resonant mode number was found to be aliased, meaning that it was not found to have any significance or bearing on the model. This is because there was significant overlap of the frequencies with various resonant modes and drill string lengths, that a model for the modes is not possible. A half-normal plot of the DOE results also shows the same results, but in a more easily readable format, Figure 5.2.

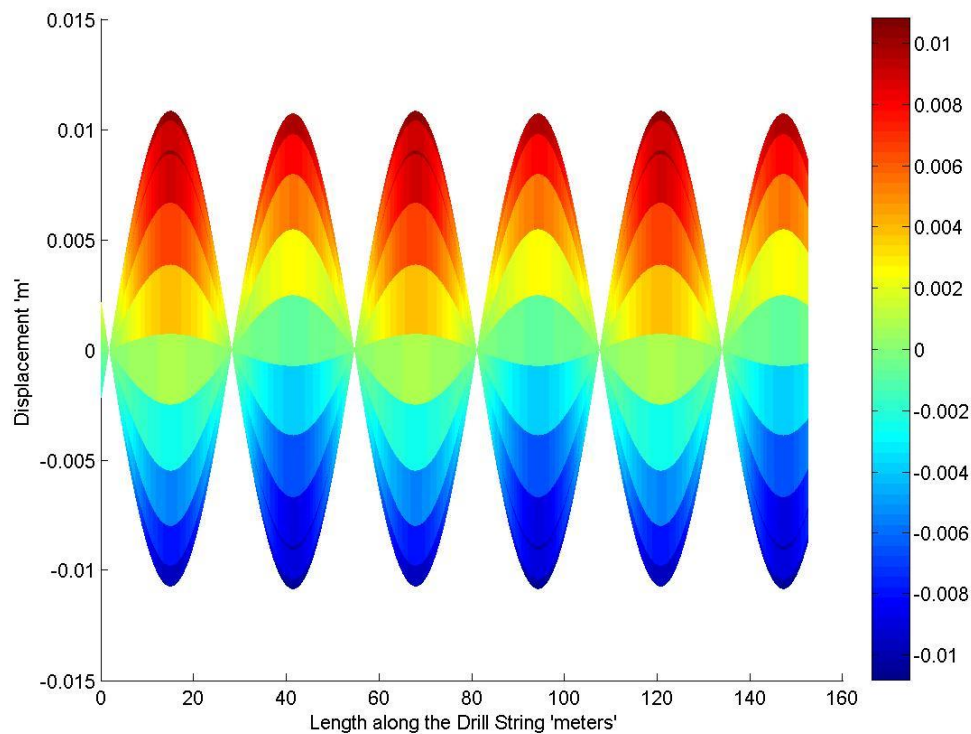


Figure 5.1. Example of an Axial Resonant Mode Shape of 6.

Table 5.2. DOE results for factors of influence of the resonant frequency.

Factor	Sum of Squares	Mean Square	Prob > F
Model	1.91E+05	3895.46	< 0.0001
A-Sonic Drill Head Mass	11575.25	5787.63	< 0.0001
D-Sonic Drill Bit Rate	6178.26	1235.65	0.0034
E-Sonic Drill Length	38874.83	9718.71	< 0.0001
AD	12634.82	1263.48	< 0.0001
AE	1.00E+05	12525.22	< 0.0001
DE	54694.43	2734.72	< 0.0001

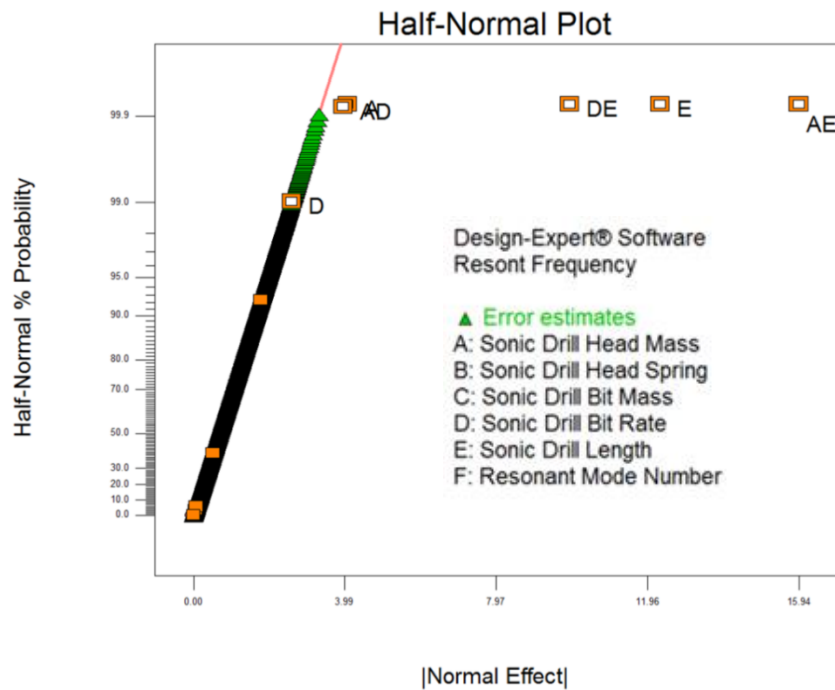


Figure 5.2. Half - Normal Plot of the DOE results for the significant factors that effect the sonic drill axial resonant frequency.

The next variable that was used to determine important factors of influence was the sonic drill bit amplitude. The results of the DOE are tabulated in Table 10.2 and a summary of the most influential variables are displayed in Table 5.3. The resonant mode number was found to be aliased, meaning that it was not found to have any significance or bearing on the model. The half – normal plot is displayed as Figure 5.3. The most

prominent factor that influences the drill bit amplitude is the combination of the sonic drill bit spring rate and the drill length.

Table 5.3. DOE results for factors of influence of the drill bit amplitude.

Factor	Sum of Squares	Mean Square	Prob > F
A-Sonic Drill Head Mass	1369.68	684.84	0.0012
B-Sonic Drill Head Spring	669.02	334.51	0.0377
C-Sonic Drill Bit Mass	1659.13	414.78	0.0027
D-Sonic Drill Bit Rate	11678.84	2335.77	< 0.0001
E-Sonic Drill Length	4773.97	1193.49	< 0.0001
AB	532.65	133.16	0.2654
AC	2391.26	298.91	0.0029
AD	4046.3	404.63	< 0.0001
AE	12081.66	1510.21	< 0.0001
BC	882.06	110.26	0.3731
BD	5211.42	521.14	< 0.0001
BE	3809.03	476.13	< 0.0001
CD	6364.75	318.24	< 0.0001
CE	5172.35	323.27	< 0.0001
DE	31102.44	1555.12	< 0.0001
ABC	2251.26	140.7	0.1414
ABE	7326.46	457.9	< 0.0001
ACD	7635.29	190.88	0.0007
ACE	17790.77	555.96	< 0.0001
BCE	5661.11	176.91	0.0063
BDE	15627.46	390.69	< 0.0001
CDE	25705.99	321.32	< 0.0001
ABCE	15153.67	236.78	< 0.0001

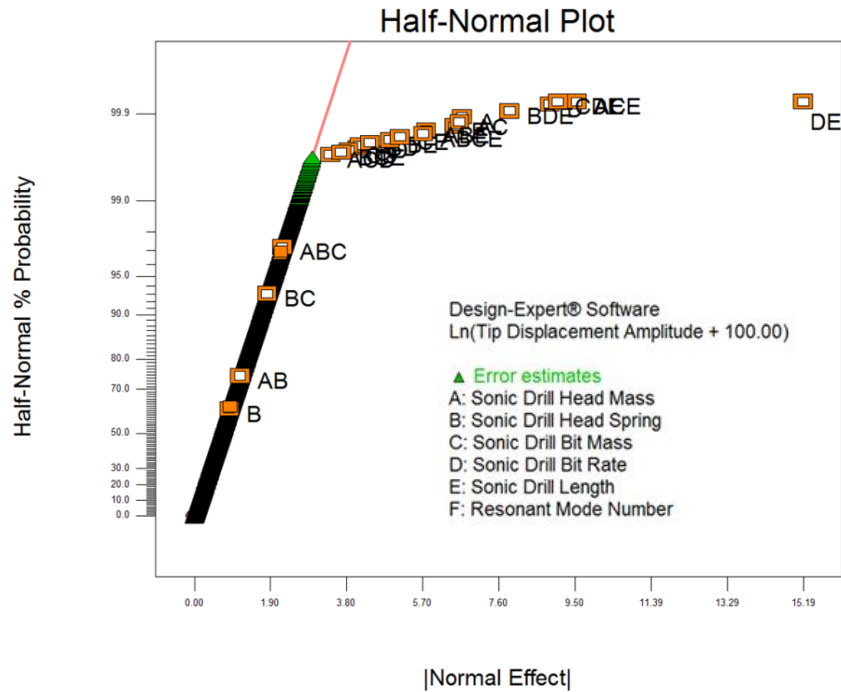


Figure 5.3. Half - Normal Plot of the DOE results for the significant factors that effect the sonic drill bit amplitude.

The next variable that was used to determine important factors of influence was the ratio of the sonic drill head amplitude to the sonic drill bit amplitude. The results of the DOE are tabulated in Table 10.3 and a summary of the most influential variables are displayed in Table 5.4. The resonant mode number was found to be aliased, meaning that it was not found to have any significance or bearing on the model. The half – normal plot is displayed as Figure 5.4. The most prominent factor that influences the drill bit amplitude is the combination of the sonic drill bit spring rate and the drill length.

Table 5.4. DOE results for factors of influence of the ratio of the sonic drill head to the drill bit amplitude.

Factor	Sum of Squares	Mean Square	Prob > F
Model	6.51E+06	1.33E+05	< 0.0001
A-Sonic Drill Head Mass	29486.69	14743.34	< 0.0001
D-Sonic Drill Bit Rate	6.25E+06	1.25E+06	< 0.0001
E-Sonic Drill Length	12218.72	3054.68	< 0.0001
AD	1.13E+05	11310.93	< 0.0001
AE	10887.52	1360.94	< 0.0001
DE	67731	3386.55	< 0.0001

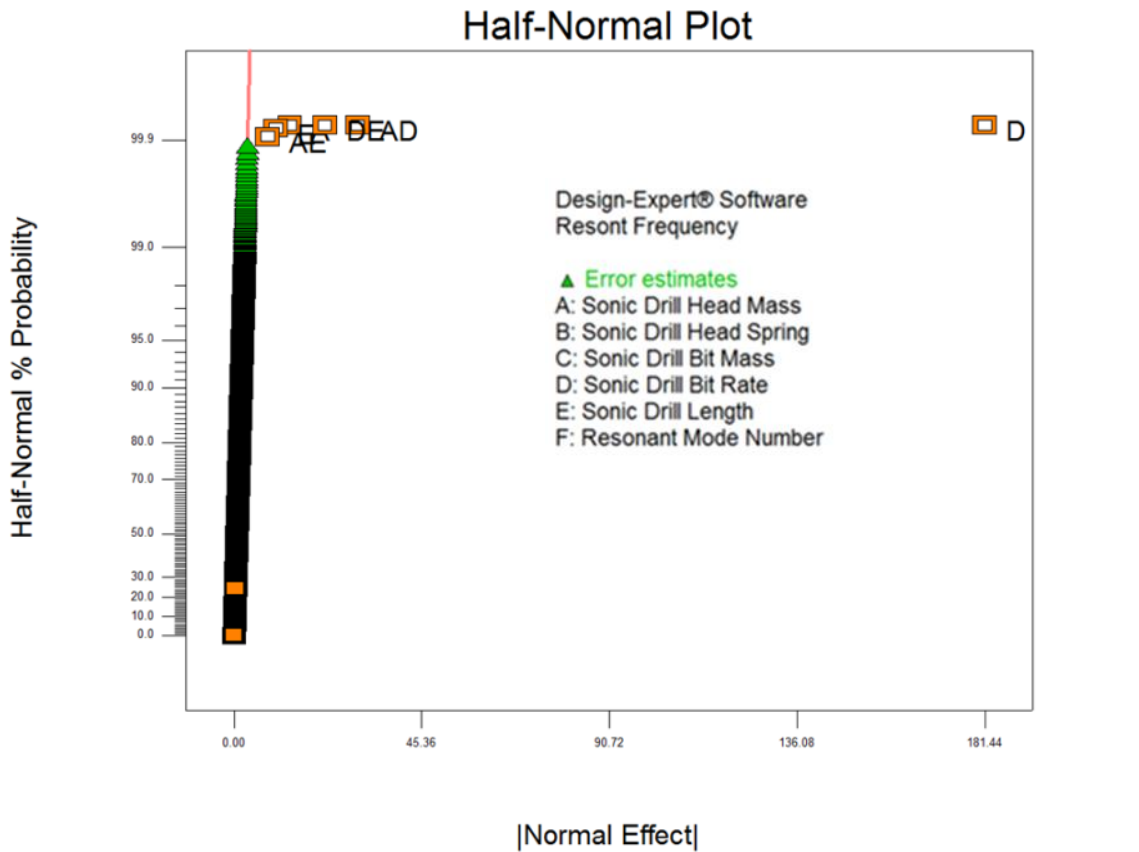


Figure 5.4. Half - Normal Plot of the DOE results for the significant factors that effect the ratio of the sonic drill head amplitude to the sonic drill bit amplitude.

The design of experiments calculated the significant variables that influence the factors specified. The sonic drill bit rate was the first variable in particular that showed great significance throughout the models. A few plots of the sonic drill head to drill bit amplitude ratio vs. the drill bit spring rate can show the magnitude of the change of the response, this is shown in Figure 5.5(a) and Figure 5.5(b). The shift to higher numbers indicates that the amplitude of the sonic drill head is large compared to the amplitude of the drill bit. When the spring rate becomes too great, the sonic drill bit end becomes fundamentally ‘fused’ with the soil, creating an anti-node at the tip. Figure 5.5(a), displays the response with various drill bit masses and a sonic drill head mass of 500 kg. Figure 5.5(b), displays the response change with various drill bit masses and a sonic drill head mass of 2000 kg.

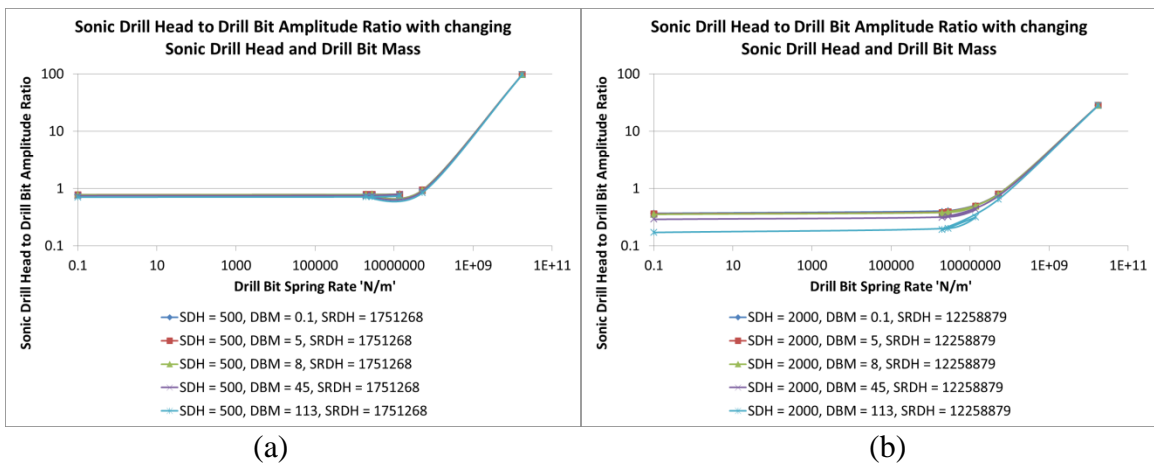


Figure 5.5. (a) Sonic drill head to drill bit amplitude ratio vs. drill bit spring rate with different curves with various drill bit masses, 500 kg sonic drill head mass, and 1,751,268 N/m sonic drill head spring rate. (b) Sonic drill head to drill bit amplitude ratio vs. drill bit spring rate with different curves with various drill bit masses, 2000 kg sonic drill head mass, and 12,258,879 N/m sonic drill head spring rate.

After the greatest influential factor, drill bit spring rate, has been fixed, the remaining individual factors can be examined. A few plots of the sonic drill head to drill bit amplitude ratio vs. the sonic drill head spring rate can show the magnitude of the change of the responses of the other individual variables, Figure 5.6(a) and Figure 5.6(b). Figure 5.6 shows that the sonic drill head spring rate has no significant affect (no change in response of the sonic drill head to drill bit amplitude ratio). The sonic drill mass has higher significance (magnitude change) of the sonic drill head to drill bit amplitude ratio than the drill bit spring rate (assuming the sonic drill spring rate doesn't go high enough to fuse the drill bit in an anti-node condition).

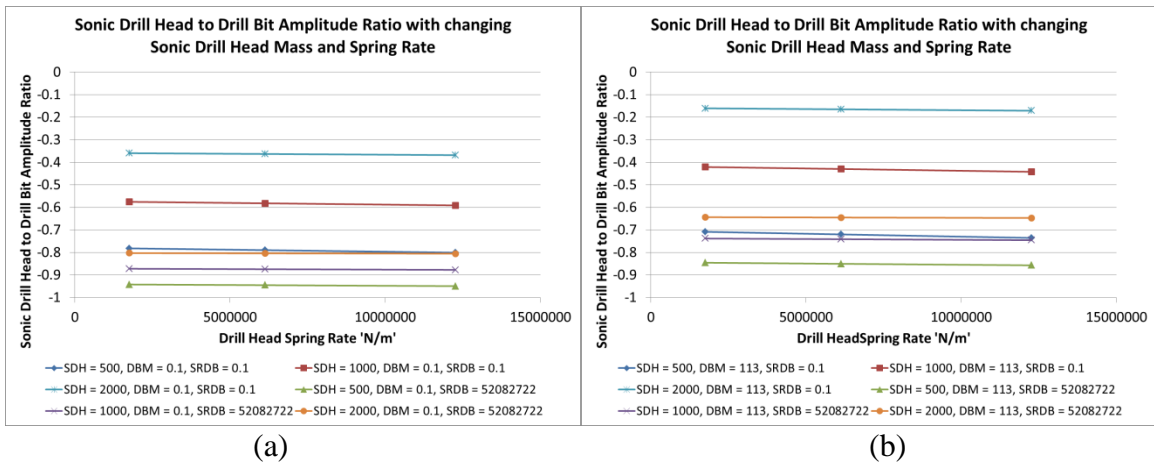


Figure 5.6. (a) Sonic drill head to drill bit amplitude ratio vs. drill head spring rate with different curves with drill bit mass of 0.1 kg, various sonic drill head masses, and the extreme sonic drill head spring rates. (b) Sonic drill head to drill bit amplitude ratio vs. drill head spring rate with different curves with drill bit mass of 113 kg, various sonic drill head masses, and the extreme sonic drill head spring rates.

Another plot was generated to show the contrast between the sonic drill head mass and the drill bit mass. In Figure 5.7, the different curves are for the different sonic drill bit masses from 0.1 kg to 113 kg. The sonic drill bit mass has less effect than the mass of the sonic drill head.

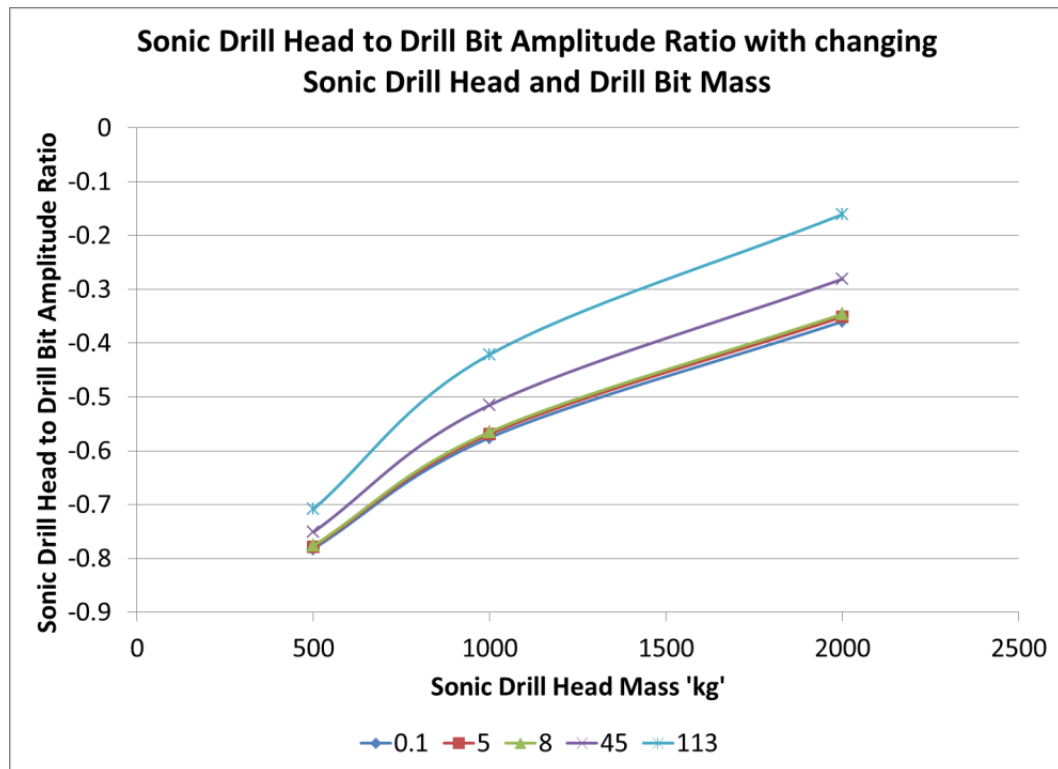


Figure 5.7. Sonic drill head to drill bit amplitude ratio vs. sonic drill head mass with different curves for varying drill bit masses.

The results of the DOE software correlate well with the curves of the raw data for the ratio of the sonic drill head to drill bit amplitude ratio. The other models of drill bit amplitude and resonant frequency also correlated with the raw data were assumed and were not verified against the raw data curves.

Variable Effects of the Strata Being Drilled

The data for this experiment was generated using the same model as previous, except that the damping was not held constant, but with the values calculated for each of the materials as given in Table 3.5. The solutions used in the DOE were generated using a drill length of 1500 ft. Because there was only one drill length used, the resonant mode significance was also found. Thus, the variables of influence that were compared for this DOE were 1) Sonic drill head mass, 2) Sonic drill head spring, 3) Sonic drill bit mass, 4) Resonant mode number, and 5) Strata Type. The three variables that were assumed influenced by the boundary condition variables were: 1) Ratio of the sonic drill head to drill bit amplitude, 2) Resonant Frequency, and 3) Drill bit amplitude. These were the same variables as used previously for the low-damped case.

The first variable of measure was the resonant frequency and the above variables were analyzed by the DOE software. A full factorial DOE was performed and all the factors and combinations of the factors were investigated (3510 possible combinations). The most significant variables were found to be, in the order of most important to least important: 1) Resonant mode, 2) Strata types, 3) Combination of sonic drill head mass, sonic drill length, and the sonic drill bit spring rate, 4) Combination of the sonic drill head mass and the strata type and 5) Combination of the sonic drill head mass and the resonant mode. The results of the DOE are listed in Table 10.4 and the summary of the most influential variables are displayed in Table 5.5. The resonant mode number was not found to be aliased, as was the case before, because only one drill string length was used.

A half-normal plot of the DOE results also shows the same results, but in an easily readable format, Figure 5.8.

The next variable used to determine important factors of influence was the sonic drill bit amplitude. The results of the DOE are tabulated in Table 10.5 and the summary of the most influential variables are displayed in Table 5.6. The most significant variables were found to be, in the order of most important to least important: 1) Resonant mode, 2) Sonic drill head mass and the resonant mode, 3) Strata types, 4) Sonic drill head mass, 5) Combination of the sonic drill head mass and the strata type. The half – normal plot is displayed as Figure 5.9.

Table 5.5. DOE results for factors of influence of the resonant frequency.

Factor	Sum of Squares	Mean Square	Prob > F
Model	3.59E+06	6.8E+04	< 0.0001
A-Sonic Drill Head Mass	1.54E+03	7.7E+02	< 0.0001
C-Sonic Drill Bit Mass	3.66E+02	9.1E+01	< 0.0001
D-Resonant Mode Number	9.18E+05	7.6E+04	< 0.0001
E-Strata Types	7.65E+02	1.5E+02	< 0.0001
AC	2.42E+02	3.0E+01	< 0.0001
AD	5.30E+02	2.2E+01	< 0.0001
AE	6.39E+02	6.4E+01	< 0.0001
CD	1.24E+02	2.6E+00	0.0010
CE	1.73E+02	8.6E+00	< 0.0001
ACE	1.75E+02	4.4E+00	< 0.0001

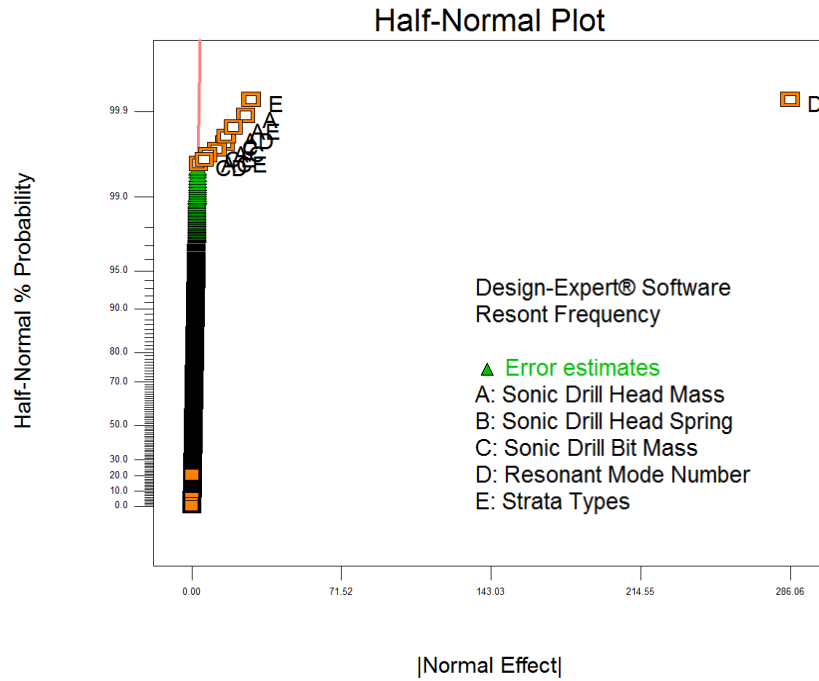


Figure 5.8. Half - Normal Plot of the DOE results for the significant factors that effect the sonic drill axial resonant frequency.

Table 5.6. DOE results for factors of influence of the drill bit amplitude.

Factor	Sum of Squares	Mean Square	Prob > F
Model	1.23E+00	2.30E-02	< 0.0001
A-Sonic Drill Head Mass	1.40E-02	6.78E-03	0.0797
D-Resonant Mode Number	1.00E-01	8.48E-03	0.0002
E-Strata Types	3.00E-01	5.90E-02	< 0.0001
AD	5.70E-01	2.40E-02	< 0.0001
AE	2.40E-01	2.40E-02	< 0.0001

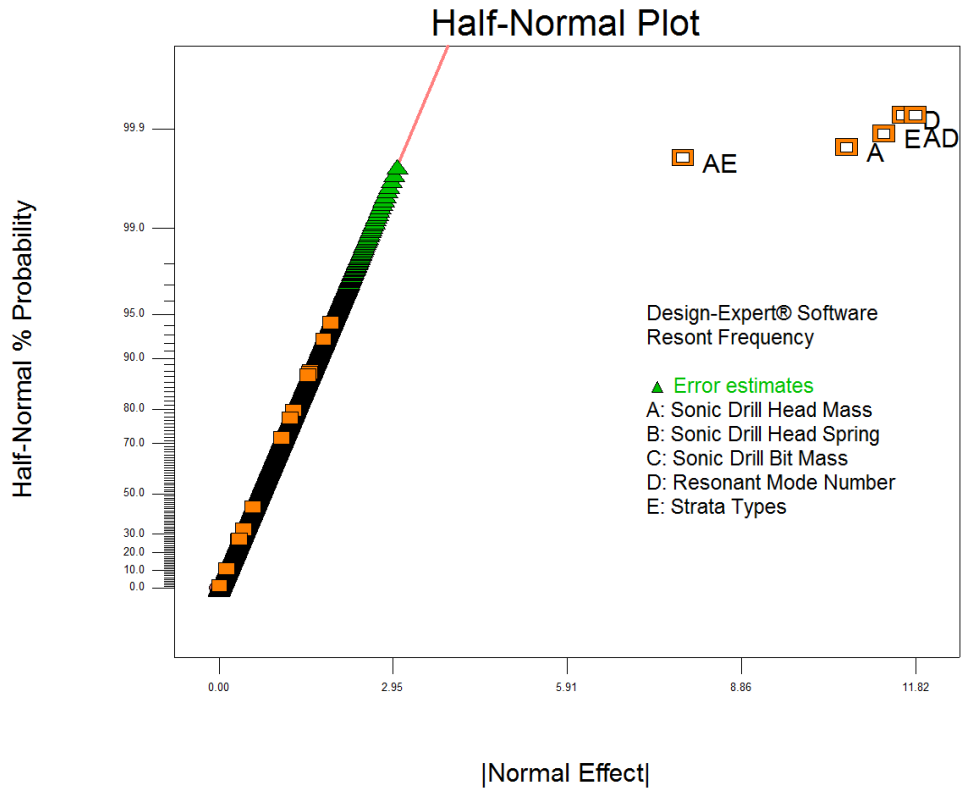


Figure 5.9. Half - Normal Plot of the DOE results for the significant factors that effect the sonic drill bit amplitude.

The next variable used to determine important factors of influence was the ratio of the sonic drill head amplitude to the sonic drill bit amplitude. The results of the DOE are listed in Table 10.6 and the summary of the most influential variables are displayed in Table 5.7. The half – normal plot is displayed as Figure 5.10. The most prominent factor that influences the drill bit amplitude is the strata type.

Table 5.7. DOE results for factors of influence of the ratio of the sonic drill head to the drill bit amplitude.

Factor	Sum of Squares	Mean Square	Prob > F
Model	3.59E+06	6.77E+04	< 0.0001
A-Sonic Drill Head Mass	2.02E+04	1.01E+04	< 0.0001
D-Resonant Mode Number	7.82E+04	6.52E+03	< 0.0001
E-Sonic Drill Bit Damping Value	3.42E+06	6.84E+05	< 0.0001
AD	2.04E+04	8.50E+02	< 0.0001
AE	1.31E+04	1.31E+03	< 0.0001

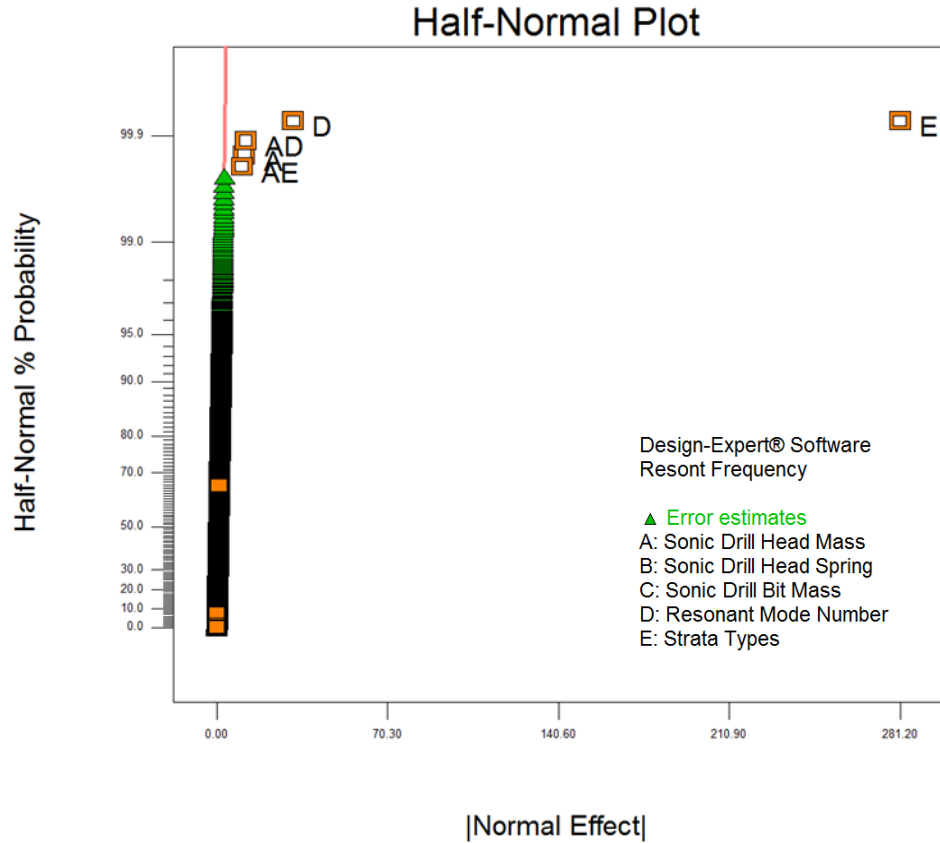


Figure 5.10. Half - Normal Plot of the DOE results for the significant factors that effect the ratio of the sonic drill head amplitude to the sonic drill bit amplitude.

Variable Effects of the Strata Damping

The data for this experiment was generated using the same model as those previously, except that the drill bit spring rate was held constant at 52,082,722 N/m. The drill string length was also held constant at 1,500 ft. The damping values were defined at values of 0.01; 0.1; 5,526; 11,695; 4,696; and 24,195 N*s/m. Because there was only one drill length used, the resonant mode significance was also found. The variables of influence that were compared for this DOE were 1) Sonic drill head mass, 2) Sonic drill head spring rate, 3) Sonic drill bit mass, 4) Resonant mode number, and 5) Drill bit damping. The three variables that were assumed to be influenced by the boundary condition variables were: 1) Ratio of the sonic drill head to drill bit amplitude, 2) Resonant Frequency, and 3) Drill bit amplitude.

The first variable of measure was the resonant frequency and the above variables were analyzed by the DOE software. A full factorial DOE was performed and all the factors and combinations of the factors were investigated (3510 possible combinations). The most significant variables were found to be, in the order of most important to least important: 1) Resonant mode, 2) Sonic drill bit mass, 3) Combination of sonic drill head mass, sonic drill length, and the sonic drill bit mass, and 4) Sonic drill head mass. The results of the DOE are listed in Table 10.7 and the summary of the most influential variables are displayed in Table 5.8. The resonant mode number was found to not be aliased, as was the case before, because only one drill string length was used.

Table 5.8. DOE results for factors of influence of the resonant frequency.

Factor	Sum of Squares	Mean Square	Prob > F
Model	9.98E+05	3.84E+04	< 0.0001
A-Sonic Drill Head Mass	3.59E+01	1.79E+01	< 0.0001
C-Sonic Drill Bit Mass	1.63E+02	4.08E+01	< 0.0001
D-Resonant Mode Number	9.82E+05	8.19E+04	< 0.0001
AC	2.19E+02	2.73E+01	< 0.0001

A half-normal plot, Figure 5.11, of the DOE results also shows the same results.

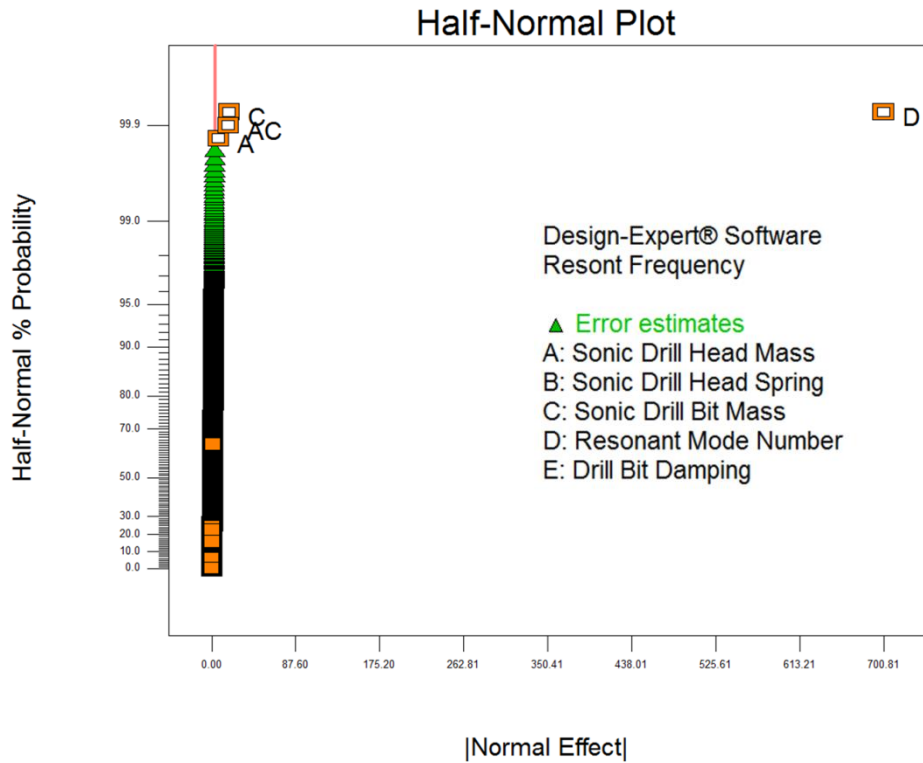


Figure 5.11. Half - Normal Plot of the DOE results for the significant factors that effect the sonic drill axial resonant frequency.

From well-known vibration theory, the resonant frequency should increase with the higher resonant modes for continuous systems. Because the DOE also predicts that the most dominant variable for this is the resonant mode is a very good indication that the

DOE is working correctly and the results are accurate. From the results, the sonic drill bit mass, sonic drill head, and the combination between the two are the only other major contributors to the resonant frequency, which also make sense, since the damping doesn't affect the un-damped natural frequency of resonant systems.

The next variable used to determine important factors of influence was the sonic drill bit amplitude. The results of the DOE are listed in Table 10.8 and the summary of the most influential variables are displayed in Table 5.9. The most significant variables on the model drill bit amplitude were found to be, in the order of most important to least important: 1) Sonic drill head spring rate, 2) Combination of the sonic drill head spring rate and the resonant mode, 3) Resonant mode, 4) Sonic drill head mass, 5) Combination of the sonic drill head and bit masses, and 5) Sonic drill bit mass. The half – normal plot is displayed as Figure 5.12.

Table 5.9. DOE results for factors of influence of the drill bit amplitude.

Factor	Sum of Squares	Mean Square	Prob > F
Model	1.64E+00	3.20E-02	< 0.0001
A-Sonic Drill Head Mass	1.70E-01	8.40E-02	< 0.0001
B-Sonic Drill Head Spring	2.55E-03	1.28E-03	0.3282
C-Sonic Drill Bit Mass	3.60E-02	9.08E-03	< 0.0001
D-Resonant Mode Number	7.30E-01	6.10E-02	< 0.0001
AC	6.60E-02	8.21E-03	< 0.0001
BD	6.20E-01	2.60E-02	< 0.0001

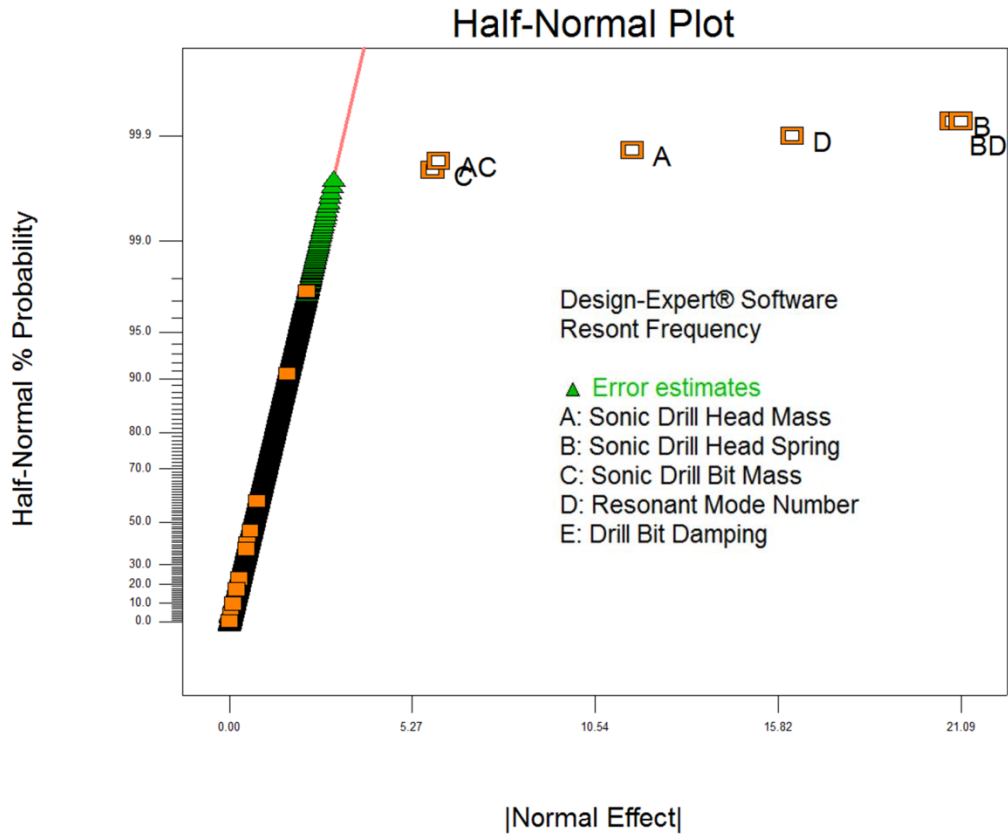


Figure 5.12. Half - Normal Plot of the DOE results for the significant factors that effect the sonic drill bit amplitude.

The next variable that was used to determine important factors of influence was the ratio of the sonic drill head amplitude to the sonic drill bit amplitude. The results of the DOE are listed in Table 10.9 and the summary of the most influential variables are displayed in Table 5.10. The half – normal plot is displayed as Figure 5.13. The most prominent factors that influence the ratio of the sonic drill head amplitude to drill bit amplitude are: 1) Sonic drill head mass, 2) Resonant mode, 3) Sonic drill bit mass, 4) Combination of sonic drill head mass and bit mass, and finally 5) Sonic drill bit damping.

Table 5.10. DOE results for factors of influence of the ratio of the sonic drill head to the drill bit amplitude.

Factor	Sum of Squares	Mean Square	Prob > F
Model	9.86E+01	3.18E+00	< 0.0001
A-Sonic Drill Head Mass	3.99E+01	1.99E+01	< 0.0001
C-Sonic Drill Bit Mass	1.18E+01	2.95E+00	< 0.0001
D-Resonant Mode Number	5.63E+01	4.69E+00	< 0.0001
E-Damping	1.40E-01	2.70E-02	0.0008
AC	3.30E-01	4.20E-02	< 0.0001

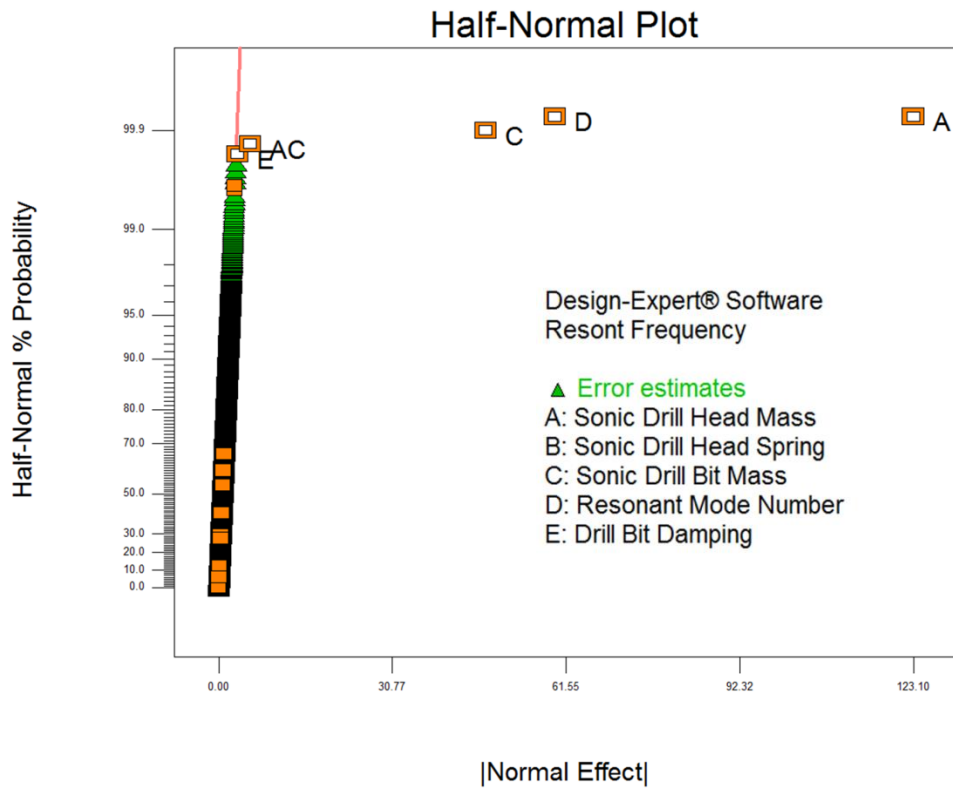


Figure 5.13. Half - Normal Plot of the DOE results for the significant factors that effect the ratio of the sonic drill head amplitude to the sonic drill bit amplitude.

Finite Element Solution

The finite element model was used for several reasons. Each of these reasons specified previously are broken up into each following subsection. The resonant modes that could be excited over the drill string lengths and boundary conditions were quantify. These resonant modes include the axial mode (primary concern) as well as bending, torsional, and breathing modes. Examples of the different mode shapes are displayed in Figure 5.14, Figure 5.15, and Figure 5.16. These mode shapes encompass the mode shapes in all degrees of freedom, whereas the previous model only concentrated on the primary axial resonant mode. A more efficient way to model the system response, by lumping the damping along the length as the damping ratio of the system was also examined. As opposed to the finite difference, the finite element can solve directly for the steady state condition of the system, without going through and solving the transient problem. A harmonic analysis can be performed using the finite element approach over a broad range of frequencies.

The resonant excitation between the axial modes and the lateral modes were investigated. The sensitivity of the damping and coupling along the length of the drill string was determined. The effect of the drill bit coupling and damping were also investigated by looking at the phase angle response, which will be used to verify the model against the empirical testing on the sonic drill system.

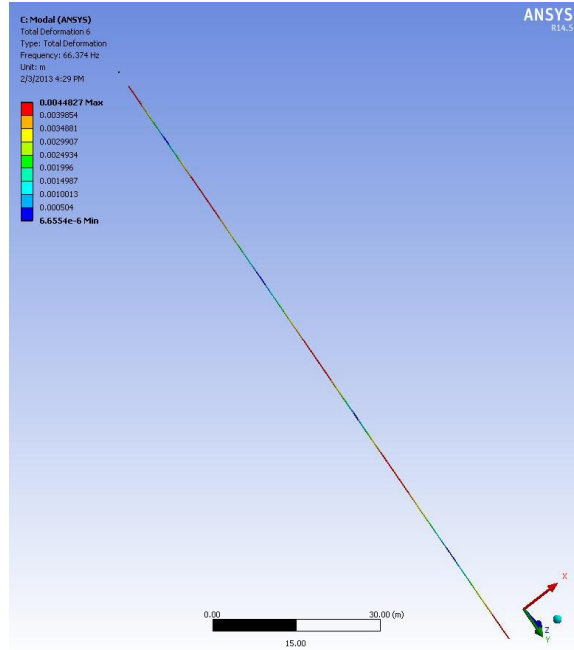


Figure 5.14. Example of an axial resonant mode resultant mode shape.

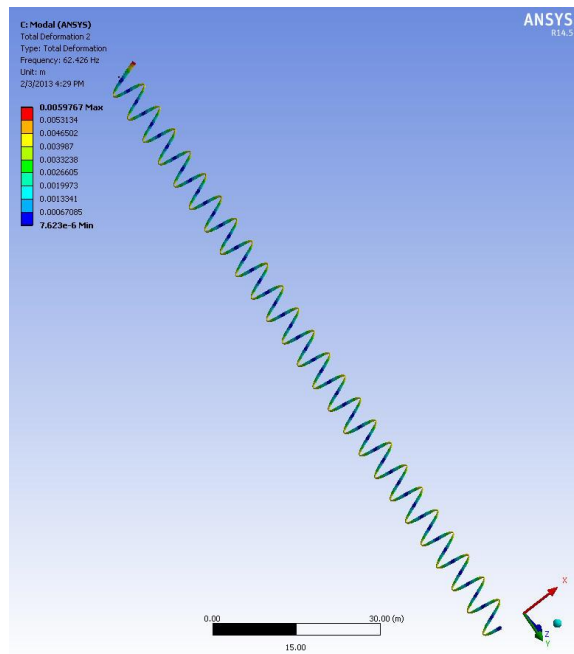


Figure 5.15. Example of a bending resonant mode resultant mode shape.

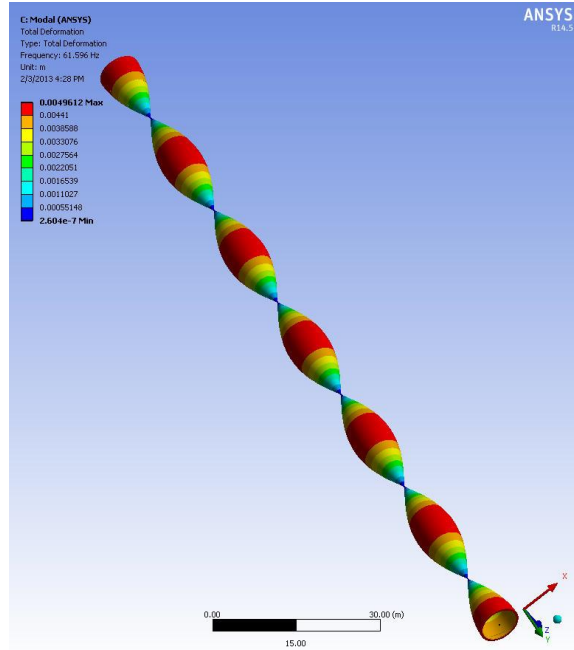


Figure 5.16. Example of a torsional resonant mode resultant mode shape.

Resonant Modes

The resonant modes were solved for a single sonic drill configuration, as outlined in Table 5.11. The ANSYS® model boundary conditions are also displayed in Figure 5.17. Standard earth gravity was also applied. The finite element system was constrained to leave all degrees of freedom free. This way it accounted for all the system dynamics.

Table 5.11. Finite Element Sonic Drill Variables.

Finite Element Sonic Drill Variables			
Sonic Head Mass	1000 lbs.	450 kg	
Elastic Spring Support	36,000 lbf/in ³	9.80E+09 N/m ³	
Drill Bit Mass	18 lbs.	8 kg	
Pipe wall thickness	0.5 inches	0.0127 m	

The resonant mode shapes were found between the operational frequencies of 60 Hz and 135 Hz. All of the mode shapes were found for drill string lengths of 50 ft, 100 ft, 120 ft, 150 ft, 250 ft, 500 ft, 750 ft, and 1000 ft. The modal results are listed in Table 10.10 through Table 10.14 in the Appendix for axial, bending, torsional, and breathing modes. The axial modes for the above conditions were found and plotted in Figure 5.18.

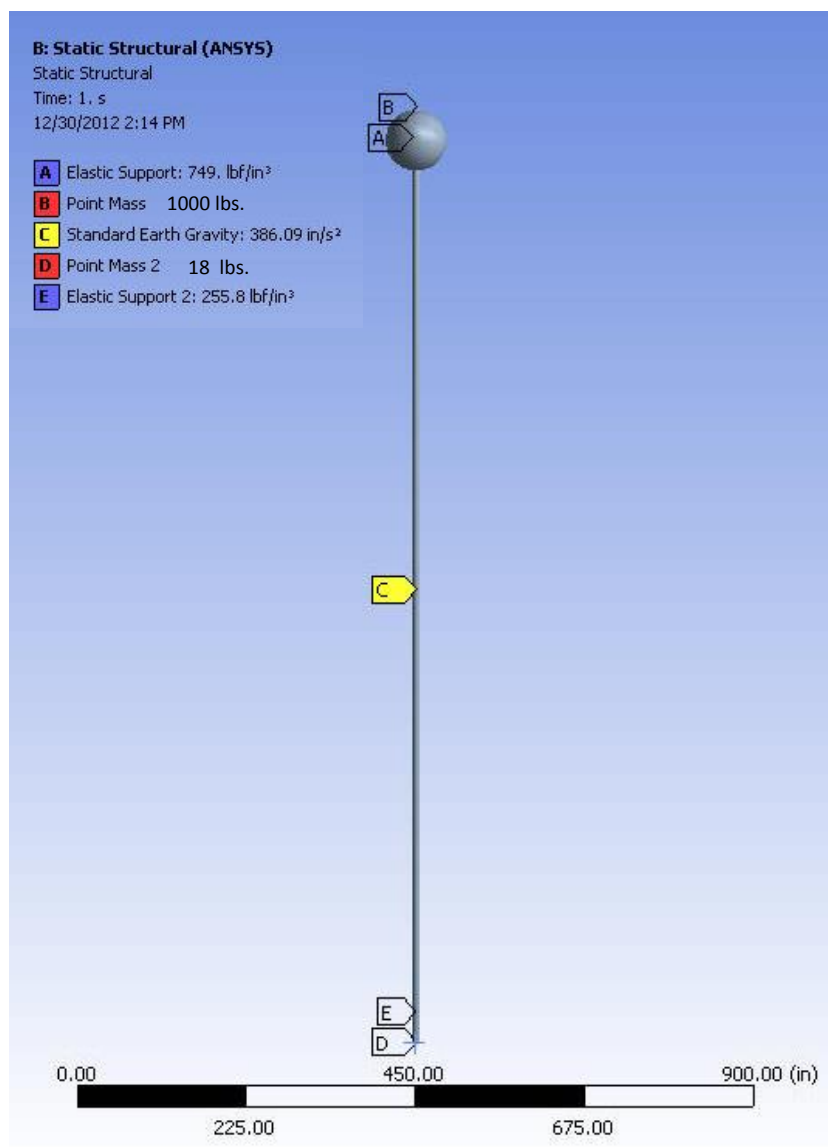


Figure 5.17. ANSYS[®] Model Boundary Conditions.

Only one axial resonant mode per drill string length was present for most of the drill string lengths up to 250 ft. Because there is only one axial resonant mode for the lower frequencies, this greatly simplifies control for sonic drill operators. After 250 ft, more than one axial resonant mode can be chosen for the operational frequency. For instance, if a particular mode is found to be useful, for example mode 8, then this mode can be used for all drill lengths between 500 ft and 1000 ft if the drill string has an operation frequency between 60 and 130 Hz. This makes operation very simple for an operator, as they would control the drill at a nearly consistent speed before and after the addition of a new drill pipe section. However, if a problem is encountered with the chosen mode and the penetration rate decreases for some reason, there has not been any documented means of determining what operating mode the operator should try/use. The methods are described in the control applications section, below.

Axial modes are not the only resonant modes that can affect a sonic drill. Lateral (or bending) modes can play a role in the dynamics of the drill string. However, if a lateral mode resonant frequency is not close to an axial mode, the input power needed to excite a lateral mode is greater than the sonic drill driver can exert in any lateral direction. The restoring forces or internal inertia of the drill string will damp out any lateral forces that are not close enough to a resonant condition. However, if the drill bit were to only impact on a single side repeatedly, it is conceivable that there could be a substantial moment loading onto the drill string that could excite the lateral (flexural) modes. This particular excitation mode was not explored in this body of work, but is mentioned in the future work section, below. The control section also has a monitoring

section that covers lateral or flexural modes, by use of accelerometers on the lateral planes.

Lateral modes are displayed in Figure 5.19. There are many more lateral modes than there are axial modes. Because they are more closely spaced, there is higher probability that they would coincide with an axial mode. When a lateral resonant mode can be excited at the same frequency as an axial resonant mode, the energy can be swapped between the two via what is commonly referred to as a ‘weak spring’ (34). The weak spring can be any compliant member that links the two resonant modes together. When energy is being swapped between the two resonant conditions, one mode will rob energy from another and subsequently give it back. The mode amplitudes will not be stable, but will beat based on the energy swap rate of the weak spring. When a bending mode is close to an axial mode the ANSYS[®] FEA analysis predicted results shows that when the axial mode is excited, the bending mode is also excited through the weak springs of the system.

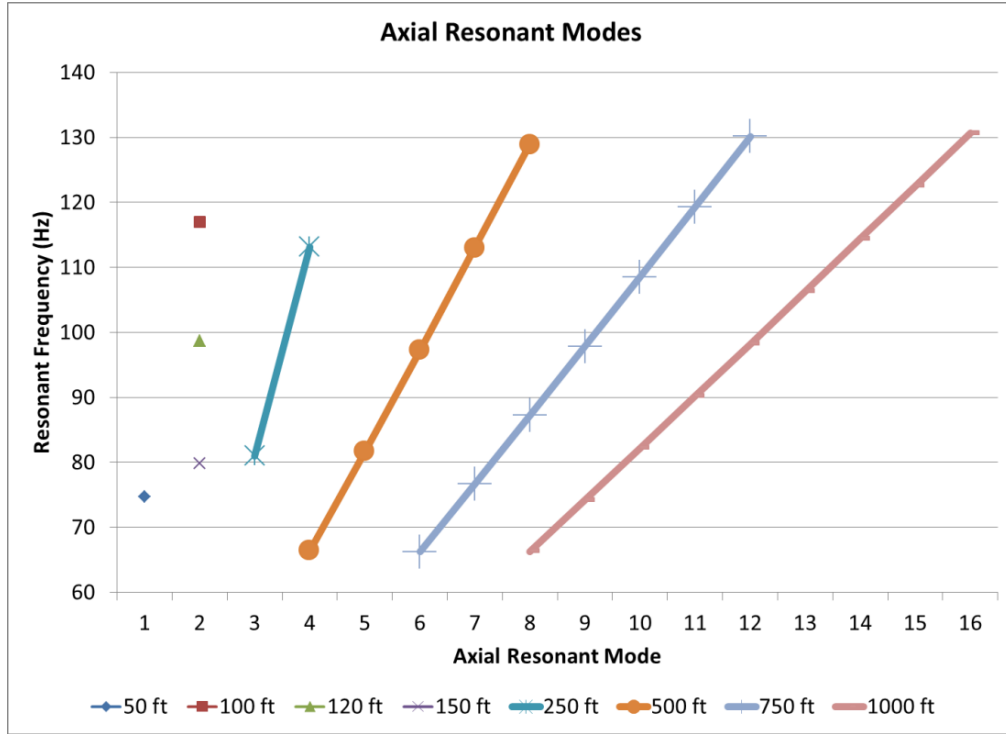


Figure 5.18. Axial resonant modes for different drill string lengths.

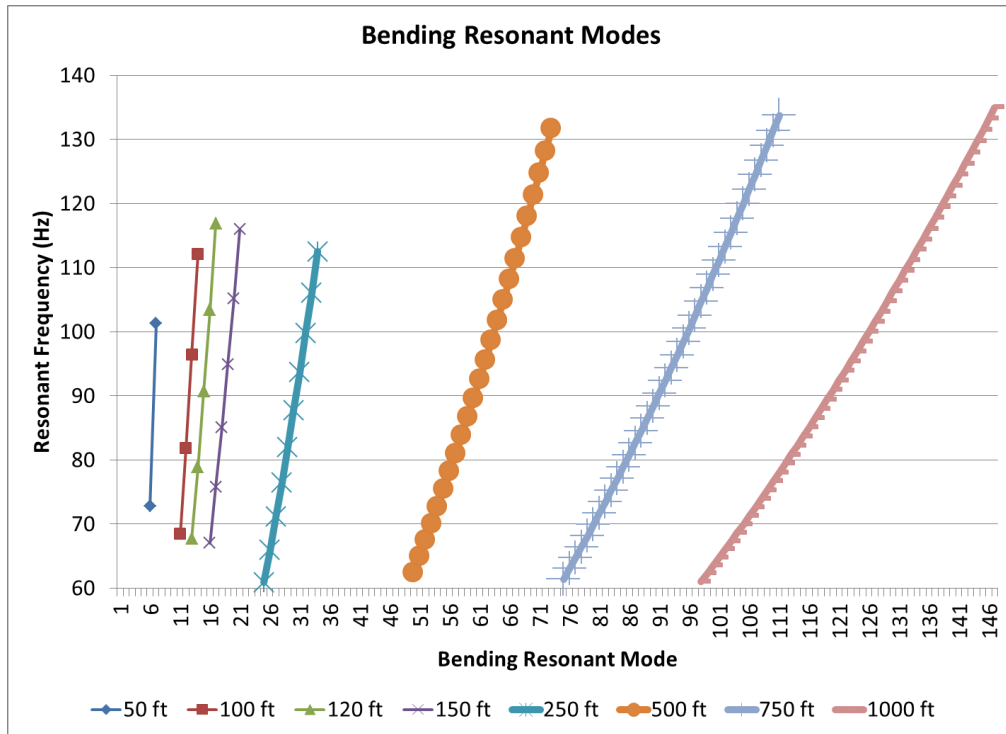


Figure 5.19. Bending resonant modes for different drill string lengths.

Figure 5.20 shows both an axial mode with a bending mode 0.2 Hz away and one that is within 1.1 Hz of the axial mode. The closer the bending mode is to an axial mode, the more susceptible it is to resonant amplification. The mode shapes are so closely packed between frequencies, that there was minor overlap between the axial and lateral modes for drill string lengths until string lengths over 750 ft. were reached. From this modal analysis, it is found that the lateral modes are difficult to excite unless they are within 1 Hz from an axial mode. The reason this is the case is that the resonant peak is very steep, as displayed in Figure 2.1 above, and that by moving less than 1 Hz off of resonance the internal losses of the system (either absorbing potential or kinetic energy) keeps the amplitude from these unwanted modes down. Not to mention that the primary forcing function is in the axial direction, reducing the probability of exciting the lateral modes due to the small lateral force vector at the sonic drill head.

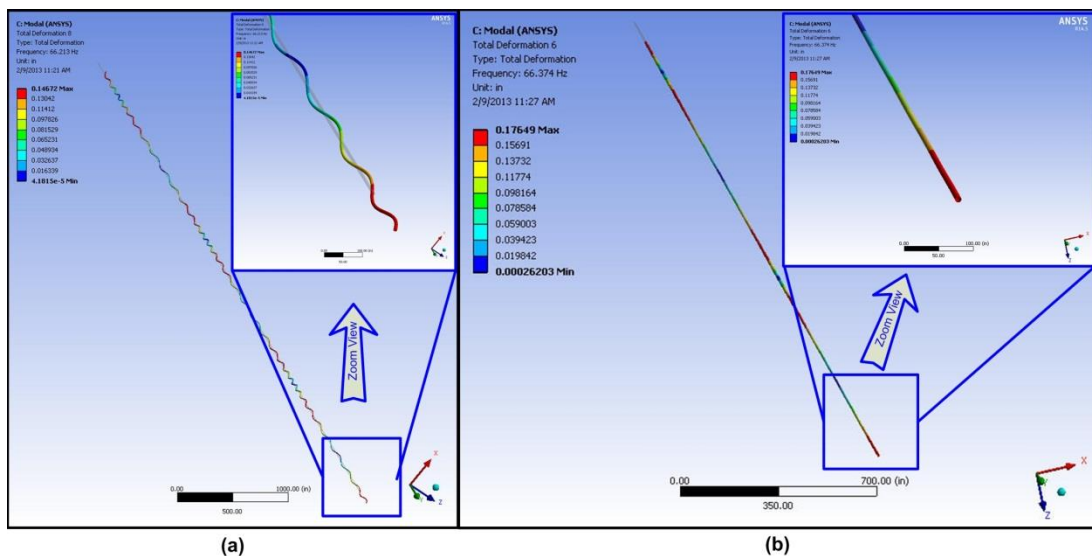


Figure 5.20. Lateral coupling with the primary axial resonant mode. (a) is the 6th resonant mode for a 750 ft. long drill string and (b) is the 4th resonant mode for a 500 ft. long drill string. The lateral mode is 0.2 Hz away from the axial for the 750 ft. long drill string mode, and 1.1 Hz away for the 500 ft. long drill string.

The torsional resonant modes found from the FEA are displayed in Figure 5.21. These modes are also challenging to excite and no cross excitation between axial and torsional modes were observed for this specific drill string pipe size and length. However, it can be envisioned that these modes could be excited by using an aggressive drilling bit that imparted torsional forces onto the drill string. There were some modes that were lightly coupled with the lateral bending modes, but these particular modes were not documented.

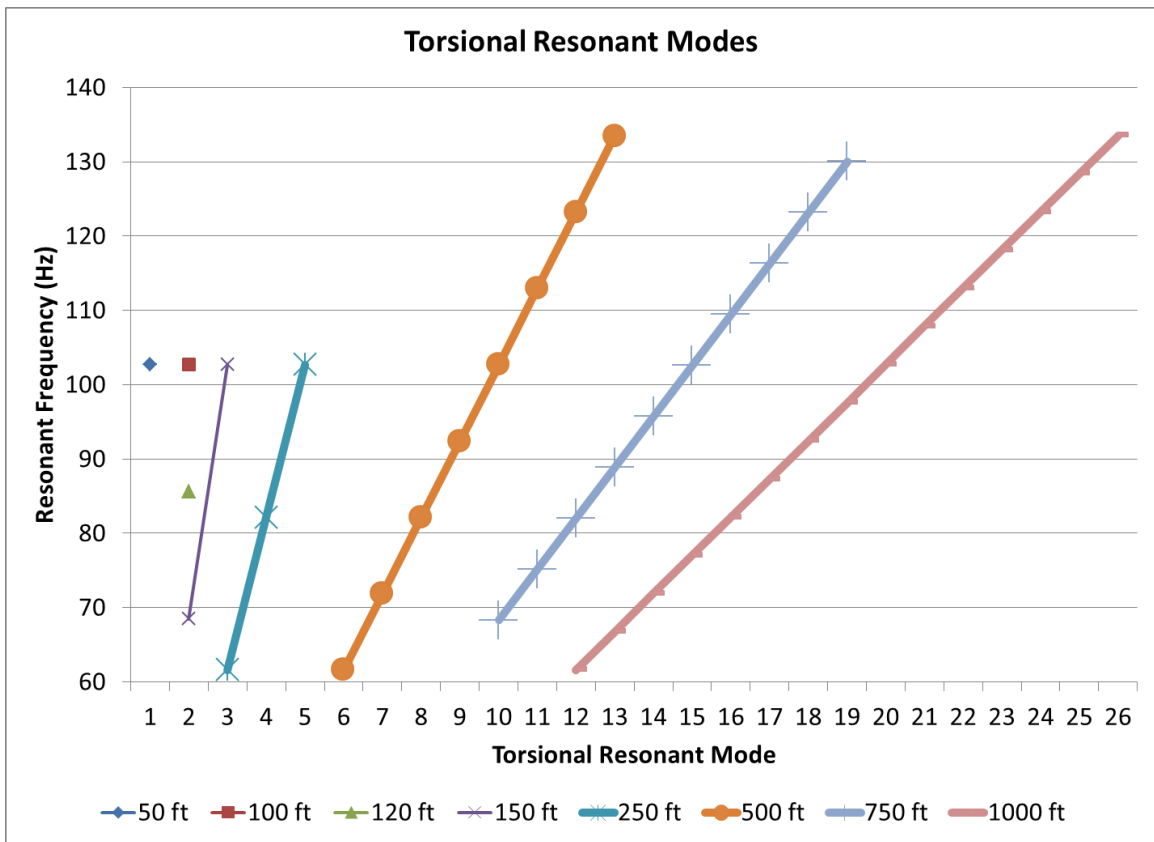


Figure 5.21. Torsional resonant modes for different drill string lengths.

Through understanding the dynamics of the system for all the different mode shapes, control of the sonic drill can be performed from the surface to monitor the

amount of bending, torsion, axial and breathing modes. Such monitoring of the sonic drill would be at the sonic drill head and would typically be done by accelerometers in the three principal directions, which would be used to determine if bending modes as well as axial modes exist. The torsional mode would require an accelerometer on the outside of the drill string, and would have to have high sensitivity for low acceleration at low frequency. The bending modes could also be determined from multiple accelerometers in the axial direction at different sides of the pipe. For example if 4 accelerometers were mounted in the axial direction at 12, 3, 6 and 9 o'clock orientation looking down the drill string, then if there were bending modes, the cross accelerometers would be out of phase in displacement, velocity, and acceleration.

Constant Damping and Restoring

A small design of experiments (DOE) was performed to determine the sensitivity of the effects drill string oscillation response due to damping and elastic coupling along the length of the drill string. The DOE sonic drill configuration tests are listed in Table 5.12. These conditions coincide with the constant damping as displayed in Figure 3.9. Figure 5.22, displays the corrected results from the FEA analysis. The results were found using a 1000 lbf for all the frequencies. The results were then scaled for the actual sonic drill force amplitude for a given frequency as calculated using the eccentric mass and radius given in Table 3.5. Figure 5.22(a) also displays that the only the axial modes are excited with any given amplitude if the input force is acting only in the vertical direction. This shows that there is no weak spring coupling between the axial and lateral modes of the sonic drill. Figure 5.22(b) shows that the sonic drill head only changes phase

between 180° and 0° and resonance is found at 90° when the phase is decreasing. This relation shows that the measured data is correct and that the sonic drill should be operated at phase angles of displacement of 90°. It is also noted that the bit can change phase between 180° and -180°.

Table 5.12. FEA design of experiments listed variables to determine the significance of the damping and elastic coupling along the drill string length.

Variable	FEA Test Condition				
	1	2	3	4	5
Damping or Coupling Type	None	None	Constant	Constant	Constant
Drill String Length	250 ft	250 ft	250 ft	250 ft	250 ft
Pipe Wall Thickness	0.5 in	0.5 in	0.5 in	0.5 in	0.5 in
Sonic Head Mass	1000 lbs	1000 lbs	1000 lbs	1000 lbs	1000 lbs
Sonic Head Spring Rate	36,000 lbf/in ³	36,000 lbf/in ³	36,000 lbf/in ³	36,000 lbf/in ³	36,000 lbf/in ³
Drill Bit Mass	18 lbs	18 lbs	18 lbs	18 lbs	18 lbs
Drill Bit Damping	0 lbf*s/in ³	0 lbf*s/in ³	0 lbf*s/in ³	0 lbf*s/in ³	0 lbf*s/in ³
Drill Bit Spring Rate	0 lbf/in ³	175 lbf/in ³	175 lbf/in ³	175 lbf/in ³	175 lbf/in ³
Drill String Equivalent Damping	0 lbf*s/in ³	0 lbf*s/in ³	0 lbf*s/in ³	0.679 lbf*s/in ³	0.253 lbf*s/in ³
Drill String Equivalent Spring Rate	0 lbf/in ³	0 lbf/in ³	342 lbf/in ³	342 lbf/in ³	342 lbf/in ³
Resonant Frequency Mode 2	66.50 Hz	66.62 Hz	66.62 Hz	71.55 Hz	71.55 Hz
Resonant Frequency Mode 3	95.34 Hz	95.43 Hz	95.43 Hz	103 Hz	103 Hz
Resonant Frequency Mode 4	125.59 Hz	125.66 Hz	125.66 Hz	Hz	Hz
Damping Ratio Mode 2	N/A	N/A	N/A	0.677	0.253
Damping Ratio Mode 3	N/A	N/A	N/A	0.61	0.228
Damping Ratio Mode 4	N/A	N/A	N/A	0.539	0.2
Ratio of Head to Bit Amplitude Mode 2	0.999	1.000	1.000		
Ratio of Head to Bit Amplitude Mode 3	0.932	0.933	0.933		
Ratio of Head to Bit Amplitude Mode 4	0.803	0.799	0.799		

The amplitude response for the head and bit for conditions 3, 4, and 5 are plotted in Figure 5.23. Conditions 4 and 5 are too heavily damped and the resonant condition is not readily found by locating a phase angle of 90°. In Test 5 the only mode that is excited and has a measured phase angle of 90° was located at 66 Hz. The higher modes are too highly damped to be found by measuring the phase angle. Test condition would indicate that dense sand and light clay should over damp the sonic drill system if applied along the length of the drill string. The light clay results make sense, but the sand results

do not. During testing of the drill as described in Chapter 6, below, the sonic drill was used to penetrate sands to a depth of 120 feet. During these tests the damping along the length of the drill string was found to be negligible. When the damping of sand along the drill string length becomes negligible, the sand must decouple with the drill string during drilling causing little energy is absorbed. The measured data wasn't taken to determine the damping of the drill system when the drill bit was not engaged with the soil because the system was too unstable. The unstable system here is defined as a system that does not have adequate damping to limit the oscillation amplitude of the drill string and the amplitudes will grow uncontrollably until the drill string or driver fails due to excessive stresses. Therefore, no empirical data was generated to match up the damping along the drill length.

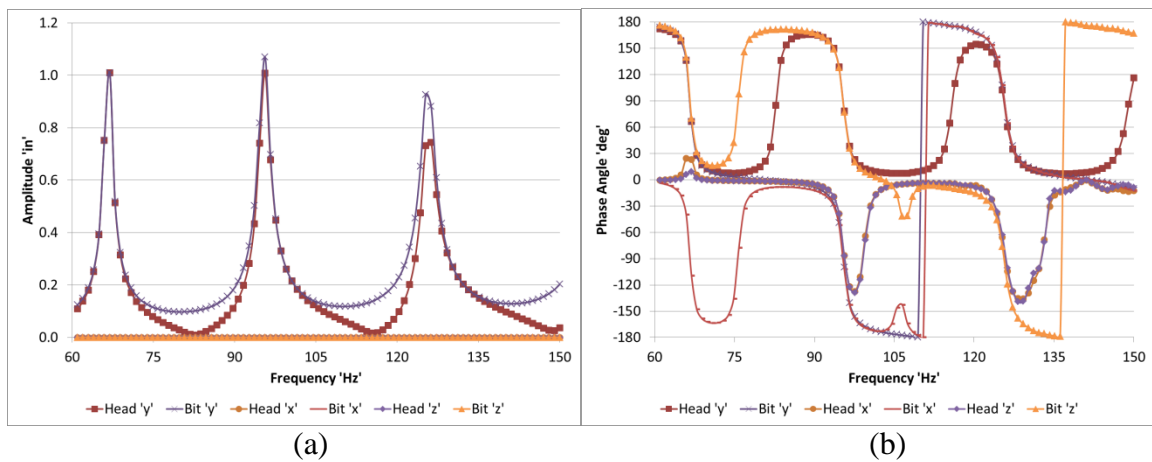


Figure 5.22. FEA test condition 3 results. (a) Amplitude response of the sonic head and drill bit. (b) Phase response for the sonic head and the drill bit.

FEM with Equivalent Damping and Restoring

The damping and spring rate types for linear, step, and impulse are displayed in Figure 3.9. The peak values were that of dense sand. The mode shapes for each system analyzed were first normalized and using equations 4.36 and 4.37 the equivalent damping and restoring values along the drill string length were determined. The damping ratio ' γ ' for the system was then found by plugging the equivalent damping, equivalent restoring and the resonant frequency into Equation 3.44. The last condition examined is for an impulse damping and restoring as extreme clay over a 10 ft (3.05 m) long section.

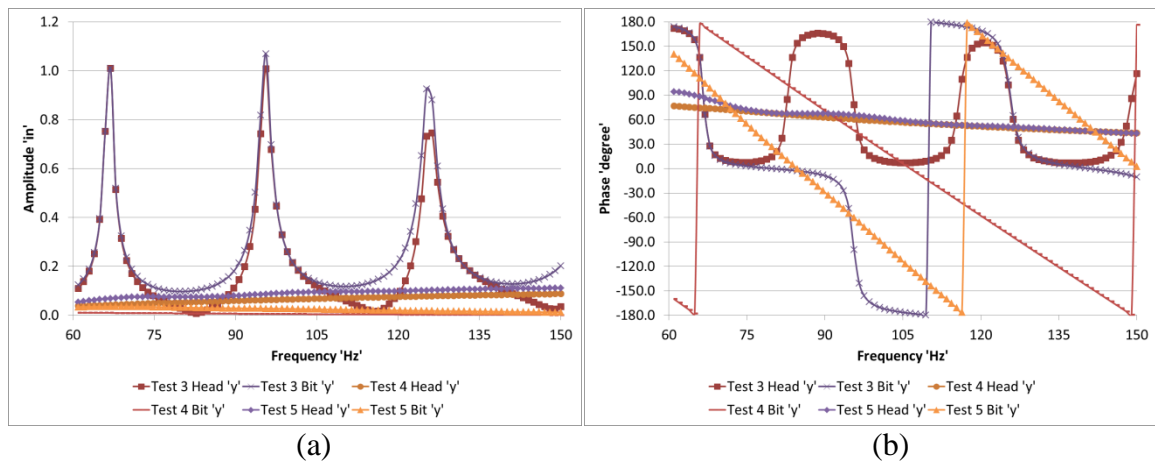


Figure 5.23. FEA test condition 3, 4, and 5 results. (a) Amplitude response of the sonic head and drill bit. (b) Phase response for the sonic head and the drill bit.

The impulse will be implemented as two separate conditions: 1) At a node and 2) At an anti-node location. This mimics a condition of swelling clay around the sonic drill string. A summary of the test conditions are listed in Table 5.13. The damping and restoring values are listed in Table 5.13 as well as displayed in Figure 5.24.

Table 5.13. Variable Damping and Restoring Along the Drill String Length.

Variable	DOE Test Condition			
	1	2	3	4
Damping or Coupling Type	Linear	Step	Impulse 'Node'	Impulse 'Anti-Node'
Drill String Length	250 ft	250 ft	250 ft	250 ft
Pipe Wall Thickness	0.5 in	0.5 in	0.5 in	0.5 in
Sonic Head Mass	1000 lbs	1000 lbs	1000 lbs	1000 lbs
Sonic Head Spring Rate	36,000 lbf/in ³	36,000 lbf/in ³	36,000 lbf/in ³	36,000 lbf/in ³
Drill Bit Mass	18 lbs	18 lbs	18 lbs	18 lbs
Drill Bit Damping	0 lbf*s/in ³	0 lbf*s/in ³	0 lbf*s/in ³	0 lbf*s/in ³
Drill Bit Spring Rate	175 lbf/in ³	175 lbf/in ³	175 lbf/in ³	175 lbf/in ³
Drill String Equivalent Damping	0.144 lbf*s/in ³	0.2 lbf*s/in ³	0.03 lbf*s/in ³	0.35 lbf*s/in ³
Drill String Equivalent Spring Rate	342 lbf/in ³	342 lbf/in ³	342 lbf/in ³	342 lbf/in ³
Resonant Frequency	66 Hz	66 Hz	66 Hz	66 Hz
Damping Ratio	0.144	0.199	0.062	0.728

Figure 5.25 displays the results for the FEA models for the linear and step conditions. The amplitudes of both show that there are resonant peaks, but they have a low 'Q'. The phase angle only went through 90° at 40 and 66 Hz. At resonant frequencies higher than 66 Hz the damping in these two conditions is too great to effectively keep the drill string operating on resonance.

The 1.3 lbf*s/in³ (3.5×10^5 N*s/m³) damping condition was applied over a 10 ft (3 m) length either at a node location and at an anti-node location along the drill string length. Figure 5.26 displays that if the damping is applied to a node and not at an anti-node location; the drill string can resonate without losing much energy to the high damping region. Therefore, if a mode is heavily damped, other resonant modes should be used to transmit more power to the drill bit. This is another reason for industry to be using a automated control system. The possible number of downhole conditions are simply too complex for the unaided driller to be able to drill effectively. Therefore, the operator cannot use “feel” for sonic drilling.

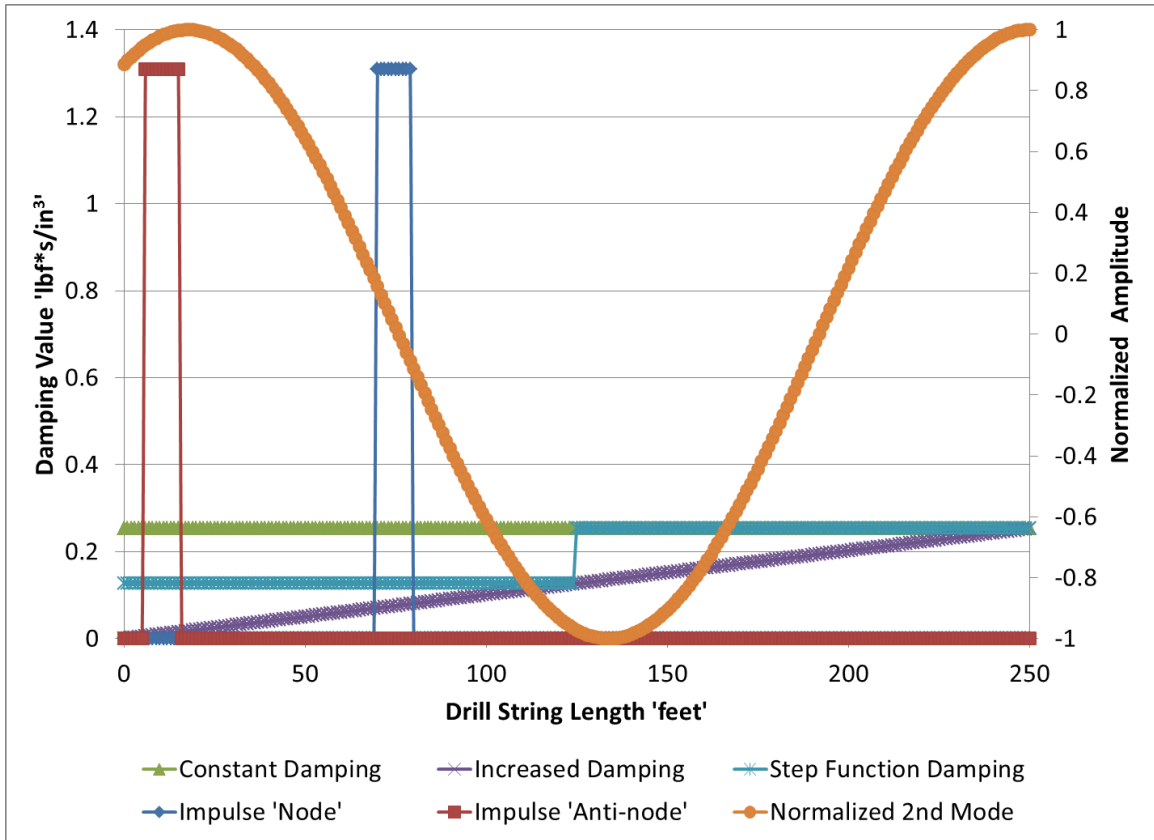


Figure 5.24. Damping Values and the normalized mode shape at 66 Hz.

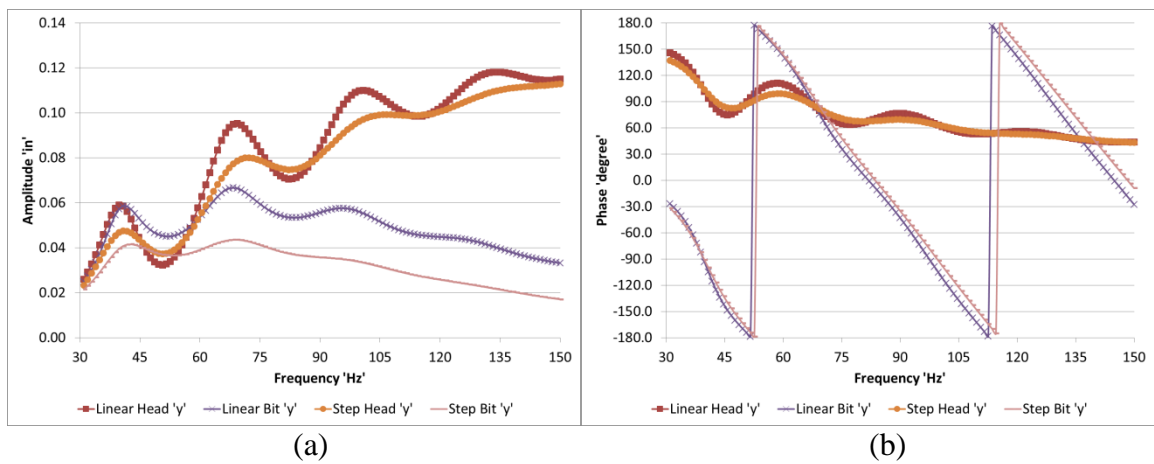


Figure 5.25. FEA linear and step condition results. (a) Amplitude response of the sonic head and drill bit. (b) Phase response for the sonic head and the drill bit.

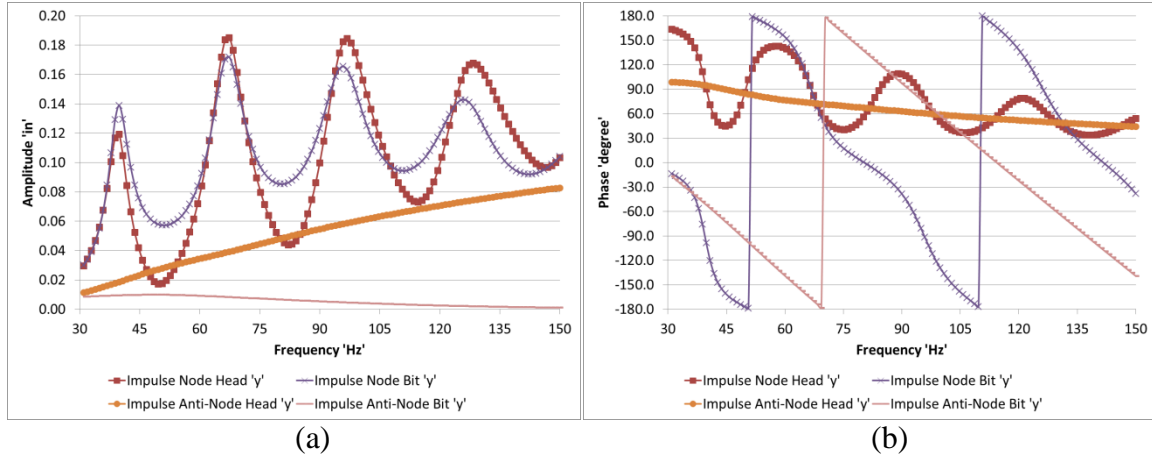


Figure 5.26. FEA impulse node and anti-node condition results. (a) Amplitude response of the sonic head and drill bit. (b) Phase response for the sonic head and the drill bit.

Boundary Condition Results Summary

The boundary condition solutions mapped the sensitivities of the parameters specified in Table 5.1, above, with respect to: 1) Ratio of sonic drill head to drill bit amplitude, resonant frequency, and drill bit amplitude. Three different design of experiments were performed to determine the different variable sensitivities relative to each other with respect to the above 3 variable criteria. A table summarizing the important parameters from most important '1' to least important '8' are listed in Table 5.14 for each of the DOE experiment numbers and 3 variables. Table 5.15 shows the same results as Table 5.14, but with the results sorted by the measured variable.

Table 5.14. Boundary Condition Variables of Influence.

Design of Experiment	Measured Variable	Factors of Influence (Most Influential '1' to least influential '8')							
		1	2	3	4	5	6	7	8
1	Resonant Frequency	AH	H	DH	A	AD			
	Bit Amplitude	DH	DCH	CAH	D	BDH	A	AC	H
	Ratio Head to Bit Amplitude	D	AD	DH	A	H	AH		
2	Resonant Frequency	G	F	A	AF	AG	C	AC	CF
	Bit Amplitude	AG	G	F	A	AF			
	Ratio Head to Bit Amplitude	F	G	AG	A	AF			
3	Resonant Frequency	G	C	AC	A				
	Bit Amplitude	B	BG	G	A	AC	C		
	Ratio Head to Bit Amplitude	A	G	CAH	AC	E			
Legend:									
	A~ Sonic Drill Head Mass								
	B~ Sonic Drill Head Spring Rate								
	C~ Sonic Drill Bit Mass								
	D~ Sonic Drill Bit Spring Rate								
	E~ Sonic Drill Bit Damping								
	F~ Strata Types								
	G~ Resonant Mode								
	H~ Sonic Drill Length								

Table 5.15. Boundary Condition Variables of Influence, sorted by Measured Variable.

Design of Experiment	Measured Variable	Factors of Influence (Most Influential '1' to least influential '8')							
		1	2	3	4	5	6	7	8
1	Bit Amplitude	DH	DCH	CAH	D	BDH	A	AC	H
2		AG	G	F	A	AF			
3		B	BG	G	A	AC	C		
1	Ratio Head to Bit Amplitude	D	AD	DH	A	H	AH		
2		F	G	AG	A	AF			
3		A	G	CAH	AC	E			
1	Resonant Frequency	AH	H	DH	A	AD			
2		G	F	A	AF	AG	C	AC	CF
3		G	C	AC	A				
Legend:									
	A~ Sonic Drill Head Mass								
	B~ Sonic Drill Head Spring Rate								
	C~ Sonic Drill Bit Mass								
	D~ Sonic Drill Bit Spring Rate								
	E~ Sonic Drill Bit Damping								
	F~ Strata Types								
	G~ Resonant Mode								
	H~ Sonic Drill Length								

The most influential sonic drill variables for each measured parameter of Bit Amplitude, Ratio of Head to Bit Amplitude and Resonant Frequency are displayed in Figure 5.27, Figure 5.28, and Figure 5.29, respectively.

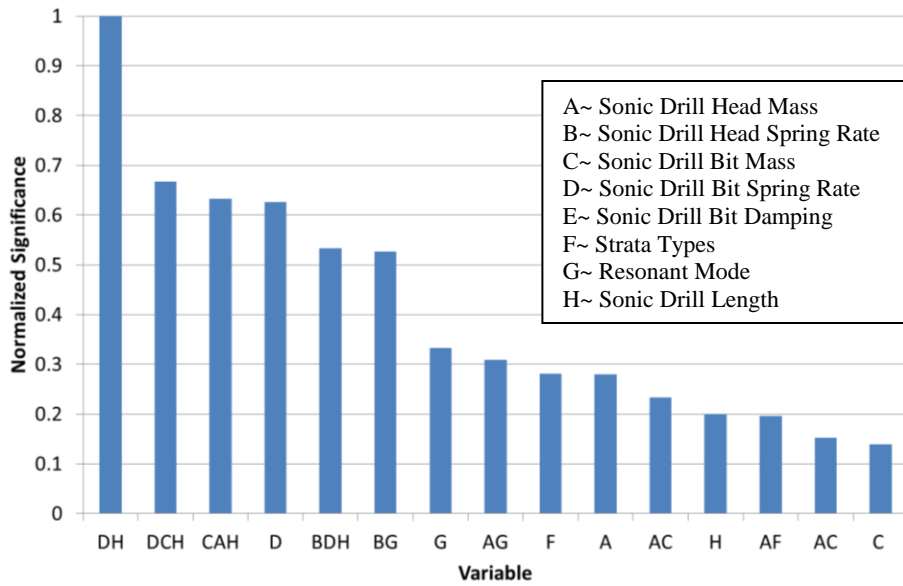


Figure 5.27. Bit Amplitude Normalized Factors of Influence. 1 being most influential.

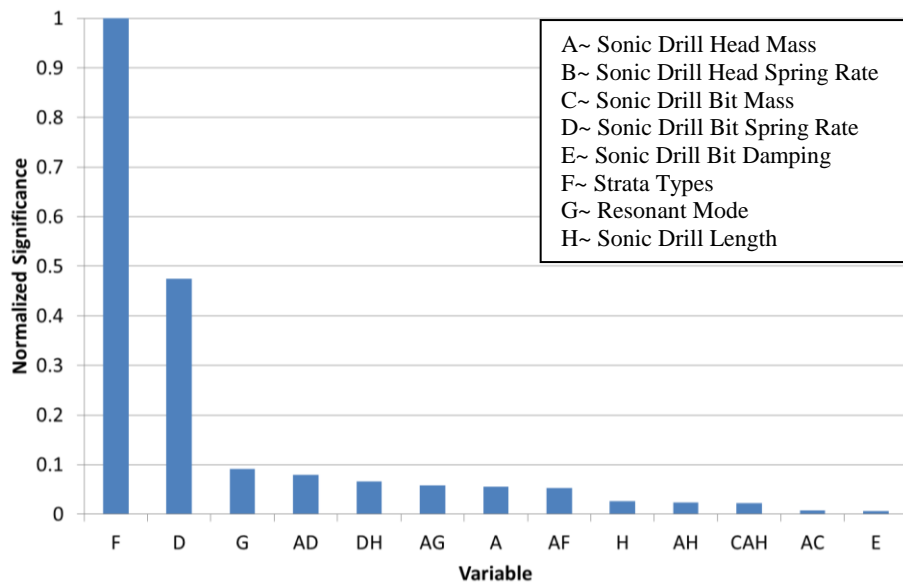


Figure 5.28. Ratio of Head to Bit Normalized Factors of Influence. 1 being most influential.

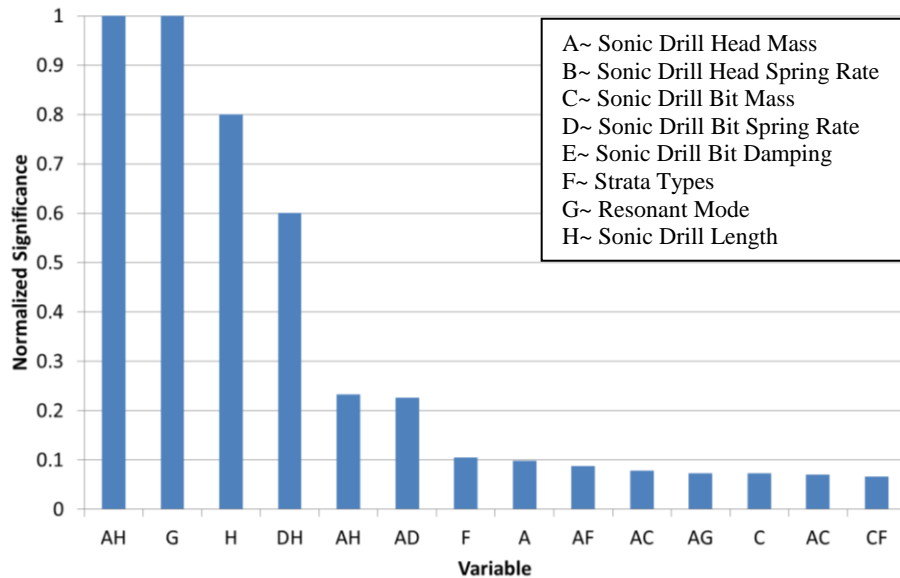


Figure 5.29. Resonant Frequency Normalized Factors of Influence. 1 being most influential.

The most influential parameters for the bit amplitude are the combination of the sonic drill bit spring rate and the sonic drill length, resonant mode, and the combination of the sonic drill head mass and resonant mode. The sonic drill bit spring rate is so influential, because within the operating conditions, it can get high enough to essentially “fuse” the drill bit with the strata and make it act as a resonant node. This essentially changes the boundary condition of the drill string at the drill bit to fixed, which drastically changes the resonant frequency. When the drill bit is a node, two things may occur. The first is that the current operating frequency does not correspond with new resonant mode from the new boundary conditions of top free (mass and spring) and the bottom in the fixed condition. The second is if the current operating frequency corresponds with a resonant mode, and the top of the drill string is putting in a lot of energy, but no energy is being delivered to the drill bit. This mode is detrimental, as all

the energy goes into the string along the length and it easily can build to an amplitude stress level that will break the drill string.

The most influential parameters for the ratio of head to bit amplitude are the drill bit spring rate, strata type (combination of the bit spring rate and bit damping), sonic drill head mass, combination of the drill head mass and the bit spring rate, drill bit spring rate and the drill length, as well as the resonant mode. Similarly as discussed above, the bit spring rate can change the boundary condition of the bit to essentially be fixed. The strata type also plays into the possibility of creating a node at the drill bit. The next most influential variable is the drill head mass. As the drill head mass is increased, the head amplitude relative to the drill bit amplitude decreases. This has two benefits for drilling: it allows more deflection of the drill bit so it can store and release more energy and it decreases the amount of oscillation at the drill head to minimize un-needed fatigue. However, sonic drills are typically designed to have as light of sonic drill heads as possible, which has the following effects: 1) It allows more energy to be input into the system, because of higher velocities where the force is input and 2) It allows more energy to drive the system above resonance, which helps create the “lock-in” condition described above.

The most influential parameter in the resonant frequency by an order of magnitude is the resonant mode, but the next most influential is the combination of the sonic head mass and the drill length, followed by the drill length, strata types, and bit mass.

Finite Element Results Summary

The finite element analysis was used to examine the relative influence of different sonic drill variables than the boundary condition model. The variables with great significance for the boundary condition model are outlined above in Table 5.14. The finite element model was used to determine the significance of the coupling and damping along the length of the drill string, because the boundary condition model cannot account for such loadings onto the system. The boundary condition model was also used to examine the longitudinal deformation of the drill string while omitting the flexure, torsional, and breathing conditions. However, the finite element method can be used to determine the sonic drill response in three dimensions. The modal results showed that there exist axial, torsional, and bending modes for the sonic drill system. The model predicted that the lateral modes could also be excited if their resonant frequency was within 1 Hz of the primary axial mode. Thus, the lateral modes should also be monitored.

The finite element models demonstrated that the drill conditions below ground can be measured at the sonic drill head. Thus, by monitoring the phase angle between the input force with respect to the displacement, velocity or acceleration, the resonant condition of the sonic drill can be monitored. Also, by monitoring the motion of the sonic drill head in the three primary translational axes (x, y, and z) the axial motion of the drill string as well as any unwanted lateral modes can be determined. By monitoring the phase angle of the lateral modes measured signals, the lateral resonant condition can be monitored and avoided.

FEA can be used to model the sonic drill system, but the damping numbers for sands as calculated by Warrington (36) for pile drivers do not hold true for sonic drilling. Empirical damping data should be collected at frequencies from 60-200 Hz for the different soil types, which could be later verified through FEA analysis. The damping of clays appeared more realistic, but empirical data for all soil types at sonic drill frequencies should be measured. The FEA analysis did show that the system dynamics can be monitored above ground and the empirical soil data, could be collected with a sonic drill if the soil conditions are known and that there is either enough soil damping to safely damp the sonic drill operation without the drill bit engaged or data should be taken off of mechanical resonance so the system will self-regulate the response by the internal potential or kinetic stored energy.

The method of equivalent spring and damping was demonstrated to work for the FEA models, but further empirical data is required to fully validate the proposed methods.

The FEA models did validate that the hypothesis of damping at an anti-node compared to a node will absorb more energy. In the case examined, we found that the anti-node location absorbed enough energy to drop the system displacement amplitude at the drill bit by over an order of magnitude which greatly limited the drills ability penetrate the strata.

CHAPTER 6

EXPERIMENTAL VERIFICATION

Introduction

The previous chapters have provided background in sonic drilling, sonic drilling models, and results for the mechanical and strata variable significance. The sonic drill model and model results show that the sonic drill is very complex. However, measurement of the system dynamics can be made above ground. Chapter 6 outlines the tests that were performed using a sonic drill, data analysis of the test data, and how the test results correlate with the model data generated and reported in chapters 4 and 5, respectively.

Tests were performed using a sonic drill system owned by Water Development Corporation. A 1” thick flat bottom piece of steel was welded to the bottom drill string and used as a drill bit to drill 120 feet into the earth while collecting measurement data at the sonic drill head. The measured data was then used to quantify and verify the sonic drilling conditions and significant operating parameters determined by the model. Through the data analysis, a few counterintuitive control conditions were determined.

Test and Measurement Setup

Testing was performed with 9 inch OD sonic drill string in 10 foot sections. The Sonic drill, displayed in Figure 6.1, used a sonic driver that produced 200,000 lbf at 100

Hz. Robert Dobush from Blue Star Enterprises was the sonic drill operator. The sonic drill was used to drill the 9 inch OD drill string to a depth of 120 feet.

The sonic drill was instrumented with an accelerometer and an eddy current sensor both on the sonic driver, displayed in Figure 6.2. An accelerometer was used to measure the sonic driver motion while drilling. An eddy current sensor was used to pick up the eccentric crank as it rotated past the accelerometer, which created a pulse square wave once every full rotation. A picture of the actual configuration is presented in Figure 6.3.

An eddy current sensor is mounted to pick up the time when the eccentric is exerting full force in the x direction. The accelerometer is mounted to measure the acceleration in the positive x direction. Test data was recorded using a National Instruments USB DAQ card through Labview software. The data was recorded at 20,000 samples per second. PZT strain sensors were mounted on the sonic drill pipe just under the sonic driver to give an indication of the phase of the pressure waves traveling down the drill string. The data was collected, but was not used for any calculations.

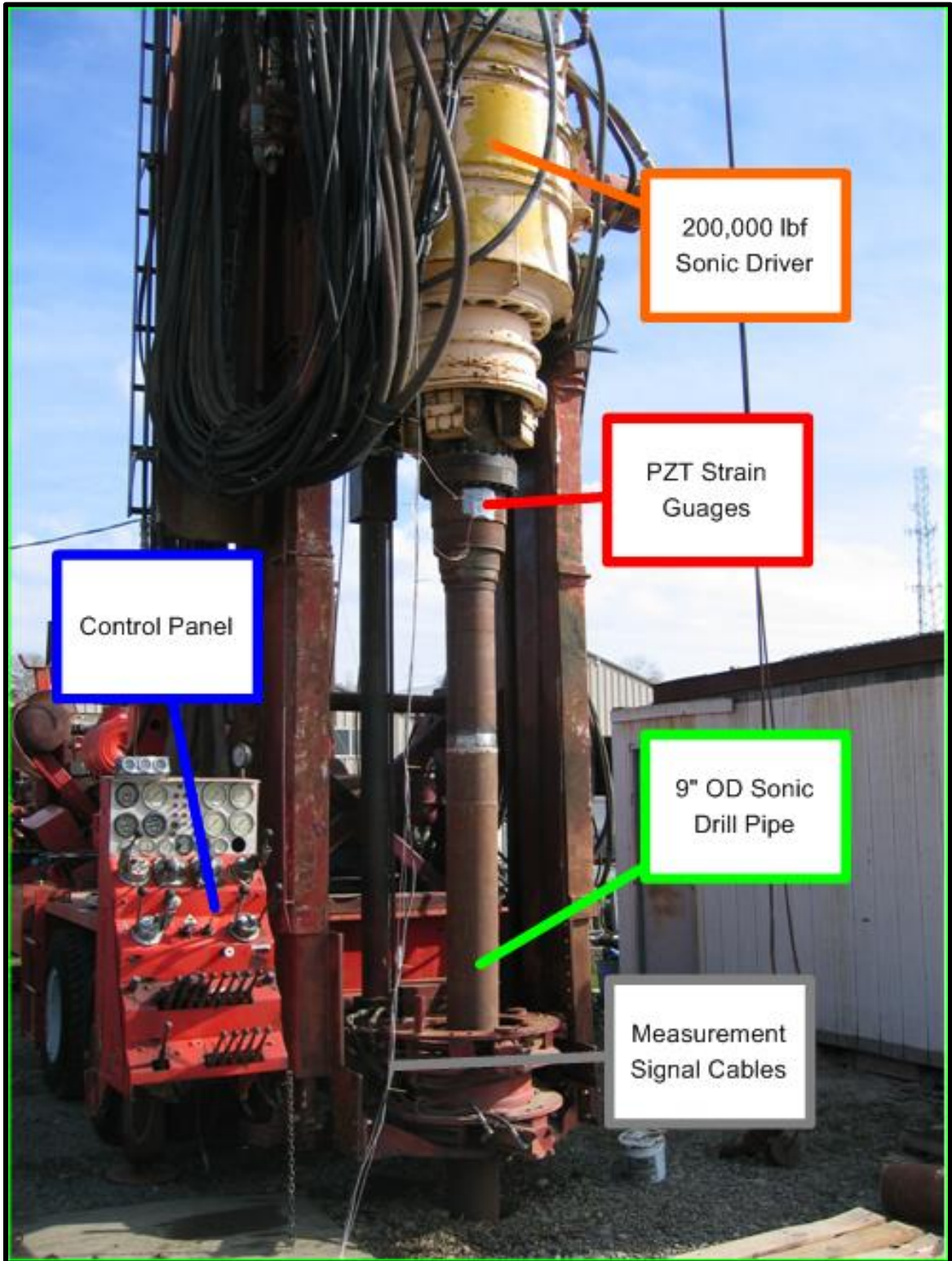


Figure 6.1. Water development technologies sonic drill system.

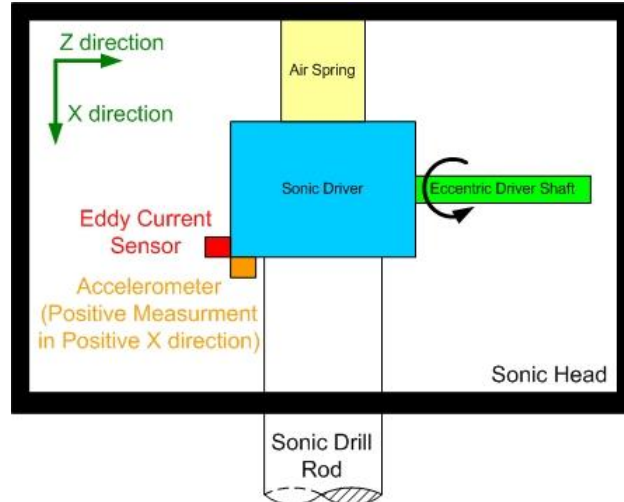


Figure 6.2. Accelerometer and eddy current sensor.

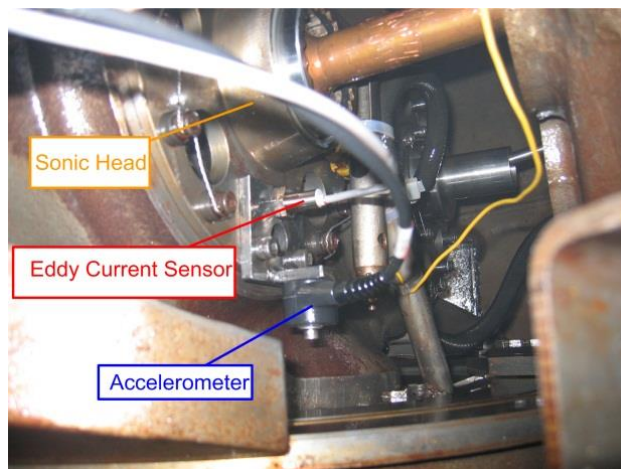


Figure 6.3. Accelerometer and eddy current sensors.

Data Analysis

Test Data and Data Construction

The accelerometer and eddy current sensor data were obtained for times that varied between 10 and 60 seconds at various intervals while as the drill string penetrated from the surface to a depth of 120 feet. The data was then saved as a .csv file and read into a MATLAB[®] script that was used to perform all data manipulation and analysis. The

eddy current sensor data was modeled by a sine wave that mapped the eccentric location. The accelerometer data was filtered, with a low pass filter with a 300 Hz cut off frequency, to take out higher frequency vibrations of the sonic head that are unimportant to the control system. An example of the refined data is depicted in Figure 6.4. Note that the amplitudes are scaled to show the relations of the measured functions to one another.

Phase Angle and Resonance

Knowledge of the phase angle ' Φ_d ' between the input force and the displacement of the sonic driver is the key to accomplish automated control of a sonic drill utilizing measurement feedback. By recording the phase angle between the input force and the displacement, velocity, or acceleration of the sonic driver, many defining characteristics about the system can be established, as presented in the system control variables section below. The salient characteristics to understand in order to determine the resonant condition are the natural frequency of the resonating system, the damping of drill bit and the amount of energy being input into the system and how much of that energy is being used to perform work. The natural frequency is salient because many useful values such as damping ratio and the maximum displacement, velocity, acceleration amplitude frequencies can be determined using the natural frequency. The damping at the drill bit is important as it is related to the amount of energy of the sonic drill system being used to perform real work (drilling). The apparent power going into the system and the real power are calculated from the measured data at the sonic drill head. The apparent and real power are used to derive the mechanical efficiency of the input power being

transferred to the drill bit to perform drilling. The system should be operating with a power factor equal to 1.

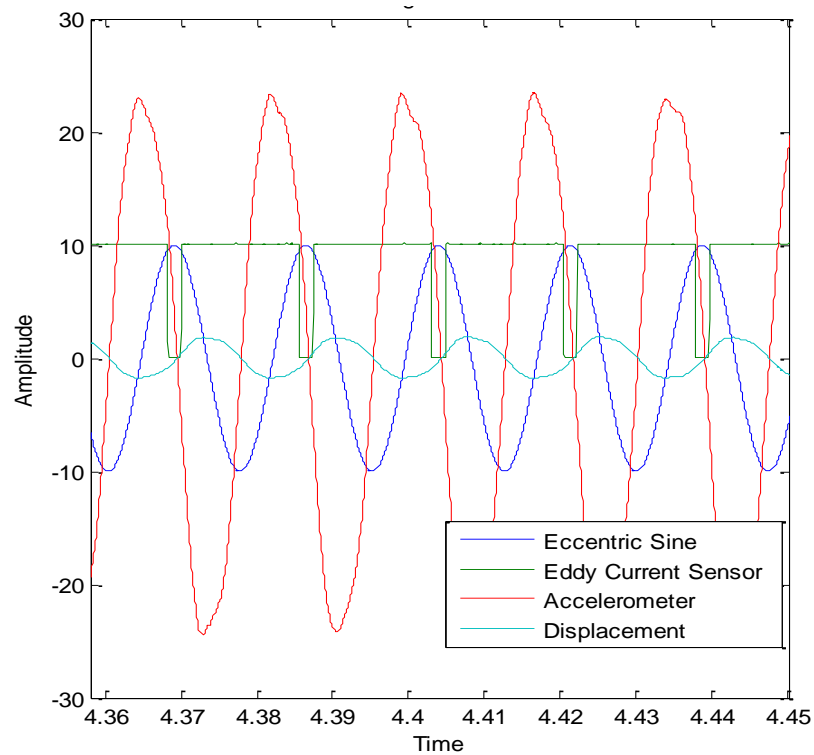


Figure 6.4. Measured signals and reconstructed eccentric motion.

The phase angle (in degrees), was determined by using the relation given in Equation 6.1. The phase angle is defined as the phase between the input force and axial acceleration of the sonic drill head. The phase angle was plotted versus frequency for each of the recorded data sets, and a sample of this is shown in Figure 6.5, which was for 80 feet of drill string.

$$\phi = \Delta t \cdot \frac{\omega_f}{2 \cdot \pi} \cdot 360 \text{ deg} \quad (6.1)$$

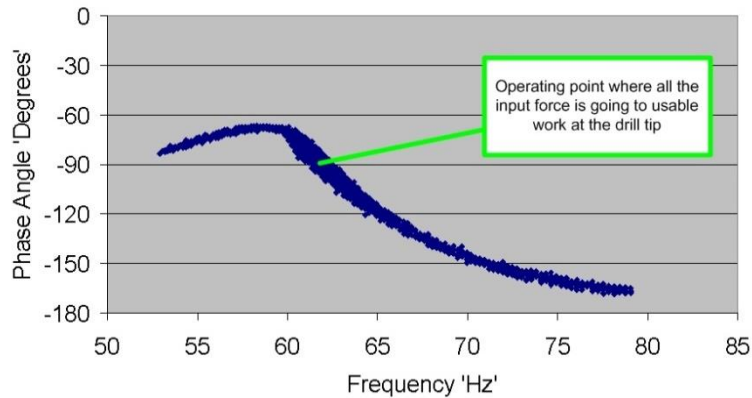


Figure 6.5. While drilling at a depth of 80 feet of drill string, the displacement vs. input force phase angle ' Φ_d ' is shown to peak over -70 degrees, which allows the drill string to pass through -90 degrees while moving into resonance.

The phase angle response for each data set was then compared with the preliminary ANSYS® predictions to determine how well the data correlated. ANSYS, as well as the closed form model, predicted that the phase will always be on -90 degrees for the un-damped natural frequency.

Push or Pull Force and Resonance

The push or pull force is the constant force applied onto the drill string by the structure. The push or pull force mainly changes the boundary conditions at the drill bit. For example, if the push force that is applied the drill bit exceeds 9000 lbf, then the drill bit will become effectively “fused” to the bottom of the hole and will act as a node. This operating condition is bad for drilling because it changes the boundary condition to a fixed condition where the sound energy is reflected back to the system and the drill bit has little to no relative motion for drilling. When the drill bit has little to no relative motion the drill bit may generate heat, which cannot be normally dissipated by the drilling action, which results in excessive heat buildup in the drill bit and under some

cases it has melted down. The actual amount of push force to cause this condition at the drill bit will need to be further quantified through empirical testing on various strata types and push forces. Figure 6.6 shows a result with a large down force (e.g., >9,000 lbf) applied and the phase angle does not reach a value of -90° , which impedes the transmission of driver power to the drill bit. In other words, the system suffers from power factor losses. The reason the phase angle does not reach -90° is that the drill bit is coupling with the media being drilled, causing the system to behave like a non-resonant pile. However, the resonant equations developed earlier, Table 3.8, are still valid and can be used to track resonance while also finding the amount of damping in the system. The heavy damped system is directly produced by applying excessive downward force in an effort to increase the penetration rate. While driving the drill string into the ground with 80 feet of drill string, the downward force was increased from 9,000 lbf to 13,800 lbf, which demonstrated that higher down force negatively impacted the resonant system. When the down force was increased the system became even more damped causing 20% less energy to be delivered to the end of the drill string, as displayed in Figure 6.7. The penetration rate also dropped from 2 to 1 feet per minute, when the down force was increased. Because of the additional damping to the system, the phase angle change did not extend much higher than -90° nearly making the system a heavily damped system (a system where it is not allowed to reach a point of zero losses for the system), as displayed in Figure 6.6. The plot shows that phase is still measurable. However, when the drill string is exited with this exact downward force at the second drill string resonant frequency with 120 ft of drill string in Figure 6.6, the damping is too high to effectively

track resonance with the same scheme. Conventional knowledge in the sonic drilling industry is that more down force will yield a higher penetration rate. The test data indicates that too much down force will cause the drill string to become too highly damped and thus create power factor losses.

The down force relation was found by the boundary condition model and was determined by the DOE as one of the significant variables. Because the coupling of the strata at the drill bit can be large enough to essentially fuse the drill bit to the strata, the down force must be monitored and adjusted to ensure the ‘fusing’ condition does not occur.

Power

The sonic drill is currently monitored by the hydraulic pressure used to drive the eccentrics. This hydraulic pressure is an indicator the amount of energy being used to drive the eccentrics. However it is important to note that, contrary to standard belief, the maximum energy input to the sonic drill does not occur at the same frequency as the maximum input power into the eccentrics. Hence, using increased hydraulic pressure as a means to improve drill string penetration (which is the commonly used methodology) can be counterproductive and increases the damping of the drill bit. This effect is illustrated below with monitored operational conditions and experimental data but first ideal operational conditions are first explored.

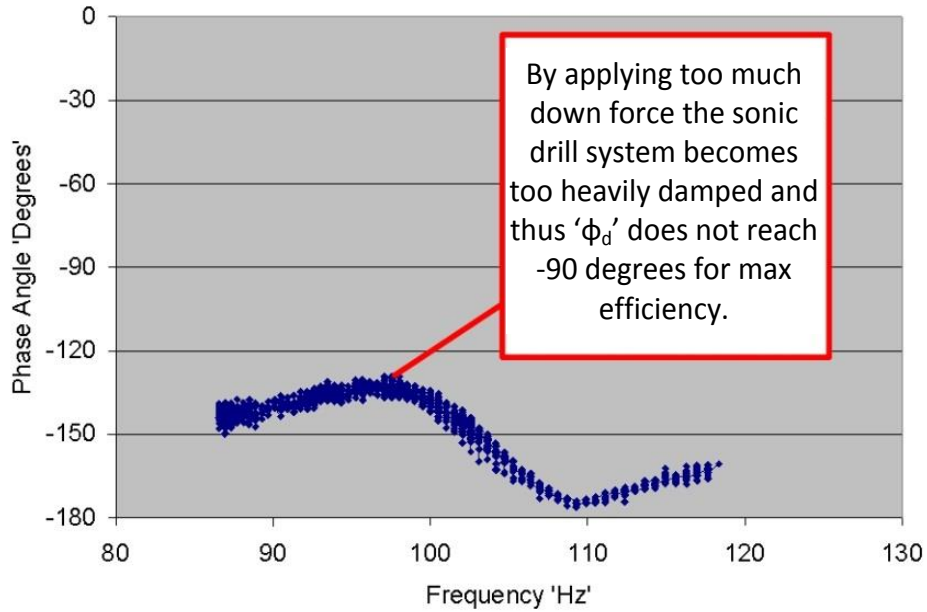


Figure 6.6. While drilling with 120 feet of drill string, the system becomes heavily damped because the operator incorrectly applied too high of a down force (9000 lbf).

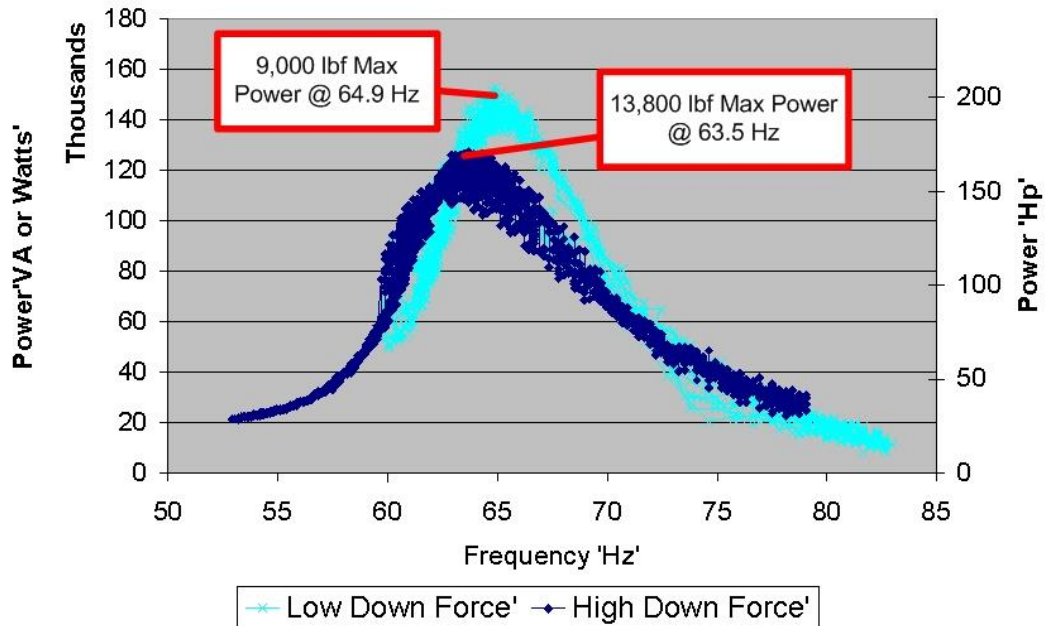


Figure 6.7. While drilling with 80 feet of drill string the operator increases the down force from 9,000 lbf to 13,800 lbf in an attempt to increase the penetration rate, but in doing so it decreases the amount of input power delivered to the drill string that could be utilized for drilling.

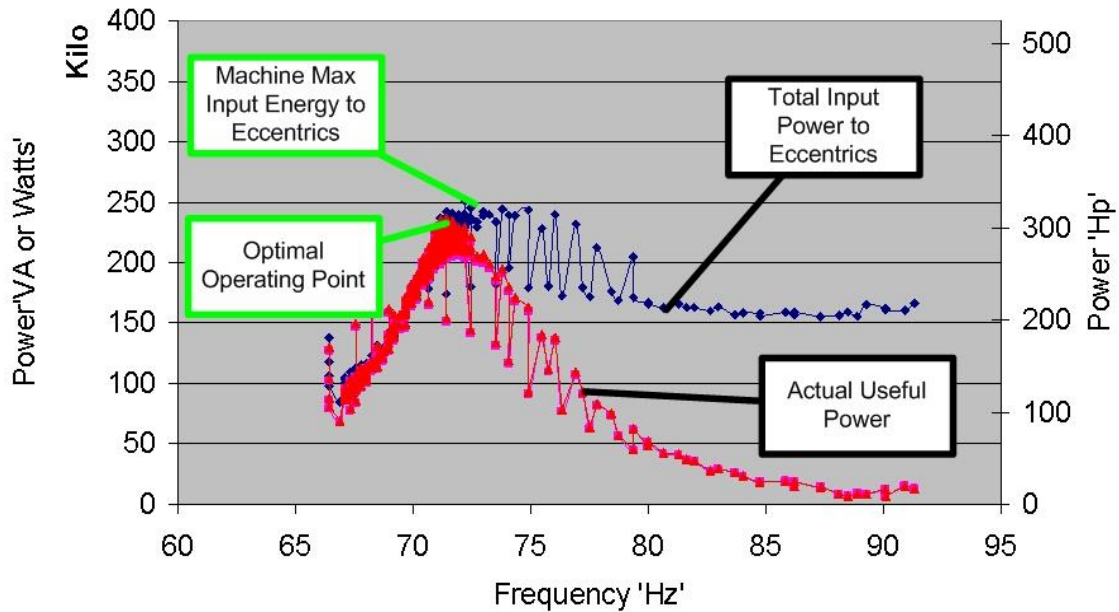


Figure 6.8. While drilling with 70 feet of drill string, the power input to the drill tip for drilling reached a maximum value of 300 hp. The large amount of power transfer was possible by an appropriately matched downward force for the length of drill string.

As shown in Figure 6.8 and Figure 6.9, the resonant system's power factor decreases from 1 to very low values as the phase angle ' Φ_d ' is drops from -90 degrees to -135 degrees-where the power factor is 0.707.

In general, sonic drill operators will monitor hydraulic pressure generated by the diesel engine, which transfers the power to the hydraulic motors that drive the eccentrics. The operator adjusts the frequency of the machine to maximize this pressure. However, as Figure 6.9 displays, the optimal operating point is found before the maximum hydraulic pressure is reached. Essentially, where the engine is producing the maximum energy to drive the eccentrics. However, as shown in Figure 6.9, operating the string by this metric results in the loss of 1/3 of its useful energy to the drill string in additional, extraneous down force exacerbates the problem.

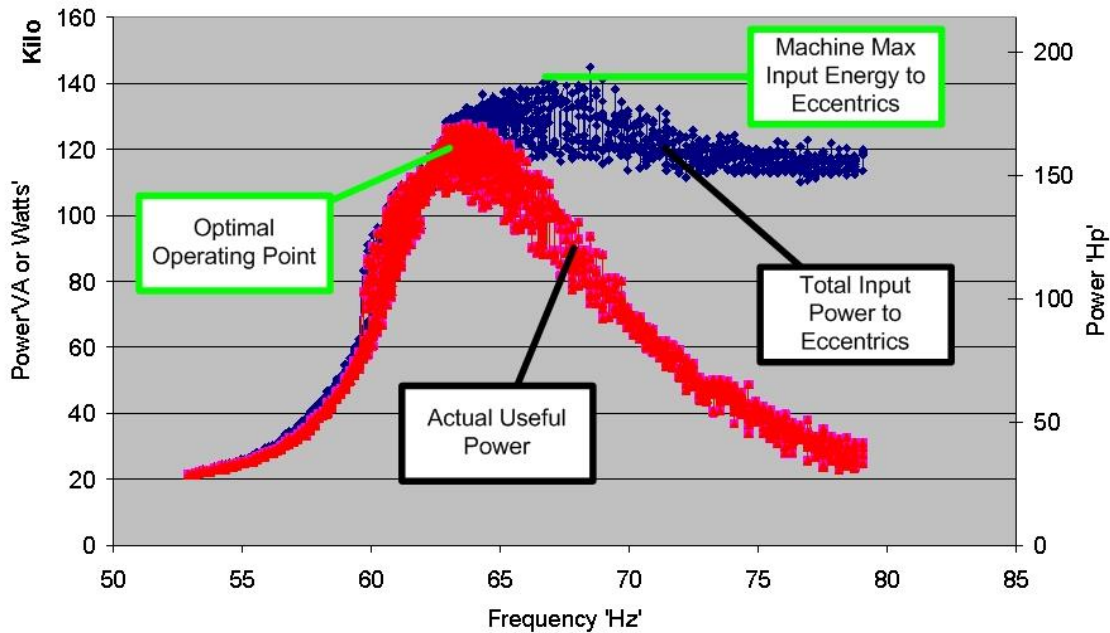


Figure 6.9. The same down force of 9,000 lbf upon the drill string results in a power to drop from 300 hp to 175 hp by adding 10 feet of drill string to the system – Extension from 70 to 80 feet in length.

As the drill sting increases in length, the power factor has a tendency to decrease because of the down force due to the added weight of the drill string. The hydraulic down force imposed by the operator is typically increased, or held constant, as more drill string is added and the hole deepens. Conventional thinking is that longer drill strings require additional down force due to increasing soil-imposed frictional interaction with the drill string. This operator action results in increased damping of the system, because the drill bit couples more with the material being drilled, causing the drill to drive with brute force like a pile driver. This method can sometimes be used successfully with unconsolidated soils. This concept is shown in Figure 6.10, where the real and total power are very different because of the power factor change caused by the large amount of damping due to the larger downward load of the drill string.

An experiment was performed in which increased the down force and the power to the eccentrics dropped from 250 hp to 200 hp while drilling with 120 feet of drill string. However, the actual useful power during this experiment decreased from 175 hp to 70 hp, displayed in Figure 6.10 and Figure 6.11. When the system becomes overdamped the peak input power corresponds with the minimum amount of useful energy transferred to the drill tip for drilling. These results demonstrate that most of the damping was caused only at the drill bit interface with the soil and not along the drill string. If the drill string was allowed to resonate by using less downward force, the total power going in to the drill string would increase and the power curve would look similar to Figure 6.9 and also, Figure 6.7 above, which display that with less downward force damping diminishes. In summary, an experienced operator would typically drive the sonic drill to where the most hydraulic pressure is located, but this is not the location for the best efficiency or penetration power, shown in Figure 6.12. This operating condition is caused by the inability of the operator to know the amount of down force to keep the sonic drill resonating over the entire range of drilling depths.

The displacement, velocity, and acceleration amplitudes are plotted in Figure 6.13. By analyzing the peak values for displacement, velocity, and acceleration, the maximum power delivered to the drill bit is located at the maximum velocity, correlating well with the modeled data above which predicts that the peak power is delivered at the maximum velocity angular frequency ' ω_v '. The maximum displacement ' ω_M ', maximum velocity ' ω_v ', and maximum acceleration ' ω_A ' angular frequencies are located at different frequencies, because velocity and acceleration are related to the displacement by the

operating frequency and operating frequency squared; respectively. The max displacement angular frequency ' ω_M ' is the most important because the work is maximized at this location.

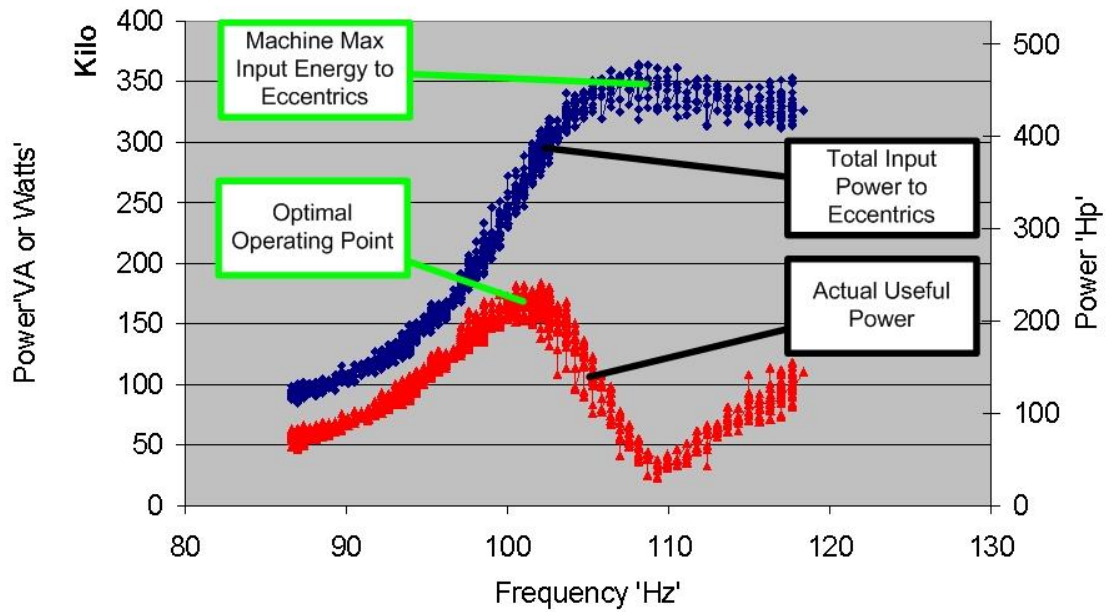


Figure 6.10. While drilling with 120 feet of drill string, high down force causes heavy damping of the system which leads to the separation of total input power (kilo VA) and the actual useful power (kW).

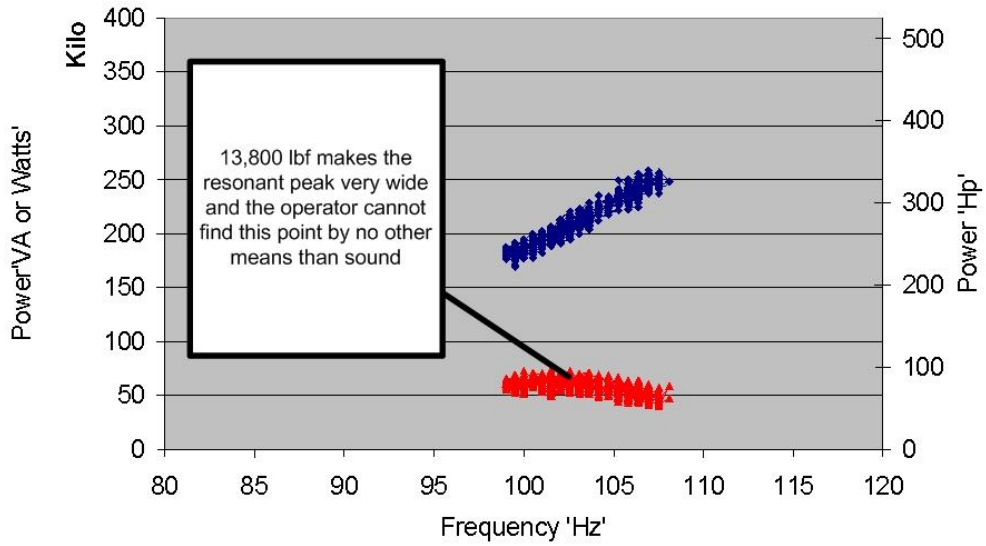


Figure 6.11. While Drilling with 120 Feet of drill string the system became so heavily damped that the resonant peak was not discernible, making it very unlikely that the operator could find resonance. The actual useful power is also below 100 hp where at 9,000 lbf of load the useful power can be as high as 225 hp.

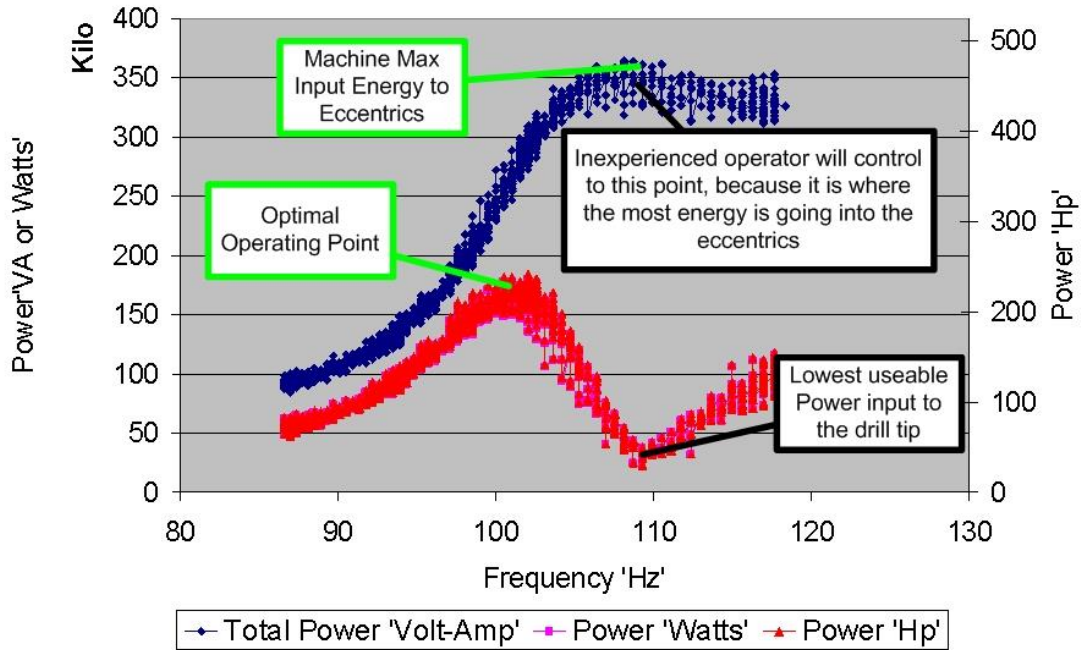


Figure 6.12. While drilling with 120 feet of string, the high down force of 9,000 lbf caused a heavily damped system, increasing the difficulty for a human operator.

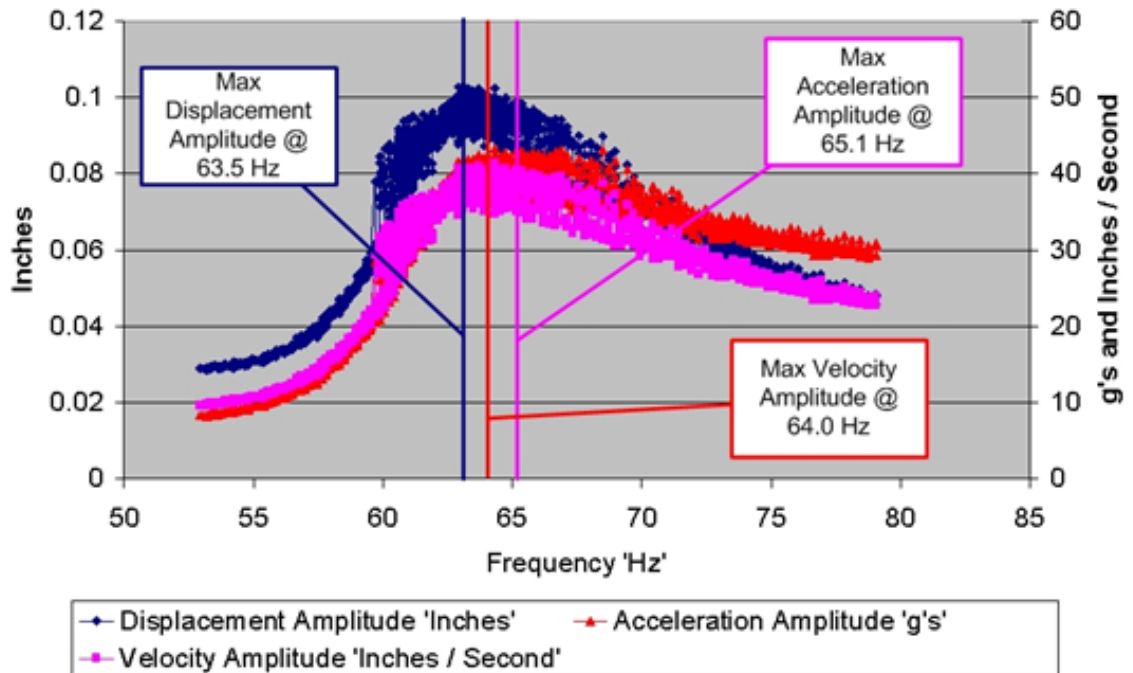


Figure 6.13. The maximum displacement ' ω_M ', max velocity ' ω_V ', and max acceleration ' ω_A ' angular frequencies.

The power relationship is also listed in Table 6.1, where the data indicates that the maximum displacement has more power going to the drill bit than maximum acceleration, even though the maximum acceleration point has 5% more input force. The maximum velocity coincides with the maximum hp, but it is only 0.5% more hp than at maximum displacement. The system is more sensitive with the frequencies above the velocity maximum amplitude natural frequency, because the maximum acceleration natural frequency has 4.9 % less hp than the maximum velocity natural frequency, which is 10 times more power required than operating at the maximum displacement frequency. A plot of the measured phase between the sonic driver displacement, velocity, and acceleration relative to the input force is also plotted in Figure 6.14. The maximum

velocity is located at a phase angle of -20 degrees. From Table 3.8 the maximum velocity is greater than the undamped resonant frequency and is a function of the damping ratio.

Table 6.1. Difference in power for the displacement, velocity, and acceleration maximum amplitude natural frequencies.

Mode	Forcing Frequency	Input force	Velocity	ϕ_v	Useful Power	% Power Loss
Max Displacement	63.5 Hz	80908 lbf	40.6 in/s	-18 degrees	236.4 hp	0.5 %
Max Velocity	64.0 Hz	82187 lbf	40.6 in/s	-20 degrees	237.5 hp	0.0 %
Max Acceleration	65.1 Hz	85037 lbf	40.5 in/s	-30 degrees	225.8 hp	4.9 %

The undamped natural frequency ' ω_n ' and damping ratio ' ζ ' were calculated by using the equations displayed in Table 3.8, which relate the peak displacement, velocity, and acceleration measured frequencies to ' ω_n ' and ' ζ '. Because there are two unknowns, two independent equations must be used. However, there are three equations to choose from. The extra equation combinations will be used as added data to give a better representation of the actual ' ω_n ' and ' ζ '.

The equations used from Table 3.8 are displayed below as equations 6.2 – 6.4. The resulting damping and undamped natural frequency values are displayed in Table 6.2. These values are influenced by measured signal noise making accurate peak amplitude quantification challenging because of the poor signal to noise ratio. A common method to achieve good operating measurements is to operate at steady state for a long time to acquire an average value for the noisy data, by averaging a block of data or using a moving average of the real time measured data. Neither method was used during this work. From the amplitude peaks found in the noisy data, the damping ratio does not

vary by more than 14% from the mean calculated value. Thus during this particular drilling condition, the damping ratio of the system is close to 0.1.

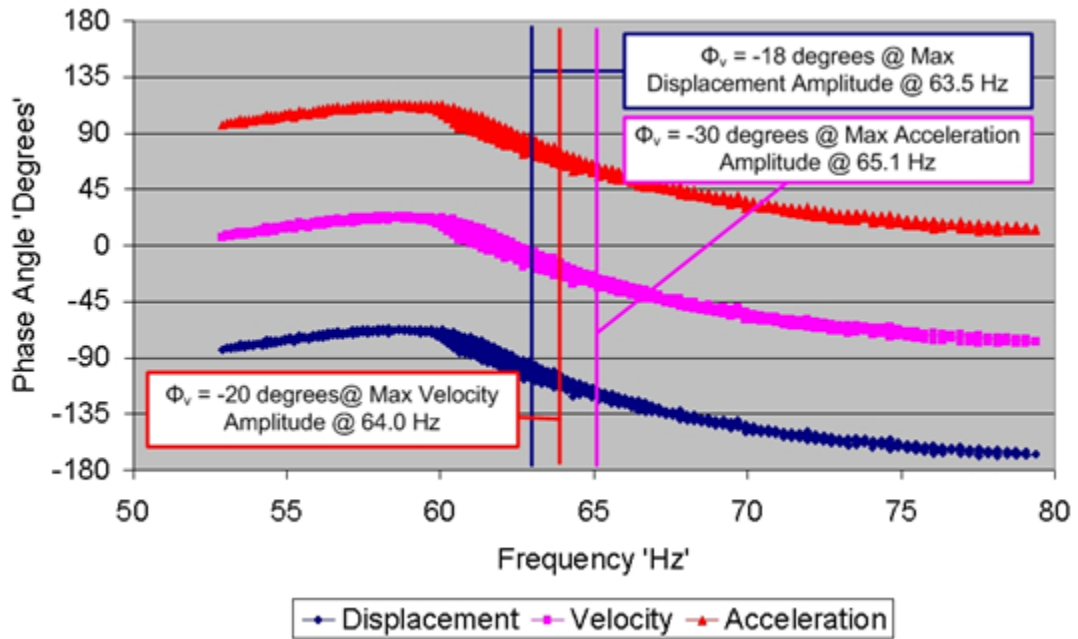


Figure 6.14. The phase between the force input and the corresponding velocity changes between the maximum displacement, velocity, and acceleration amplitude frequencies.

$$\omega = \frac{\omega_n}{\sqrt{1-2\zeta^2}} \quad (6.2)$$

$$\omega = \omega_n \sqrt{2.0 - 1.0\sqrt{16\zeta^4 - 16\zeta^2 + 1.0} - 4\zeta^2} \quad (6.3)$$

$$\omega = \omega_n \sqrt{1.5 - 0.5\sqrt{36\zeta^4 - 36\zeta^2 + 1.0} - 3\zeta^2} \quad (6.4)$$

Table 6.2. Calculated undamped natural frequency and damping ratio.

Equations Used	Undamped Natural Frequency	Damping Ratio ' ζ '
6.2 and 6.3	63.03 Hz	0.086
6.2 and 6.4	62.82 Hz	0.103
6.3 and 6.4	62.30 Hz	0.113

This premature damping of the drill bit (as displayed in Figure 6.10 through Figure 6.12) is due to excessive push down force. The excessive push force arises from a lack of understanding on drill string dynamics and force coupling at greater depths. The current maximum depths of 500-700 feet can be attributed to the drill string becoming sufficiently heavy that the rig actually needs to apply pulling instead of push force to be able to resonate the drill string with the drill bit in the free condition, displayed in Figure 6.15, and not fuse the drill bit to the strata to be drilled (fixed boundary condition). Based on the amount of power and damping encountered during the tests, the goal of drilling to depths greater than 1,500 feet becomes feasible as the power is sufficient to drill to these depths considering the amount of damping on the drill string sides.

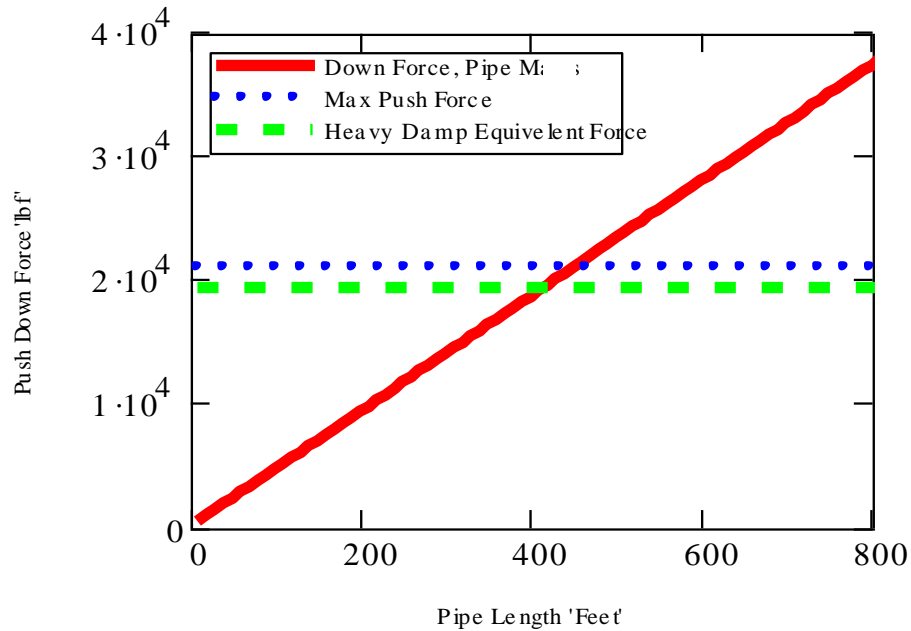


Figure 6.15. The drill string mass is aiding in the push down force for penetration. Based on the tests the Equivalent pull down force for a heavy damped system was calculated and found to be very close to the drill string's own weight at about 400 feet. This is the onset of where the drill string will behave more like a pile driver than a sonic drill. The drill will still penetrate, but at a reduced rate to the maximum depths between the 500 and 700 foot ranges.

Experimental Results

Through collection of data at the sonic drill head, experiments were performed to measure the power going into the drill string as well as the power delivered to the drill bit to perform drilling. The experimental tests outlined above were used to derive the counterintuitive system responses for drilling. The first and most important counterintuitive aspect to sonic drilling is that the down force is critical to system dynamics. Drilling operators are trained to apply more down force that applies additional push force onto the drill bit. In standard rotary drilling, this will increase the force on the drill bit causing additional shear of material and subsequently increasing the penetration

rate. However, when this rule of thumb is applied to sonic drilling, the drill bit becomes fused to the bottom of the hole and drilling stops. When the drill bit becomes fused to the bottom of the hole, the results on the power and efficiency of drilling are displayed in Figure 6.16.

Figure 6.16 describes the sonic drilling performance data, labeled as ‘A’, ‘B’ and ‘C’, that were obtained to establish the sonic drilling performance over a range of different operating conditions.

The optimum operating point for this specific test and series of formulations, labeled ‘A’, shows that the drill bit is receiving nearly 100% of the input power to utilize for drilling at the drill bit. The drill string was measured to be in resonance at this point. This operating condition resulted in a high penetration rate, about 5 ft/min.

The method used to obtain and maintain this optimal operating point is “not-obvious” and it has been determined that this condition can only be achieved, and maintained, by use of automated control methodology, which simultaneously monitors, evaluates and controls the status of the drill string and the sonic head.

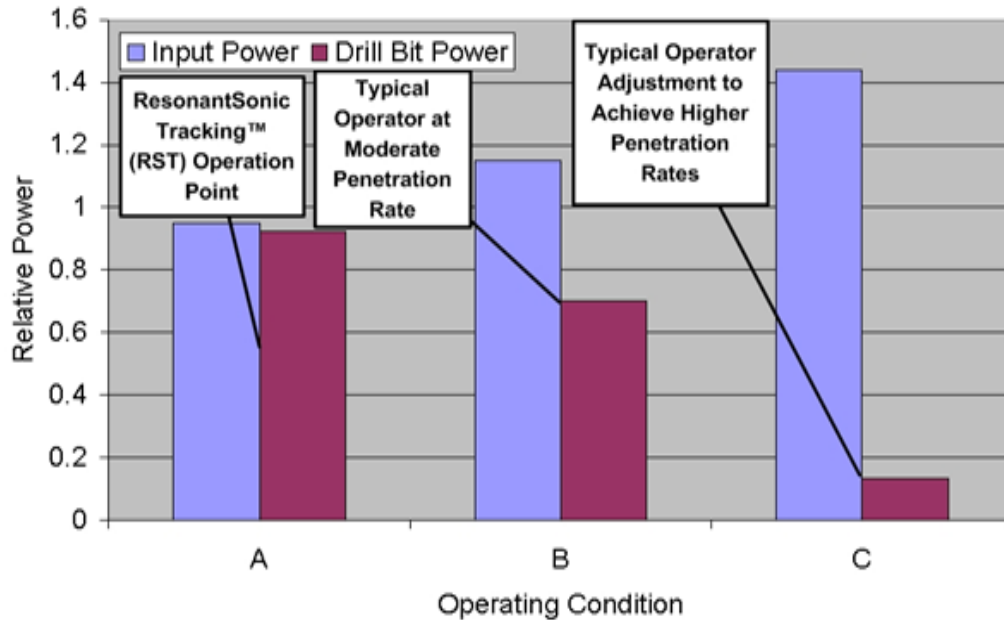


Figure 6.16. Sonic drilling performance data.

During the operating condition labeled ‘B’ the transferred power to the drill bit is about 22% less than the input power to the sonic driver. This operating condition occurs at the resonant condition of the drill string, but not at optimal operating conditions. This operating condition is typical for an operator-controlled system and is perceived by a trained operator as optimal conditions.

Two performance characteristics can be observed from a comparison of the two power functions for conditions moving from operating condition ‘B’ to ‘C’. First, as the operator adjusts the input power past peak power level to the drill bit, the power to the drill bit plummets. This is a result of the drill string falling off of resonance and the drill string penetration rate slows from 5 ft/min at condition ‘A’, shown in Figure 6.8, above, to about 3 ft/min at ‘B’ for this specific test and series of formations. Secondly, as the operator takes action, applying additional down force to keep the drill string moving

downward (condition 'C') it becomes clear that the power transferred to the drill bit actually decreases. This decrease in power transferred from the driver to the drill bit (loss of 83%) was accompanied by a reduction in the drill string penetration rate for this specific test and series of formulations, slows from 3 ft/min at condition 'B' to about ½ ft/min at 'C'.

Contrary to conventional belief, and as shown Figure 6.16, the maximum power to the driver does not directly correlate to the maximum power being delivered to the drill bit. During operating condition labeled 'C', the maximum input power to the sonic driver was being achieved, however at the same condition the minimum amount of energy was delivered to the drill bit. This condition was taken from Figure 6.10, above.

Another way to evaluate the data presented in Figure 6.16, is the drilling efficiency as displayed in Figure 6.17.

The bar charts, shows in Figure 6.17 above show efficiency of input power to power being delivered to the drill bit for the three different operating points; 'A', 'B' and 'C'. (These are the same 'A', 'B' and 'C' operating points that were shown in Figure 6.16.) Even though the input power was increased for the operating points 'A' to 'C' in ascending order, the energy transfer efficiency progressively decreases. The point of this figure is to graphically illustrate that when the sonic drill system is incorrectly controlled, severe losses in drill penetration performance result.

The means to overcome these huge losses in drilling efficiency is to provide automated control. The proposed automated control is described in the commercial applications section and is termed ResonantSonic Tracking™ (RST™). RST™ is

required because operating conditions needed to maintain the best drilling performance as the drill string penetrates the earth are counterintuitive and are not achievable by manual control.

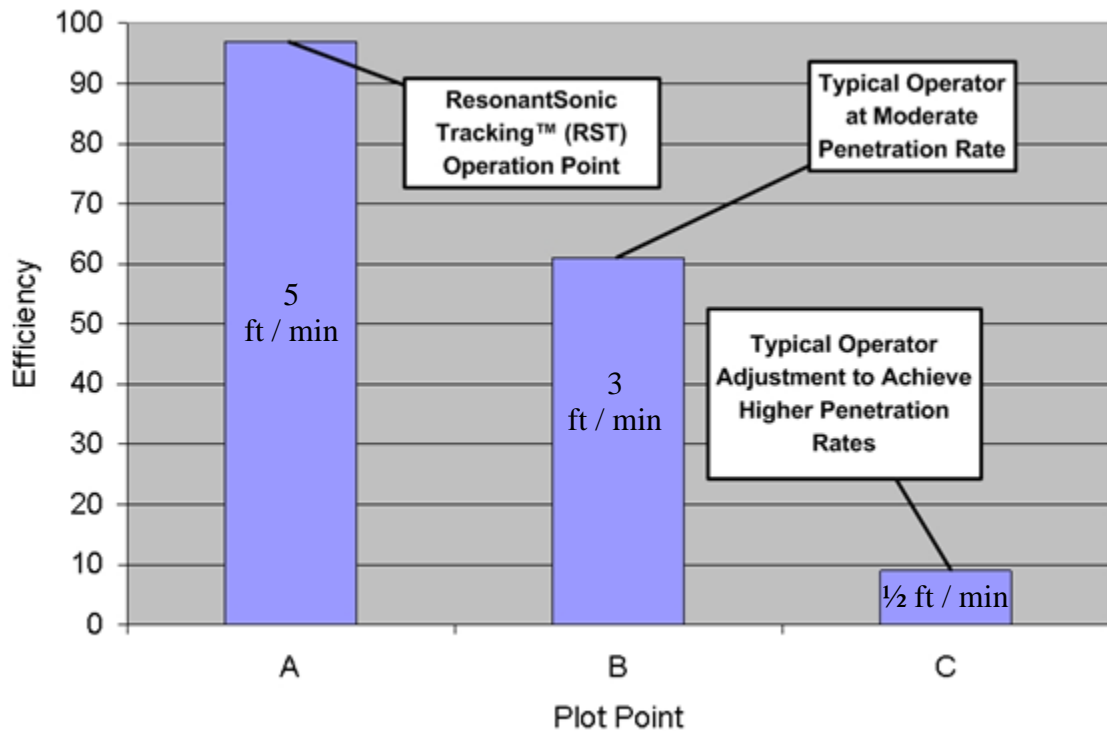


Figure 6.17. Sonic drilling efficiency.

Another result of this research relates to the down force. As the drill string becomes longer, the drill string weight increases. As the drill string weight increases due to increased lengths, the added weight also adds down force onto the drill bit. A plot of the increased down force is displayed, in Figure 6.15, above and suggests that to effectively perform drilling to depths greater than 500 feet (for the 9" OD drill pipe) that pull force on the drill string must be applied. The drill string will still move down because the weight of the drill string is much greater than the pull force applied, but it is

counter intuitive that this force is necessary to drill. This is why the sonic drills are limited to 1000 – 1500 feet, because the drill string weight is enough to fully fuse the tip of the bit to the soil at these drill lengths based on the testing data.

Experimental Conclusions

The test data confirms the findings from the model that coupling between the sonic drill bit and the drilling strata is the most important variable. This variable greatly limits the drilling ability of the sonic drill at deeper depths and is thus, the reason why sonic drilling has a perceived maximum drilling depth of 1000-1500 feet.

Three counterintuitive items were found by experimental testing and data analysis. First, the sonic drill down force can essentially ‘fuse’ the drill bit to the strata. This changes the drill resonant conditions and doesn’t impart sufficient force to drill strata, because it is just acting to reflect the sound waves back up the string and act as a fixed boundary condition.

The second counterintuitive item was that the impact of the down force becomes worse with increased drill string length. Therefore, it was determined that when drilling depths greater than 500 feet, using drill and drill pipe, pull force instead of push force should be applied at the sonic drill head while drilling to achieve optimum drilling.

The third counterintuitive item found, was that the sonic drill operators should not control the drill at the maximum hydraulic pressure being delivered to drive the eccentrics. However, because of the aforementioned down force, the resonant system would excite a resonant mode, that would push energy back onto the sonic driver requiring additional pressure to perform minimal work at the drill bit. Thus, the sonic

drill hydraulic pressure doesn't represent the drilling condition and should not be used as a point of monitoring or target for control.

In addition to the counterintuitive findings, the sonic drilling condition was verified that it could be measured and quantified at the sonic drill head. The system control variables are described in more detail in the next section, System Control Variables. Because of the counterintuitive items, and the current means of controlling sonic drill systems, an automated control system to operate the sonic drill to the optimum drilling conditions is required.

CHAPTER 7

SYSTEM CONTROL VARIABLES

Introduction

One of the primary goals of the research effort was to identify the governing control variables for the sonic drill and identify the degree of importance of each, Chapter 5. The important variables of influence were listed in the conclusions section of Chapter 5 in Table 5.14 and Table 5.15. It was also determined that the damping along the length could be influential, but the means of finding the significance by measuring the phase angle of the input force and the resultant sonic head acceleration amplitude, was verified in Chapter 6. A means of measuring and controlling each of the variables was also identified in chapter 6. A process control schematic was developed, which demonstrates the actual process control needed for an automated control system.

An explanation of the modeling of the hydraulic system was covered in previous chapters and is only represented as a block diagram in this chapter. When the drill is drilling through high damping material and suddenly breaks through to a layer of very low damping material great amounts of energy being input into the drill and it can no longer dissipate the energy during drilling. Thus it will begin to store the added energy very rapidly to the drill system. The energy stored in the drill string grows uncontrollably until the sonic drill string breaks or the drill reaches a layer of high damping where the energy can again be dissipated. The rapid growth of oscillations can be detected at the sonic drill head. In this condition, the sonic drill rate of penetration will typically also

increase, which can also be detected at the sonic drill rig. This rapid growth in oscillation amplitude condition is referred to as an unsafe or unstable system. The system in this condition is not able to reach equilibrium and ultimately results in a failure in the mechanical system.

The sonic drill system is driven by eccentric masses, which are typically powered by a hydraulic system. The design of the control matrix is to minimize input power, but maximizing the penetration rate. By creating higher penetration rates while expending less energy will decrease the cost to implement sensors by drilling boreholes. Also the associated cost due to mechanical failures will be greatly mitigated sensing and automated control of the mechanical resonance system, allowing responses more rapidly than an operator.

It was determined from the boundary condition model, that the most influential variable was the coupling of the strata at the drill bit. It was also verified through testing that this coupling with the strata at the drill bit and be adjusted by use of the push or pull force above ground. The frequency of input force was also an influential parameter that can allow the system to resonate at different mechanical resonant modes of the sonic drill system. The next section describes these monitoring and control variables and how to adjust them to choose the optimal resonant mode as well as how to control to high power efficiency. The other parameters for the boundary system are system specific and not used for control.

Measurements above Ground

Sonic Drill Head Response

Both the axial and lateral amplitudes are important to monitor. The axial displacement and velocity amplitudes are used to identify when the sonic drill is approaching the resonant condition. The velocity amplitude can be used to conclude when the maximum amount of energy can be input into the system; however, this may not be at the ideal operating condition. The ideal power consumption condition can be monitored and controlled by measuring the phase of the input force with the resultant sonic drill head velocity and controlling the input frequency until they are in phase with one another. This will give the system a power factor of one.

The lateral motion at the sonic drill head can be used to determine if any bending moment resonant modes are coupled with the primary axial mode. The axial mode should be free of any weak coupling to the closest lateral mode. Otherwise the lateral mode will rob and release energy back to the axial mode, causing control issues by making the control algorithms unstable. This phenomenon is well known and is typically taught in early mechanical vibration courses, and will not be included in this body of work (34).

It has also been observed with other research by Jeffery Barrow and his team (20) that axial acceleration spikes at the sonic drill head may indicate that the drill string might be approaching a condition that will limit the drilling penetration rate and possibly damage the drill string. This observation was not validated in this body of work, but it is

also a consideration that could be measured for extended control measures for safety and drilling efficiency.

The axial amplitude at the sonic drill head can also be used to determine the resultant sonic drill motion below the surface. This was demonstrated in that the mode shapes could be found using the boundary condition method and the fact that damping along the length of the drill string damps the entire mode shape, but the relative deflection ratios along the length of the string are consistent. With that being said, displacements along the length can be used to find the relative stresses along that length, for which algorithms can be developed to monitor and control the sonic drill head amplitudes to keep the string at safe stress levels. This is explained further in the Control Applications chapter.

Phase Relation and Input Power

The input force phase relative to the sonic drill head velocity and the input power are used to determine the efficiency of drilling. If the phase difference of the input force and the sonic drill head velocity is not 0, then energy is being stored in the drill string and released back onto the hydraulic motors performing the work. In this way, the system becomes less efficient. As described earlier, the input power can be calculated by multiplying the RMS input force with the RMS input velocity and the cosine of the phase between the two.

It is also proposed that the power required to drill along with the down force can be correlated to the type of strata being drilled. It should also be noted, that the use of

flushing material and the rate of rotation may also affect the correlation and will probably be less significant variables in the model.

Through empirical tests, the input power calculated using the input force and velocity of the sonic drill head, should be used for control. The input power (VA) calculated can also be broken down into both the real and reactive power. The real power (Watts) is used to perform work, while the reactive power (VARs) is stored by the system and reacted back onto the driver. The hydraulic pressure and flow driving the eccentrics provides the operator with the total apparent power (VA) being delivered to the system, but doesn't provide the operator with how much of the power is going into real work (Watts) or power being stored and reacted by the system (VARs).

Rate of Penetration

The rate of penetration and input power are used to determine the true drilling efficiency. The rate of penetration should be maximized while minimizing the input power. We have identified that the weight on bit must be controlled in order to have high drilling efficiency. In addition, the sonic drill system frequency should be on a resonant condition with a power factor of one. It was modeled in Chapter 5 and verified in Chapter 6 that the amount of down force on the drill bit can affect the rate of penetration. The methods of applying pull force to regulate the amount of down force was described in Chapter 6 and will not be repeated here, but to reiterate that first the force on the bit must be adjusted to ensure good coupling before the rest of the control can be implemented.

Axial Resonance Mode Choice

From the finite element model: as the drill string become longer, more axial resonant modes are available in the sonic drill operating range for the control system or user to select. The optimum drilling mode can be found mathematically or empirically, the next two subsections describe these methods.

Mathematically

The method to determine the resonant modes mathematically also depends on acquisition of accurate data on strata types already penetrated. The resonant modes are derived mathematically by using measured data, a plot similar to that displayed in Figure 3.18, and converting into damping and spring values along the length using equations 4.36 and 4.37. Using the methods described, the sonic drill conditions are displayed in Table 7.1, the mode shapes were solved using the closed form model coded in MATLAB[®].

Table 7.1. Sonic Drill Variables used for Example.

Sonic Drill Variables			
Sonic Drill String Length	250 ft	76.2	m
Sonic Head Mass	1000 lbs.	450	kg
Elastic Spring Support	72,000 lbf/in	1.20E+07	N/m
End Mass	18 lbs.	8	kg
Pipe wall thickness	0.5 inches	0.0127	m

Then the mode shapes from the finite element model were found for the given length, for this particular example, 250 ft. Figure 5.18 shows that two resonant modes can be excited between 60 Hz and 135 Hz. These two sonic drill mode shapes are

displayed in Figure 7.1, the corresponding natural frequencies are 59 Hz and 90 Hz. The normalized mode shapes for these frequencies are displayed in Figure 7.2.

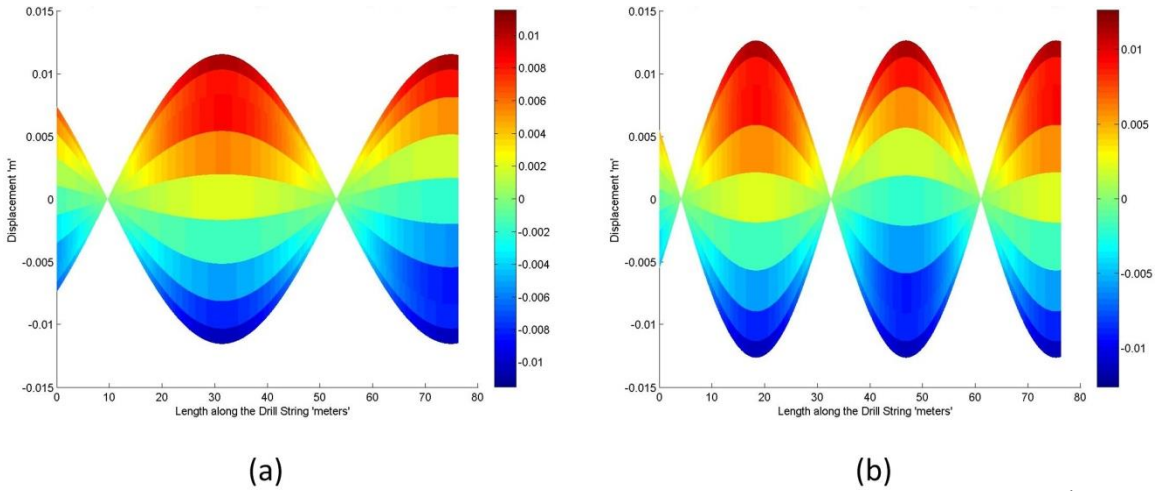


Figure 7.1. Sonic drill mode shapes for a 76.2 m (250 ft) long drill string. (a) 2nd mode shape and (b) 3rd mode shape.

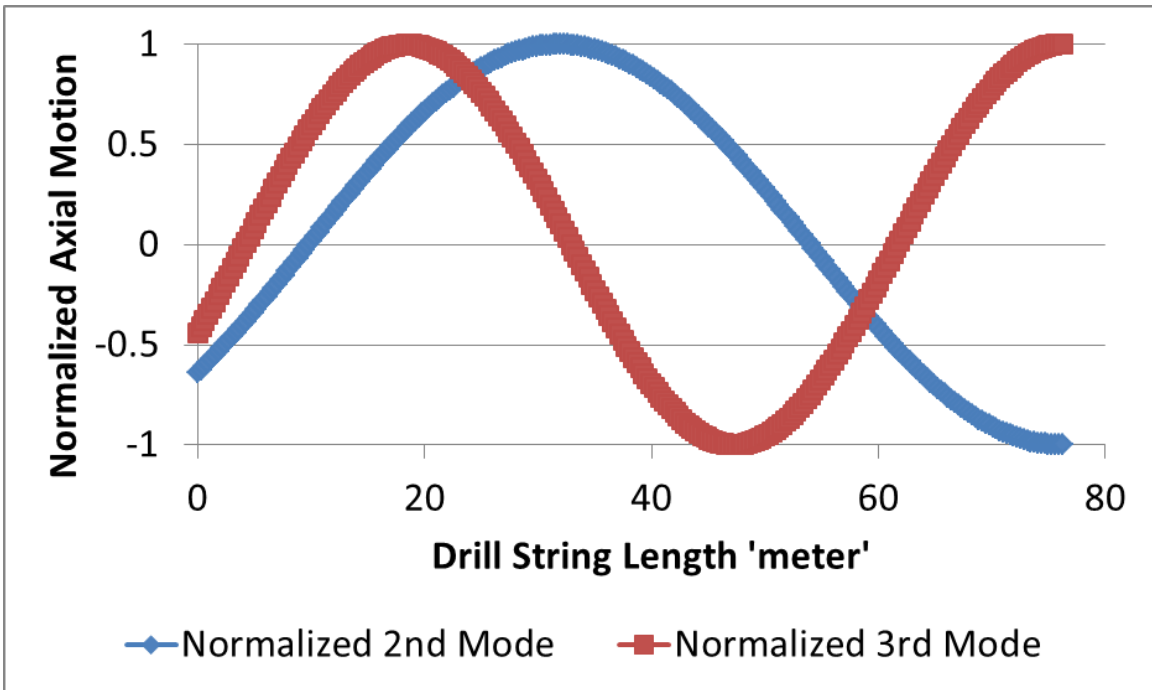


Figure 7.2. Normalized mode shape for a 76.2 m (250 ft) long drill string.

Sonic drill mode shapes found using the closed form model are normalized to 1. By using equations 3.46 and 3.47, the damping ratio can be used as a metric to identify the best mode. Three different damping and spring rate conditions were examined: 1) Constant rate, 2) Increased rate, and 3) Step function rate, displayed in Figure 7.3 and Figure 7.4. The better resonant mode has the lowest effective damping value. In the example of a 250 ft long drill string, there are few instead of many nodes in the mode shape, which causes error in the damping calculation. The uncorrected damping numbers are listed in Table 7.2. By correcting for the error, by calculating a correction coefficient for each mode to make the constant damping and spring calculation for both modes equal to the constant value input (43.2 lbf*s/in). The corrected effective damping and spring rates are listed in Table 7.3. The 3rd resonant mode is chosen because it has an effective damping value of 26 lbf*s/in, which is 3.8% lower than the 2nd mode. However, the 2nd mode is chosen for the step condition because it has 10 % lower damping.

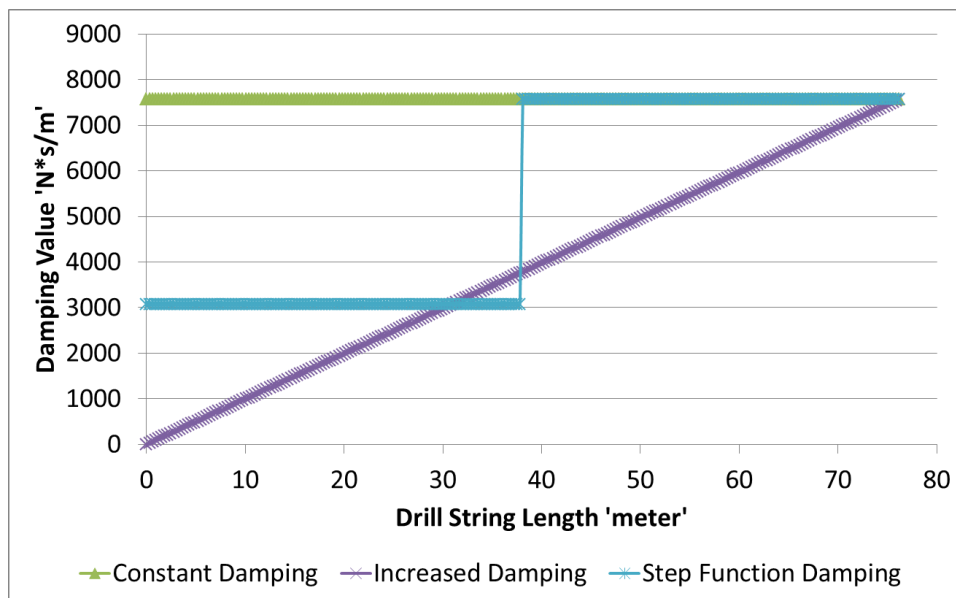


Figure 7.3. Three different damping conditions along the length of the drill string.

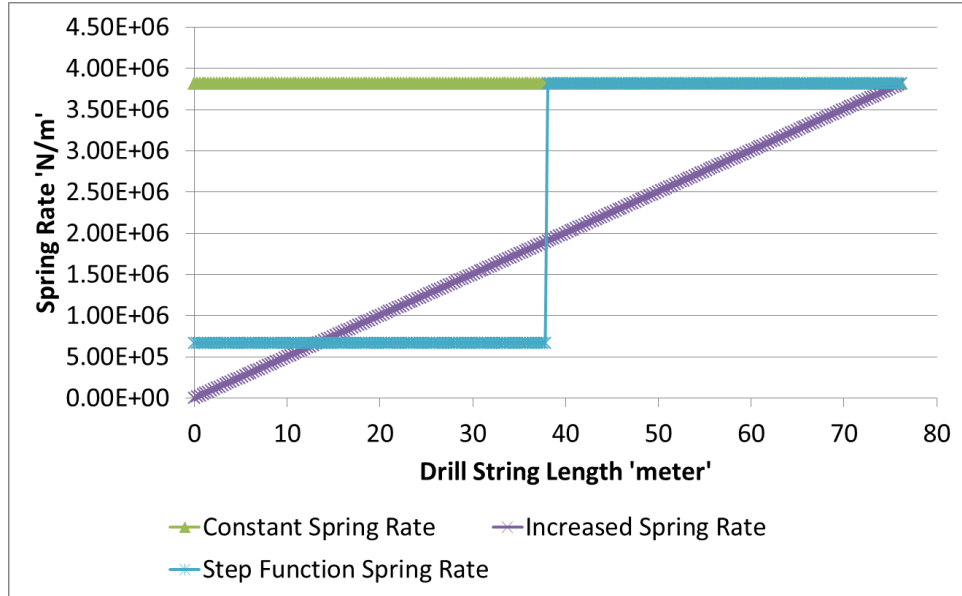


Figure 7.4. Three different spring rate conditions along the length of the drill string.

Table 7.2. Equivalent damping and spring constants along the length of the drill string without RMS correction.

Equivalent Damping Constant					
Damping Condition	2 nd Mode	3 rd Mode	Percent Difference	2 nd Mode	3 rd Mode
Constant	41.4 lbf*s/in	42.3 lbf*s/in	2.3%	7242 N*s/m	7409 N*s/m
Increased	25.8 lbf*s/in	25.4 lbf*s/in	1.6%	4523 N*s/m	4453 N*s/m
Step Function	31.0 lbf*s/in	34.2 lbf*s/in	10.2%	5435 N*s/m	5987 N*s/m
Equivalent Spring Constant					
Damping Condition	2 nd Mode	3 rd Mode	Percent Difference	2 nd Mode	3 rd Mode
Constant	20840.6 lbf/in	21318.7 lbf/in	2.3%	3649749 N/m	3733484 N/m
Increased	13016.1 lbf/in	12813.8 lbf/in	1.6%	2279473 N/m	2244047 N/m
Step Function	14639.3 lbf/in	16482.0 lbf/in	12.6%	2563741 N/m	2886441 N/m

Table 7.3. Equivalent damping and spring constants along the length of the drill string with RMS correction.

Equivalent Damping Constant					
Damping Condition	2nd Mode	3rd Mode	Percent Difference	2nd Mode	3rd Mode
<i>Constant</i>	43.2 lbf*s/in	43.2 lbf*s/in	0.0%	7565 N*s/m	7565 N*s/m
<i>Increased</i>	27.0 lbf*s/in	26.0 lbf*s/in	3.8%	4725 N*s/m	4547 N*s/m
<i>Step Function</i>	32.4 lbf*s/in	34.9 lbf*s/in	7.7%	5678 N*s/m	6114 N*s/m
Equivalent Spring Constant					
Damping Condition	2nd Mode	3rd Mode	Percent Difference	2nd Mode	3rd Mode
<i>Constant</i>	21770.0 lbf/in	21770.0 lbf/in	0.0%	3812511 N/m	3812511 N/m
<i>Increased</i>	13596.6 lbf/in	13085.1 lbf/in	3.8%	2381128 N/m	2291548 N/m
<i>Step Function</i>	15292.2 lbf/in	16830.9 lbf/in	10.1%	2678073 N/m	2947539 N/m

The above method was also used with the finite element model results in Chapter 5 for the different damping and spring rate conditions along the drill string length.

Empirically

The empirical method involves a frequency sweep or a chirp signal with the sonic drill driver and using the half-power bandwidth method to determine the damping ratio for each mode. The half-power responses and their corresponding frequencies can be used in Equation 7.1 to estimate the damping ratio of a single-degree-of freedom viscously damped system (34). Figure 7.5 below shows the plot of oscillation amplitude versus frequency.

After identifying the resonant peak frequency and measuring the frequencies at the half-power amplitude, the factored damping ratio ‘ ζ ’ can be determined.

$$2\zeta = \frac{\omega_2}{\omega_n} - \frac{\omega_1}{\omega_n} \quad (7.1)$$

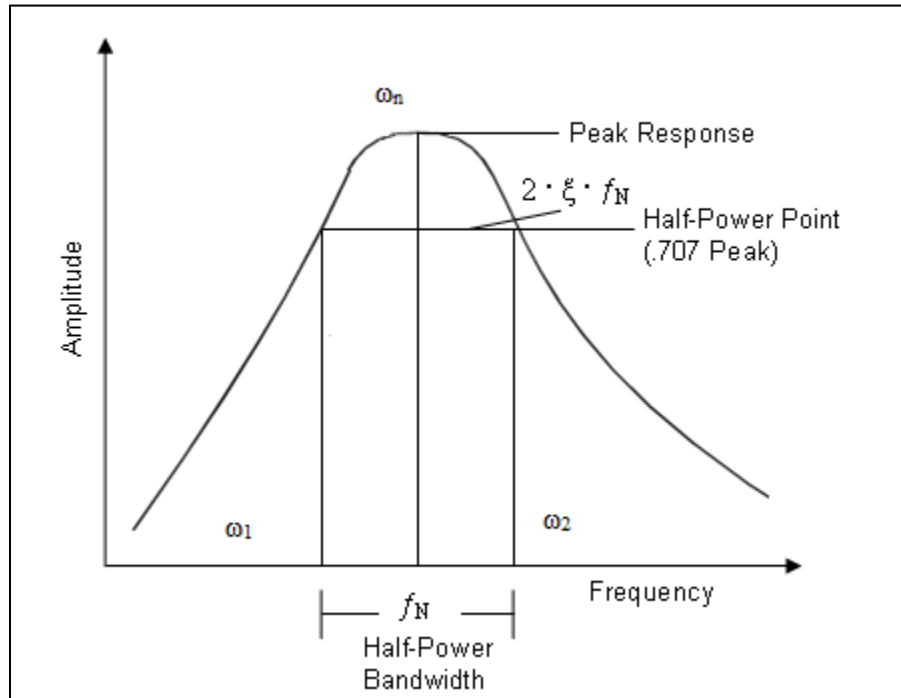


Figure 7.5. Half-power bandwidth method to determine the damping ratio. (34)

The highest frequency mode, with the lowest damping ratio should be chosen. The axial and bending resonant frequencies can be easily measured using accelerometers mounted on the sonic drill head. Axial modes that have lateral modes within 2 Hz should be skipped, as weak spring coupling could affect the control system.

The above two systems of control work for determining steady state operating conditions, however, if a sudden change exists in the drilling system at the drill bit, the system should react quickly. The next section discusses the ideal response when a sudden change in drilling at the drill bit occurs.

Other Measurement Control Conditions

Rapidly changing drilling conditions can cause unsafe operating conditions. One such change in conditions is when a void is encountered while drilling. The void causes a rapid decoupling of drill bit from the surrounding drilled media. When this occurs, there is insufficient damping of the sonic drill system to limit the magnitude of drill rig oscillations and thus the drill string starts to “runaway.” A runaway condition on resonance allows the energy to grow in the system until either the structure undergoes mechanical failure or a safe equilibrium between the input force and damping returns. The control system guards against this type of damage by constantly monitoring system operating parameters, including phase angle and amplitude of the displacement of the sonic drill head. Monitoring any value related to either of these two metrics can also be used. Because a sonic drill operates in mechanical resonance, oscillations can grow in a controlled fashion, allowing the control system to detect and change the operating conditions, such as the input force frequency, input force amplitude, push or pull force, rate of drill bit rotation, and flow rate of the flushing media. In Figure 7.6, two conditions are displayed. The first is the response of the sonic drill while drilling through hard rock and the second is the system response if a void is encountered. While drilling hard rock with a sonic drill at 55 Hz, Figure 7.6 shows that the drill configuration is operating in stable safe conditions. However, if the same drill then were to drill into a void, or a cavern, then the drill would start to build amplitude to unsafe operating conditions. These unsafe operating conditions were stated above and were defined when the system is in a runaway state.. Other unsafe operating conditions can be defined as

operating outside the bounds of the control system, operating at unsafe stress conditions on the drill string and sonic drill head, operating with little motion on the drill bit which can cause bit failure due to excessive heat, and operating at down forces that could cause buckling of the drill string. Normal operation within the specified parameters of the control system are deemed safe operating conditions. Therefore, it is necessary for the control system to detect and stop the runaway condition before damage occurs to the sonic drill system.

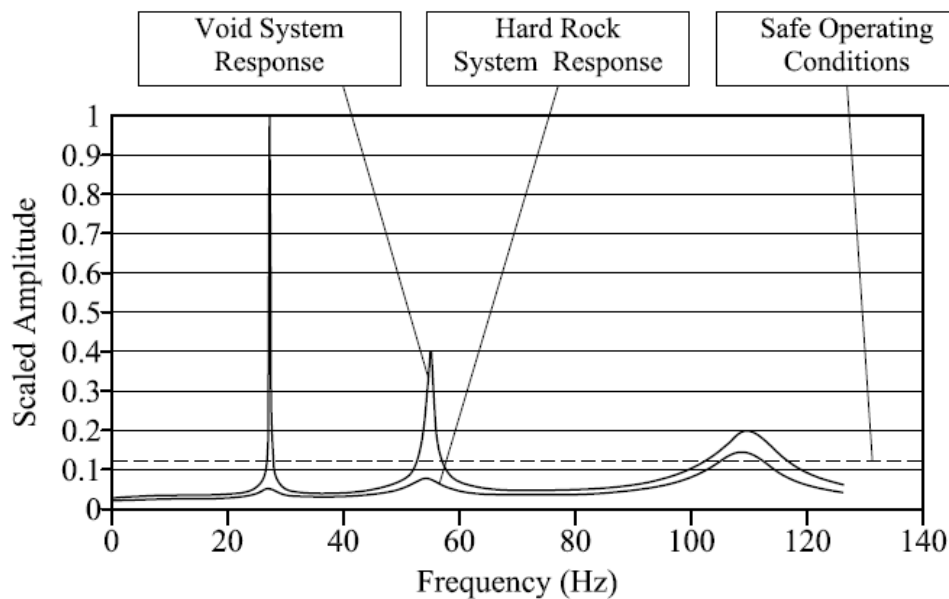


Figure 7.6. Sonic drill operating conditions for drilling through rock and a void.

When designing a control system, one must recognize that if some of the measurement devices used to sense the movement of parts of the sonic drill are mounted on moving parts, they will eventually fail. Therefore, an electric circuit that can detect a lost signal is required. Another critical aspect of design is: if communication is lost

between human machine interface and the controller, then the control system must be able to detect the condition and shut the sonic drill down safely.

CHAPTER 8

CONTROL APPLICATIONS

Introduction

The overall goal of this research was to identify if a control system could manage and optimize sonic drill operation by using measurement devices above ground. The modeling demonstrated that the salient sonic drill variable was the coupling and damping of the strata at the drill bit, Chapters 3, 4 and 5. This coupling could be controlled by the force applied at the sonic drill head. The frequency of operation was also found to be critical in the control, which it is required to operate on the optimal resonant mode that yields the highest efficiency of transmitted power to the drill bit to perform drilling, Chapters 3, 4, and 5. The modeling and testing effort showed that a control system could be implemented based on measurement devices above ground, as demonstrated in Chapter 6. Chapter 7 showed the methods on how to utilize these measured variables to control the sonic drill system. In this chapter, the actual control methodology is described by using block diagrams and high level schematics. The concepts for the control system presented were tested in Chapter 6 and 7. Because a control system was proven feasible to control a sonic drill, as shown in chapter 6, the main variables and design considerations were completed beyond the conceptual design and are presented in this chapter. The system presented was also filed on May 26, 2009 in patent application number 12/736,742 (Publication number: US20110056750).

Sonic Drilling

As previously shown in the above chapters, sonic drilling is a complex system that has been commercialized without an understanding of the fundamental aspects of the drilling phenomenon. Commercial sonic drills are operated by specially trained operators using intuition and feel. The control system outlined for a sonic drill system uses a mathematical model as a foundation for the control logic, mechanical control actuators, electrical sensors, and a human machine interface. The sonic drill system outlined in this chapter is designed for a hydraulically-driven counter-rotating eccentric system. However, the same concepts can be applied to other sonic drill systems with other driving configurations.

The sonic drill control system is termed ResonantSonic Tracking™ (RST™). The RST™ system is designed around a particular transfer functions that were developed in Chapter 3, Equation 3.27. This equation has the overall ability to model the resonant system in the longitudinal direction, but the same form of the equation can also be derived from the flexure and torsional resonant modes and included in the control system. There is no transfer function currently made for the degree of down force and how the down force relates to the coupling of the drill bit to the strata. In addition, there is also no direct transfer function to determine the optimal available resonant mode, but methods were developed to determine the optimal available resonant mode, which delivers the greatest amount of energy to the drill bit to perform drilling. A conceptual design of the RST™ system is displayed in Figure 8.1. In Figure 8.1, the lines in green are the

electrical control, the red lines are the electrical sensors, and the black lines are the hydraulic/mechanical feed systems.

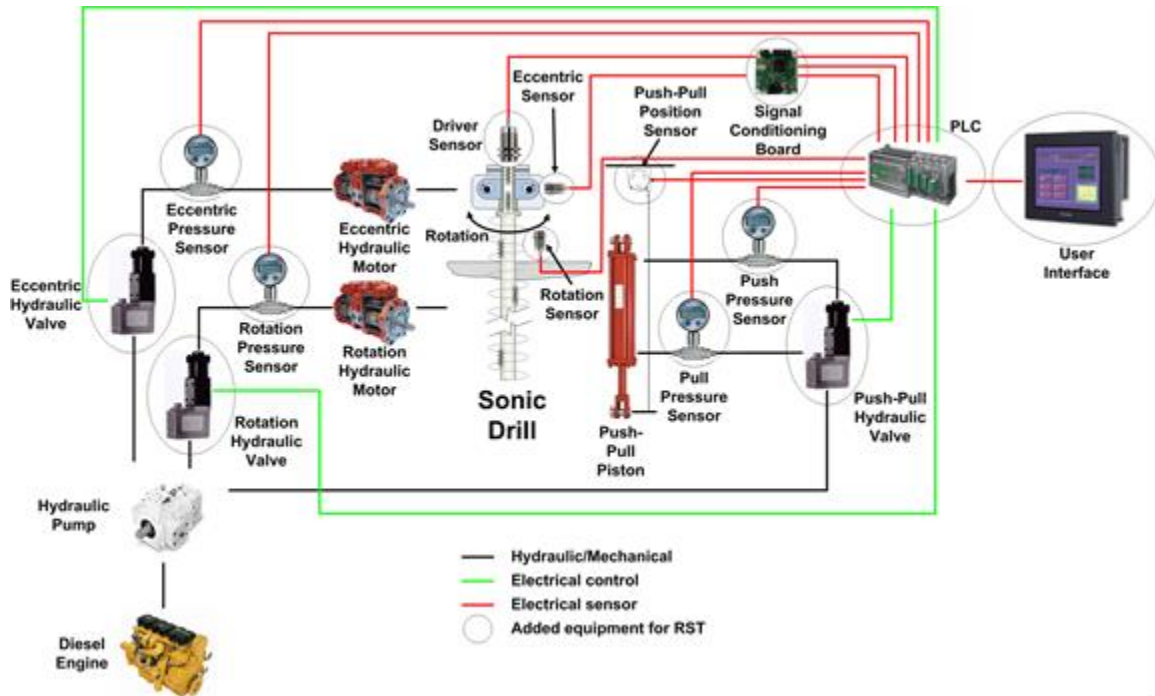


Figure 8.1. RST™ instrumentation and control system schematic. (Courtesy of Resodyn Corporation.)

The required controls hardware components are as follows:

- Eccentric Sensor – an inductive eddy current displacement sensor that will measure the angular speed of the eccentric rotor by providing one pulse per revolution to the Signal Conditioning Board. This pulse will be used with the driver sensor to determine resonant frequency.
- Driver Sensor – an inductive eddy current displacement sensor that will measure the displacement of the Sonic Driver. This voltage signal will be sent to the Signal Conditioning Board where it will be used with the eccentric

sensor to determine resonant frequency.

- Rotation Sensor – an inductive eddy current displacement sensor that will measure the angular speed of the rotation axis.
- Rotation Hydraulic Valve – hydraulic valve that will control the speed of the rotation axis hydraulic motor
- Eccentric Hydraulic Valve – hydraulic valve that will control the speed of the eccentric hydraulic motor
- Push-Pull Hydraulic Valves – hydraulic valve that will control the force of the push-pull hydraulic piston.
- Push–Pull Piston Sensor – a cable extension transducer that will provide push-pull piston sensor that will be used to calculate penetration rate.
- Eccentric Pressure Sensor – a hydraulic pressure sensor that will provide feedback for controlling the speed of the eccentric.
- Rotation Pressure Sensor – a hydraulic pressure sensor that will provide feedback for controlling the speed of the rotation axis.
- Push Pressure Sensor – a hydraulic pressure sensor that will provide feedback for controlling the force of the push on the Push-Pull Piston.
- Pull Pressure Sensor – a hydraulic pressure sensor that will provide feedback for controlling the force of the pull on the Push-Pull Piston.
- PLC and I/O modules – a PLC (Programmable Logic Controller) will be used

as the supervisory control system. It will receive analog signals from all previously mentioned sensors into input modules, act on these signals to provide control signals through the output modules to the hydraulic valves that control the hydraulic motors and pistons. This device will also communicate with the User Interface and Signal Conditioning Board.

- User Interface – a touch screen or LCD panel that will communicate with the PLC to obtain operational status and display this information to the operator. The User Interface will also provide buttons for the operator to select operational modes and controls to enter numeric values.

The hydraulic motor and the push-pull piston control design is the most critical for the design, as the hydraulic motor controls the oscillation frequency and the push-pull piston controls the weight on the bit. In order to control to at the level needed to meet the RST™ system performance criteria, a closed loop control system is required. A schematic of the eccentric speed and push-pull control loops are displayed in Figure 8.2.

The high level control schematic is displayed in Figure 8.3, which shows the empirical method of finding the correct resonant mode.

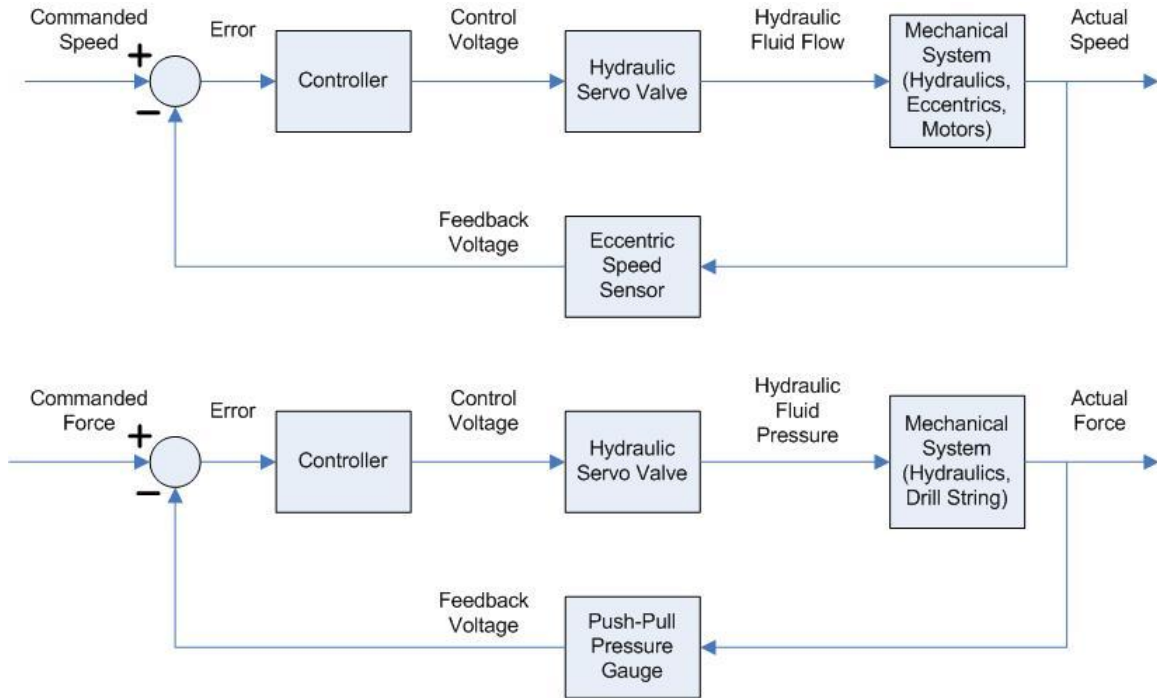


Figure 8.2. Eccentric speed and push-pull control loops. (Courtesy of Resodyn Corporation.)

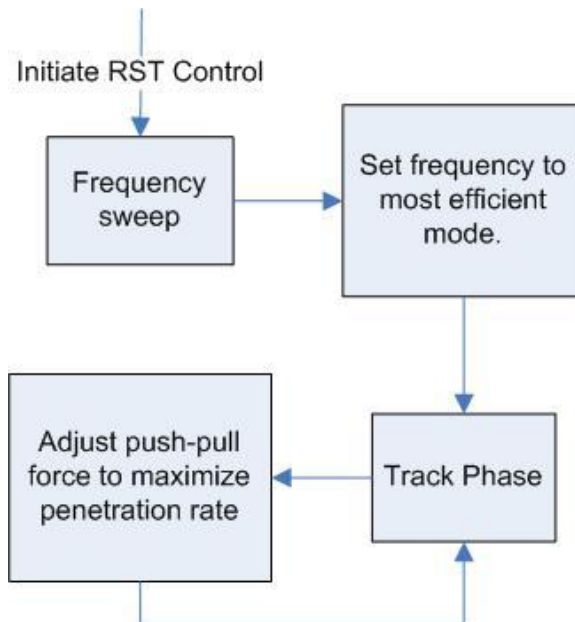


Figure 8.3. High level RST™ flowchart. (Courtesy of Resodyn Corporation.)

However, the high level control chart alone does not provide sufficient detail to control the sonic drill. A control patent was filed by Resodyn Corporation, on May 26, 2009 for the automatic control of oscillatory penetration apparatus (46). The patent application was published March 10, 2011 and was assigned publication number US 2011/0056750 A1. The following sections describe the control patent methods in more detail.

As shown in Figure 8.4, the control system can operate at a higher frequency than observed upon which the system will decrease the operating frequency until the desired phase angle between the input force and the displacement amplitude of the sonic drill head is attained. Then the operating system is further refined as shown in Figure 8.5 which outlines the proper operating conditions to adjust the Push/Pull force (weight on bit), so that the optimum drilling conditions to maximize the penetration rate are performed. The diagram also describes adjusting the rate of rotation, input force, flushing fluid rate, and operating frequency to maximize the penetration rate. If the drilling conditions cannot be met, then a feedback loop and fail safe loop bring the system to adjust the operating point shown in Figure 8.4.

In addition to the control of parameters to optimize the penetration rate, a supervisory control system to ensure the drill is operating under safe operating conditions is required. The control system block diagram for the supervisory control under safe operating conditions is displayed in Figure 8.6.

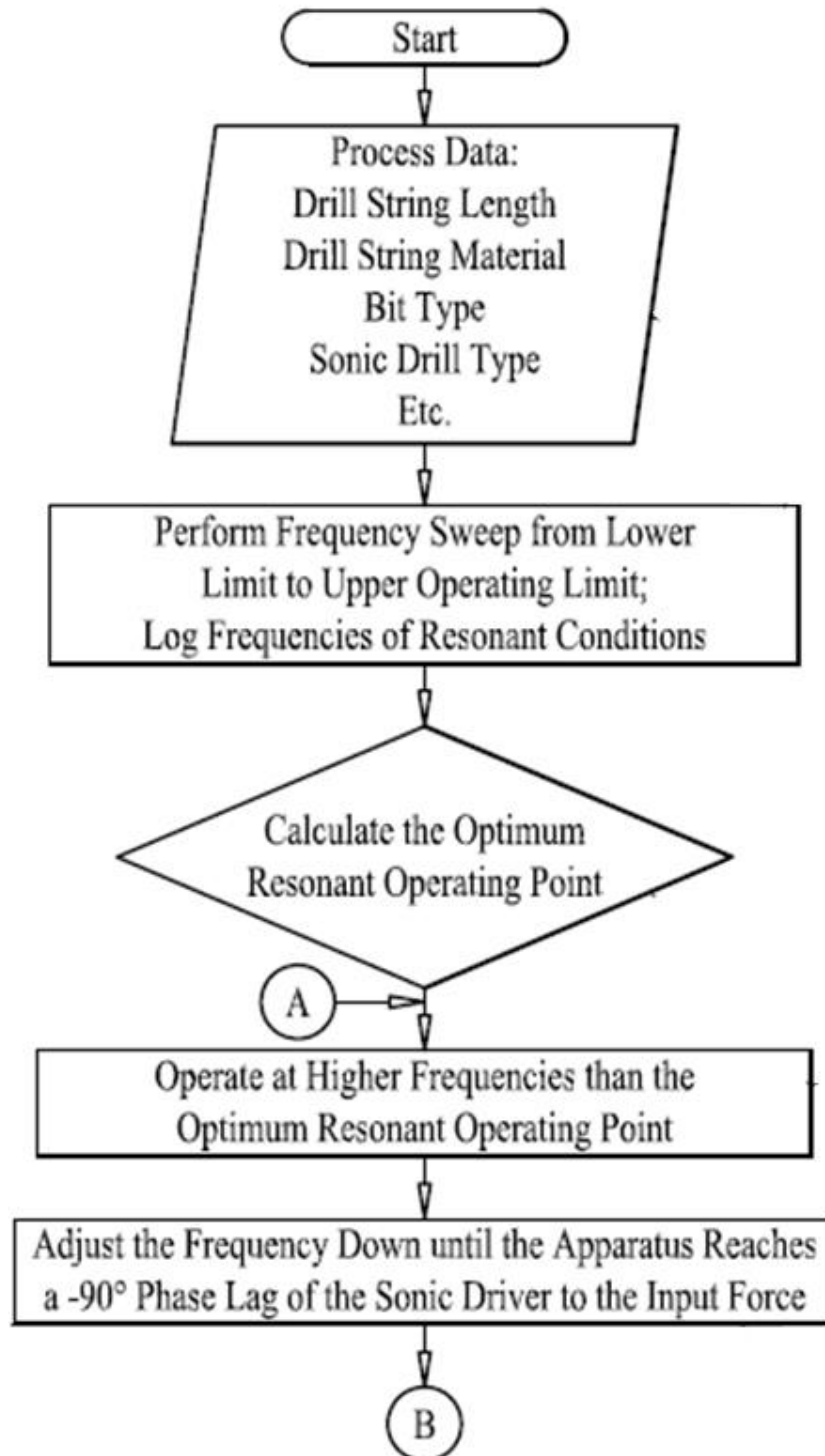


Figure 8.4. Sonic drill starting control algorithms.

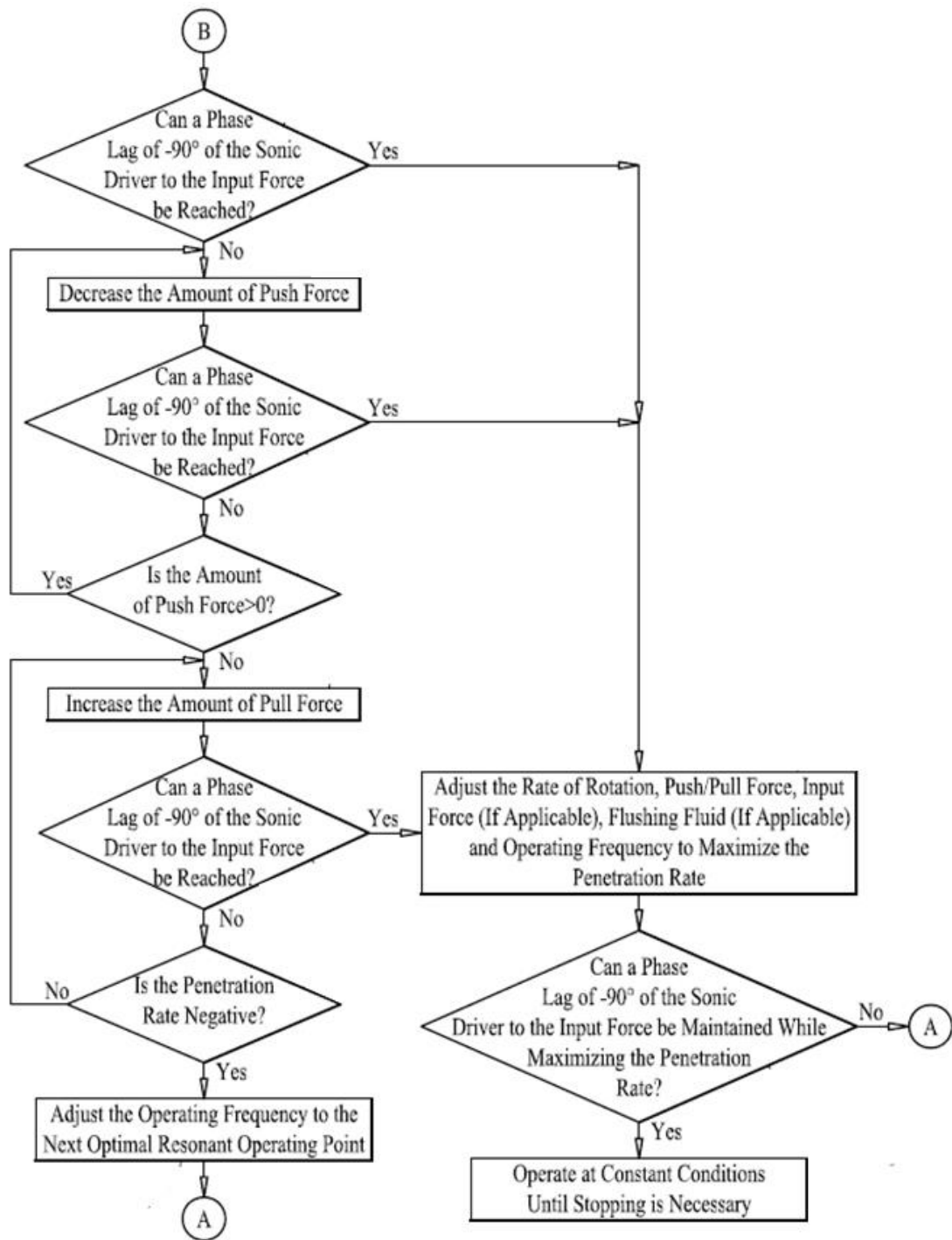


Figure 8.5. Sonic drill control algorithms.

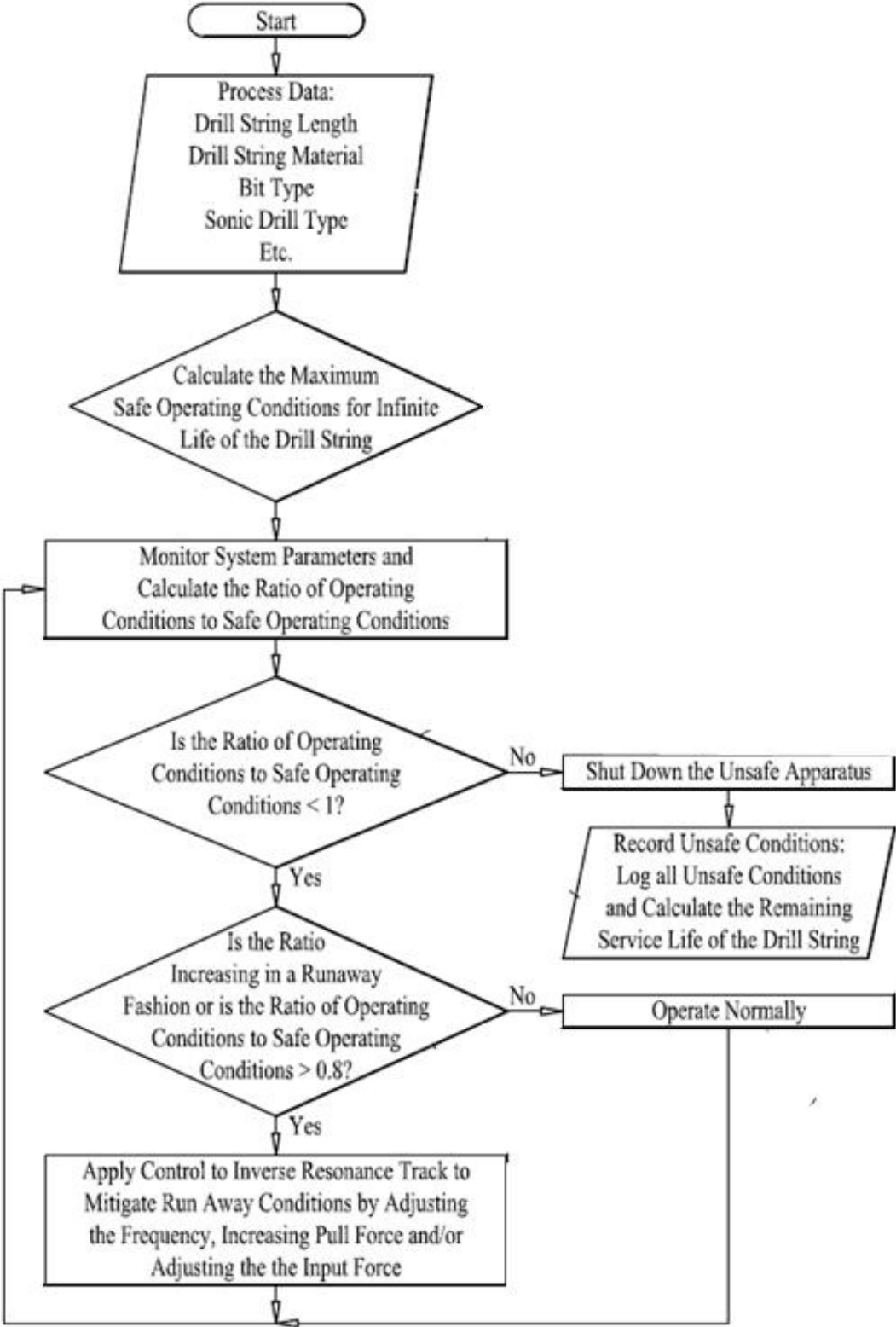


Figure 8.6. Block diagram of the supervisory safe conditions control system.

Figure 8.6, above, presents the steps of a safety control process that runs in the background during the drilling process. Processes data such as drill string length, drill string material, drill bit mass and type, sonic drill type, etc. for sonic drill apparatus are input to control system. In calculate maximum safe operating condition step, maximum safe operating conditions (e.g., maximum safe scaled displacement amplitude) for sonic drill apparatus are calculated by the control system. The maximum safe scaled displacement amplitude is determined by the size of the drill pipe, joint design, drill pipe material, and desired safety fatigue factor using standard machine design practices. Such standard machine design practices include those taught in machine design courses and which are used by those having ordinary skill in the art of mechanical engineering, for example, see those described in *Shigley's Mechanical Engineering Design* (47). The description of which is incorporated by reference as if fully set forth herein. Appropriate safety fatigue factors are determined using the ultimate tensile strength and cyclic fatigue knock down factors of the pipe material, size of drill pipe, length of drill pipe in the drilled hole, etc.

Sonic drill operating conditions are monitored in the “monitor apparatus” step. In this step, the control system measures the actual displacement amplitude of sonic drill apparatus. The actual amplitude is then scaled by creating a ratio of the actual amplitude relative to the predetermined safe displacement amplitude. Maintaining the ratio at a value less than 1 prevents damage to the apparatus.

The resulting actual operation condition (e.g., scaled amplitude) is then compared to the safe operating condition (e.g., safe scaled operating amplitude) in the “compare

amplitudes” step. If the ratio of the condition is greater than one, the apparatus is shut down in the “shutdown unsafe apparatus” step and all unsafe conditions are logged and the remaining service life of drill string is calculated in the record “unsafe conditions” step. If the ratio of conditions is less than one, then the ratio is tested again in “retest conditions” step. If the ratio is increasing in a runaway fashion or if the ratio is greater than a preselected value (e.g., 0.8), then control actions are taken by control system in apply “control actions” step. In this step, the control system may adjust the frequency of the input force, increase the push force, decrease the pull force and/or adjust the magnitude of the input force. If the ratio is not increasing in a runaway fashion or if the ratio is not greater than 0.8, then normal operation continues in the “operate normally” step. After either of the steps: Apply control to “inverse resonance track” or “operate normally” are performed, the control passes back to step “monitor system parameters”.

All of these supervisory and control algorithms are built-in and inaccessible to the operator. However, the operator does have some awareness of what is happening by what is shown on the human machine interface as explained below.

The human machine interface (HMI) will be a direct replacement of the control panel, displayed in Figure 2.4. The panel will still contain dial indicators to give the new configuration the same look and feel to what the operators are currently used to, but controls will all be automated. Because the control code will be written in ladder logic in a personal logic controller (PLC), it will be able to monitor each gauge every 5 ms, where a normal operator can only monitor one or two gauges at any given second. If the control system operated to a point outside of its preset values, it will automatically shut down to

prevent a runaway condition that may cause the failure of a critical component. A sample of the RST HMI control center is displayed in Figure 8.7 and the manual control page, Figure 8.8 is so that the operator can control the machine if the control system fails to drill.

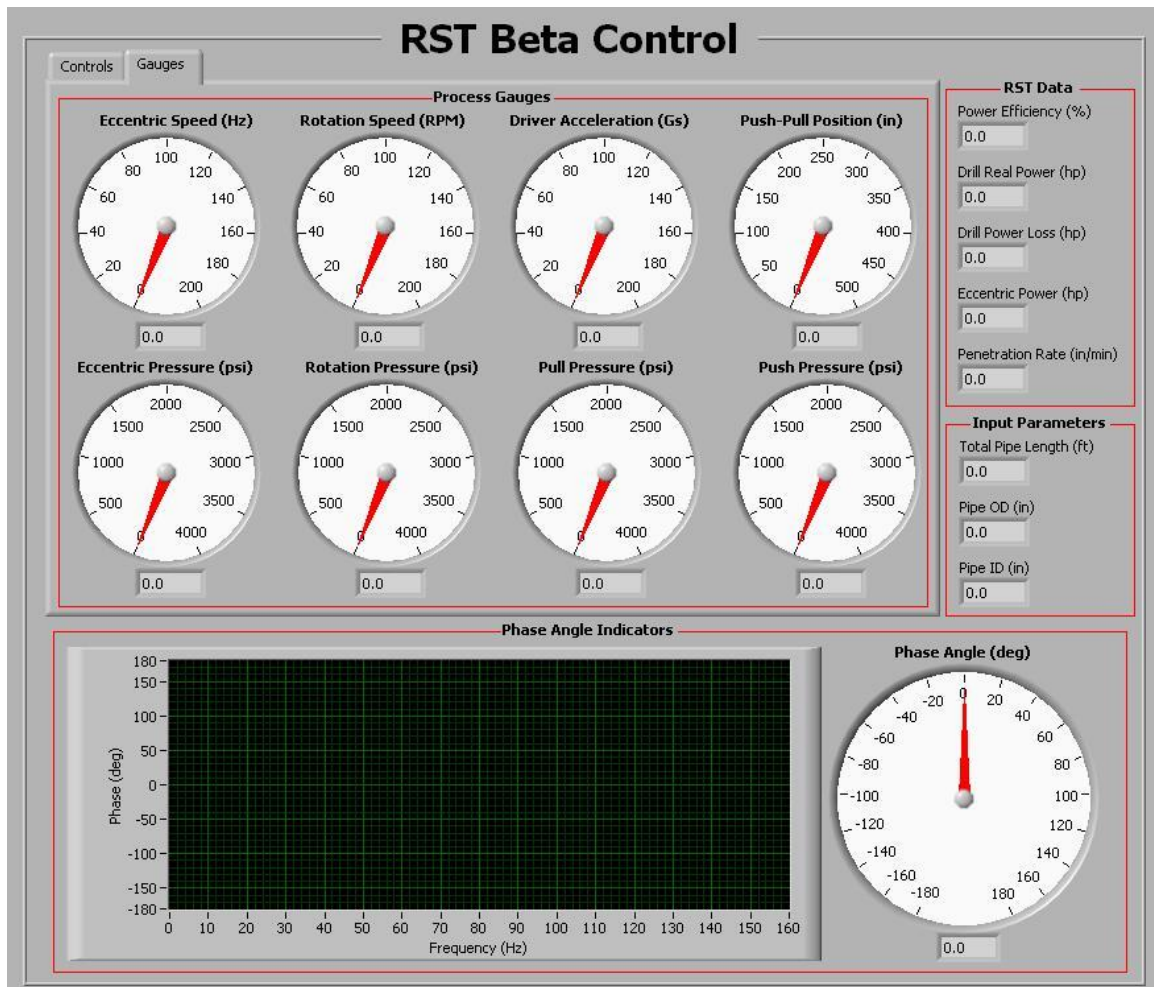


Figure 8.7. RST HMI control center replacement.

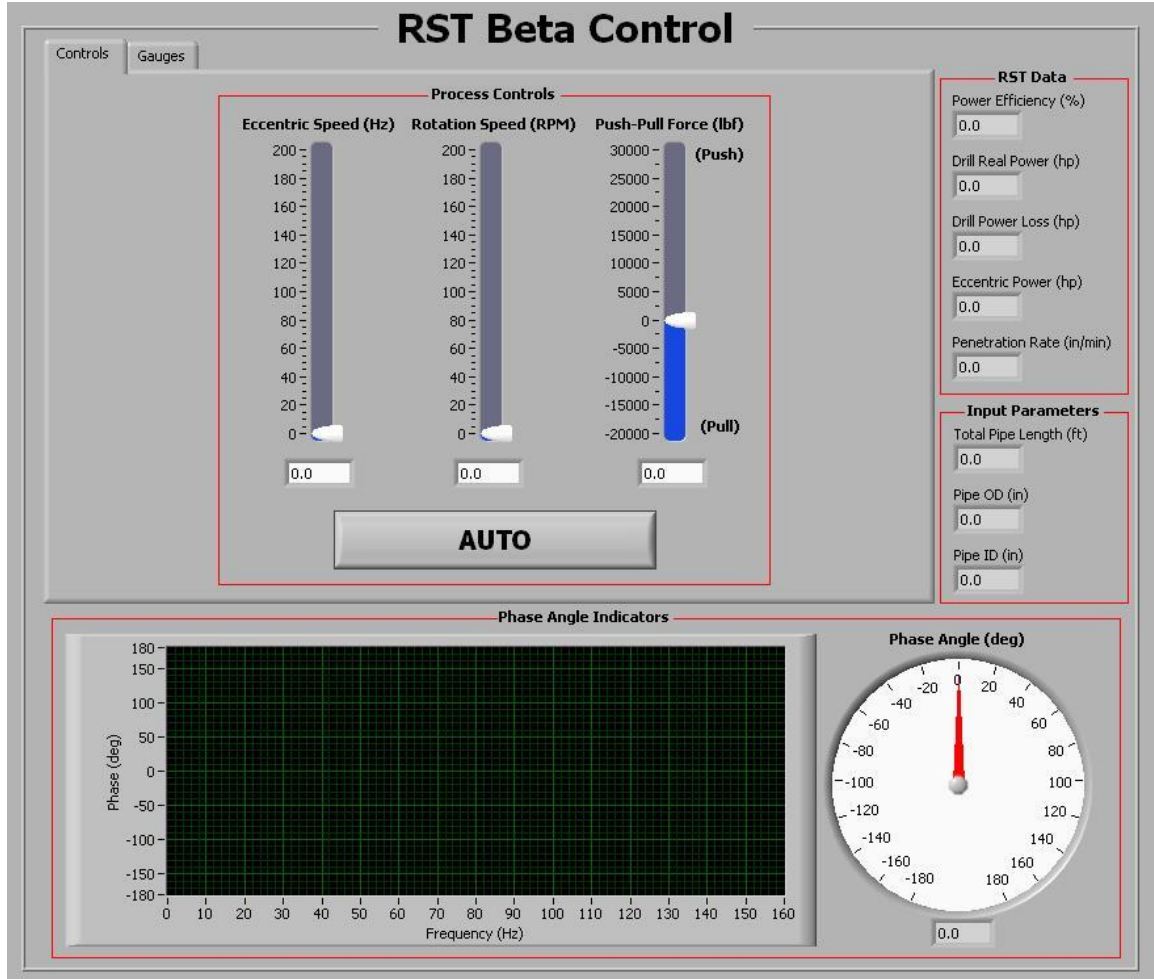


Figure 8.8. Manual control screen.

Advantages for utilization of ResonantSonic Tracking™ (RST™) technology:

1. Tracking to ensure maximum fraction of input energy is delivered to the drill bit
 - a. Demonstrated to have more than 400 % increased power to the drill bit
 - b. Drill penetration rates increased for large penetration resistance changes:
 - i. Along the drill string length
 - ii. At the drill bit
2. Monitoring system to ensure longevity of drill string sections:
 - a. Monitors force input to ensure stresses along the drill length are within fatigue limits at all times

- b. Monitors the cyclic fatigue time and magnitude on each drill string rod and can estimate the probability of the remaining useful life of the drill pipe
3. Automatic algorithm based control system seeks the optimum penetration rates
4. Mapping of formation being drilled:
 - a. By monitoring damping at the drill tip the types of soils can be mapped. Typically in sonic drilling, the lithology of formations being penetrated is determined by retrieving cores to the surface
 - b. Establishes the resonant mode that should be used subsequent in drilling to avoid potential high damping zones, e.g., a predictive model
5. By drilling with this control system, the need for flushing fluid will be minimized and less waste will be generated.
6. Core samples can be collected faster.
7. Operator intervention for maximum sonic head performance unnecessary, allowing for the faster training of operators to take over sonic drilling machine operations.
8. The control system will be durable, robust, and safe for all weather conditions.

Non-resonant Systems

The modeling and control technology can be applied to non-resonant systems as well, but will only have applications where the system is designed to keep the mechanical system off mechanical resonance. A few chosen systems that are designed to operate off mechanical resonance, but have the capability to resonate are: 1) Drive shafts, 2) Machining end mills and drill bits, 3) Machinists lathes, and 4) Computer hard drive reading arms. All of these are designed for potential vibratory applications, but the operation on mechanical resonance has demonstrated a history of failure.

CHAPTER 9

CONCLUSIONS

Sonic drilling has been used in industry for many years. Universities have had minimal modeling of the sonic drill due to the lack of funding and industry interest. The majority of the research has been performed by private industry where they have kept the knowhow that they have developed internal and proprietary. Because of this reason, limited information about sonic drilling is available in peer reviewed literature. The research presented in this work combines both empirical testing and mathematical modeling techniques to quantify the significant variables that affect the sonic drill system. The significant variables were used as the foundation of a control system, which was outlined and subsequently described in detail.

The first chapter outlined the available information about sonic drilling in peer reviewed literature as well as marketing information from various private companies. Chapter 2 provides definitions of the sonic drill variables, by providing a review and summary of current knowledge with rules of thumb. The modeling, Chapter 3, included background of how a sonic drill system is similar to a single degree of freedom spring-mass-damper system. The same tools used to analyze a single degree of freedom model were also used to analyze the sonic drill system. Governing differential equations of motion for the sonic drill were derived from both force balance and energy balance. Closed form boundary condition solutions and numerical solutions using finite element models were used to solve for the system dynamics. Chapter 4 describes the design of experiments that was used to determine the sensitivity of the sonic drill variables which

include: : 1) sonic drill head mass, 2) sonic drill head spring rate, 3) sonic drill bit spring rate, 4) sonic drill bit mass, 5) resonant mode, 6) strata types, 7) sonic drill bit damping, and 8) sonic drill length.

The results for the design of experiments described in Chapter 5 for both the boundary condition model and the finite element model are:

Boundary Condition Model

- The most influential parameter in the resonant frequency, by an order of magnitude, is the resonant mode, but the next most influential is the combination of the sonic head mass and the drill length, followed by the drill string length, strata types, and bit mass.
- The most influential parameters for the bit amplitude are the combination of the sonic drill bit spring rate and the sonic drill length, resonant mode, and the combination of the sonic drill head mass and resonant mode. The sonic drill bit spring rate is highly influential, because within the operating conditions, it can get high enough to essentially “fuse” the drill bit with the strata and make it act as a resonant node. This essentially changes the boundary condition of the drill string at the drill bit to fixed, which drastically changes the resonant frequency. When the drill bit is a node, two things may occur. The first is that the current operating frequency does not correspond with new resonant mode from the new boundary conditions of top free (mass and spring) and the bottom in the fixed condition. The second is if the current operating frequency corresponds with a resonant mode, and the top of the drill string is putting in a lot of energy, but no energy is

being delivered to the drill bit. This mode is detrimental, as all the energy goes into the string along the length and it easily can build to an amplitude stress level that will break the drill string.

- The most influential parameters for the ratio of head to bit amplitude are the drill bit spring rate, strata type (combination of the bit spring rate and bit damping), sonic drill head mass, combination of the drill head mass and the bit spring rate, drill bit spring rate and the drill length, as well as the resonant mode. Similarly as discussed above, the bit spring rate can change the boundary condition of the bit to essentially be fixed. The strata type also plays into the possibility of creating a node at the drill bit. The next most influential variable is the drill head mass. As the drill head mass is increased, the head amplitude relative to the drill bit amplitude decreases.

Finite Element Model

- The finite element analysis showed that the bending resonant modes were not excited unless they were within a few Hertz in frequency from the primary axial mode.
- It was determined that the finite element method could be used as a tool to model the sonic drill dynamics for the damping and restoring along the drill string length and at the drill bit.

- A method was derived to estimate the equivalent damping and spring rate along the length of the drill string, which the lowest resultant equivalent damping resonant mode should be chosen for operation.
- The FEA models were used to validate the equivalent damping method.
- The results of this analysis showed that the soil damping constants derived by Warrington, do not seem valid for the sonic drill model and the constants should be empirically found.
- Methods to perform the empirical experiments to determine the soil damping and coupling constants were identified.
- The FEA models also solved the sonic drill problem for all 6 degrees of freedom (3 translational and 3 rotation), which included the axial, bending, breathing and torsional modes. The breathing modes were not found in our sonic drill conditions examined for the 9” outer diameter drill pipe up to depths of 1000 ft. However, different diameters and wall thickness of drill pipe should be examined to see if the breathing modes will exist for the drill string length.
- The lateral (flexural) modes were found to have weak coupling with the axial modes if they were within 1 Hz of the closest axial resonant mode. Therefore, monitoring and control schemes were delineated to avoid lateral mode excitation during operation.

The sonic drill experimentation and testing was described in Chapter 6. The conclusions from this were that there were three counterintuitive empirical findings verified through the mathematical modeling.

- First, the sonic drill down force can essentially ‘fuse’ the drill bit to the strata and act as a fixed boundary condition. A fixed boundary condition changes the drill resonant conditions and doesn’t impart sufficient force to drill strata, because it is just acting to reflect the sound waves back up the string.
- The second counterintuitive item was that the impact of the down force becomes worse with increased drill string length. Therefore, it was determined that when drilling depths greater than 500 feet, using pull force instead of push force should be applied at the sonic drill head while drilling to achieve optimum drilling. This could also be a subset of the first, but was separated, because this is non-obvious to the drilling community.
- The third counterintuitive item found, was that the sonic drill operators should not control the drill at the maximum hydraulic pressure being delivered to drive the eccentrics. However, because of the aforementioned down force, the resonant system would excite a resonant mode, that would push energy back onto the sonic driver requiring additional pressure to perform minimal work at the drill bit. Thus, the sonic drill hydraulic pressure doesn’t represent how much energy is being used for drilling at the bit and should not be used as a point of monitoring or target for control by the sonic drill operator.

In addition to the counterintuitive findings, the sonic drilling condition was verified that it could be measured and quantified at the sonic drill head.

The variables that will be used for the control system are described in Chapter 7. The control system, which is patent pending, primarily for Resonant Sonic Drilling and other applications that utilize the control methodologies were described in Chapter 8.

CHAPTER 9

FUTURE WORK

As with most research, the further a system is explored, more unknown phenomena are revealed that have yet to be understood. In this chapter, the additional research topics for a sonic drill system that became apparent during this body of work are outlined in a bulleted format. These research topics further the understanding of the physics and dynamics of the sonic drill system.

- Creating more realistic relations for the various strata coupling and damping along the length of the drill string and at the drill bit.
- Quantifying the coupling and importance of the flexure modes of the sonic drill during operation.
- Testing the proposed automatic control system on a sonic drill to determine how well the control and existing transfer functions work.
 - Quantify by measuring the improved penetration rate.
 - Quantify by measuring the improved gain in power efficiency.
- Use an array of at least 6 independent accelerometers to determine all 6 degrees of freedom at the sonic drill head. These measurements can be used to quantify the longitudinal, torsional, and two flexure resonant modes relative displacement amplitudes as well as other dynamic motion that may exist, and energies of each resonant mode.

- Identify and explore other resonant systems that the control system could be used to control.

REFERENCES CITED

1. http://www.sonicdrilling.com/Flash/learn_more.html. *www.sonicdrilling.com*. [Online] [Cited: April 6, 2013.]
2. **Swanson, Gloria J.** Rotasonic Revisited. *Water Well Journal*. October 1994, pp. 58-63.
3. **Roussy, Ray.** Sonic Drill Tackles Massive Earthfill Dam. *Water Well Journal*. January 1998, pp. 120-123.
4. The Development of Sonic Drilling Technology. *GeoDrilling International*. December 2002, pp. 7-10.
5. *Exploration Drilling: hunting cost efficiency*. 2, 2012, Mining World, Vol. Volume 9.
6. **Bernat, Henry.** <http://www.dea-global.org/projects/status/115.html>. [Online]
7. **Barrow, J C.** *The Resonant Sonic Drilling Method*. 1994. pp. 153-160, Ground Water Monitoring and Remediation.
8. www.rockhog.com. [Online] November 15, 2007.
9. **Albert G. Bodine, Jr.** *Sonic Drilling Device*. 3,684,037 United States of America, 10 5, 1970. Mechanical System.
10. —. *Acoustic Method and Apparatus for Driving Piles*. 2,975,846 United States of America, March 8, 1957. Mechanical System.
11. —. *Earth Boring Apparatus*. 2,554,005 United States of America, December 11, 1950. Mechanical System.
12. —. *Method for Sonic Earth Boring by use of Resonant Wave Pattern Transmitted from Ground Surface*. 2,942,849 United States of America, June 2, 1958. Mechanical System.
13. —. *Acoustic apparatus for Driving Piles*. 3,054,463 United States of America, January 24, 1958. Hardware.
14. —. *Sonic Method and Apparatus for Installing Pile Member, Casing Members or the like, in Earthen Formations*. 3,379,263 United States of America, February 1, 1966. Mechanical System.
15. —. *Sonic Pile Driver*. 3,189,106 United States of America, January 9, 1962. Mechanical System.
16. —. *Transmission of Sonic Waves by a Column of Elements*. 3,391,748 United States of America, January 24, 1966. Mechanical System.

17. —. *Oscillator Means for Sonic Pile Drivers*. 3,291,227 United States of America, Jan 28, 1965. Mechanical System.
18. **Hueter, Theodor F. Bolt and Richard H.** *Sonics*. New York : John Wiley & Sons, 1955. B002K03YLA.
19. **Rockefeller, W C.** *Mechanical Resonant Systems in High-Power Applications*. s.l. : United Engineering Center, 1967.
20. **Barrow, Jeff.** *Sonic Drill Instrumentation Interim Report FY-96*. None : None, 1996. None.
21. **Barrow, Jeffrey.** President of Water Development Corporation. *Various Phone Conversations*. 2006-2012.
22. **Arvani, Farid.** Project manager at Memorial University. *Phone Conversation*. 2012.
23. *Retrieving Stuck Liners, Tubing, Casing, and Drillpipe with Vibratory Resonant Techniques*. **Gonzalez, Orlando J., Pool Co.-Resotek**. 3, s.l. : Society of Petroleum Engineers, 1987, Vol. 2. 14759-PA.
24. **Various.** *Coiled Tubing: State of the Industry and Role for NETL*. s.l. : Department of Energy, June 2005. Topical Report.
25. *The application of Microhole Technology to the Development of Coalbed Methane Resources at Remote Locations*. **Albright J., Clough, J., Dreesen, D.** s.l. : Division of Geological And Geophysical Surveys, 2001.
26. *Assessing coalbed methane gas for rural Alaska energy needs*. **Clough, J.G.** s.l. : Workshop on Opportunities in Alaska Coalbed Methane, Anchorage, Alaska, March 1-3, 2000.
27. *Rural Alaska natural gas study - a profile of natural gas energy substitution in rural Alaska*. **Foster, M.** s.l. : Final report prepared for the State of Alaska, Department of Community and Regional Affairs, Division of Energy., 1997.
28. *Economic analysis of drilling three coalbed methane wells in rural Alaska*. **Ogbe, D. O., J.E. Bott, and M. Hawley.** s.l. : R of Alaska Department of Natural Resources, Division of Geological and Geophysical Surveys to the State, 1998.
29. **Barrow, J C.** *Resonant Sonic Drilling*. U.S. Department of Energy, Hanford, WA. s.l. : U.S. Department of Energy, Hanford, WA, 1995. Innovative Technology Summary Report.
30. **Barkan, D D.** *Dynamics of Bases and Foundations*. [ed.] Translated from Russian by L. Drashevskaya. New York : McGraw-Hill Book Co., 1962.

31. *Skin Friction For Steel Piles in Sand*. **Coyle, H.M., and Sulaiman, I.H.** SM6, s.l. : ASCE, 1967, Vol. 93.
32. **Youd, T. L.** *Densification and Shear of Sand during Vibration*. May 1970, Vol. 96, SM3, p. 7272.
33. *Pile Driving By Means of Longitudinal and Torsional Vibrations*. **Kovacs, Austin and Michitti, Frank.** Special Report 141, Cold Regions Research and Engineering Laboratory, Hanover, New Hampshire : Corps of Engineers, U.S. Army.
34. **Dimarogonas, Andrew.** *Vibration for Engineers*. New Jersey : Prentice-Hall, Inc., 1996. p. 269. 0-13-456229-1.
35. **Rao, Singiresu S.** *Vibration of Continous Systems*. Hoboken : John Wiley and Sons. Inc., 2007. 978-0-471-77171-5.
36. **Warrington, Don C.** *Closed form Solution of the Wave Equation for Piles*. 1997. Masters Thesis for the University of Tennessee at Chattanooga.
37. *Modeling Percussive Drilling Performance using Simulated Visco-Elasto-Plastic Rock Medium*. **Sazidy, M.S., Rideout, D.G., Butt, S.D. and Arvani, F.** Salt Lake City, UT : American Rock Mechanics Association, 2010. ARMA 10-434.
38. **Unknown.** *GEOL 615 at Stanford University*. [Online] [Cited: Oct 8th, 2012.] <http://www.stanford.edu/~tyzhu/Documents/Some%20Useful%20Numbers.pdf>.
39. **Various.** *Wikipedia*. [Online] [Cited: October 8, 2012.] <http://en.wikipedia.org/wiki/Porosity>.
40. *Wikipedia*. [Online] [Cited: 10 9, 2012.] http://en.wikipedia.org/wiki/Poisson%27s_ratio.
41. **DAS, B.M.** *Priciples of Foundation Engineering*. Boston : PWS Publishers, 1984.
42. **Lysmer, J.** *Vertical Motion of Rigid Footings*. Defense Atomic Support Agency NWER Subtask 13. Vicksburg, MS : U.S. Army Corps of Engineers, Waterways Experiment Station, 1965. Contract Report Number. 3-115.
43. *Modeling of Dynamic Behavior at the Pile Base*. **Holeyman, A.E.** Vancouver, BC : Bi-Tech Publishers, 1988. Proceedings of the Third International Conference on the Applictaion of stress-Wave Theory to Piles, pp. 174-185.
44. *Anisotropic elasticity of a natural clay*. **Houlsby, J. Graham and G. T.** 2, s.l. : Geotechnique, 1983, Vol. 33, pp. 165-180.

45. **Erling Fjaer, Rune M. Holt, Per Horsrud, and Arne M. Raaen.** *Petroleum Related Rock Mechnaics*. New York : Elsevier, 1992. pp. 322-324. 0-444-88913-2.
46. **Lucon, Peter A.** *Automatic Control of Oscillatory Penetration Apparatus*.
Publication Number: US 2011/0056750 A1 USA, May 26th, 2009.
47. **Joseph Shigley, Charles Mischke, and Richard Budynas.** *Shigley's Mechanical Engineering Design*. s.l. : McGraw-Hill Science/Engineering/Math, 2010. 978-0073529288.
48. **Terry, D B, et al., et al.** *Resonant Sonic Drilling at Three Former MGP Sites: Benefits and Limitations*. s.l. : GEI Consulatants Inc., 2003.
49. **Eurocopter.** *AS 350 B3 Ecureuil Performance Specifications* . s.l. : Eurocopter.
50. **Baker Oil Tools.** *Resonant Systems Product No. 140-52*. 1994. Product Report number PR/FS/94002/2M/4-94.
51. **Longyear, Boart.**
http://www.boartlongyear.com/c/document_library/get_file?uuid=32576257-601c-47eb-a25a-a5c70ac7422d&groupId=10138. *Boart Longyear*. [Online]

APPENDICES

APPENDIX A

MATLAB[®] CODE

```

%%-Dissertation--Sonic Drill Model-----%
-----%
% Created By: Peter A. Lucon
% Program Name: BC_Program_all_modes_Final
% Created On: 02-07-12
% Modified By:-----Rev:-----Modified Name:-----Modified Date:--
Notes:-----%
% Peter A. Lucon 001 BC_Res_Sol_001 10-31-12
% Peter A. Lucon 002 BC_Program_all_modes_Final 10-31-12.

%% Program Description-----%
-----%
% This program first defines all the sonic drill variables that are used to find the
roots to the boundary conditions
% equations that determine the undamped natural frequencies for the sonic drill system.

% Takes all the variables of the drill string (length, density, cross sectional area, mass
and spring at the ends.
% Finds the solution and then plots the solution as well as creates an output file to
excel called
% BC_Solution_XXX.xlsx.

%% Initialize Program-----%
-----%
clear;clc;clf;close all;format compact;format short g
disp('Program Running')

%% Conversion Variables
ft_m = 0.3048; %'m/ft' % Converts ft to meters
%% Variables-----%
-----%
% Define Initial Conditions (Initial Variables and Conditions of the Drill String)
% Variable 'Unit' 'Description'
N_p = 25; % '#' % Number of sections of pipe.
L_p_s = 10; % 'ft' % Length of each section of pipe.
L_p_ft = N_p*L_p_s; % 'ft' % length of pipe. (Input in multiples of 10
ft as each section of pipe)
nn = 10; % % Number of nodes per each section of pipe.
dx_ft = L_p_s/(nn); % 'ft' % Distance between nodes.
nn_s = nn*N_p+1; % % Total number of nodes in the system. One
is added as the initial node.
u0 = zeros(1,nn_s); % 'm' % Initial Displacements of the Nodes. The
system starts at rest.

% Converting all english variables to Metric for ease of solving:
% Variable 'Unit' 'Description'
L_p = L_p_ft*ft_m; % 'm' % Converts ft to meters.
dx = dx_ft*ft_m; % 'm' % Distance between nodes in 'm'.

% Sonic Drill Physical and Material Properties:
% Variable 'Unit' 'Description'
rho = 7850; % 'kg/m^3' % Density of Steel Pipe.
E_p = 2.068e11; % 'Pa' % Youngs Modulus of Steel Pipe.
m_ecc = 28.4; % 'kg' % Mass of the two eccentrics.
r_ecc = .06; % 'm' % Eccentricity of the Eccentrics.
k_ti = [12258879]; % 'N/m' % Spring Rate of Air Spring on top of the
Sonic Drill.
c_t = 10; % 'N*s/m' % Damping Rate of Air Spring on top of the
Sonic Drill.
m_ti = [1000]; % 'kg' % Mass of the Sonic Drill Head.
k_bi = [0.1];%21616000;%11.75127e2; % 'N/m' % Spring Rate of the drill bit while drilling
(coupling with the soil).
c_bi = [1e-2];%[0.1,5526,11695,4696,24195,5423668];%31.554*.1;%1.75e5;
% 'N*s/m' % Damping Rate of Drill bit while drilling.
m_bi = [8]; % 'kg' % Mass of the Sonic Drill Bit.
b_p = 0; % 'N*s/m^4' % Damping Constant Along the Length of the
Drill String.

```

```

k_p = 0; % 'N/m^4' % Coupling Constant Along the Length of the
Drill String.
A_p = 8.6e-3; % 'm^2' % Cross sectional Area of the Pipe.
f_hz = 60; % 'Hz' % Operating Frequency
w = f_hz*2*pi; % 'Rad/sec' % Operating Frequency
F_amp = m_ecc*r_ecc*w^2; % 'N' % Amplitude of the Forcing Function onto the
Sonic Drill.
n_osc = 10; % % Number of oscillations.
x = [0:dx:L_p]'; % 'm' % Discretized length of the drill pipe.
c0 = sqrt(E_p/rho); % 'm/s' % Speed of sound through the Steel Drill
String.

% Solution Variables
f_max = 120; % 'Hz' % Maximum Frequency to look for the Resonant
Frequency
f_min = 50; % 'Hz' % Minimum Frequency to look for the Resonant
Frequency
%% Solution-----%
-----%
% Defining the equation to determine the roots:
lk_ti = length(k_ti); % Vector Length of the Spring Rate of the Air Spring
lm_ti = length(m_ti); % Vector Length of the Mass of the Sonic Drill Head
lm_bi = length(m_bi); % Vector Length of the Mass of the Drill Bit
lc_bi = length(c_bi); % Vector Length of the Drill Bit Spring and Damping
Values
f_in_g = zeros(lm_ti*lk_ti*lm_bi*lc_bi,2);
Var = zeros(lm_ti*lk_ti*lm_bi*lc_bi,5);
W = f_in_g;
for c1 = 1:lm_ti
    m_t = m_ti(c1);
    for c2 = 1:lk_ti
        k_t = k_ti(c2);
        for c3 = 1:lm_bi
            m_b = m_bi(c3);
            for c4 = 1:lc_bi;
                c_b = c_bi(c4);
                k_b = k_bi(c4);
                B = @(w) -tan(w*sqrt(rho)/sqrt(E_p)*L_p)+...
                    (((A_p*E_p*w*sqrt(rho)/sqrt(E_p))/(k_b-m_b*w^2))-
                    (A_p*E_p*w*sqrt(rho)/sqrt(E_p))/(k_t+...
                    -m_t*w^2)))/(((A_p*E_p*w*sqrt(rho)/sqrt(E_p))^2/((k_b-m_b*w^2)*(k_t-
                    m_t*w^2)))-1));
            for count = f_min:f_max;
                X(count,1) = B(count*2*pi());
                f_hz(count,1) = count;
            end
            count1 = 0;
            for count = f_min:f_max;
                if X(count,1)<0 & X(count-1,1)>0
                    count1 = count1+1;
                    f_in_g(c1*lk_ti*lm_bi*lc_bi-lk_ti*lm_bi*lc_bi...
                    +c2*lm_bi*lc_bi-lm_bi*lc_bi+c3*lc_bi-lc_bi+c4,count1) =
f_hz(count-1,1);
                    % Finding the Initial guesses for the Natural Frequencies.
                    x_l = f_in_g(c1*lk_ti*lm_bi*lc_bi-lk_ti*lm_bi*lc_bi...
                    +c2*lm_bi*lc_bi-lm_bi*lc_bi+c3*lc_bi-lc_bi+c4,count1)*2*pi;
                    x_u = (f_in_g(c1*lk_ti*lm_bi*lc_bi-lk_ti*lm_bi*lc_bi...
                    +c2*lm_bi*lc_bi-lm_bi*lc_bi+c3*lc_bi-
                    lc_bi+c4,count1)+1)*2*pi;
                    c = 0; % Counter
                for the While Loop
                    E_ar = 100; % Start
                % Error Guess
                    while E_ar > .2
                        c = c + 1;
                        f_l = B(x_l);
                        f_u = B(x_u);
                        x_r = x_u - (f_u*(x_l-x_u))/(f_l-f_u);

```

```

        f_r = B(x_r);
        if sign(f_r) == sign(f_l) && sign(f_r) ~= sign(f_u)
            Ea(c) = (x_r-x_l)/(x_l)*100;
            x_l = x_r;
        elseif sign(f_r) == sign(f_u) && sign(f_r) ~= sign(f_l)
            Ea(c) = (x_r-x_u)/(x_u)*100;
            x_u = x_r;
        else
            error('Not in the bound')
        end
        E_ar = abs(Ea(c));
    end
    if sign(f_r) == sign(f_l)
        root = x_l;
    elseif sign(f_r) == sign(f_u)
        Ea(c) = (x_r-x_u)/(x_u)*100;
        root = x_u;
    else
        end
        W(c1*lm_ti*lm_bi*lc_bi-lk_ti*lm_bi*lc_bi...
            +c2*lm_bi*lc_bi-lm_bi*lc_bi+c3*lc_bi-lc_bi+c4,count1,1) =
root;
        else
        end
    end
    Var(c1*lm_ti*lm_bi*lc_bi-lk_ti*lm_bi*lc_bi...
        +c2*lm_bi*lc_bi-lm_bi*lc_bi+c3*lc_bi-lc_bi+c4,:) =
[m_t,k_t,m_b,c_b,k_b];
    end
end
end
F_root = W./(2*pi);
[x1,x2] = size(F_root);
for g1 = 1:x2
    root_n = g1
    RTA = root_n; % Root number in the frequency set.
    nsheet = num2str(g1);
    sheet = ['s',nsheet];
    fname_exl = ['BC_Solution_',num2str(L_p_ft),'.xlsx'];
    xlswrite(fname_exl,Var, sheet, 'A3:E272');
    xlswrite(fname_exl,f_in_g, sheet, 'F3:H272');
    xlswrite(fname_exl,F_root, sheet, 'I3:K272');
    FS = 1; % 'Hz' % Frequency Step
    NS = 40; % % Number of steps on each side of the
undamped natural frequency
    SF = F_root(2)-FS*NS; % 'Hz' % Starting Frequency
    EF = F_root(2)+FS*NS; % 'Hz' % Ending Frequency
    FI = [SF:FS:EF]; % 'Hz' % Frequency Matrix
    % figure(2)
    % plot(F_root)
    % title('Natural Frequencies')
    % ylabel('Natural Frequency ''Hz''')
    % xlabel('Mode Shape')

%% Finding the Constants for the solution of the drill given a forcing function and
frequencies.
count = 1;
wABCD = zeros(lm_ti*lk_ti*lm_bi*lc_bi,5);

for c1 = 1:lm_ti
    m_t = m_ti(c1);
    for c2 = 1:lk_ti
        k_t = k_ti(c2);
        for c3 = 1:lm_bi
            m_b = m_bi(c3);
            for c4 = 1:lc_bi;
                c_b = c_bi(c4);

```

```

k_b = k_bi(c4);
Theta = w/c0; D = 0.00001; B = 10; A = 1000; C = 0.0001; Di = D; Bi = B;
Ai = A; Ci = C;
eq1 = @(D,A,B,C,w,Theta,F_amp) -A_p*E_p*w*B*D/c0 + k_t*A*D - c_t*w*A*C -
m_t*w^2*A*D + F_amp;
eq2 = @(C,A,B,D,w,Theta,F_amp) -A_p*E_p*w*B*C/c0 + k_t*A*C + c_t*w*A*D -
m_t*w^2*A*C;
eq3 = @(A,B,C,D,w,Theta,F_amp) E_p*A_p*Theta*(B*cos(Theta*L_p) -
A*sin(Theta*L_p))*D + (A*cos(Theta*L_p)+B*sin(Theta*L_p))*(-k_b*D - c_b*w*C + m_b*w^2*D);
eq4 = @(B,A,C,D,w,Theta,F_amp) E_p*A_p*Theta*(B*cos(Theta*L_p) -
A*sin(Theta*L_p))*C + (A*cos(Theta*L_p)+B*sin(Theta*L_p))*(-k_b*C + c_b*w*D + m_b*w^2*C);
eq5 = @(C,A,B,D,w,Theta,F_amp) -A_p*E_p*w*B*D/c0 + k_t*A*D - c_t*w*A*C -
m_t*w^2*A*D + F_amp;
eq6 = @(D,A,B,C,w,Theta,F_amp) -A_p*E_p*w*B*C/c0 + k_t*A*C + c_t*w*A*D -
m_t*w^2*A*C;
eq7 = @(B,A,C,D,w,Theta,F_amp) E_p*A_p*Theta*(B*cos(Theta*L_p) -
A*sin(Theta*L_p))*D + (A*cos(Theta*L_p)+B*sin(Theta*L_p))*(-k_b*D - c_b*w*C + m_b*w^2*D);
eq8 = @(A,B,C,D,w,Theta,F_amp) E_p*A_p*Theta*(B*cos(Theta*L_p) -
A*sin(Theta*L_p))*C + (A*cos(Theta*L_p)+B*sin(Theta*L_p))*(-k_b*C + c_b*w*D + m_b*w^2*C);
eq9 = @(A,B,C,D,w,Theta,F_amp) -A_p*E_p*w*B*D/c0 + k_t*A*D - c_t*w*A*C -
m_t*w^2*A*D + F_amp;
eq10 = @(B,A,C,D,w,Theta,F_amp) -A_p*E_p*w*B*C/c0 + k_t*A*C + c_t*w*A*D -
m_t*w^2*A*C;
eq11 = @(D,A,B,C,w,Theta,F_amp) E_p*A_p*Theta*(B*cos(Theta*L_p) -
A*sin(Theta*L_p))*D + (A*cos(Theta*L_p)+B*sin(Theta*L_p))*(-k_b*D - c_b*w*C + m_b*w^2*D);
eq12 = @(C,A,B,D,w,Theta,F_amp) E_p*A_p*Theta*(B*cos(Theta*L_p) -
A*sin(Theta*L_p))*C + (A*cos(Theta*L_p)+B*sin(Theta*L_p))*(-k_b*C + c_b*w*D + m_b*w^2*C);
eq13 = @(B,A,C,D,w,Theta,F_amp) -A_p*E_p*w*B*D/c0 + k_t*A*D - c_t*w*A*C -
m_t*w^2*A*D + F_amp;
eq14 = @(A,B,C,D,w,Theta,F_amp) -A_p*E_p*w*B*C/c0 + k_t*A*C + c_t*w*A*D -
m_t*w^2*A*C;
eq15 = @(C,A,B,D,w,Theta,F_amp) E_p*A_p*Theta*(B*cos(Theta*L_p) -
A*sin(Theta*L_p))*D + (A*cos(Theta*L_p)+B*sin(Theta*L_p))*(-k_b*D - c_b*w*C + m_b*w^2*D);
eq16 = @(D,A,B,C,w,Theta,F_amp) E_p*A_p*Theta*(B*cos(Theta*L_p) -
A*sin(Theta*L_p))*C + (A*cos(Theta*L_p)+B*sin(Theta*L_p))*(-k_b*C + c_b*w*D + m_b*w^2*C);

c_all = 1; % Start
count of the total iterations.
E_ABCD = 100;
Test(1,:) = [1,1,1,1];
for cn = root_n:length(FI)
cn; f_hz = F_root(c1*lk_ti*lm_bi*lc_bi-lk_ti*lm_bi*lc_bi...
+c2*lm_bi*lc_bi-lm_bi*lc_bi+c3*lc_bi-lc_bi+c4,cn)-1;
w = f_hz*2*pi; % 'Rad/sec' % Operating Frequency in
'Rad/sec'.
F_amp = m_ecc*r_ecc*w^2; % 'N' % Amplitude of the
Forcing Function onto the Sonic Drill.
c_all = 1;
E_ABCD = 100;
Theta = w/c0; D = 0.1; B = 100; A = 1000; C = 0.1; Di = D; Bi = B; Ai
= A; Ci = C; c_all = 1;
Check(c1*lk_ti*lm_bi*lc_bi-lk_ti*lm_bi*lc_bi...
+c2*lm_bi*lc_bi-lm_bi*lc_bi+c3*lc_bi-lc_bi+...
c4,2:5) = [100,2000,3000,20000];
while c_all < 30 & E_ABCD > .00001 &
abs(sum(Check(c1*lk_ti*lm_bi*lc_bi-lk_ti*lm_bi*lc_bi...
+c2*lm_bi*lc_bi-lm_bi*lc_bi+c3*lc_bi-lc_bi+...
c4,2:4))) > 500
c_all= c_all +1;
A = fzero(@(A,B,C,D) eq8(A,B,C,D,w,Theta,F_amp),1,A,B,C,D);
Ai(c_all,1) = A;
B = fzero(@(B,A,C,D) eq7(B,A,C,D,w,Theta,F_amp),1,B,A,C,D);
Bi(c_all,1) = B;
C = fzero(@(C,A,B,D) eq5(C,A,B,D,w,Theta,F_amp),1,C,A,B,D);
Ci(c_all,1) = C;

```

```

D = fzero (@(D,A,B,C) eq6(D,A,B,C,w,Theta,F_amp),1,D,A,B,C);
Di(c_all,1) = D;
A = fzero (@(A,B,C,D) eq3(A,B,C,D,w,Theta,F_amp),1,A,B,C,D);
Ai(c_all,2) = A;
B = fzero (@(B,A,C,D) eq4(B,A,C,D,w,Theta,F_amp),1,B,A,C,D);
Bi(c_all,2) = B;
C = fzero (@(C,A,B,D) eq2(C,A,B,D,w,Theta,F_amp),1,C,A,B,D);
Ci(c_all,2) = C;
D = fzero (@(D,A,B,C) eq1(D,A,B,C,w,Theta,F_amp),1,D,A,B,C);
Di(c_all,2) = D;
C = fzero (@(C,A,B,D) eq2(C,A,B,D,w,Theta,F_amp),1,C,A,B,D);
Ci(c_all,3) = C;
B = fzero (@(B,A,C,D) eq4(B,A,C,D,w,Theta,F_amp),1,B,A,C,D);
Bi(c_all,3) = B;
D = fzero (@(D,A,B,C) eq1(D,A,B,C,w,Theta,F_amp),1,D,A,B,C);
Di(c_all,3) = D;
A = fzero (@(A,B,C,D) eq3(A,B,C,D,w,Theta,F_amp),1,A,B,C,D);
Ai(c_all,3) = A;
B = fzero (@(B,A,C,D) eq4(B,A,C,D,w,Theta,F_amp),1,B,A,C,D);
Bi(c_all,4) = B;
D = fzero (@(D,A,B,C) eq1(D,A,B,C,w,Theta,F_amp),1,D,A,B,C);
Di(c_all,4) = D;
C = fzero (@(C,A,B,D) eq2(C,A,B,D,w,Theta,F_amp),1,C,A,B,D);
Ci(c_all,4) = C;
A = fzero (@(A,B,C,D) eq14(A,B,C,D,w,Theta,F_amp),1,A,B,C,D);
Ai(c_all,4) = A;
B = fzero (@(B,A,C,D) eq13(B,A,C,D,w,Theta,F_amp),1,B,A,C,D);
Bi(c_all,4) = B;

Test(c_all,:) =
[eq1(D,A,B,C,w,Theta,F_amp),eq2(C,A,B,D,w,Theta,F_amp),eq3(A,B,C,D,w,Theta,F_amp),eq4(B,A
,C,D,w,Theta,F_amp)];
E_ABCD = abs((Test(c_all,1)-Test(c_all-1,1)) +...
(Test(c_all,2)-Test(c_all-1,2)) +...
(Test(c_all,3)-Test(c_all-1,3)) +...
(Test(c_all,4)-Test(c_all-1,4)));
Check(c1*lk_ti*lm_bi*lc_bi-lk_ti*lm_bi*lc_bi...
+c2*lm_bi*lc_bi-lm_bi*lc_bi+c3*lc_bi-lc_bi+...
c4,:) =
[f_hz,eq1(D,A,B,C,w,Theta,F_amp),eq2(C,A,B,D,w,Theta,F_amp),...
eq3(A,B,C,D,w,Theta,F_amp),eq4(B,A,C,D,w,Theta,F_amp)];

end
C_all(c1*lk_ti*lm_bi*lc_bi-lk_ti*lm_bi*lc_bi...
+c2*lm_bi*lc_bi-lm_bi*lc_bi+c3*lc_bi-lc_bi+...
c4,1) = c_all;
%A_n(cn,1) = A; B_n(cn,1) = B; C_n(cn,1) = C; D_n(cn,1) = D;
w_n(cn,1) = w;
wABCD(c1*lk_ti*lm_bi*lc_bi-lk_ti*lm_bi*lc_bi...
+c2*lm_bi*lc_bi-lm_bi*lc_bi+c3*lc_bi-lc_bi+c4,:) =
[w,A,B,C,D];
Check(c1*lk_ti*lm_bi*lc_bi-lk_ti*lm_bi*lc_bi...
+c2*lm_bi*lc_bi-lm_bi*lc_bi+c3*lc_bi-lc_bi+...
c4,:) =
[f_hz,eq1(D,A,B,C,w,Theta,F_amp),eq2(C,A,B,D,w,Theta,F_amp),...
eq3(A,B,C,D,w,Theta,F_amp),eq4(B,A,C,D,w,Theta,F_amp)];
count = count +1;
end
end
end
end
l_n = nn*N_p+1; % Number of nodes in the length direction of
the string.
nts = 16; % Number of time steps in each oscillation.
u = zeros(l_n,length(wABCD));
f_hz_n = zeros(length(wABCD),1);
for c1 = 1:length(wABCD)

```

```

w = wABCD(c1,1);
dt = (f_hz)^-1;
f_hz_n(c1,1) = f_hz;
for c3= 1 : l_n
    L = dx*(c3-1);
    time = dt/4;
    u(c3,c1) =
(wABCD(c1,2)*cos(wABCD(c1,1)/c0*L)+wABCD(c1,3)*sin(wABCD(c1,1)/c0*L))* (wABCD(c1,4)*cos(w*
time)+wABCD(c1,5)*sin(w*time));

end
Phase(1,c1) = atan(wABCD(c1,5)/wABCD(c1,4))*180./pi();
for c2 = 1:20
    time = dt*c2*1/20;
    for c3= 1 : l_n
        L = dx*(c3-1);
        %time = dt/4;
        ub(c3,c2) =
(wABCD(c1,2)*cos(W(1,RTA)/c0*L)+wABCD(c1,3)*sin(W(1,RTA)/c0*L))* (wABCD(c1,4)*cos(w*time-
Phase(1,c1))+wABCD(c1,5)*sin(w*time-Phase(1,c1)));
    end
end
figure(1)
surface(1:20,x',ub,'EdgeColor','none')%surface(x,time,u')
xlabel('Time')
ylabel('Length along the Drill String 'meters'')
zlabel('Displacement 'm'')
colorbar
set(gca,'XDir','rev')%'ZScale','log',
freq = num2str(F_root(c1,root_n),'%0.2g');
MSDH = num2str(Var(c1,1),'%0.0f');
SRSDH = num2str(Var(c1,2),'%0.0f');
MDB = num2str(Var(c1,3),'%0.1f');
SRDB = num2str(Var(c1,5),'%0.1f');
Hz = ('Hz, ');
view([90 0])
titlefig = ['Sonic Drill Mode Shape Full Wave ',freq,' ',Hz,'MSDH ',MSDH,'kg, SRSDH
',SRSDH,'Nperm, MDB ',MDB,'kg, SRDB ',SRDB, 'Nperm'];
title(titlefig)
filename = [titlefig,'.jpg'];
saveas(gcf,filename)%title('Sonic Drill Mode Shape')
pause(1);
gcf;clf;
end
for c1 = 1%: length(F_root);
figure(1)
freq = num2str(F_root(c1,root_n),'%0.2g');
MSDH = num2str(Var(c1,1),'%0.0f');
SRSDH = num2str(Var(c1,2),'%0.0f');
MDB = num2str(Var(c1,3),'%0.1f');
SRDB = num2str(Var(c1,5),'%0.1f');
Hz = ('Hz');
titlefig = ['Sonic Drill Mode Shape ',freq,' ',Hz,' MSDH ',MSDH,' kg, SRSDH ',SRSDH,'
Nperm, MDB ',MDB,' kg, SRDB ',SRDB, ' Nperm'];
plot(x,u(:,c1))
xlabel('Length along the Drill String 'meters'')
ylabel('Displacement 'm'')
title(titlefig)
filename = [titlefig,'.jpg'];
saveas(gcf,filename)
pause(1);
gcf;
clf;
end
% Finding the Resonant Mode Shape by finding the number of anti-nodes
ui(:,gl) = u(:,1);
mode = zeros(length(wABCD),1);
for c1 = 1:length(wABCD)

```

```

    for c3= 2 : l_n
        if sign(u(c3,c1)) ~= sign(u(c3-1,c1))
            mode(c1,1) = mode(c1,1)+1;
        else
            end
        end
    end
end

ratio = (u(1,:)./u(end,:))';
Data1 = [ratio,mode];% ,F_root(:,root_n)];
% % plot(ratio)
% figure(1)
% surface(f_hz_n(1:5,1),x',u(:,1:5),'EdgeColor','none')%surface(x,time,u')
% xlabel('Frequency 'Hz'')
% ylabel('Length along the Drill String 'meters'')
% zlabel('Displacement 'm'')
% colorbar
% set(gca,'XDir','rev')% 'ZScale','log',
% title('Sonic Drill Mode Shape')
% view(3)
% figure(2)
% plot(wABCD(:,1)'. /2/pi,Phase)
xlswrite(fname_exl,wABCD,sheet,'M3:Q272');
xlswrite(fname_exl,Check(:,2:5),sheet,'R3:U272');
xlswrite(fname_exl,Data1,sheet,'V3:X272');
xlswrite(fname_exl,u(end,:),sheet,'Z3:Z272');
xlswrite(fname_exl,u(1,:),sheet,'AB3:AB272');
end
Min = abs(min(ui)); Max = abs(max(ui));
Maximum = max(Min,Max);
u_norm = [ui(:,1) ./Maximum(1,1),ui(:,2) ./Maximum(1,2)];
figure(2)
plot(x,u_norm)
%% Closing Program-----%
-----%
disp('Program Finished')

```

APPENDIX B

SUPPLEMENTAL DATA AND GRAPHS

Table 10.1. DOE results for factors of influence of the resonant frequency.

Term	SumSqr	F Value	Prob>F	% Contribution
A-Sonic Drill Head Mass	6922.34	0.0001	9.12878	0.278187
B-Sonic Drill Head Spring	24.971	0.9676	0.03293	0.0010035
C-Sonic Drill Bit Mass	2960.24	0.099	1.9519	0.118963
D-Sonic Drill Bit Rate	5291.03	0.016	2.791	0.212629
E-Sonic Drill Length	57879.2	< 0.0001	38.1638	2.32598
F-Resonant Mode Number	Aliased			
AB	43.5723	0.9984	0.02873	0.00175103
AC	2220.53	0.6633	0.732075	0.0892359
AD	12634.8	0.0002	3.33241	0.507753
AE	100202	< 0.0001	33.0351	4.02679
AF	Aliased			
BC	166.062	0.9999	0.054748	0.0066735
BD	119.183	1	0.031434	0.00478957
BE	15.5047	1	0.005112	0.000623085
BF	Aliased			
CD	777.566	1	0.102541	0.0312479
CE	2879.59	0.9599	0.47468	0.115722
CF	Aliased			
DE	54694.4	< 0.0001	7.21278	2.19799
DF	Aliased			
EF	Aliased			
ABC	150.085	1	0.024741	0.00603145
ABD	349.731	1	0.046121	0.0140546
ABE	116.517	1	0.019207	0.00468243
ABF	Aliased			
ACD	768.525	1	0.050674	0.0308846
ACE	2296.07	1	0.189245	0.0922716
ACF	Aliased			
ADE	Aliased			
ADF	Aliased			
AEF	Aliased			
BCD	143.764	1	0.009479	0.0057774
BCE	267.663	1	0.022061	0.0107565
BCF	Aliased			
BDE	587.582	1	0.038744	0.0236131
BDF	Aliased			
BEF	Aliased			
CDE	1527.73	1	0.050367	0.0613945
CDF	Aliased			
CEF	Aliased			
DEF	Aliased			
ABCD	330.853	1	0.010908	0.0132959
ABCE	683.23	1	0.028156	0.0274568
ABCF	Aliased			
ABDE	Aliased			
ABDF	Aliased			
ABEF	Aliased			
ACDE	Aliased			

Table 10.2. DOE results for factors of influence of the drill bit amplitude.

Term	SumSqr	F Value	Prob>F	% Contribution
A-Sonic Drill Head Mass	4991.35	< 0.0001	24.6239	0.614362
B-Sonic Drill Head Spring	195.852	0.3806	0.966198	0.0241065
C-Sonic Drill Bit Mass	2560.12	< 0.0001	6.31494	0.315114
D-Sonic Drill Bit Rate	9652.17	< 0.0001	19.0469	1.18804
E-Sonic Drill Length	5407.3	< 0.0001	13.338	0.66556
F-Resonant Mode Number	Aliased			
AB	546.141	0.2498	1.34714	0.067222
AC	6693.08	< 0.0001	8.25476	0.82382
AD	3879.92	< 0.0001	3.82817	0.477561
AE	11895.8	< 0.0001	14.6714	1.4642
AF	Aliased			
BC	1479.96	0.0676	1.82527	0.182161
BD	4175.12	< 0.0001	4.11944	0.513897
BE	4347.59	< 0.0001	5.36201	0.535125
BF	Aliased			
CD	5295.34	0.0001	2.61236	0.651779
CE	6279.04	< 0.0001	3.87206	0.772858
CF	Aliased			
DE	30754.6	< 0.0001	15.1722	3.78544
DF	Aliased			
EF	Aliased			
ABC	2899.3	0.027	1.7879	0.356862
ABD	3374.78	0.0316	1.66488	0.415385
ABE	7219.14	< 0.0001	4.45179	0.888571
ABF	Aliased			
ACD	7635.29	0.0006	1.88336	0.939792
ACE	17824.2	< 0.0001	5.49579	2.1939
ACF	Aliased			
ADE	Aliased			
ADF	Aliased			
AEF	Aliased			
BCD	4312.84	0.3624	1.06383	0.530847
BCE	6888.2	0.0002	2.12385	0.847837
BCF	Aliased			
BDE	15627.5	< 0.0001	3.85476	1.92351
BDF	Aliased			
BEF	Aliased			
CDE	25706	< 0.0001	3.17039	3.16403
CDF	Aliased			
CEF	Aliased			
DEF	Aliased			
ABCD	10688	0.031	1.31818	1.31554
ABCE	15153.7	< 0.0001	2.33618	1.86519
ABCF	Aliased			
ABDE	Aliased			
ABDF	Aliased			
ABEF	Aliased			
ACDE	Aliased			

Table 10.3. DOE results for factors of influence of the ratio of sonic drill head amplitude to the drill bit amplitude.

Term	SumSqr	F Value	Prob>F	% Contribtion
A-Sonic Drill Head Mass	22446.32	< 0.0001	86.45156038	0.732578071
B-Sonic Drill Head Spring	66.90699	0.7728	0.257690958	0.002183636
C-Sonic Drill Bit Mass	1.644903	1.0000	0.003167656	5.36845E-05
D-Sonic Drill Bit Rate	2070070	< 0.0001	3189.132865	67.56063142
E-Sonic Drill Length	13898.57	< 0.0001	26.76504328	0.453606244
F-Resonant Mode Number	Aliased			
AB	17.21287	0.9979	0.033147512	0.000561774
AC	16.7868	1.0000	0.016163512	0.000547869
AD	113109.3	< 0.0001	87.1276752	3.691536854
AE	10887.52	< 0.0001	10.48326303	0.355334644
AF	Aliased			
BC	17.6188	1.0000	0.016964614	0.000575023
BD	276.3903	0.9952	0.212902322	0.009020518
BE	25.897	1.0000	0.024935446	0.000845198
BF	Aliased			
CD	26.88109	1.0000	0.0103532	0.000877315
CE	31.7989	1.0000	0.015309105	0.001037817
CF	Aliased			
DE	67731	< 0.0001	26.08645934	2.210528993
DF	Aliased			
EF	Aliased			
ABC	29.35413	1.0000	0.014132108	0.000958028
ABD	79.33795	1.0000	0.030556855	0.002589344
ABE	54.61586	1.0000	0.026293988	0.001782492
ABF	Aliased			
ACD	67.072	1.0000	0.012916324	0.002189021
ACE	37.93569	1.0000	0.009131786	0.001238103
ACF	Aliased			
ADE	Aliased			
ADF	Aliased			
AEF	Aliased			
BCD	83.26291	1.0000	0.016034272	0.002717442
BCE	40.62141	1.0000	0.009778286	0.001325757
BCF	Aliased			
BDE	105.7194	1.0000	0.020358808	0.003450352
BDF	Aliased			
BEF	Aliased			
CDE	51.81881	1.0000	0.004989478	0.001691205
CDF	Aliased			
CEF	Aliased			
DEF	Aliased			
ABCD	140.0161	1.0000	0.013481735	0.004569691
ABCE	63.23119	1.0000	0.007610427	0.002063669
ABCF	Aliased			
ABDE	Aliased			
ABDF	Aliased			
ABEF	Aliased			
ACDE	Aliased			

Table 10.4. DOE results for factors of influence of the resonant frequency.

Term	SumSqr	F Value	Prob>F	% Contribution
A-Sonic Drill Head Mass	987.5914	< 0.0001	301.4701252	0.134301779
B-Sonic Drill Head Spring	0.674131	0.8140	0.205783721	9.16745E-05
C-Sonic Drill Bit Mass	399.3016	< 0.0001	60.94499678	0.054300714
D-Resonant Mode Number	727198.2	< 0.0001	36997.17301	98.89111507
E-Strata Types	1225.708	< 0.0001	149.6628326	0.166683055
AB	1.071831	0.9568	0.163592405	0.000145757
AC	256.9865	< 0.0001	19.61179537	0.034947397
AD	529.6997	< 0.0001	13.47458636	0.072033443
AE	650.5564	< 0.0001	39.71750347	0.088468656
BC	1.72314	0.9979	0.13150052	0.000234328
BD	6.34855	1.0000	0.161495454	0.000863334
BE	4.613492	0.9853	0.281661027	0.000627385
CD	124.4285	0.0069	1.582616677	0.016920939
CE	166.6563	< 0.0001	5.087316226	0.02266346
DE	Aliased			
ABC	3.032623	1.0000	0.115716529	0.000412404
ABD	Aliased			
ABE	5.199224	1.0000	0.158710462	0.000707038
ACD	Aliased			
ACE	175.051	< 0.0001	2.671785376	0.023805047
ADE	Aliased			
BCD	20.21165	1.0000	0.128536798	0.002748566
BCE	7.625326	1.0000	0.116384569	0.001036962
BDE	Aliased			
CDE	Aliased			
ABCD	Aliased			
ABCE	13.70652	1.0000	0.104600572	0.001863938
ABDE	Aliased			
ACDE	Aliased			
BCDE	Aliased			
ABCDE	Aliased			

Table 10.5. DOE results for factors of influence of the drill bit amplitude.

Term	SumSqr	F Value	Prob>F	% Contribution
A-Sonic Drill Head Mass	0.317885	< 0.0001	59.3298	3.55641
B-Sonic Drill Head Spring	0.006756	0.2836	1.2609	0.0755823
C-Sonic Drill Bit Mass	0.019589	0.1207	1.82802	0.219153
D-Resonant Mode Number	0.469891	< 0.0001	14.6167	5.257
E-Strata Types	0.3882	< 0.0001	28.9813	4.34307
AB	0.007969	0.5622	0.743651	0.0891534
AC	0.029294	0.2061	1.36686	0.327735
AD	0.570232	< 0.0001	8.86896	6.37958
AE	0.24365	< 0.0001	9.09493	2.72589
BC	0.015381	0.6762	0.717652	0.172073
BD	0.085784	0.1283	1.33421	0.95972
BE	0.034707	0.227	1.29553	0.388289
CD	0.157865	0.1374	1.22766	1.76615
CE	0.082114	0.0612	1.53257	0.918666
DE	Aliased			
ABC	0.038839	0.5618	0.906097	0.434513
ABD	Aliased			
ABE	0.042229	0.7307	0.788164	0.472449
ACD	Aliased			
ACE	0.142459	0.0819	1.32942	1.59378
ADE	Aliased			
BCD	0.181344	0.9862	0.705124	2.02883
BCE	0.078922	0.8882	0.736497	0.882956
BDE	Aliased			
CDE	Aliased			
ABCD	Aliased			
ABCE	0.193165	0.7207	0.901301	2.16107
ABDE	Aliased			
ACDE	Aliased			
BCDE	Aliased			
ABCDE	Aliased			

=

Table 10.6. DOE results for factors of influence of the ratio of sonic drill head amplitude to the drill bit amplitude.

Term	SumSqr	F Value	Prob>F	% Contribtion
A-Sonic Drill Head Mass	12542.4	< 0.0001	57.6545	0.345
B-Sonic Drill Head Spring	7.99589	0.9639	0.0367554	0.000219942
C-Sonic Drill Bit Mass	417.841	0.4281	0.960364	0.0114935
D-Resonant Mode Number	97672.8	< 0.0001	74.8302	2.68667
E-Strata Types	3251170	< 0.0001	5977.97	89.4293
AB	83.7207	0.9424	0.192423	0.00230289
AC	174.733	0.9908	0.200803	0.00480635
AD	20395.8	< 0.0001	7.81294	0.561024
AE	13094.6	< 0.0001	12.0386	0.36019
BC	7.93565	1	0.00911962	0.000218285
BD	458.14	1	0.175498	0.012602
BE	92.2374	0.9999	0.0847991	0.00253716
CD	958.796	1	0.183641	0.0263734
CE	179.213	1	0.0823804	0.00492958
DE	Aliased			
ABC	4.10088	1	0.00235636	0.000112802
ABD	Aliased			
ABE	422.388	1	0.194163	0.0116185
ACD	Aliased			
ACE	260.159	1	0.0597948	0.00715615
ADE	Aliased			
BCD	107.645	1	0.0103088	0.00296098
BCE	43.2712	1	0.00994542	0.00119025
BDE	Aliased			
CDE	Aliased			
ABCD	Aliased			
ABCE	29.9856	1	0.00344594	0.000824809
ABDE	Aliased			
ACDE	Aliased			
BCDE	Aliased			
ABCDE	Aliased			

Table 10.7. DOE results for factors of influence of the resonant frequency.

Term	SumSqr	F Value	Prob>F	% Contribtion
A-Sonic Drill Head Mass	38.43424	< 0.0001	27.63457785	0.003903306
B-Sonic Drill Head Spring	0.220821	0.8532	0.158772533	2.24262E-05
C-Sonic Drill Bit Mass	225.1521	< 0.0001	80.94322725	0.022866006
D-Resonant Mode Number	982440.1	< 0.0001	117730.6	99.77469471
E-Drill Bit Damping	0.796626	0.9500	0.229112632	8.09038E-05
AB	2.782639	0.4060	1.000371866	0.000282599
AC	218.5938	< 0.0001	39.29275402	0.022199964
AD	Aliased			
AE	0.299319	1.0000	0.043042574	3.03982E-05
BC	3.191417	0.8003	0.573664665	0.000324114
BD	4.538353	0.9998	0.271926488	0.000460906
BE	0.156723	1.0000	0.022537117	1.59165E-05
CD	Aliased			
CE	0.415717	1.0000	0.029890448	4.22194E-05
DE	Aliased			
ABC	7.366598	0.8334	0.662081571	0.000748137
ABD	Aliased			
ABE	0.572671	1.0000	0.041175613	5.81594E-05
ACD	Aliased			
ACE	1.822876	1.0000	0.065533248	0.000185128
ADE	Aliased			
BCD	Aliased			
BCE	1.00374	1.0000	0.036084907	0.000101938
BDE	Aliased			
CDE	Aliased			
ABCD	Aliased			
ABCE	1.757673	1.0000	0.03159459	0.000178506
ABDE	Aliased			
ACDE	Aliased			
BCDE	Aliased			
ABCDE	Aliased			

Table 10.8. DOE results for factors of influence of the drill bit amplitude.

Term	SumSqr	F Value	Prob>F	% Contribution
A-Sonic Drill Head Mass	0.160526	< 0.0001	69.7945	3.32576
B-Sonic Drill Head Spring	0.504257	< 0.0001	219.244	10.4471
C-Sonic Drill Bit Mass	0.0512983	< 0.0001	11.1519	1.06279
D-Resonant Mode Number	0.355405	< 0.0001	25.7542	7.36325
E-Drill Bit Damping	0.0107483	0.0964	1.86928	0.222682
AB	0.00207239	0.7721	0.450522	0.0429355
AC	0.0656364	< 0.0001	7.13444	1.35985
AD	Aliased			
AE	0.0232857	0.0274	2.02486	0.482431
BC	0.00290354	0.9605	0.315605	0.0601553
BD	0.617529	< 0.0001	22.3744	12.7939
BE	0.0102316	0.542	0.889711	0.211977
CD	Aliased			
CE	0.0204469	0.6018	0.889002	0.423617
DE	Aliased			
ABC	0.00551473	0.9966	0.299716	0.114254
ABD	Aliased			
ABE	0.0236864	0.4218	1.02985	0.490732
ACD	Aliased			
ACE	0.0419638	0.6285	0.912263	0.869402
ADE	Aliased			
BCD	Aliased			
BCE	0.0332378	0.9023	0.722566	0.688617
BDE	Aliased			
CDE	Aliased			
ABCD	Aliased			
ABCE	0.0782217	0.8248	0.850242	1.62059
ABDE	Aliased			
ACDE	Aliased			
BCDE	Aliased			
ABCDE	Aliased			

Table 10.9. DOE results for factors of influence of the ratio of sonic drill head amplitude to the drill bit amplitude.

Term	SumSqr	F Value	Prob>F	% Contribtion
A-Sonic Drill Head Mass	39.9768	< 0.0001	3567.03	32.2413
B-Sonic Drill Head Spring	0.069316	0.0021	6.1849	0.0559034
C-Sonic Drill Bit Mass	11.8153	< 0.0001	527.125	9.52904
D-Resonant Mode Number	56.273	< 0.0001	836.851	45.3842
E-Damping	0.135689	0.0002	4.84287	0.109433
AB	0.026129	0.324	1.16571	0.021073
AC	0.333673	< 0.0001	7.44321	0.269108
AD	Aliased			
AE	0.07262	0.2267	1.29594	0.0585679
BC	0.035441	0.611	0.790572	0.0285829
BD	0.294931	0.0007	2.193	0.237862
BE	0.062864	0.3413	1.12183	0.0506994
CD	Aliased			
CE	0.040209	0.996	0.358776	0.0324286
DE	Aliased			
ABC	0.090964	0.4373	1.01456	0.0733625
ABD	Aliased			
ABE	0.08409	0.7755	0.750314	0.0678185
ACD	Aliased			
ACE	0.175916	0.8315	0.784828	0.141876
ADE	Aliased			
BCD	Aliased			
BCE	0.221701	0.4903	0.989091	0.178802
BDE	Aliased			
CDE	Aliased			
ABCD	Aliased			
ABCE	0.493319	0.2564	1.10044	0.397861
ABDE	Aliased			
ACDE	Aliased			
BCDE	Aliased			
ABCDE	Aliased			

Table 10.10. Axial Mode Frequencies for Various Drill Pipe Lengths.

Mode	Pipe Length							
	50 ft	100 ft	120 ft	150 ft	250 ft	500 ft	750 ft	1000 ft
1	75 Hz	Hz	Hz	Hz	Hz	Hz	Hz	Hz
2	Hz	117 Hz	99 Hz	80 Hz	Hz	Hz	Hz	Hz
3	Hz	Hz	Hz	Hz	81 Hz	Hz	Hz	Hz
4	Hz	Hz	Hz	Hz	113 Hz	66 Hz	Hz	Hz
5	Hz	Hz	Hz	Hz	Hz	82 Hz	Hz	Hz
6	Hz	Hz	Hz	Hz	Hz	97 Hz	66 Hz	Hz
7	Hz	Hz	Hz	Hz	Hz	113 Hz	77 Hz	Hz
8	Hz	Hz	Hz	Hz	Hz	129 Hz	87 Hz	66 Hz
9	Hz	Hz	Hz	Hz	Hz	Hz	98 Hz	74 Hz
10	Hz	Hz	Hz	Hz	Hz	Hz	109 Hz	82 Hz
11	Hz	Hz	Hz	Hz	Hz	Hz	119 Hz	90 Hz
12	Hz	Hz	Hz	Hz	Hz	Hz	130 Hz	98 Hz
13	Hz	Hz	Hz	Hz	Hz	Hz	Hz	106 Hz
14	Hz	Hz	Hz	Hz	Hz	Hz	Hz	114 Hz
15	Hz	Hz	Hz	Hz	Hz	Hz	Hz	123 Hz
16	Hz	Hz	Hz	Hz	Hz	Hz	Hz	131 Hz

Frequencies in Red are loosely coupled with the bending mode.

Table 10.11. Torsional Mode Frequencies for Various Drill Pipe Lengths.

Mode	Pipe Length										
	50 ft	100 ft	120 ft	150 ft	250 ft	500 ft	750 ft	1000 ft			
1	103 Hz	Hz	Hz	Hz	Hz	Hz	Hz	Hz	Hz	Hz	Hz
2	Hz	103 Hz	86 Hz	68 Hz	Hz	Hz	Hz	Hz	Hz	Hz	Hz
3	Hz	Hz	Hz	103 Hz	62 Hz	Hz	Hz	Hz	Hz	Hz	Hz
4	Hz	Hz	Hz	Hz	82 Hz	Hz	Hz	Hz	Hz	Hz	Hz
5	Hz	Hz	Hz	Hz	103 Hz	Hz	Hz	Hz	Hz	Hz	Hz
6	Hz	Hz	Hz	Hz	Hz	62 Hz	Hz	Hz	Hz	Hz	Hz
7	Hz	Hz	Hz	Hz	Hz	72 Hz	Hz	Hz	Hz	Hz	Hz
8	Hz	Hz	Hz	Hz	Hz	82 Hz	Hz	Hz	Hz	Hz	Hz
9	Hz	Hz	Hz	Hz	Hz	92 Hz	Hz	Hz	Hz	Hz	Hz
10	Hz	Hz	Hz	Hz	Hz	103 Hz	68 Hz	Hz	Hz	Hz	Hz
11	Hz	Hz	Hz	Hz	Hz	113 Hz	75 Hz	Hz	Hz	Hz	Hz
12	Hz	Hz	Hz	Hz	Hz	123 Hz	82 Hz	62 Hz	Hz	Hz	Hz
13	Hz	Hz	Hz	Hz	Hz	133 Hz	89 Hz	67 Hz	Hz	Hz	Hz
14	Hz	Hz	Hz	Hz	Hz	Hz	96 Hz	72 Hz	Hz	Hz	Hz
15	Hz	Hz	Hz	Hz	Hz	Hz	103 Hz	77 Hz	Hz	Hz	Hz
16	Hz	Hz	Hz	Hz	Hz	Hz	109 Hz	82 Hz	Hz	Hz	Hz
17	Hz	Hz	Hz	Hz	Hz	Hz	116 Hz	87 Hz	Hz	Hz	Hz
18	Hz	Hz	Hz	Hz	Hz	Hz	123 Hz	92 Hz	Hz	Hz	Hz
19	Hz	Hz	Hz	Hz	Hz	Hz	130 Hz	98 Hz	Hz	Hz	Hz
20	Hz	Hz	Hz	Hz	Hz	Hz	Hz	103 Hz	Hz	Hz	Hz
21	Hz	Hz	Hz	Hz	Hz	Hz	Hz	108 Hz	Hz	Hz	Hz
22	Hz	Hz	Hz	Hz	Hz	Hz	Hz	113 Hz	Hz	Hz	Hz
23	Hz	Hz	Hz	Hz	Hz	Hz	Hz	118 Hz	Hz	Hz	Hz
24	Hz	Hz	Hz	Hz	Hz	Hz	Hz	123 Hz	Hz	Hz	Hz
25	Hz	Hz	Hz	Hz	Hz	Hz	Hz	128 Hz	Hz	Hz	Hz
26	Hz	Hz	Hz	Hz	Hz	Hz	Hz	134 Hz	Hz	Hz	Hz

Frequencies in Red are loosely coupled with the bending mode.

Table 10.12. First 50 Bending Modes for Various Drill Pipe Lengths.

Mode	Pipe Length								
	50 ft	100 ft	120 ft	150 ft	250 ft	500 ft	750 ft	1000 ft	
1	Hz	Hz	Hz	Hz	Hz	Hz	Hz	Hz	Hz
2	Hz	Hz	Hz	Hz	Hz	Hz	Hz	Hz	Hz
3	Hz	Hz	Hz	Hz	Hz	Hz	Hz	Hz	Hz
4	Hz	Hz	Hz	Hz	Hz	Hz	Hz	Hz	Hz
5	Hz	Hz	Hz	Hz	Hz	Hz	Hz	Hz	Hz
6	73 Hz	Hz	Hz	Hz	Hz	Hz	Hz	Hz	Hz
7	101 Hz	Hz	Hz	Hz	Hz	Hz	Hz	Hz	Hz
8	Hz	Hz	Hz	Hz	Hz	Hz	Hz	Hz	Hz
9	Hz	Hz	Hz	Hz	Hz	Hz	Hz	Hz	Hz
10	Hz	Hz	Hz	Hz	Hz	Hz	Hz	Hz	Hz
11	Hz	68 Hz	Hz	Hz	Hz	Hz	Hz	Hz	Hz
12	Hz	82 Hz	Hz	Hz	Hz	Hz	Hz	Hz	Hz
13	Hz	96 Hz	68 Hz	Hz	Hz	Hz	Hz	Hz	Hz
14	Hz	112 Hz	79 Hz	Hz	Hz	Hz	Hz	Hz	Hz
15	Hz	Hz	91 Hz	Hz	Hz	Hz	Hz	Hz	Hz
16	Hz	Hz	103 Hz	67 Hz	Hz	Hz	Hz	Hz	Hz
17	Hz	Hz	117 Hz	76 Hz	Hz	Hz	Hz	Hz	Hz
18	Hz	Hz	Hz	85 Hz	Hz	Hz	Hz	Hz	Hz
19	Hz	Hz	Hz	95 Hz	Hz	Hz	Hz	Hz	Hz
20	Hz	Hz	Hz	105 Hz	Hz	Hz	Hz	Hz	Hz
21	Hz	Hz	Hz	116 Hz	Hz	Hz	Hz	Hz	Hz
22	Hz	Hz	Hz	Hz	Hz	Hz	Hz	Hz	Hz
23	Hz	Hz	Hz	Hz	Hz	Hz	Hz	Hz	Hz
24	Hz	Hz	Hz	Hz	Hz	Hz	Hz	Hz	Hz
25	Hz	Hz	Hz	Hz	61 Hz	Hz	Hz	Hz	Hz
26	Hz	Hz	Hz	Hz	66 Hz	Hz	Hz	Hz	Hz
27	Hz	Hz	Hz	Hz	71 Hz	Hz	Hz	Hz	Hz
28	Hz	Hz	Hz	Hz	76 Hz	Hz	Hz	Hz	Hz
29	Hz	Hz	Hz	Hz	82 Hz	Hz	Hz	Hz	Hz
30	Hz	Hz	Hz	Hz	88 Hz	Hz	Hz	Hz	Hz
31	Hz	Hz	Hz	Hz	94 Hz	Hz	Hz	Hz	Hz
32	Hz	Hz	Hz	Hz	100 Hz	Hz	Hz	Hz	Hz
33	Hz	Hz	Hz	Hz	106 Hz	Hz	Hz	Hz	Hz
34	Hz	Hz	Hz	Hz	112 Hz	Hz	Hz	Hz	Hz
35	Hz	Hz	Hz	Hz	Hz	Hz	Hz	Hz	Hz
36	Hz	Hz	Hz	Hz	Hz	Hz	Hz	Hz	Hz
37	Hz	Hz	Hz	Hz	Hz	Hz	Hz	Hz	Hz
38	Hz	Hz	Hz	Hz	Hz	Hz	Hz	Hz	Hz
39	Hz	Hz	Hz	Hz	Hz	Hz	Hz	Hz	Hz
40	Hz	Hz	Hz	Hz	Hz	Hz	Hz	Hz	Hz
41	Hz	Hz	Hz	Hz	Hz	Hz	Hz	Hz	Hz
42	Hz	Hz	Hz	Hz	Hz	Hz	Hz	Hz	Hz
43	Hz	Hz	Hz	Hz	Hz	Hz	Hz	Hz	Hz
44	Hz	Hz	Hz	Hz	Hz	Hz	Hz	Hz	Hz
45	Hz	Hz	Hz	Hz	Hz	Hz	Hz	Hz	Hz
46	Hz	Hz	Hz	Hz	Hz	Hz	Hz	Hz	Hz
47	Hz	Hz	Hz	Hz	Hz	Hz	Hz	Hz	Hz
48	Hz	Hz	Hz	Hz	Hz	Hz	Hz	Hz	Hz
49	Hz	Hz	Hz	Hz	Hz	Hz	Hz	Hz	Hz
50	Hz	Hz	Hz	Hz	Hz	62 Hz	Hz	Hz	Hz

Table 10.13. Bending Modes 51 – 100 for Various Drill Pipe Lengths.

Mode	Pipe Length								
	50 ft	100 ft	120 ft	150 ft	250 ft	500 ft	750 ft	1000 ft	
51	Hz	Hz	Hz	Hz	Hz	65 Hz	Hz	Hz	Hz
52	Hz	Hz	Hz	Hz	Hz	67 Hz	Hz	Hz	Hz
53	Hz	Hz	Hz	Hz	Hz	70 Hz	Hz	Hz	Hz
54	Hz	Hz	Hz	Hz	Hz	73 Hz	Hz	Hz	Hz
55	Hz	Hz	Hz	Hz	Hz	75 Hz	Hz	Hz	Hz
56	Hz	Hz	Hz	Hz	Hz	78 Hz	Hz	Hz	Hz
57	Hz	Hz	Hz	Hz	Hz	81 Hz	Hz	Hz	Hz
58	Hz	Hz	Hz	Hz	Hz	84 Hz	Hz	Hz	Hz
59	Hz	Hz	Hz	Hz	Hz	87 Hz	Hz	Hz	Hz
60	Hz	Hz	Hz	Hz	Hz	90 Hz	Hz	Hz	Hz
61	Hz	Hz	Hz	Hz	Hz	93 Hz	Hz	Hz	Hz
62	Hz	Hz	Hz	Hz	Hz	96 Hz	Hz	Hz	Hz
63	Hz	Hz	Hz	Hz	Hz	99 Hz	Hz	Hz	Hz
64	Hz	Hz	Hz	Hz	Hz	102 Hz	Hz	Hz	Hz
65	Hz	Hz	Hz	Hz	Hz	105 Hz	Hz	Hz	Hz
66	Hz	Hz	Hz	Hz	Hz	108 Hz	Hz	Hz	Hz
67	Hz	Hz	Hz	Hz	Hz	111 Hz	Hz	Hz	Hz
68	Hz	Hz	Hz	Hz	Hz	115 Hz	Hz	Hz	Hz
69	Hz	Hz	Hz	Hz	Hz	118 Hz	Hz	Hz	Hz
70	Hz	Hz	Hz	Hz	Hz	121 Hz	Hz	Hz	Hz
71	Hz	Hz	Hz	Hz	Hz	125 Hz	Hz	Hz	Hz
72	Hz	Hz	Hz	Hz	Hz	128 Hz	Hz	Hz	Hz
73	Hz	Hz	Hz	Hz	Hz	132 Hz	Hz	Hz	Hz
74	Hz	Hz	Hz	Hz	Hz	Hz	Hz	Hz	Hz
75	Hz	Hz	Hz	Hz	Hz	Hz	61 Hz	Hz	Hz
76	Hz	Hz	Hz	Hz	Hz	Hz	63 Hz	Hz	Hz
77	Hz	Hz	Hz	Hz	Hz	Hz	65 Hz	Hz	Hz
78	Hz	Hz	Hz	Hz	Hz	Hz	66 Hz	Hz	Hz
79	Hz	Hz	Hz	Hz	Hz	Hz	68 Hz	Hz	Hz
80	Hz	Hz	Hz	Hz	Hz	Hz	70 Hz	Hz	Hz
81	Hz	Hz	Hz	Hz	Hz	Hz	72 Hz	Hz	Hz
82	Hz	Hz	Hz	Hz	Hz	Hz	73 Hz	Hz	Hz
83	Hz	Hz	Hz	Hz	Hz	Hz	75 Hz	Hz	Hz
84	Hz	Hz	Hz	Hz	Hz	Hz	77 Hz	Hz	Hz
85	Hz	Hz	Hz	Hz	Hz	Hz	79 Hz	Hz	Hz
86	Hz	Hz	Hz	Hz	Hz	Hz	81 Hz	Hz	Hz
87	Hz	Hz	Hz	Hz	Hz	Hz	83 Hz	Hz	Hz
88	Hz	Hz	Hz	Hz	Hz	Hz	85 Hz	Hz	Hz
89	Hz	Hz	Hz	Hz	Hz	Hz	86 Hz	Hz	Hz
90	Hz	Hz	Hz	Hz	Hz	Hz	88 Hz	Hz	Hz
91	Hz	Hz	Hz	Hz	Hz	Hz	90 Hz	Hz	Hz
92	Hz	Hz	Hz	Hz	Hz	Hz	92 Hz	Hz	Hz
93	Hz	Hz	Hz	Hz	Hz	Hz	94 Hz	Hz	Hz
94	Hz	Hz	Hz	Hz	Hz	Hz	96 Hz	Hz	Hz
95	Hz	Hz	Hz	Hz	Hz	Hz	98 Hz	Hz	Hz
96	Hz	Hz	Hz	Hz	Hz	Hz	101 Hz	Hz	Hz
97	Hz	Hz	Hz	Hz	Hz	Hz	103 Hz	Hz	Hz
98	Hz	Hz	Hz	Hz	Hz	Hz	105 Hz	61 Hz	Hz
99	Hz	Hz	Hz	Hz	Hz	Hz	107 Hz	62 Hz	Hz
100	Hz	Hz	Hz	Hz	Hz	Hz	109 Hz	64 Hz	Hz

